One-Pot Synthesis of Chemicals Using CO_2 as Chemical Feedstock

March 2024

Koichi Nakaoka

(Doctor's Course)

Graduate School of Natural Science and Technology

Okayama University, Japan

Contents

Chapter 1

General Introduction

1.1 Carbon dioxide fixation

Carbon dioxide (CO_2) is a greenhouse gas giving severe damage to the global environment as well as a cheap, abundant, and renewable C1 building block, and the development of effective technologies of CO_2 utilization is essential for the creation of carbon-neutral societies.[1] CO_2 is the most oxidized form of carbon with high stability, and the effective and efficient conversions of CO_2 into useful chemical products are still challenging. The thermodynamic stability of CO_2 can be overcome by reacting with high-energy chemicals or providing heat or electric current while suitable catalysts can be used to lower the kinetic barriers. There are reductive and non-reductive transformations of CO_2, and both of them have attracted much attention of chemists from the viewpoint of energy and sustainable organic chemistry.[1]

The reductive conversions of CO_2 can produce bulk chemicals and fuels such as CO, carboxylic acids, alcohols, and hydrocarbons. Reductants such as hydrogen, hydrosilane, and hydroborane are often used. In addition, solar or renewable electric energy can also promote CO_2 reduction.

On the other hand, the syntheses of urea, (poly)carbonates, and (poly)urethanes from CO_2 are non-reductive CO_2 transformations making new C–O or C–N bonds, and some of them have already been industrialized. In particular, the reactions of CO_2 with epoxides in the presence of catalysts giving (poly)carbonates with 100% atom efficiency have gained increasing attention during the past few decades.[2,3]

1.2 The ring-opening copolymerization (ROCOP) of epoxides and CO_2 and the terpolymerization of epoxides, CO_2, and comonomers.

ROCOP of epoxides and CO_2 for the synthesis of aliphatic polycarbonates is a green and sustainable synthetic technology with 100% atom economy (Scheme 1a).[2,3] Since the first report in 1969,[4] the catalytic ROCOP of epoxides and CO_2 has been intensively studied. ROCOP of epoxides and CO_2 competes with the ring-opening polymerization (ROP) of epoxides giving polyether (Scheme 1b), and many kinds of catalysts that can selectively promote the ROCOP of epoxides and CO_2 have been developed. However, aliphatic polycarbonates sometimes display poor chemical and mechanical properties, although various types of epoxides have been screened. The incorporation of the third comonomer can be one of the most useful methods for the improvement of the physical properties of aliphatic polycarbonates derived from epoxides and CO_2.

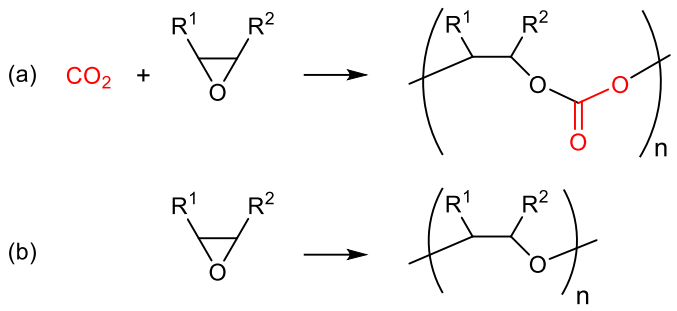

Scheme 1. (a) ROCOP of epoxides and CO_2 and (b) ROP of epoxides.

The terpolymerization of epoxides, CO_2, and comonomers, such as cyclic acid (thio)anhydrides,[5] lactones,[6] lactides,[7] and heteroallenes[8,9] is an effective strategy for the development of new CO_2-based polymers (Scheme 2). The thermal, optical, mechanical or degradation properties can be added or tuned by not only incorporating new polymer backbones derived from the comonomers but also controlling the sequences of terpolymers such as random, block, and gradient polymers. On the other hand, two catalytic processes need to proceed on the same polymer chains to give sequence-controlled terpolymers, which makes these polymerizaitons challenging. Here, the terpolymerizations of epoxides, CO_2, and comonomers are overviewed. The terpolymerizations of two different epoxides and CO_2 are excluded, although the resulting terpolymers often have interesting properties.[10]

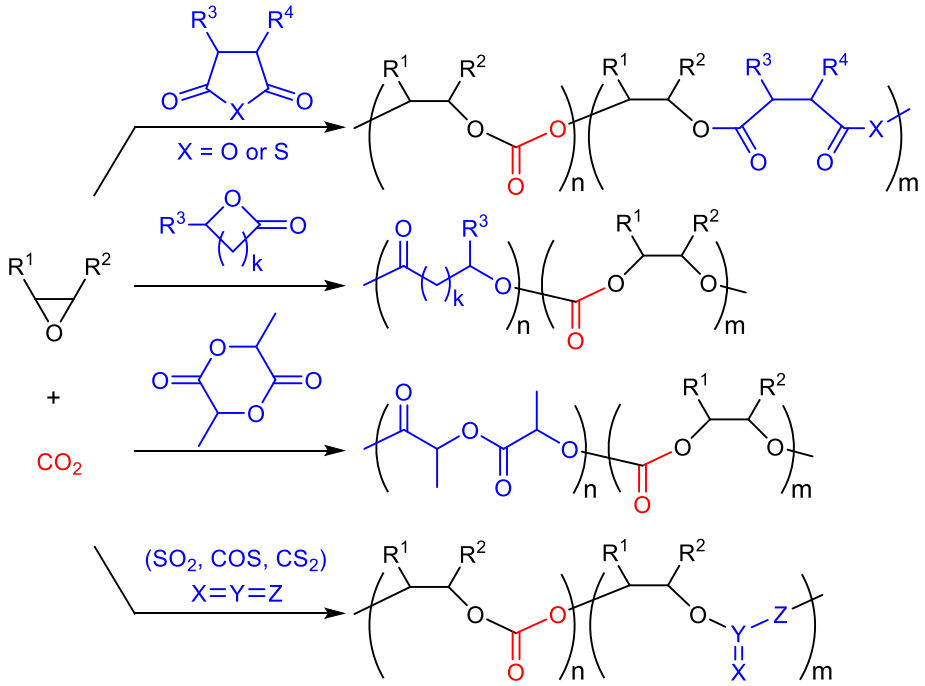

Scheme 2. Classification of the terpolymerizations of epoxides, CO_2, and comonomers.

1.3 Terpolymerization of epoxides, CO_2, and cyclic acid (thio)anhydrides

The terpolymerization of epoxides, CO_2, and cyclic acid (thio)anhydrides gives poly(carbonate-ester)s (Scheme 3a). The carbonate and ester linkages are biodegradable to different degrees, and it is possible to adjust the degradability of the poly(carbonate-ester)s by regulating the ratio of the polyester linkage to the polycarbonate linkage. The representative catalytic cycles, catalysts, and conditions for the terpolymerization of epoxides, CO_2, and cyclic acid (thio)anhydrides are shown in Scheme 3b, Figure 1, and Table 1, respectively.

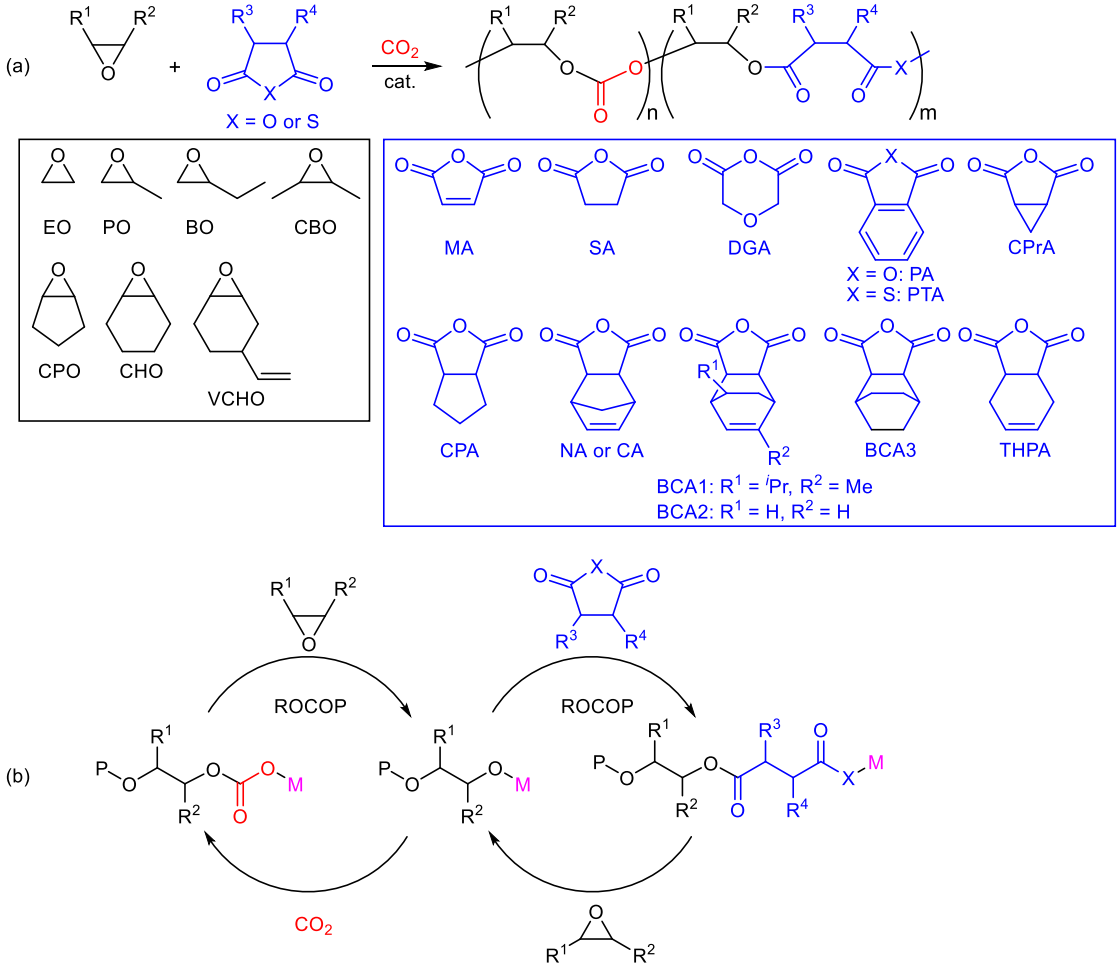

Scheme 3. (a) Representative reactions and (b) catalytic cycles.

In 2006, Huang and co-workers reported the terpolymerization of propylene oxide (PO), CO_2, and maleic anhydride (MA) by using polymer-supported bimetallic complex (PBM) **1** as a catalyst.[5a] The viscosity, grass transition temperature (T_g), and decomposition temperature of the terpolymers were much higher than those of poly(propylene carbonate) (PPC). The terpolymers also had higher degradability than PPC, and their degradation rates increased with increasing the content of MA in the terpolymers.

In 2008, Coates and co-workers developed an excellent homogeneous catalytic system using β-diiminate (BDI) zinc complex **2**, which enabled the first block terpolymerization of cyclohexene oxide (CHO) or vinyl cyclohexene oxide (VCHO), CO_2, and diglycolic anhydride (DGA) or succinic

anhydride (SA) under mild reaction conditions in a simple one-step procedure.[5b] This discovery led to the development of several other selective catalysts.

In the same year, Meng and co-workers found that zinc glutarate catalyst (s-ZnGA) **3** prepared from zinc oxide and glutaric acid was a versatile supported catalyst for the terpolymerization of PO, CO_2, and MA.[5c] The T_g values of the terpolymers increased with increasing the molecular weights. The decomposition temperatures of the terpolymers were enhanced in proportion to the MA content because the double bonds derived from MA readily underwent crosslinking at high temperature. Tensile tests also indicated that the mechanical properties of the terpolymers increased with increasing the molecular weight. The same group also reported the terpolymerization of PO, CO_2, and phthalic anhydride (PA) using zinc glutarate (ZnGA) **4**.[5g] In this system, CO_2 was much more reactive than PA. The introduction of a small amount of PA enhanced the thermal properties of the terpolymers. In 2015, they reported the terpolymerizations of PO, CO_2, and MA using zinc adipate (ZnAA) **5**, and the sulfonation of the resulting terpolymers afforded new biodegradable surfactants.[5j] The terpolymer with comparable hydrophilic and hydrophobic segments exhibited the best surface activity.

In 2010, Zhang and co-workers achieved the one-pot terpolymerization of CHO, CO_2, and MA to afford a poly(ester-carbonate) with a low content of the ether unit using heterogeneous Zn–Co^{III} double metal cyanide (DMC) catalyst **6**.[5d] THF used as a solvent dramatically inhibited polyether formation owing to the coordination of THF to the Zn center. Moreover, the polycarbonate chain containing a small amount of the polyester linkage showed slightly higher degradation temperature than the fully alternating polycarbonate.

In 2011, Duchateau and co-workers achieved the terpolymerization of CHO, CO_2, and cyclic acid anhydride using chromium tetraphenylporphyrin complex (Cr(TPP)Cl, **7**) or salophen complex (Cr(salophen)Cl, **8**) as a catalyst and 4-(*N,N*-dimethylamino)pyridine (DMAP) as a co-catalyst.[5e] SA, cyclopropane-1,2-dicarboxylic acid anhydride (CPrA), cyclopentane-1,2-dicarboxylic acid anhydride (CPA) or PA was used as an anhydride comonomer. Both **7** and **8** in combination with DMAP afforded perfect poly(ester-carbonate)s, and the presence of CO_2 suppressed the formation of the polyether linkage associated with the homopolymerization of CHO.

Darensbourg and co-workers studied the kinetics of the terpolymerization of CHO, CO_2, and PA using Cr(salen)Cl (**9**) as a catalyst and bis(triphenylphosphine)iminium chloride (PPNCl) as a co-catalyst to afford diblock copolymers with very little tapering.[5f] The polyester formation was much faster than the polycarbonate formation; in the latter case, the epoxide ring opening is much slower, and CO_2 insertion into the metal–alkoxide intermediate is highly reversible.

In 2014, Liu and co-workers performed the terpolymerization of PO, CO_2, and norbornene anhydride (NA) using Co(salen)NO_3 catalyst **10**.[5h] The reaction afforded diblock copolymers containing a reactive norbornyl ring, which could be applied to the thiol-ene click reaction. In the same year, Lee and co-workers reported Co(salen)NO_3 catalyst **11** tethering four quaternary ammonium salts, which showed a high activity of 2.2 kg-polymer/g-catalyst for the terpolymerization of PO, CO_2, and PA.[5i] The T_g value of the terpolymer was higher than that of the PO/CO_2 alternating copolymer (PPC) and lower than that of the PO/PA alternating copolymer.

In 2015, Williams and co-workers used dinuclear zinc complex catalyst **12** in the terpolymerization of CHO, CO_2, and PA. The polyester was initially produced selectively, and poly(cyclohexene carbonate) (PCHC) was then formed, delivering poly(ester-*b*-carbonate)s in a one-step manner.[5k] They also studied the block selective copolymerization from a mixture of CHO and PA under 1 atm CO_2 using dinuclear zinc catalyst **13** to obtain poly(ester-*b*-carbonate)s.[5l] DFT calculations indicated that PA insertion to CHO was more favorable than CO_2 insertion to CHO. In 2017, they also reported catalysts **13** and **14** for the terpolymerization of bio-derived anhydrides (BCA1–3), carbic anhydride (CA), or 1,2,3,6-tetrahydrophthalic anhydride (THPA).[5m] Both catalysts **13** and **14** showed excellent selectivity for ester linkages, and block copolymers were obtained from BCA1, CHO, and CO_2. Zn-based catalyst **13** initially catalyzed CHO/BCA1 polymerization, after which alternating CHO/CO_2 polymerization occurred to give poly(ester-*b*-carbonate)s. Interestingly, Mg-based catalyst **14** formed the polycarbonate block first, and after the removal of CO_2, CHO/BCA1 copolymerization proceeded to give poly(carbonate-*b*-ester)s. DSC analysis showed high T_g values, which could be further controlled by the carbonate/ester block ratio. In particular, materials with greater amounts of carbonate blocks (>70%) showed slightly lower T_g values, while those containing greater proportions of ester blocks (>60%) showed T_g values of up to 113 °C. In 2021, they found that different block structures are possible with the same types of dinuclear catalysts **13**–**15** by changing the metal combinations; $Zn^{II}Zn^{II}$ complex **13** yielded poly(ester-*b*-carbonate)s, $Mg^{II}Mg^{II}$ complex **14** or $Mg^{II}Co^{II}$ complex **15b** delivered poly(carbonate-*b*-ester)s, and $Mg^{II}Zn^{II}$ complex **15a** furnished random copolymers from mixtures of acid anhydride (PA or BCA1), CHO, and CO_2.[5p] The most active and selective catalyst, $Mg^{II}Co^{II}$ complex **15b**, gave precision triblock, pentablock, and heptablock polymers by changing the atmosphere of CO_2 or N_2 (1 bar). They also reported that a trinuclear $Zn^{II}Na^{I}Zn^{II}$ catalyst **16** catalyzed CHO/PA ROCOP, CHO/CO_2 ROCOP, and CHO ROP from mixtures of PA and CHO by using the gas atmosphere of CO_2 or N_2.[5q]

In 2018, Liu, Lu, and co-workers reported the one-pot terpolymerization of CHO, CO_2, and PA with the dinuclear chromium complex **17**. PA was consumed completely within 2 h to give the polyesters, and then the polymerization entered the second phase, leading to the formation of poly(ester-*b*-carbonate)s without the formation of the polyether unit.[5n] More recently, they reported the asymmetric terpolymerizations of *meso*-epoxides, CO_2, and PA, giving terpolymers with a random distribution of carbonate and ester units, which is different from that observed for tapered or gradient terpolymers, using chiral bimetallic aluminum complex **18**.[5v] Various epoxides such as *cis*-2,3-butene oxide (CBO), CHO, cyclopentene oxide (CPO) were reactive and terpolymerized enantioselectively with PA and CO_2 in up to 99% *ee*.

Plajer and coworkers reported the terpolymerization of epoxides, CO_2, and phthalic thioanhydride (PTA) forming random poly(ester-thioester-carbonates) by employing heterobimetallic Cr(III)-based catalysts (**19**) or **9**.[5x] These terpolymers degraded into oligomers under UV irradiation owing to the selective degradation of thioester linkages. They also conducted quaterpolymerization of CHO, CO_2, PTA, and PA, which showed that the terpolymerization of CHO, CO_2, and PA occurred until PA was consumed, followed by the terpolymerization of CHO, CO_2, and PTA.

Metal-free catalysts have also been developed since the discovery of the epoxides/CO_2 ROCOP with BEt_3 (**19**) and onium salts by Gnanou, Feng, and co-workers.[3a] In 2021, Xiao, Meng, and co-workers reported the terpolymerization of PO, CO_2, and PA using **20** and PPNCl.[5r] A random poly(ester-carbonate) segment forms first, and a long PPC-enriched segment was given after the consumption of PA. The terpolymers with 43 mol% aromatic polyester moieties displayed T_g that was about 9 °C higher than that of commercial PPC and a tensile strength of 37.6 MPa. The terpolymers also exhibited satisfactory degradation behaviors. They also reported the copolymerization of CHO, PO, PA, and CO_2 using **20**.[5o] Recently, Xiao, Meng, and co-workers reported that gradient terpolymers were successfully synthesized by the one-pot terpolymerization of ethylene oxides (EO), CO_2, and PA using **20** and tetrabutyl ammonium salt of *m*-phthalic acid (A-*m*PhA).[5u] TG analysis shows that the terpolymers have two fast decomposition stages, and the first weight loss peak corresponds to the decomposition of poly(ethylene carbonate) (PEC) sequence, and the second weight loss peak belongs to the thermal degradation of PA/EO polyester. The terpolymers possess better thermal stabilities than pure PEC. Liu, Kang, Li, and co-workers achieved both ROCOP of epoxide/CO_2 and ROCOP of epoxide/anhydride using **20**.[5s] CHO/PA/CO_2 terpolymerization in a one-step manner gave diblock copolymers with very little tapering (gradient character). Furthermore, the sequential ROCOP of CHO/PA and ROCOP of CHO/CO_2 by changing the atmosphere from N_2 to CO_2 afforded well-defined diblock poly(ester-*b*-carbonate)s. Other epoxides including PO and 1,2-butylene oxide (BO) were also used to construct diblock poly(ester-*b*-carbonate)s. All materials showed one T_g values between the T_g values for the corresponding polyester and polycarbonate homopolymers. Liu, Zhong, Li, and co-workers also reported the chemoselective terpolymerization of CHO, CO_2, and PA using **20** and phosphazenes (C_3N_3-Py-P_3) as binary organocatalysts.[5w] The terpolymers with block, tapered, or random structures could be selectively synthesized by changing the molar ratio of C_3N_3-Py-P_3 to **20**. DFT calculations clarified the effect of the molar ratio of C_3N_3-Py-P_3 to **20** on the chemoselectivity. Gnanou, Feng, and co-workers also demonstrated the terpolymerization of PO or CHO, SA or PA, and CO_2 in the presence of **20** and PPNCl or tetrabutylammonium azide (Bu_4NN_3).[5t] Only a single glass transition was observed for all the terpolymers, and the T_g value could be tuned by varying the ester contents.

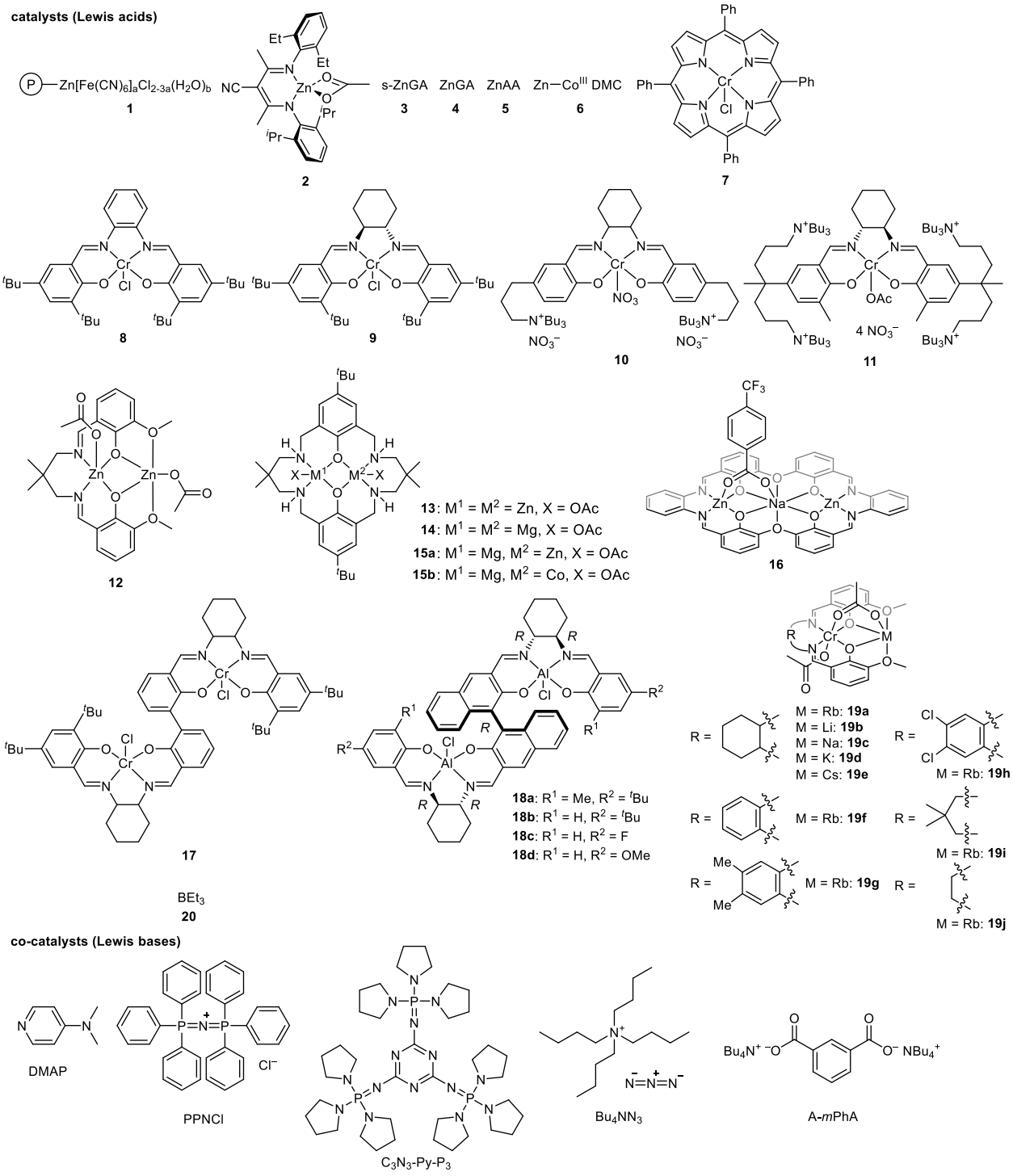

Figure 1. Catalysts and co-catalysts for the terpolymerization of epoxides, CO_2, and cyclic acid (thio)anhydrides.

Table 1. Terpolymerization of epoxides, CO_2, and cyclic acid (thio)anhydrides.

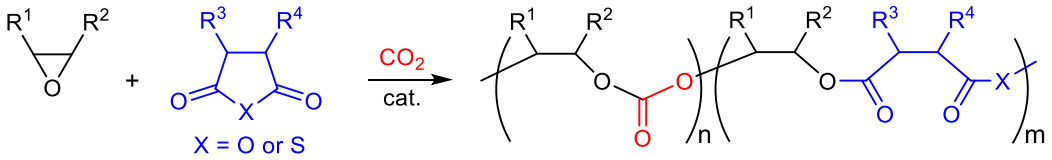

entry	epoxide	CO_2 (MPa)	anhydride	cat.	co-cat.	T (°C)	M_n (kg mol^{-1})[a]	ref
1	PO	3.5–4	MA	**1**	none	50–80	78.1	5a
2	CHO, VCHO	0.34–5.5	DGA, SA	**2**	none	50–55	37.0	5b
3	PO	5.2	MA	**3**	none	60	67.1	5c
4	PO	0.5–5.0	PA	**4**	none	75	221	5g
5	PO	2.5–5.0	MA	**5**	none	75	152	5j
6	CHO	1.0–4.0	MA	**6**	none	75–90	14.1	5d
7	CHO	5.0	SA, CPrA, CPA, PA	**7, 8**	DMAP	80	16	5e
8	CHO	3.4	PA	**9**	PPNCl	80	–	5f
9	PO	3.0	NA	**10**	none	60	94.4	5h
10	PO	3.5	PA	**11**	none	80	381	5i
11	CHO	3.0	PA	**12**	none	100	7.1	5k
12	CHO	0.10	PA	**13**	none	100	–	5l
13	CHO	0.10	BCA1–3, CA, THPA	**13**, **14**	none	100	11.8	5m
14	CHO	0.10–2.0	PA, BCA1	**13**, **14**, **15**	none	100	19.4	5p
15	CHO	0.10	PA	**16**	none	90–100	4.06	5q
16	CHO	1.0	PA	**17**	PPNCl	80	10.2	5n
17	CBO, CPO, CHO	0.5–2.0	PA	**18**	PPNCl	0–60	30.0	5v
18	CHO, BO	0.4	PTA	**19**, **9**	none, PPNCl	100	16.9	5x
19	PO	0.5–3.0	PA	**20**	PPNCl	60–100	58.3	5r
20	EO	1.0	PA	**20**	A-*m*PhA	40–45	273	5u
21	CHO, PO, BO	1.0	PA	**20**	PPNCl	80	29.8	5s
22	CHO	1.0	PA	**20**	C_3N_3-Py-P_3	80	15.5	5w
23	CHO, PO	1.0	SA, PA	**20**	Bu_4NN_3 or PPNCl	60–80	22.7	5t

[a] Maximum value.

1.4 Terpolymerization of epoxides, CO_2, and lactones

Polymers containing carbonate and ester linkages are also obtained by the terpolymerization of epoxides, CO_2, and lactones, where the ROCOP and ROP mechanisms are involved (Scheme 4a). This approach is accessible to the copolymers that cannot be synthesized by the terpolymerization of epoxides, CO_2, and cyclic acid anhydrides. The representative catalytic cycles, catalysts, and conditions for the terpolymerization of epoxides, CO_2, and lactones are shown in Scheme 4b, Figure 2, and Table 2, respectively.

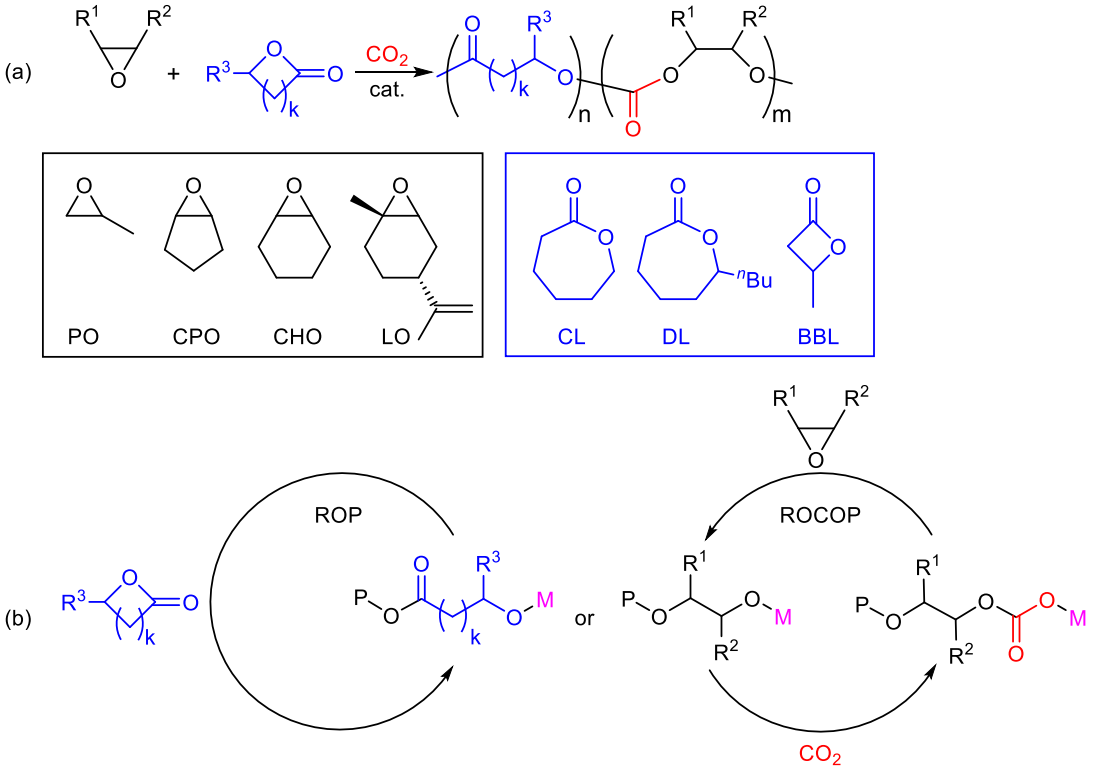

Scheme 4. (a) Representative reactions and (b) catalytic cycles.

In 2003, Ree and co-workers carried out the terpolymerization of PO, CO_2, and ε-caprolactone (CL) using zinc glutarate (ZnGA, **4**) as a catalyst, producing aliphatic carbonate-ester terpolymers with improved biodegradability.[6a,6b] All the terpolymers showed a single T_m, which originated from the CL blocks, and only a single T_g, which originated from the PC blocks. The terpolymers also underwent enzymatic degradation with a lipase in a phosphate buffer (pH 7.0) at 37 °C for 10 days. In 2006, Huang and co-workers reported the terpolymerization of PO, CO_2, and CL with PBM catalyst **1**.[6c] The introduction of CL increased the viscosity, glass transition temperature, and the degradation rate of the terpolymers.

In 2014, Williams and co-worker reported the selective synthesis of poly(cyclohexene carbonate-caprolactone)s from CHO, CL, and CO_2 using dizinc catalyst **13**, which also catalyzed epoxides/cyclic acid anhydrides/CO_2 ROCOP as mentioned above.[6d] This is the first example of a single catalyst that was not only active for two distinct polymerizations but also switched between them by the addition of exogeneous switch reagents, epoxide or CO_2. The catalytic mechanism was

studied by using both experiments and DFT calculations.[6h] They also reported the same terpolymerization with dizinc catalyst **21**, giving an ABA-type block polymer, poly(ester-*b*-carbonate-*b*-ester)s, in one pot from a mixture of the three monomers.[6e] The ROCOP of epoxides/CO_2 occurred first to produce polycarbonate polyols, and after removal of CO_2, the subsequent selective ROP of CL produced triblock copolymers. The copolymers showed controllable T_g values from –54 °C to 34 °C, which depended on the block compositions. In 2020, they reported one-pot switchable catalysis for the synthesis of PCHC-*b*-poly(decalactone) (PDL)-*b*-PCHC triblock polymers using heterodinuclear $Zn^{II}Mg^{II}$ catalyst **22**.[6k] These block copolymers showed not only good thermal stability, high toughness, and very high elongation at break, but also degradation behaviors upon gentle heating under acidic conditions.

In 2015, Xiao, Meng, and co-workers reported the terpolymerization of CHO, CO_2, and CL with Schiff base trizinc complexes **23**.[6f] In this terpolymerization system, CL was much more active than CHO, and the incorporation of CL dramatically improved the decomposition temperatures of the terpolymers. This is the first report on catalysts capable of synthesizing poly(carbonate-ester) in one step.

The highly efficient one-step terpolymerization of CHO, CO_2, and CL in the presence of zinc–cobalt double metal cyanide **6** and stannous octoate (**24**) was reported by Zhang and co-workers.[6g] CHO/CO_2 copolymerization catalyzed by **6** and ROP of CL catalyzed by **24** were combined to give multiblock copolymers, which was the first example of biodegradable polycarbonate-polyester blocks. The multiblock copolymers showed improved elongation as compared with PCHC and PCHC/poly(ε-caprolactone) (PCL) blend.

In 2017, Rieger and co-workers developed the terpolymerization of epoxides, CO_2, and (*rac*)-*β*-butyrolactone (BBL), which is less reactive than CL or lactide, utilizing complex **25**.[6i] The polymerizations could be regulated and switched between ROP of BBL and CHO/CO_2 ROCOP, and the following three terpolymerization procedures were established. The first procedure provided the block structures by ROP of BBL in the beginning followed by the addition of 40 bar CO_2 starting the epoxide/CO_2 ROCOP, and the second one was the reverse procedure of the epoxide/CO_2 ROCOP followed by the ROP of BBL. In the third procedure, lowering the CO_2 pressure to 3 bar allowed to give a random terpolymers composed of epoxides, CO_2, and BBL. Not only CHO and CPO but also the bio-based monomer, limonene oxide (LO), was successfully terpolymerized with CO_2 and BBL.[6j] Although the terpolymers with a block structure showed two T_g values because of the phase separation, only one T_g was observed for those with a random structure. As for mechanical behaviors, the Young's modulus for each of the block and the random structures was smaller than that of PCHC due to the incorporation of soft poly(3-hydroxybutyrate) segments.

Recently, Pang and co-workers developed AB-type diblock copolymers or ABA-type triblock copolymers by the terpolymerization of CHO, CO_2, and CL using Mn salen catalyst **26**.[6l] In this catalyst system, cyclic acid anhydrides were also used as comonomers, and the one-step switchable copolymerization of different anhydrides, epoxides, CO_2, and CL from the mixture delivered precise block copolymers. They also reported a facile method for the synthesis of gradient poly(carbonate-

ester), PCHC-*g*-PCL, from monomer mixtures of CHO, CO_2, and CL with Cr complex **27**.[6m] Compared with Cr(salen)Cl complex, this catalyst had an exceptional ability to synthesize biodegradable terpolymers with gradient character. The polymerization initially produced a PCHC segment, which was then transformed to a PCL-enriched segment by a cross-propagation reaction, and the chain configurations could be modulated by adjusting reaction conditions. When the proportion of PCL chains in the terpolymers was increased, a melting peak appeared, and the degradation temperature increased.

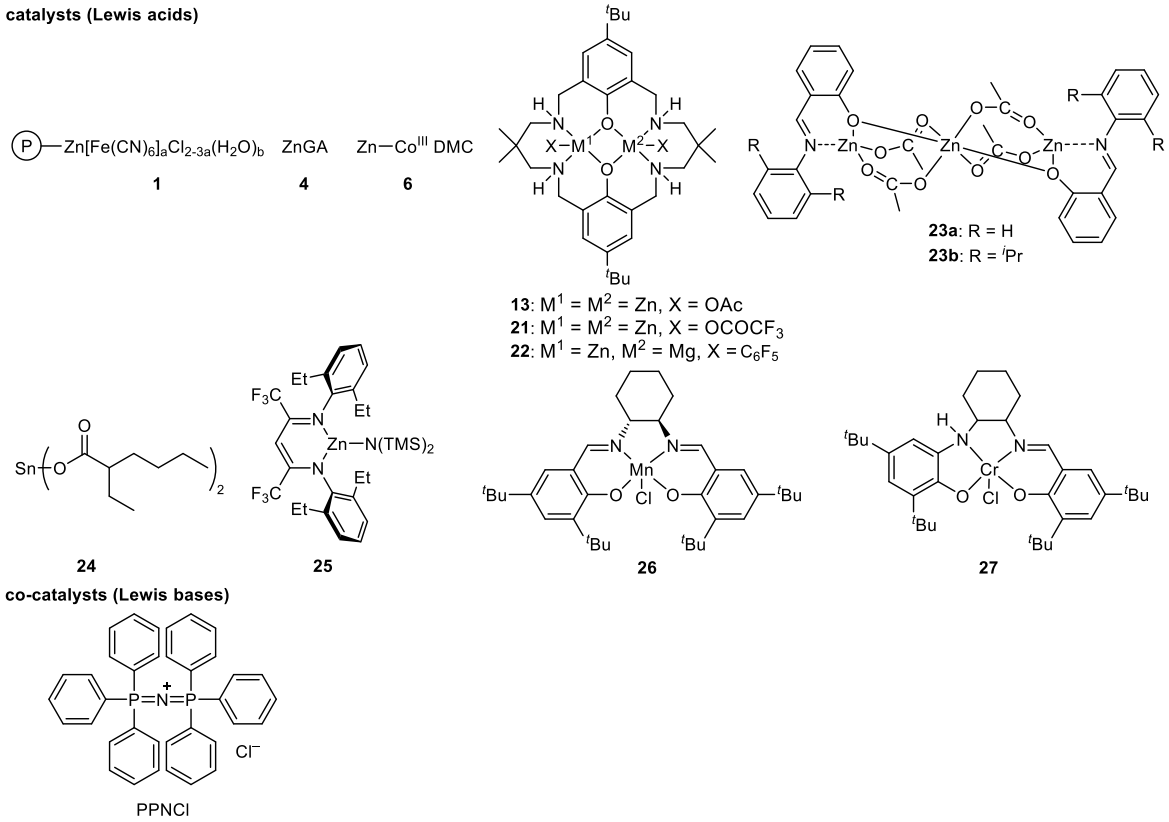

Figure 2. Catalysts and co-catalysts for the terpolymerization of epoxides, CO_2, and lactones.

Table 2. Terpolymerization of epoxides, CO_2, and lactones.

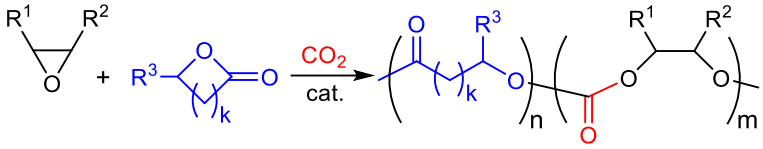

entry	epoxide	CO_2 (MPa)	lactone	cat.	co-cat.	*T* (°C)	M_n (kg mol^{-1})[a]	ref
1	PO	2.8	CL	**4**	none	60	275	6a, 6b
2	PO	4.0	CL	**1**	none	50–90	73.6	6c
3	CHO	0.10	CL	**13**	none	80	4.81	6d
4	CHO	0.10	CL	**21**	none	80	13.8	6e
5	CHO	2.0	DL	**22**	none	80	71.9	6k
6	CHO	5.0	CL	**23**	none	70–100	234.3	6f
7	CHO	4.0	CL	**6**, **24**	none	100	35.2	6g
8	CHO, CPO	0.1–5.0	BBL	**25**	none	50–60	174	6i
9	CHO, CPO, LO	0.3–4.0	BBL	**25**	none	40–60	233	6j
10	CHO	1.5	CL	**26**	PPNCl	80	41.8	6l
11	CHO	1.0–4.0	CL	**27**	PPNCl	60–100	67.1	6m

[a] Maximum value.

1.5 Terpolymerization of epoxides, CO_2, and lactides

Polylactide (PLA), which can be derived from renewable resources, has a T_g of 60 °C, high crystallinity, and biodegradability although brittleness restricts potential applicability. Therefore, poly(carbonate-ester)s synthesized by the terpolymerization of epoxides, CO_2, and lactides (Scheme 5a) may have excellent properties originating from both PLA and polycarbonate. The representative catalytic cycles, catalysts, and conditions for the terpolymerization of epoxides, CO_2, and lactones are shown in Scheme 5b, Figure 3, and Table 3, respectively.

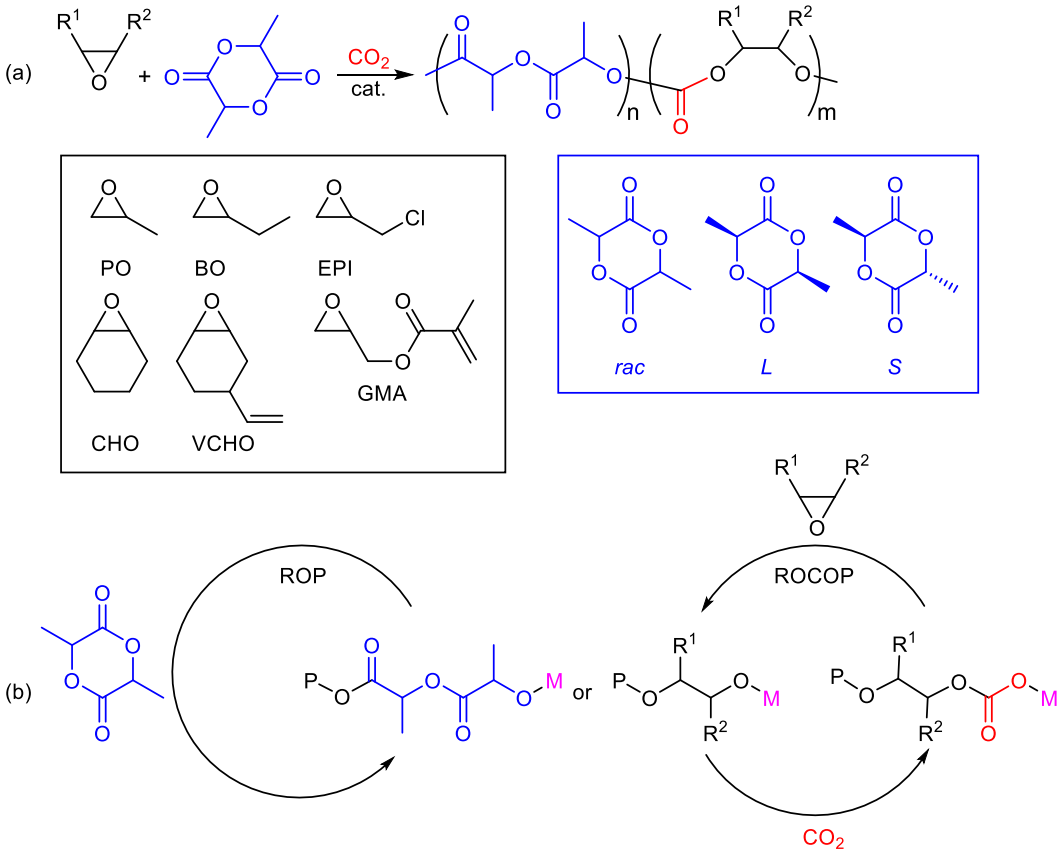

Scheme 5. (a) Representative reactions and (b) catalytic cycles.

In 2006, Kröger, Döring, and co-workers reported the first example of the terpolymerization of CHO, CO_2, and lactides with zinc complexes **28**, giving poly(cyclohexene carbonate–lactide), whose composition was adjusted by monomer feeding.[7a] The T_g values of the terpolymers fell between those for pure PLA and pure PCHC and increased with increasing the PCHC content, which indicates that the terpolymers have the random structures.

In 2011, Liu and co-workers synthesized terpolymers from PO, CO_2, and *rac*-lactides by using PBM **1**.[7b] The terpolymers showed higher degradability in Tris buffer (pH 7.4) over 10 weeks than PPC.

In 2012, Wang and co-workers conducted that the one-pot terpolymerization of PO, CO_2, and *L*-lactide using $Y(CCl_3CO_2)_3$-$ZnEt_2$-glycerin ternary catalyst **29** in short polymerization time.[7c] The thermal decomposition temperature increased by 32 °C relative to pure PPC. The elongation at break reached 40.5%, which is three times larger than that of pure PPC.

In 2015, Wang, Meng, and coworkers reported the one-step synthesis of carbonate-ester terpolymers with a long *L*-lactide-rich sequence via the terpolymerization of PO, CO_2, and *L*-lactide using ZnAA **5**.[7e] The thermal stability of the terpolymers was greatly improved; the thermal decomposition temperature was improved from 257.3 °C to 302.1 °C. This is because the activation energy of PLA decomposition (280 kJ/mol) is much higher than that of PPC decomposition (80 kJ/mol). Regarding the mechanical properties, all terpolymers exhibited higher tensile strengths than PPC; the tensile strength increased from 27.1 to 49.5 MPa with increasing the PLA content because of the increase in crystalline domains. The same catalyst system was also reported by Sakharov and co-workers.[7d]

In 2018, the one-pot regioselective and stereoselective terpolymerization of PO, CO_2, and *rac*-lactide was reported by Xie and co-workers.[7f] Interestingly, M(TPP)Cl **7** or **30** with PPNCl catalyzed the stereoselective polymerization to produce isotactic-enriched PLA despite the use of achiral catalyst and racemic starting materials. They also reported the one-step terpolymerization of 4-vinyl-1-cyclohexene-1,2-epoxide (VCHO), CO_2, and *rac*-lactide by using **30b**.[7k]

Pang, Chen, and co-workers developed a switchable system with **31a** and DBU (1,8-diazabicyclo[5.4.0]undec-7-ene) to achieve chemoselective block copolymerization between lactide ROP and PO/CO_2 ROCOP in one pot.[7g] This catalyst system is based on the reversible adsorption of CO_2 to DBU and the chain shuttling polymerization using *i*-PrOH as a chain shuttling reagent. Pang and co-workers also devised a new ternary catalyst system comprising Co^{II}(salen) (**31b**, **c**, **32a**), Co^{III}(salen) (**31d**, **e**, **32b**), and PPNCl, giving 100% poly(ester-carbonate) with no polyether structures from a mixture of PO, CO_2, and *L*-lactide.[7h] The resultant polymers were biodegradable and had T_g values that were tunable between 38 and 52 °C, which contrasts with PPC having a T_g value of 35–40 °C. The mechanistic investigation revealed that Co^{III}(salen) and Co^{II}(salen) catalyzed PO/CO_2 ROCOP and lactide ROP, respectively, and the combined polymers were formed via chain transfer. Styrene oxide (SO) and CHO were also reactive in this copolymerization. They also developed trinuclear Co^{III}(salen) complex **33** for the terpolymerization of PO, CO_2, and lactides without any nucleophilic co-catalyst to produce multiblock copolymers.[7i] Although only polycarbonates were obtained when epoxides, CO_2, and lactides were mixed using Co^{III}(salen) catalyst with a co-catalyst, **33** could catalyze the lactide ROP and PO/CO_2 ROCOP separately without co-catalysts to give the terpolymers. Recently, Pang, Chen, and co-workers developed an electrochemically controlled switchable copolymerization system with **34** for the synthesis of multi-block copolymers.[7n] In this system, the ROP of lactide proceeded, and the ROCOP of epoxide and CO_2 did not occur when the heteronuclear catalysts were in a reduced state. In contrast, the ROCOP of epoxide and CO_2 proceeded, and ROP of lactide did not occur after the electro-oxidation of the catalyst.

Pang, Deng, and co-workers reported a heterogeneous ternary catalyst system composed of **32b**, **4**, and PPNCl for the terpolymerization of epoxides, CO_2, and *L*-lactide.[7l] Co^{III}(salen) could not catalyze the ROCOP of PO/CO_2 and the ROP of lactide simultaneously owing to the strong coordination of CO_2, preventing the ROP of lactide. ZnGA **4** was also inactive for the ROP of lactide. The intermolecular cooperation between cobalt and zinc realized this terpolymerization forming

multiblock copolymers with PLA and PPC blocks having the highest molecular weight. They also reported several types of homogeneous catalyst systems called ternary catalyst systems (TCSs); TCS I was composed of **32a**, **32b**, and PPNCl, while TCS III_a consisted of **32b**, **32c**, and PPNCl, and TCS III_b comprised **32c**, O_2 and PPNCl.[7m] Compared to TCS I, TCS III_a and TCS III_b showed higher activities and remained active even under a low catalyst loading.

In 2020, Lin, Zhu, and co-workers reported Zn–Fe double metal cyanide (DMC) (**35**) and quaternary ammonium salt for the terpolymerization of PO, CO_2, and lactide.[7j] This catalyst system was synthesized from $ZnBr_2$ with $K_3Fe(CN)_6$ and quaternary ammonium salt via ball grinding, and Zn–Fe DMC with triethylmethylammonium chloride showed the highest activity.

Recently, Castro-Osma, Lara-Sánchez, and co-workers developed bimetallic indium complex **36** as a catalyst for the terpolymerization of CHO, CO_2, and *L*-lactide.[7o] The terpolymers were obtained with no co-catalyst, and the degree of the incorporation of CO_2 could be modulated by changing the CO_2 pressure and the amount of the monomer. The terpolymers exhibited single T_g values between those for pure PLA and pure PCHC, which suggested the formation of random copolymers, and T_g increased as the ratio of CHO to *L*-lactide increased. The terpolymer with the highest ratio of [CHO] to [*L*-lactide] showed good stability up to 244 °C because of the higher PCHC content.

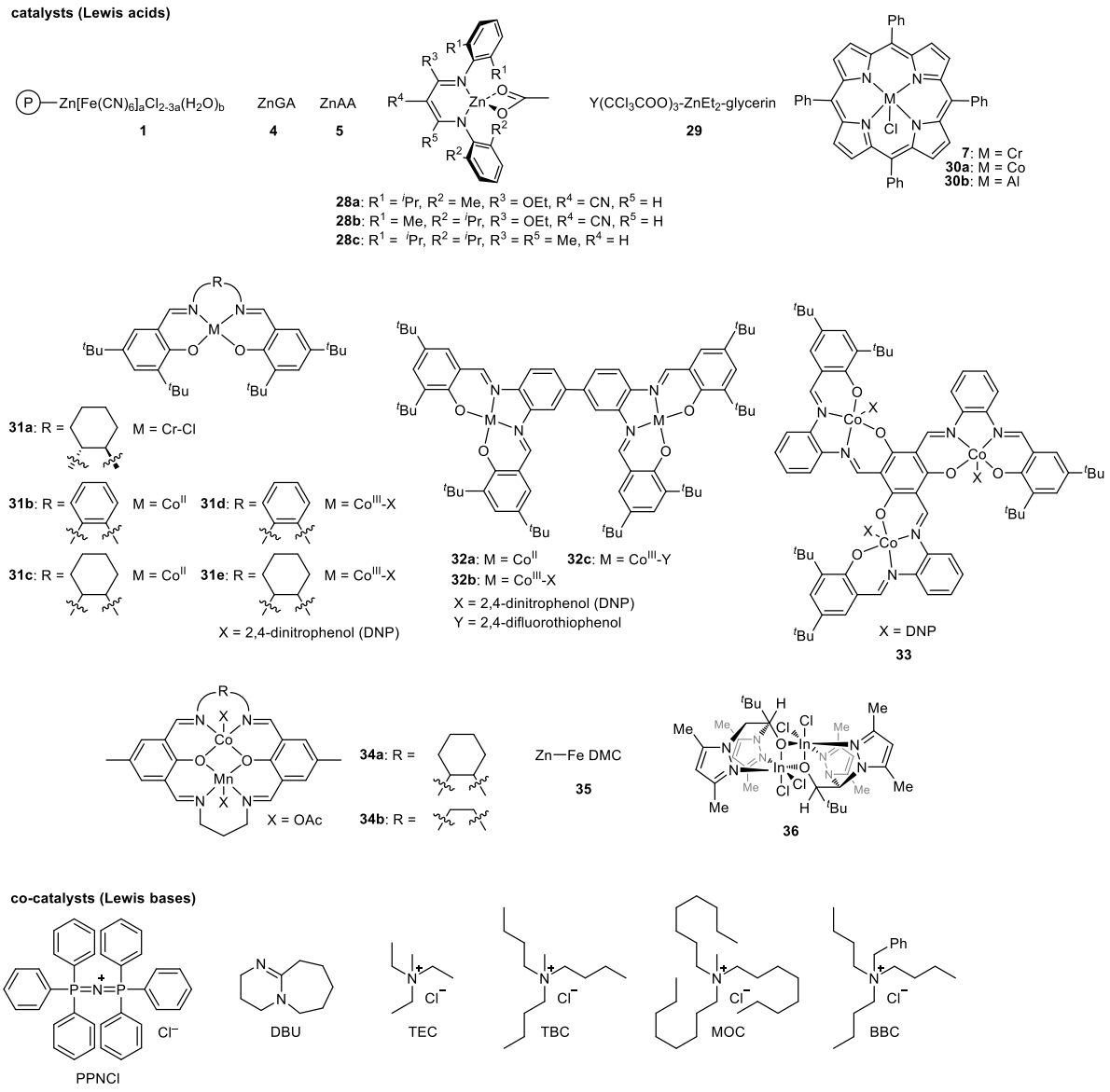

Figure 3. Catalysts and co-catalysts for the terpolymerization of epoxides, CO_2, and lactides.

Table 3. Terpolymerization of epoxides, CO_2, and lactides.

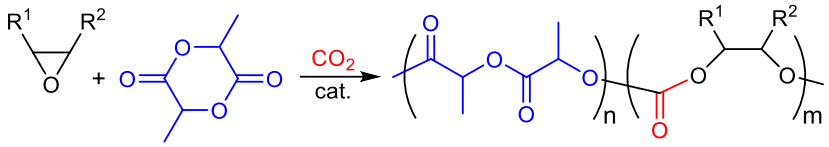

entry	epoxide	CO_2 (MPa)	lactide	cat.	co-cat.	*T* (°C)	M_n (kg mol^{-1})[a]	ref
1	CHO	4.0	*rac, S*	**28**	none	90	41.6	7a
2	PO	3.5	*rac*	**1**	none	70	24.5	7b
3	PO	4.0	*L*	**29**	none	60–80	154	7c
4	PO	5.0	*L*	**5**	none	60–90	132	7e
5	PO	CO_2 : PO = 1 : 1	*L*	**5**	none	70	68	7d
6	PO	0.1–4.0	*rac*	**7**, **30**	PPNCl	23–60	14.7	7f
7	VCHO	0.10–4.1	*rac*	**30b**	PPNCl	25–70	8.2	7k
8	PO	2.0	*L*	**31a**	DBU	rt, 40	7.15	7g
9	PO, SO, CHO	2.0	*L*	**31b–e** **32a, b**	PPNCl	60	13.6	7h
10	PO	3.0	*L*	**33**	none	25–60	15.3	7i
11	PO, EPI, GMA	1.0–4.0	*rac*	**34**	PPNCl	60	49.3	7n
12	PO, BO	0.20–2.0	*L*	**32b**, **4**	PPNCl	60	698	7l
13	PO, BO	0.20–2.0	*L*	**32**	PPNCl, O_2	60	28.7	7m
14	PO	3.5	*rac*	**35**	TEC, TBC, MOC, BBC	55	11.3	7j
15	CHO	0.5–4.0	*L*	**36**	none	60	9.1	7o

[a] Maximum value.

1.6 Terpolymerization of epoxides, CO_2, and heteroallenes

Heteroallenes such as CO_2, isocyanates, isothiocyanates, sulfur dioxide (SO_2), carbonyl sulfide (COS), and carbon disulfide (CS_2) are important reagents in organic chemistry. Epoxide/heteroallene ROCOP can introduce new linkages into the main chain of polymers, which may improve their thermal, mechanical, or optical properties (Scheme 6a). On the other hand, the terpolymerization of epoxides, CO_2, and other heteroallenes is challenging because of the large difference in reactivity between CO_2 and other heteroallenes.[8] Indeed, there are only a few reports on this type of terpolymerization to the best of our knowledge. The representative catalytic cycles, catalysts, and conditions for the terpolymerization of epoxides, CO_2, and heteroallenes are shown in Scheme 6b, Figure 4, and Table 4, respectively.

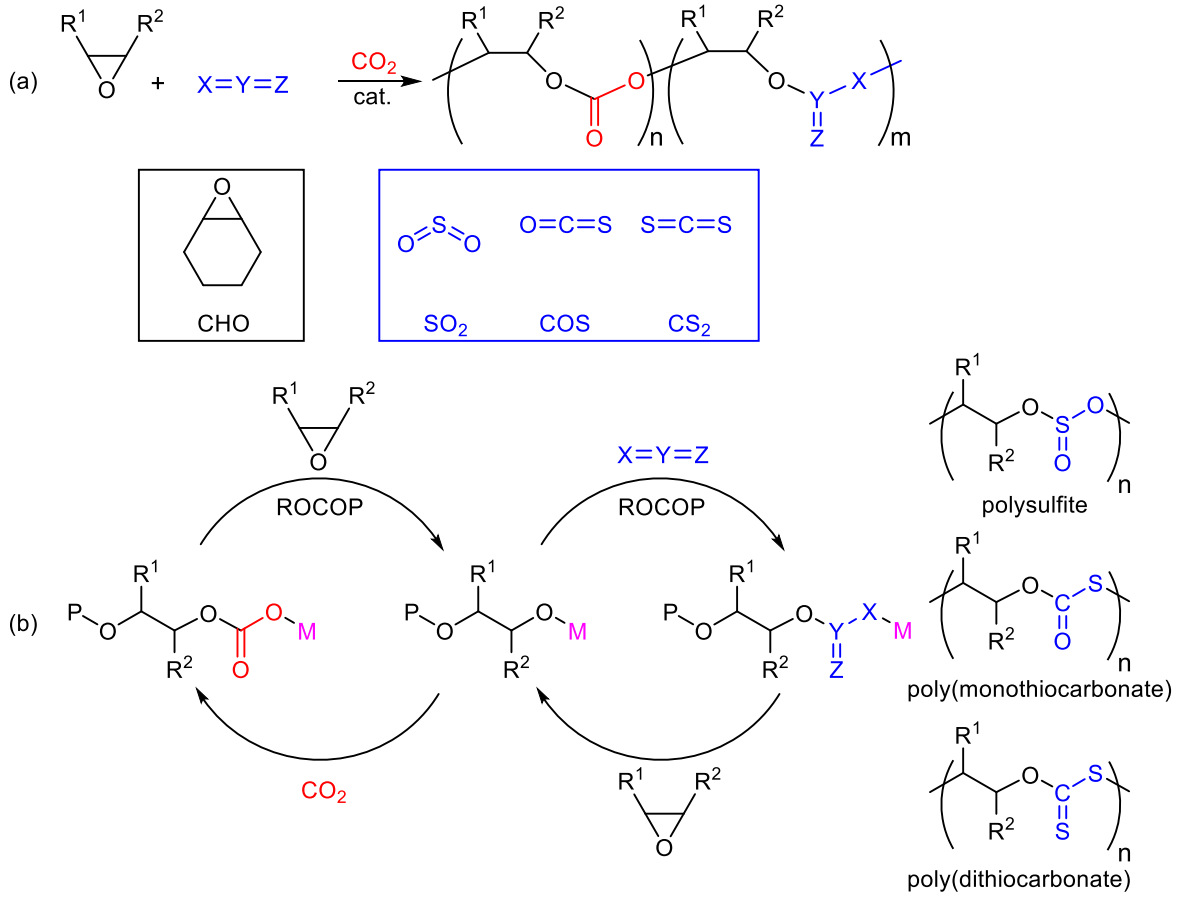

Scheme 6. (a) Representative reactions and (b) catalytic cycles.

Jia, Shan, and co-workers achieved the terpolymerization of epoxides, CO_2, and SO_2 using Co^{III}(salen)Cl **9** to synthesize poly(cyclohexene carbonate-cyclohexene sulfite)s.[9a] They found that no nucleophilic co-catalyst was necessary for the terpolymerization of CHO and SO_2 because SO_2 acted as a nucleophile as well as a reactant.

Ren, Darensbourg, and co-workers demonstrated the synthesis of terpolymers with tunable randomly distributed sulfur atoms from CHO, CO_2, and COS using **37** or **38** as a catalyst.[9b] By changing the CO_2 pressure, random polycarbonates with different COS contents in the terpolymers could be prepared, and the polymers showed good optical properties such as the Abbe number as high

as 48.6 and a refractive index of 1.501. The Abbe number of the random terpolymers was greater than those of either the blends of CHO/CO_2 and CHO/COS copolymers or the diblocked copolymers.

Neale, Plajer, and coworkers reported the terpolymerization of CHO, CO_2, and CS_2 using heterobimetallic Cr(III)-based catalysts (**19a**).[9c] The terpolymers had similar T_gs and refractive indexes to those of PCHC. These terpolymers degraded into oligomers under aqueous H_2O_2 owing to the selective degradation of poly(dithiocarbonate) linkages.

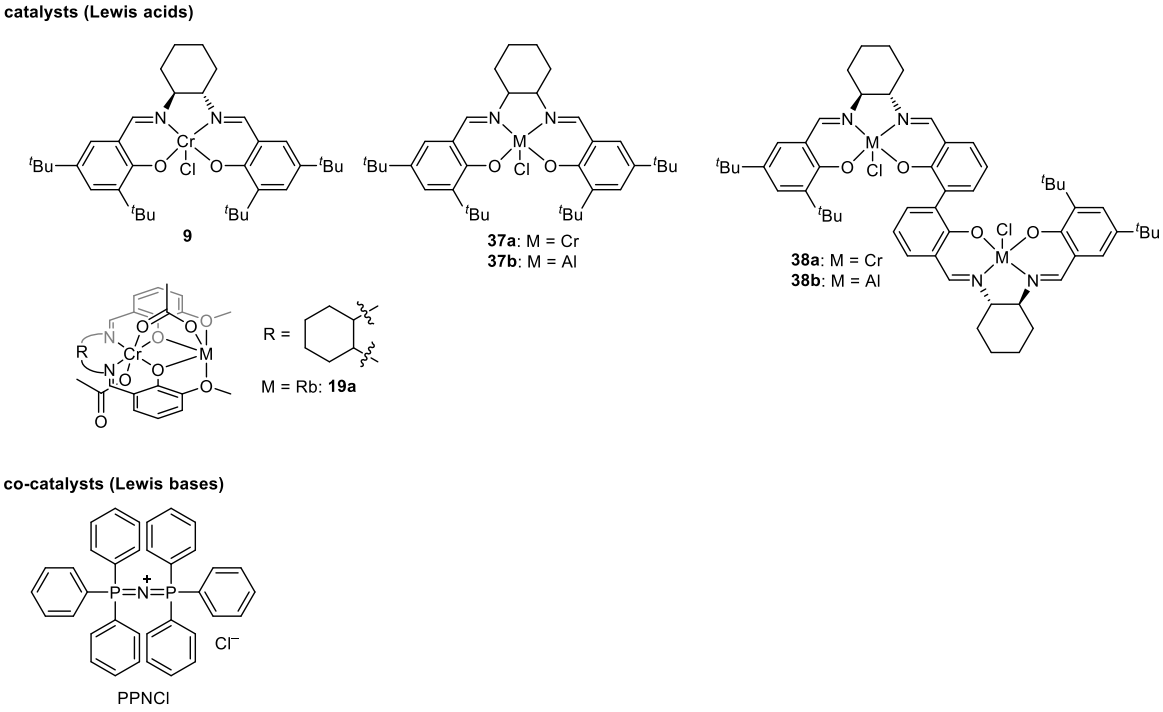

Figure 4. Catalysts and co-catalysts for the terpolymerization of epoxides, CO_2, and heteroallenes.

Table 4. Terpolymerization of epoxides, CO_2, and heteroallenes.

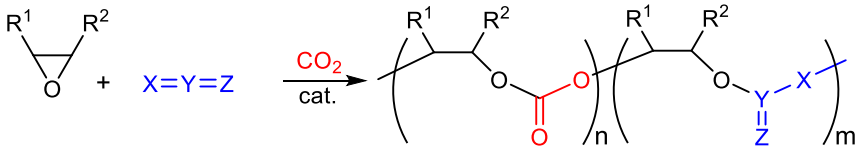

entry	epoxide	CO_2 (MPa)	heteroallene	cat.	co-cat.	T (°C)	M_n (kg mol^{-1})[a]	ref
1	CHO	SO_2 : CO_2 = 1 : 4–1 : 16	SO_2	**9**	none, PPNCl	40–90	9.99	9a
2	CHO	0.6–3.0	COS	**37**, **38**	PPNCl	25–80	50.2	9b
3	CHO	0.4	CS_2	**19a**	none	100	12.7	9c

[a] Maximum value.

1.7 Reductive transformation of CO_2 into value-added chemicals

Considerable efforts have been devoted to the reduction of CO_2 to C1 chemicals such as formic acid, formaldehyde, methanol and methane.[1a,d,e] On the other hand, deoxygenative CO_2 conversions making C–H and C–C bonds remain unexplored although value-added chemicals, such as aldehydes,[11] alcohols,[12] alkenes,[13] and heterocyclic compounds, can be obtained.[14]

1.8 Reductive transformation of CO_2 to aldehydes

There are two main synthetic approaches to aldehydes from CO_2. One involves the generation of CO from CO_2 with hydrogen or hydrosilane followed by the formation of C–C and C–H bonds. The other involves the generation of silyl formates from CO_2 and hydrosilane, which is used to form C–C bonds. Transition metal catalysts or reagents are often used in both approaches (Scheme 7).

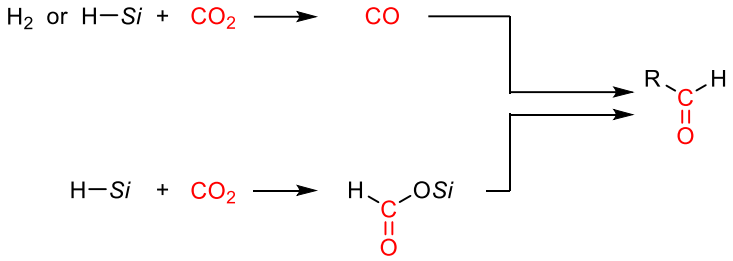

Scheme 7. Two approaches to aldehydes from CO_2.

In 2014, Liu and co-workers developed the first direct formylation of aromatic iodides to aryl aldehydes from CO_2 (1 MPa) and poly(methylhydrosiloxane) (PMHS) using Pd/C and DBU under mild conditions (Scheme 8).[11a] They also reported the first synthesis of aryl aldehydes by the formylation of aryl bromides with CO_2 and PMHS using 1,3-bis(diphenylphosphino)propane (dppp)-Pd catalyst, Pd(dppp)Cl_2, and DBU.[11b]

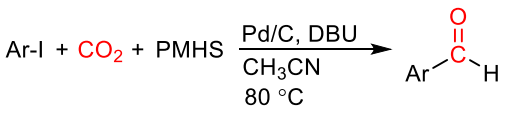

Scheme 8. Direct formylation of aryl iodides.

Milstein and co-workers achieved the photocarbonylation of benzene to give benzaldehyde in 2016 (Scheme 9).[11c] Rhodium hydride PNP (2,6-bis(di-*tert*-butylphosphinomethyl)pyridine) pincer complex effected the reductive cleavage of CO_2, and the photocarbonylation of benzene took place on the resultant rhodium–carbonyl complex, (PNP)RhCO, under UV irradiation. Finally, *p*-toluenesulfonic acid (TsOH) promoted the release of benzaldehyde from the Rh complex.

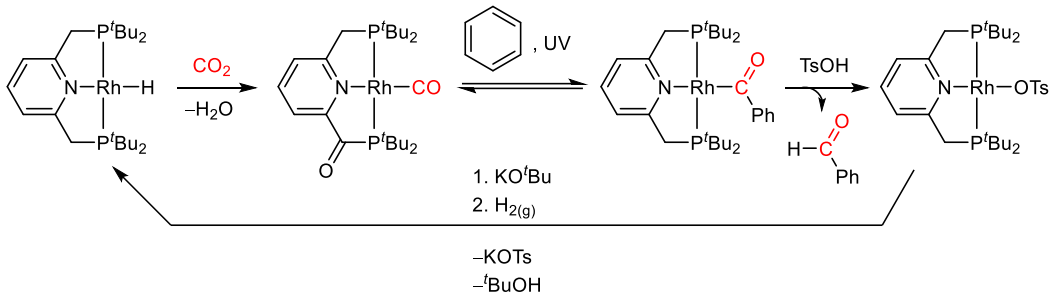

Scheme 9. Stepwise synthesis of benzaldehyde from benzene and CO_2.

In 2017, Xia, Ding, and co-workers reported the rhodium-catalyzed hydroformylation of olefins with CO_2, hydrosilane, and H_2 (Scheme 10).[11d] CO was generated *in situ* by CO_2 reduction with PMHS, and conventional rhodium-catalyzed hydroformylation with CO/H_2 proceeded. This is the first synthesis of aldehydes from alkenes and CO_2.

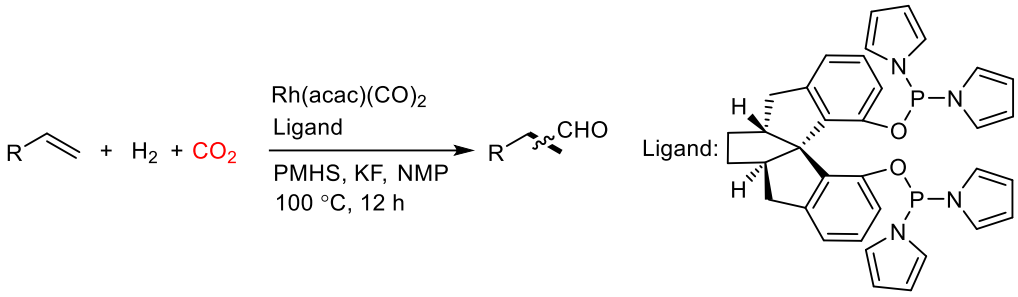

Scheme 10. Rhodium-catalyzed hydroformylation of olefins with CO_2 and hydrosilane.

In 2018, Liu and co-workers developed the reductive formylation of aryl halides to give aryl aldehydes using CO_2/H_2 for the first time (Scheme 11).[11e] RhI_3/PPh_3 and Ac_2O reacted with HCO_2H generated *in situ* to give CO and CH_3CO_2H, and aryl aldehydes were produced in good to excellent yields via oxidative addition and CO insertion followed by reductive elimination.

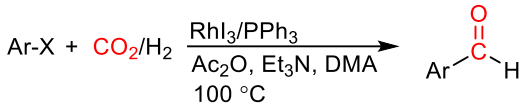

Scheme 11. Rhodium-catalyzed formylation of aryl halides with CO_2 and H_2.

In 2020, Hasegawa, Ema, and co-workers found that tetrabutylammonium acetate (TBAA) worked as a catalyst for both the hydrosilylation of CO_2 (1 atm) and the *N*-formylation of amines with hydrosilane to give various formamides including Weinreb formamide, Me(MeO)NCHO (Scheme 12).[11f] Taking advantage of solvent-free conditions, Weinreb formamide was successively converted into aldehydes by one-pot treatment with Grignard reagents.

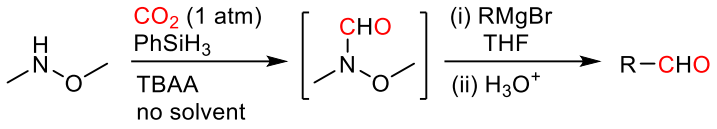

Scheme 12. Synthesis of formamides and aldehydes via the solvent-free hydrosilylation of CO_2.

1.9 Reductive transformation of CO_2 to alcohols

The synthesis of alcohols from CO_2 can be achieved by copper catalysts in combination with hydrosilanes. The reaction of copper catalysts with hydrosilanes generates copper hydrides, and the addition of copper hydrides to double or triple bonds gives organocopper intermediates, which react with CO_2 to form copper carboxylates. The hydrosilanes further reduce the copper carboxylates to copper alkoxides. Further reaction of the copper alkoxide with hydrosilane gives silyl ether, regenerating the copper hydride (Scheme 13).

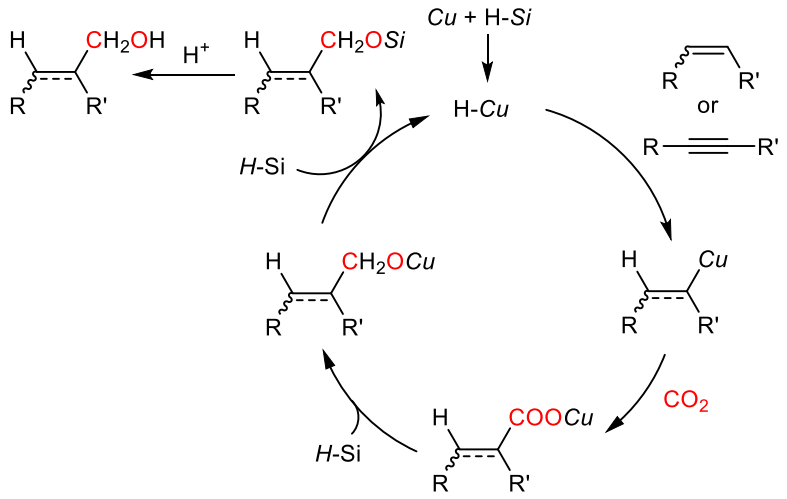

Scheme 13. Possible reaction mechanism.

In 2015, Fujihara, Tsuji, and co-workers reported the first example of the transformation of CO_2 to alcohol with concomitant C–C bond formation (Scheme 14).[12a] By employing a copper/4,5-bis(bis(3,5-dimethylphenyl)phosphino)-9,9-dimethylxanthene catalyst system and $Me(OMe)_2SiH$, various allenes reacted with CO_2 regioselectively to give homoallylic alcohols.

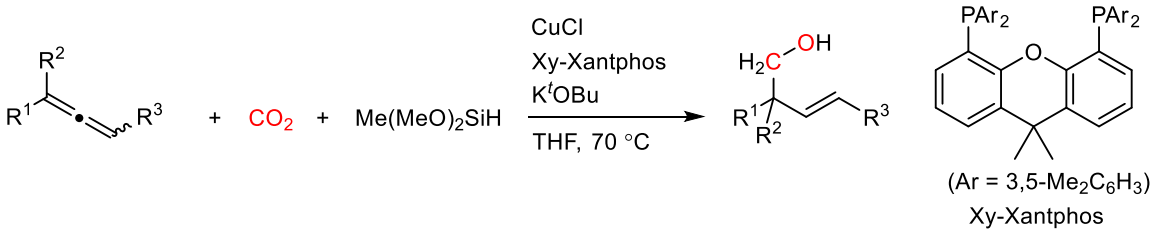

Scheme 14. Copper-catalyzed transformation of CO_2 to alcohols.

Lan, Yu, and co-workers developed the asymmetric Cu-catalyzed reductive hydroxymethylation of 1,1-disubstituted 1,3-dienes using CO_2 and $Me(OMe)_2SiH$ with high chemo-, regio-, *E*/*Z*-, and enantioselectivities (Scheme 15).[12b] This method can provide chiral all-carbon quaternary

stereocenters.

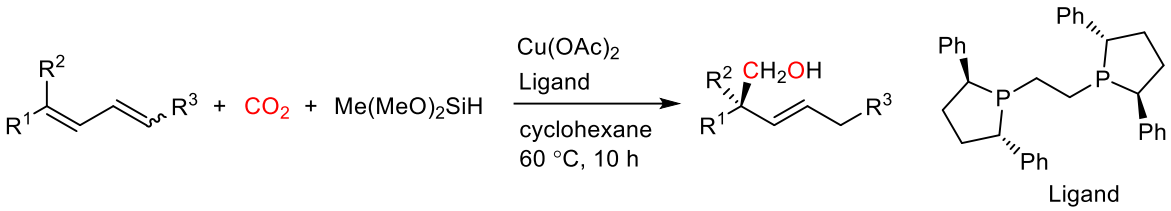

Scheme 15. Asymmetric Cu-catalyzed hydroxymethylation of dienes.

He, Ma, and co-workers studied the copper-catalyzed and proton-directed selective hydroxymethylation of alkynes with CO_2 and $(EtO)_3SiH$ (Scheme 16).[12d] With the protonation strategy, direct alkyne hydroxymethylation and reductive hydroxymethylation can be performed selectively, giving a series of allylic alcohols and homobenzylic alcohols, respectively.

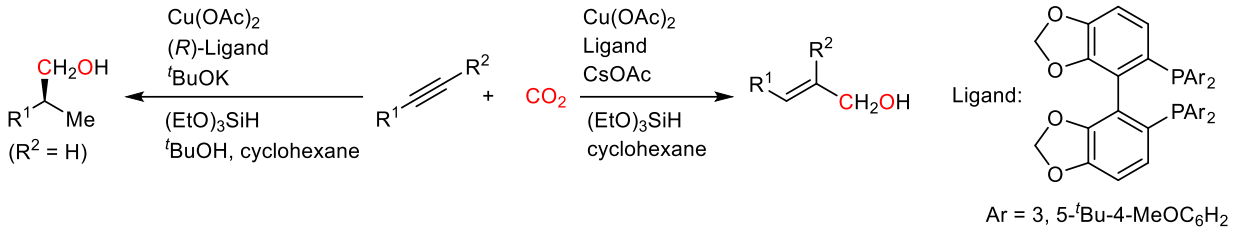

Scheme 16. Copper-catalyzed and proton-directed selective hydroxymethylation of alkynes.

Tian, Shen, He, and co-workers have reported the synthesis of alcohols from CO_2 involving the reductive hydroformylation of alkenes using heterobimetallic ruthenium–cobalt catalyst (Scheme 17).[12c] The acid-promoted reverse water-gas shift (RWGS) of CO_2 and H_2 was catalyzed by the ruthenium catalyst to generate CO, and the hydroformylation of alkenes and the reduction of the resulting aldehydes were mediated by the cobalt and ruthenium catalyst, respectively.

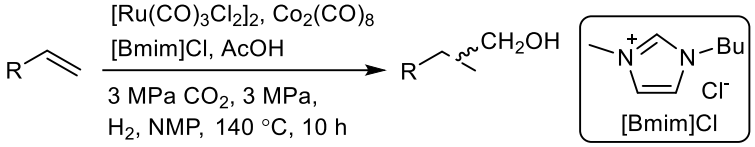

Scheme 17 Synthesis of alcohols via reductive hydroformylation of alkenes.

Bontemps and co-workers studied the selective dimerization of CO_2 into glycolaldehyde in a one-pot two-step manner for the first time (Scheme 18).[12e] In the first step, the reduction of CO_2 with 9-BBN catalyzed by $Fe(H)_2(dmpe)_2$ gave formaldehyde via the controlled hydrolysis of bis(boryl)acetal compound. In the second step, the NHC-catalyzed C–C bond formation delivered glycoaldehyde.

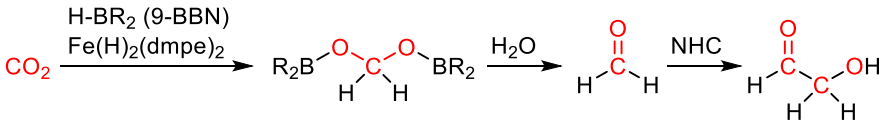

Scheme 18. Selective dimerization of CO_2 into glycolaldehyde.

Bontemps and co-workers reported the synthesis of a borylated C_3-carbohydrate from CO_2 for the first time (Scheme 19).[12f] $[Fe(H)_2(dmpe)_2]$ catalyzes the selective reduction of CO_2 into bis(boryl)acetal followed by a one-pot carbene-mediated C–C coupling reaction. According to the DFT calculations, an S_N2-type reaction between bis(boryl)acetal and carbene followed by the release of boronic acid gives the *O*-borylated Breslow (OBB) intermediate. This intermediate plays an important role in the C−C coupling reactions.

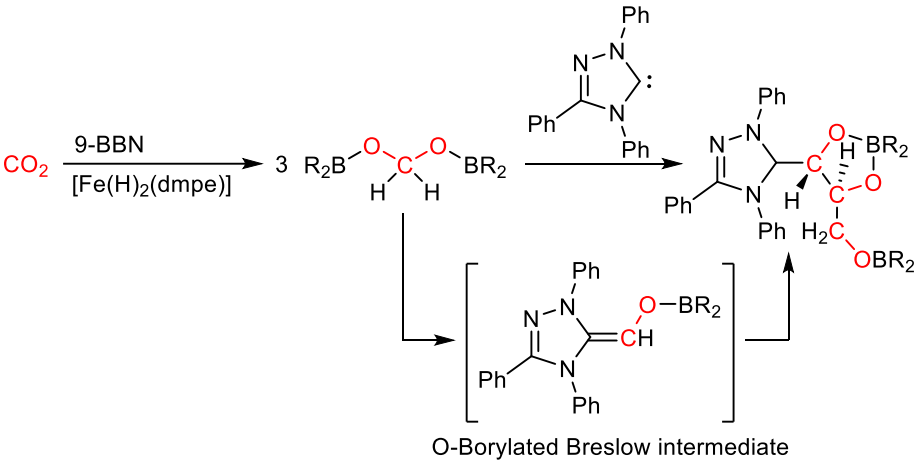

Scheme 19. Synthesis of a borylated C_3-carbohydrate from CO_2.

1.10 Reductive transformation of CO_2 to olefins

Olefins were synthesized from CO_2 through the reactions of bis(silyl)acetals or bis(boryl)acetals, generated from CO_2 and hydrosilanes or hydroboranes, with phosphorus ylides (Scheme 20).

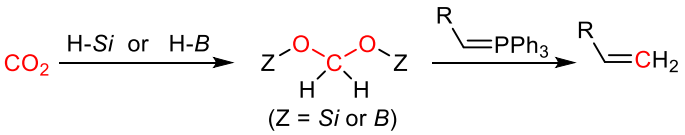

Scheme 20. Olefin synthesis from CO_2 via bis(silyl)acetals or bis(boryl)acetals.

In 2015, Sabo-Etienne, Bontemps, and co-workers achieved the iron-catalyzed selective reduction of CO_2 to bis(boryl)acetals using 9-BBN, and the subsequent Wittig reaction gave styrenes (Scheme 21).[13a]

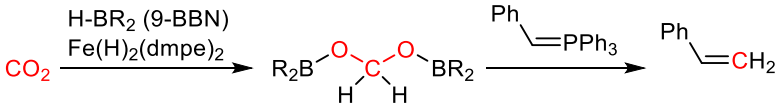

Scheme 21. Iron-catalyzed reduction of CO_2 and the synthesis of styrene.

In 2018, Xia and co-workers developed the first transition-metal-free reductive olefination reaction via bis(silyl)acetals (Scheme 22).[13b] First, the reduction of CO_2 with PMHS produces bis(silyl)acetal in the presence of a catalytic amount of NaO^{t}Bu. The nucleophilic addition of phosphorus ylides to bis(silyl)acetals affords alkene products, which are *β*-unsubstituted acrylates or vinyl ketones.

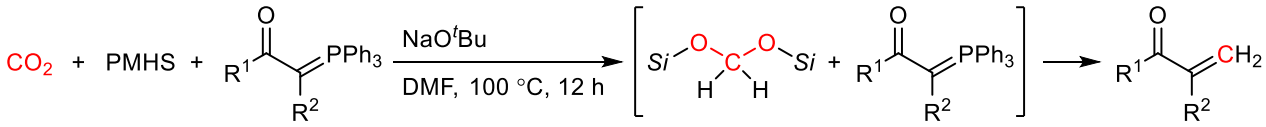

Scheme 22. Transition-metal-free synthesis of olefins with CO_2.

In 2019, Parkin and co-workers achieved the selective reduction of CO_2 to bis(silyl)acetals using $PhSiH_3$ and a [Tism$^{i\text{-PrBenz}}$]MgX/$B(C_6F_5)_3$ catalytic system (Tism$^{i\text{-PrBenz}}$ = tris[(1-isopropylbenzimidazol-2-yl)dimethylsilyl]methyl ligand) followed by the reaction with $MeOC(O)C(H)PPh_3$ or $PhCH_2OC(O)C(H)PPh_3$ in the presence of CsF to afford methyl acrylate or benzyl acrylate, respectively (Scheme 23).[13c] The treatment of the bis(silyl)acetals with CsF generates formaldehyde, which reacts with phosphonium ylides to give olefins.

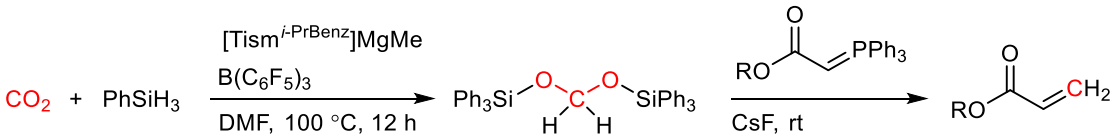

Scheme 23. Selective reduction of CO_2 to bis(silyl)acetals followed by transformation to olefins.

1.11 Reductive transformation of CO_2 to heterocyclic compounds

There are several reports on the synthesis of heterocyclic compounds involving the C−H and C−C bond formation with CO_2, and representative examples are shown below. In 2017, Xia and co-workers reported a metal-free reductive tandem C−C and C−N bond-forming reaction with CO_2 and $PhSiH_3$ to synthesize spiro-indolepyrrolidines (Scheme 24).[14b] The TBD catalyst facilitates the reaction of CO_2 with $PhSiH_3$, leading to the formation of bis(silyl)acetals, which react with the amino group of the substrate and undergoes cyclization via the nucleophilic addition of the indole ring.

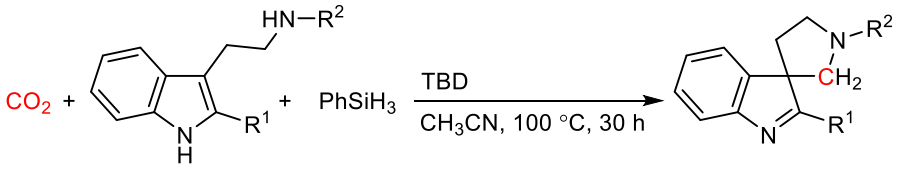

Scheme 24. Synthesis of spiro-indolepyrrolidines from CO_2.

In 2020, Zhao and co-workers developed a new reductive tandem C_{sp2}–C_{sp3} bond-forming reaction using CO_2, $PhSiH_3$, and enaminones catalyzed by a combination of TBD and $ZnCl_2$ (Scheme 25).[14c] ^{n}BuNH$_2$ significantly promoted this deoxymethylenation partly because CO_2 reacts with the primary amine to form carbamic acid, essentially increasing the effective concentration of CO_2 in the solution.

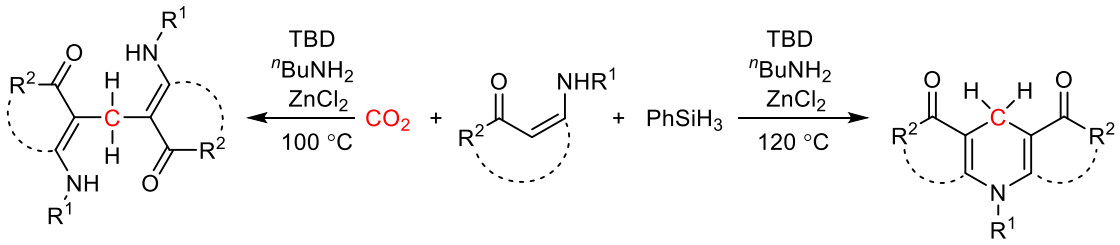

Scheme 25. The bridging of enaminones and the synthesis of 1,4-dihydropyridines from CO_2.

Zhao, Yan, You, Jiang, and co-workers reported the one-pot methylenation−cyclization of arylamines and enaminones with two molecules of CO_2 using the same catalyst system (Scheme 26).[14d] Control experiments and DFT calculations revealed that the TBD-catalyzed reduction of CO_2 with $PhSiH_3$ leads to the production of bis(silyl)acetal, which generates formaldehyde, and the condensation of aniline with formaldehyde gives imines, which then undergoes the aza-Diels−Alder reaction.

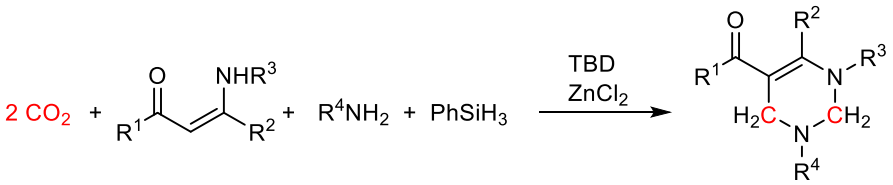

Scheme 26. One-pot methylenation–cyclization using two molecules of CO_2.

Zhao, You, and co-workers also reported the synthesis of fused-tetrahydropyridines from cyclic enamines, primary aromatic amines, and two molecules of CO_2 using Cs_2CO_3 and ZnI_2 as catalysts (Scheme 27).[14e] Bis(silyl)acetal is generated from the reaction of CO_2 with $PhSiH_3$ followed by the condensation of arylamines and the aza-Diels–Alder reaction.

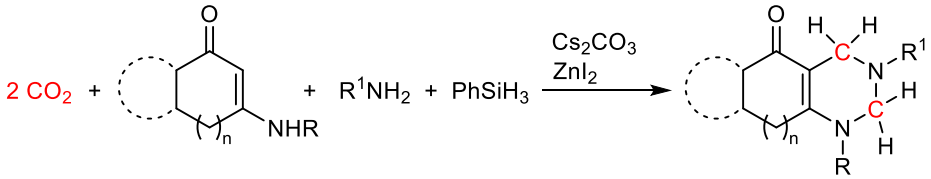

Scheme 27. The synthesis of fused-tetrahydropyrimidines from CO_2.

Takaishi, Ema, and co-workers reported the one-pot synthesis of dihydropyranes via CO_2 reduction and the domino Knoevenagel/oxa-Diels–Alder reactions (Scheme 28).[14g] The unique macrocyclic pentanuclear Zn^{II} catalyst could be prepared by the self-assembly of a binaphthyl−bipyridyl ligand and $Zn(OAc)_2{\cdot}2H_2O$. These reactions proceeded under mild conditions in the presence of only 0.07 mol% catalyst.

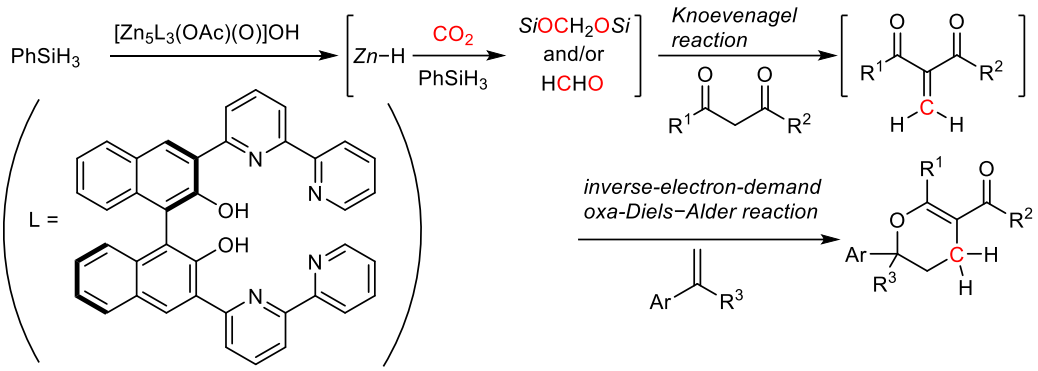

Scheme 28. Synthesis of dihydropyrans from CO_2.

Zhu, Xia, and co-workers developed the iron-catalyzed Pictet–Spengler-type cyclization with heteroarylethylamines using CO_2 (Scheme 29).[14f] Bis(silyl)acetal is formed from the reaction of CO_2 with $PhSiH_3$ in the presence of the Fe catalyst, and the reaction of typtamine with bis(silyl)acetal affords a hemiaminal intermediate via C–N bond formation and generates a silanol as a byproduct. The subsequent release of another silanol gives the iminium intermediate followed by the intramolecular nucleophilic addition of the indole moiety to give the spiroindoline intermediate. Finally, tetrahydro-β-carbolines are formed via the rearrangement of the spiroindolenine intermediate.

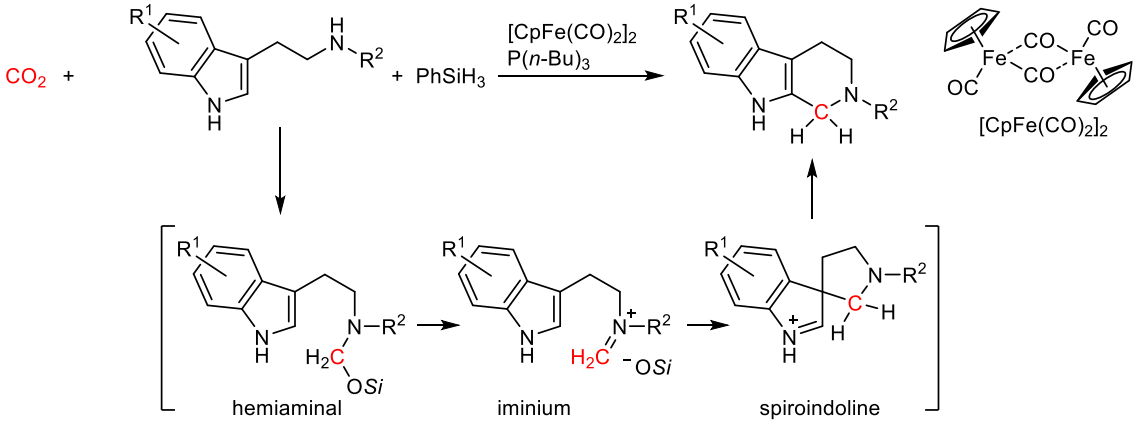

Scheme 29. Synthesis of tetrahydro-β-carbolines from CO_2.

Beller and co-workers reported the catalytic methylation of C–H bonds using CO_2 and H_2 in the presence of a ruthenium triphos catalyst and methanesulfonic acid (Scheme 30).[14a] The cationic $[Ru–H]^+$ species is generated, and CO_2 is reduced by the Ru–H species to give the formate complex, which is attacked by the carbon nucleophiles to form the corresponding acetal. Finally, the hydrogenolysis of the acetal intermediate produces the *C*-methylated product.

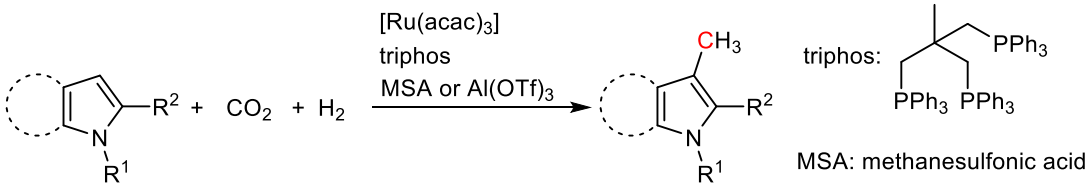

Scheme 30. Synthesis of pyrroles from CO_2.

1.12 Summary of This Thesis

Both reductive and non-reductive conversions of CO_2 have attracted considerable attention of chemists from the viewpoint of sustainable organic synthesis. Reductive transformation of CO_2 can make not only C–H bonds but also C–C and/or C–N bonds to give value-added chemicals. Among non-reductive conversions of CO_2, the terpolymerizations of epoxides, CO_2, and comonomers can provide several CO_2-based polymers, whose thermal, optical, mechanical or degradation properties can be tuned by changing the structure and composition of epoxides or/and comonomers.

In Chapter 2, the new terpolymerization of CHO, CO_2, and isothiocyanates using bifunctional Al^{III} porphyrin catalysts with quaternary ammonium bromides under solvent-free conditions was investigated (Scheme 31a). The kinetic studies and the degradation behaviors indicated that the terpolymers had gradient character, where the composition of the polycarbonate and thioimidocarbonate units changed gradually along the polymer chain. We also achieved the new terpolymerization of CHO, CO_2, and isocyanates to give poly(carbonate–urethane)s with tertiary carbamate linkages (Scheme 31b). The slow dropwise addition of isocyanates under 1 atm of CO_2 suppressed the trimerization of isocyanates, cyclic trimeric byproducts. We have also carried out the quaterpolymerizations of epoxides, CO_2, isocyanates, and isothiocyanates.

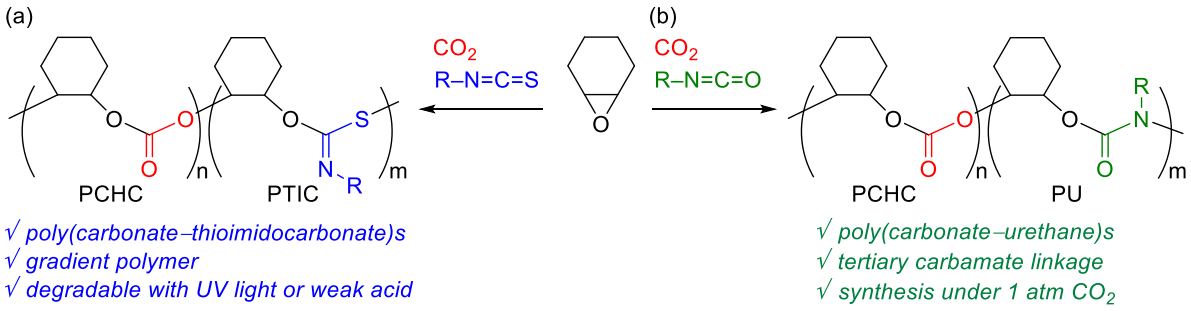

Scheme 31. Terpolymerization of CHO, CO_2, and (a) isothiocyanates or (b) isocyanates.

In Chapter 3, tetrabutylammonium acetate (TBAA) and $Cu(OAc)_2$ acted as a binary catalyst system for the solvent-free *N*-formylation of amines with CO_2 and $PhSiH_3$. This catalysis making C−H and C−N bonds with CO_2 was coupled with the subsequent C−C bond-forming reactions such as the Peterson reactions or Vilsmeier–Haack reactions to achieve the one-pot synthesis of enamines, aldehydes, and nitriles (Scheme 32).

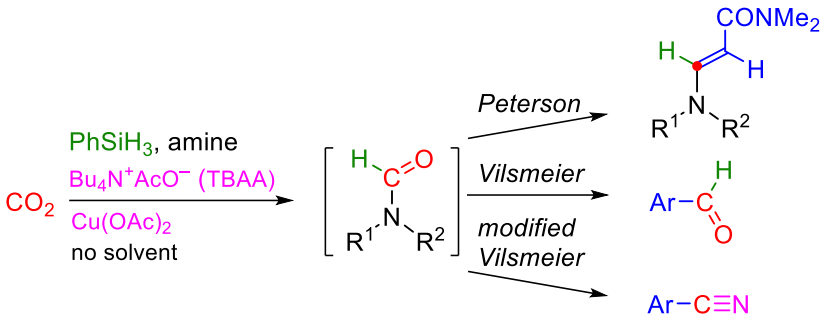

Scheme 32. Solvent-free *N*-formylation of amines with CO_2 and $PhSiH_3$ to give formamides, and the subsequent one-pot synthesis of enamines, aldehydes, and nitriles.

In Chapter 4, the solvent-free *N*-formylation of 2-(methylamino)pyridine with CO_2 and phenylsilane was catalyzed by $Cu(OAc)_2$ alone (Scheme 33). The ^1H NMR spectra of solutions containing $Cu(OAc)_2$, 2-(methylamino)pyridine, and phenylsilane showed a singlet signal assigned to a catalytically active Cu−H species, and this signal disappeared upon exposure to CO_2. The product of *N*-formylation called Comins-Meyers formamide was directly subjected to the Grignard reactions in THF for the one-pot synthesis of aldehydes or alcohols (Scheme 33).

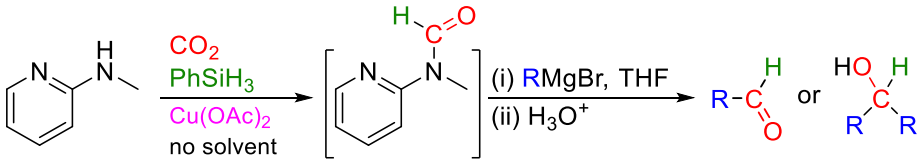

Scheme 33. Solvent-free *N*-formylation of 2-(methylamino)pyridine with CO_2 and $PhSiH_3$ to give Comins-Meyers formamide, and the subsequent one-pot synthesis of aldehydes and alcohols.

References

(1) Recent Reviews: (a) Artz, J.; Müller, T. E.; Thenert, K. *Chem. Rev*. **2018**, *118*, 434–504. (b) Hepburn, C.; Adlen, E.; Beddington, J.; Carter, E. A.; Fuss, S.; Dowell, N. M.; Minx, J. C.; Smith, P.; Williams, C. K. *Nature* **2019**, *575*, 87–97. (c) Kim, C.; Yoo, C.-J.; Oh, H.-S.; Min, B. K.; Lee, U. *J. CO2 Util*. **2022**, *65*, 102239. (d) Challa, P.; Paleti, G.; Madduluri, V. R.; Gadamani, S. B.; Pothu, R.; Burri, D. R.; Boddula, R.; Perugopu, V.; Kamaraju, S. R. R. *Catal. Surv. Asia*. **2022**, *26*, 80–91. (e) Qiu, L.-Q.; Yao, X.; Zhang, Y.-K.; Li, H.-R.; He, L.-N. *J. Org. Chem*. **2023**, *88*, 4942–4864.

(2) Reviews: (a) Coates, G. W.; Moore, D. R. *Angew. Chem. Int. Ed*. **2004**, *43*, 6618–6639. (b) Darensbourg, D. J. *Chem. Rev*. **2007**, *107*, 2388–2410. (c) Kember, M. R.; Buchard, A.; Williams, C. K. *Chem. Commun.* **2011**, *47*, 141–163. (d) Klaus, S.; Lehenmeier, M. W.; Anderson, C. E.; Rieger, B. *Coord. Chem. Rev.* **2011**, *255*, 1460–1479. (e) Lu, X.-B.; Darensbourg, D. J. *Chem. Soc. Rev.* **2012**, *41*, 1462–1484. (f) Taherimehr, M.; Pescarmona, P. P. *J. Appl. Polym. Sci.* **2014**, *131*, 41141. (g) Darensbourg, D. J.; Yeung, A. D. *Polym. Chem.* **2014**, *5*, 3949–3962. (h) Trott, G.; Saini, P. K.; Williams, C. K. *Phil. Trans. R. Soc. A* **2016**, *374*, 20150085. (i) Poland, S. J.; Darensbourg, D. J. *Green Chem.* **2017**, *19*, 4990–5011. (j) Wang, Y.; Darensbourg, D. J. *Coord. Chem. Rev*. **2018**, *372*, 85–100. (k) Kozak, C. M.; Ambrose, K.; Anderson, T. S. *Coord. Chem. Rev*. **2018**, *376*, 565–587. (l) Scharfenberg, M.; Hilf, J.; Frey, H. *Adv*. *Funct. Mater.* **2018**, *28*, 1704302. (m) Darensbourg, D. J. *Green Chem.* **2019**, *21*, 2214–2223. (n) Kamphuis, A. J.; Picchioni, F.; Pescarmona, P. P. *Green Chem.* **2019**, *21*, 406–448. (o) Paradiso, V.; Capaccio, V.; Lamparelli, D. H.; Capacchione, C. *Catalysts* **2020**, *10*, 825. (p) Huang, J.; Worch, J. C.; Dove, A. P.; Coulembier, O. *ChemSusChem* **2020**, *13*, 469–487. (q) Bhat, G. A.; Darensbourg, D. J. *Green Chem.* **2022**, *24*, 5007–5034. (r) Lidston, C. A. L.; Severson, S. M.; Abel, B. A.; Coates, G. W. *ACS Catal.* **2022**, *12*, 11037–11070.

(3) Recent examples: (a) Zhang, D.; Boopathi, S. K.; Hadjichristidis, N.; Gnanou, Y.; Feng, X. *J. Am. Chem. Soc.* **2016**, *138*, 11117–11120. (b) Reiter, M.; Vagin, S.; Kronast, A.; Jandl, C.; Rieger, B. *Chem. Sci.* **2017**, *8*, 1876–1882. (c) Huang. Z.; Wang, Y.; Zhang, N.; Zhang, L.; Darensbourg, D. J. *Macromolecules* **2018**, *51*, 9122–9130. (d) Nagae, H.; Aoki, R.; Akutagawa, S.; Kleemann, J.; Tagawa, R.; Schindler, T.; Choi, G.; Spaniol, T. P.; Tsurugi, H.; Okuda, J.; Mashima, K. *Angew. Chem. Int. Ed*. **2018**, *57*, 2492–2496. (e) Duan, R.; Hu, C.; Sun, Z.; Zhang, H.; Pang, X.; Chen, X. *Green Chem.* **2019**, *21*, 4723–4731. (f) Patil. N. G.; Boopathi, S. K.; Alagi, P.; Hadjichristidis, N.; Gnanou, Y.; Feng, X. *Macromolecules* **2019**, *52*, 2431–2438. (g) Asaba, H.; Iwasaki, T.; Hatazawa, M.; Deng, J.; Nagae, H.; Mashima, K.; Nozaki, K. *Inorg. Chem.* **2020**, *59*, 7928–7933. (h) Lindeboom, W.; Fraser, D. A. X.; Durr, C. B.; Williams, C. K. *Chem. Eur. J.* **2021**, *27,* 12224–12231. (i) Zhang, R.; Kuang, Q.; Cao, H.; Liu, S.; Chen, X.; Wang, X.; Wang, F. *CCS Chem.* **2022**, *5*, 750–760. (j) Yang, G.-W.; Xu, C.-K.; Xie, R.; Zhang, Y.-Y.; Lu, C.; Qi, H.; Yang, L.; Wang, Y.; Wu, G.-P. *Nat. Synth.* **2022**, *1,* 892–901. (k) Li, Y.-N.; Yang, H.-H.; Lu, X.-B. *J. Polym. Sci.* **2022**, *60,* 2078–2085. (l) Nagae, H.; Matsushiro, S.; Okuda, J.; Mashima, K. *Chem. Sci.* **2023**, *14*, 8262–8268.

(4) Inoue, S.; Koinuma, H.; Tsuruta, T.; *J. Polym. Sci., Part B: Polym. Lett.* **1969**, *7*, 287–292.

(5) (a) Liu, Y.; Huang, Y. L.; Peng, D.; Wu, H. *Polymer* **2006**, *47*, 8453–8461. (b) Jeske, R. C.; Rowley, J. M.; Coates, G. W. *Angew. Chem. Int. Ed*. **2008**, *47*, 6041–6044. (c) Song, P. F.; Xiao, M.; Du, F. G.; Wang, S. J.; Gan, L. Q.; Liu, G. Q.; Meng, Y. Z. *J. Appl. Polym. Sci*. **2008**, *109*, 4121–4129. (d) Sun, X.-K.; Zhang, X.-H.; Chen, S.; Du, B.-Y.; Wang, Q.; Fan, Z.-Q.; Qi, G.-R. *Polymer* **2010**, *51*, 5719–5725. (e) Huijser, S.; HosseiniNejad, E.; Sablong, R.; de Jong, C.; Koning, C. E.; Duchateau, R. *Macromolecules* **2011**, *44*, 1132–1139. (f) Darensbourg, D. J.; Polang, R. R.; Escobedo, C. *Macromolecules* **2012**, *45*, 2242–2248. (g) Liu, Y.; Xiao, M.; Wang, S.; Xia, L.; Hang, D.; Cui, G.; Meng, Y. *RSC Adv.* **2014**, *4*, 9503–9508. (h) Duan, Z.; Wang. X.; Gao, Q.; Zhang, L.; Liu, B.; Kim II, *J. Polym. Sci.* **2014**, *52*, 789–795. (i) Jeon, J. Y.; Eo, S. C.; Varghese, J. K.; Lee, B. Y. *Beilstein. J. Org. Chem.* **2014**, *10*, 1787–1795. (j) Liu, Y.; Deng, K.; Wang, S.; Xiao, M.; Han, D.; Meng, Y. *Polym.Chem.* **2015**, *6*, 2076–2083. (k) Thevenon, A.; Garden, J. A.; White, A. J. P.; Williams, C. K. *Inorg. Chem.* **2015**, *54*, 11906–11915. (l) Romain, C.; Zhu, Y.; Dingwall, P.; Paul, S.; Rzepa, H. S.; Buchard, A.; Williams, C. K. *J. Am. Chem. Soc.* **2016**, *138*, 4120–4131. (m) Saini, P. K.; Fiorani, G.; Mathers, R. T.; Williams, C. K. *Chem. Eur. J.* **2017**, *23*, 4260–4265. (n) Liu, Y.; Guo, J.-Z.; Lu, H.-W.; Wang, H.-B.; Lu, X.-B. *Macromolecules* **2018**, *51*, 771–778. (o) Ye, S.; Wang, W.; Liang, J.; Wang, S.; Xiao, M.; Meng, Y. *ACS Sustainable Chem. Eng.* **2020**, *8*, 17860–17867. (p) Rosetto, G.; Deacy, A. C.; Williams, C.K. *Chem. Sci*. **2021**, *12*, 12315–12325. (q) Plajer, A. J.; Williams, C. K. *Angew. Chem. Int. Ed*. **2021**, *60*, 13372–13379. (r) Liang, J.; Ye, S.; Wang, W.; Fan, C.; Wang, S.; Han, D.; Liu, W.; Cui, Y.; Hao, L.; Xiao, M.; Meng, Y. *J. CO2 Util.* **2021**, *49*, 101558. (s) Zhang, J.; Wang, L.; Liu, S.; Kang, X.; Li, Z. *Macromolecules* **2021**, *54*, 763–772. (t) Chidara, V. K.; Boopathi, S. K.; Hadjichristidis, N.; Gnanou, Y.; Feng, X. *Macromolecules* **2021**, *54*, 2711–2719. (u) Ye, S.; Ren. Y.; Liang, J.; Wang, S.; Huang, S.; Han, D.; Huang, Z.; Liu, W.; Xiao, M.; Meng, Y. *J. CO2 Util.* **2022**, *65*, 102223. (v) He, G.-H.; Ren, B.-H.; Wang, S.; Liu, Y.; Lu, X.-B. *Angew. Chem. Int. Ed*. **2023**, e202304943. (w) Ma, Y.; You, X.; Zhang, J.; Wang, X.; Kou, X.; Liu, S.; Zhong, R.; Li, Z. *Angew. Chem. Int. Ed*. **2023**, e202303315. (x) Stühler, M. R.; Gallizioli, C.; Rupf, S. M.; Plajer, A. J. *Polym. Chem.* **2023**, *14*, 4848–4855.

(6) (a) Hwang, Y.; Jung, J.; Ree, M.; Kim, H. *Macromolecules* **2003**, *36*, 8210–8212. (b) Hwang, Y.; Kim, H.; Ree, M. *Macromol. Symp.* **2005**, *224*, 227–237. (c) Liu, S.; Xiao, H.; Huang, K.; Lu, L.; Huang, Q. *Polym. Bull.* **2006**, *56*, 53–62. (d) Romain, C.; Williams, C. K. *Angew. Chem. Int. Ed*. **2014**, *53*, 1607–1610. (e) Paul, S.; Romain, C.; Shaw, J.; Williams, C. K. *Macromolecules* **2015**, *48*, 6047–6056. (f) Xu, Y.; Wang, S.; Lin, L.; Xiao, M.; Meng, Y. *Polym. Chem*. **2015**, *6*, 1533–1540. (g) Li, Y.; Hong, J.; Wei, R.; Zhang, Y.; Tong, Z.; Zhang, X.; Du, B.; Xu, J.; Fan, Z. *Chem. Sci*. **2015**, *6*, 1530–1536. (h) Romain, C.; Zhu, Y.; Dingwall, P.; Paul, S.; Rzepa, H. S.; Buchard, A.; Williams, C. K. *J. Am. Chem. Soc*. **2016**, *138*, 4120–4131. (i) Kernbichl, S.; Reiter, M.; Adams, F.; Vagin, S.; Rieger, B. *J. Am. Chem. Soc*. **2017**, *139*, 6787–6790. (j) Kernbichl, S.; Reiter, M.; Mock, J.; Rieger, B. *Macromolecules* **2019**, *52*, 8476–8483. (k) Sulley, G. S.; Gregory, G. L.; Chen, T. T. D.; Carrodeguas, L. P.; Trott, G.; Santmarti, A.;

Lee, K.-Y.; Terrill, N. J.; Williams, C. K. *J. Am. Chem. Soc*. **2020**, *142*, 4367–4378. (l) Yang, Z.; Hu, C.; Cui, F.; Pang, X.; Huang, Y.; Zhou, Y.; Chen, X. *Angew. Chem. Int. Ed*. **2022**, *61*, e202117533. (m) Zhou, Y.; Gao, Z.; Hu, C.; Meng, S.; Duan, R.; Sun, Z.; Pang, X. *Macromolecules* **2022**, *55*, 9951–9959.

(7) (a) Kröger, M.; Folli, C.; Walter, O.; Döring, M. *Adv. Synth. Catal.* **2006**, *348*, 1908–1918. (b) Liu, S.; Wang, J.; Huang, K.; Liu, Y.; Wu, W. *Polym. Bull*. **2011**, *66*, 327–340. (c) Gu, L.; Qin, Y.; Gao, Y.; Wang, X.; Wang, F. *Chin. J. Chem.* **2012**, *30*, 2121–2125. (d) Nysenko, Z. N.; Said-Galiev, E. E.; Buzin, M. I.; Belevtsev, Y. E.; Il'in, M. M.; Nikiforova, G. G.; Sakharov, A. M. *Mendeleev Commun.* **2014**, *24*, 236–238. (e) Tang, L.; Luo, W.; Xiao, M.; Wang, S.; Meng, Y. *J. Polym. Sci., Part A: Polym. Chem.* **2015**, *53*, 1734–1741. (f) Xie, D.; Yang, Z.; Wu, L.; Zhang, C.; Chisholm, M. H. *Polym. Int.* **2018**, *67*, 883–893. (g) Hu, C.; Duan, R.; Yang, S.; Pang, X.; Chen, X. *Macromolecules* **2018**, *51*, 4699–4704. (h) Li, X.; Hu, C.; Pang, X.; Duan, R.; Chen, X. *Catal. Sci. Technol.* **2018**, *8*, 6452–6457. (i) Duan, R.; Hu, C.; Sun, Z.; Zhang, H.; Pang, X.; Chen, X. *Green Chem.* **2019**, *21*, 4723–4731. (j) Liu, N.; Gu, C.; Chen, M.; Zhang, J.; Yang, W.; Zhan, A.; Zhang, K.; Lin, Q.; Zhu, L. *ChemistrySelect* **2020**, *5*, 2388–2394. (k) Chen, Y.; Wang, W.; Xie, D.; Wu, L.; Zhang, C. *J. Polym. Sci.* **2021** *59*, 1528–1539. (l) Li, X.; Duan, R.-L.; Hu, C.-Y.; Pang, X.; Deng, M.-X. *Polym. Chem.* **2021**, *12*, 1700–1706. (m) Li, X.; Hu, C.-Y.; Duan, R.-L.; Liang, Z.-Z.; Pang, X.; Deng, M.-X. *Polym. Chem.* **2021**, *12*, 3124–3131. (n) Huang, Y.; Hu, C.; Pang, X.; Zhou, Y.; Duan, R.; Sun, Z.; Chen, X. *Angew. Chem. Int. Ed*. **2022**, *61*, e202202660. (o) Martínez de Sarasa Buchaca, M.; de la Cruz-Martínez, F.; Sánchez-Barba. L. F.; Tejeda, J.; Rodríguez, A. M.; Castro-Osma, J. A.; Lara-Sánchez, A. *Dalton Trans.* **2023**, *52*, 3482–3492.

(8) Li, Z.; Mayer, R. L.; Ofial, A. R.; Mayr, H. *J. Am. Chem. Soc*. **2020**, *142*, 8383–8402.

(9) (a) Zhi, Y.; Miao, Y.; Zhao, W.; Wang, J.; Zheng, Y.; Su, H.; Jia, Q.; Shan, S. *Polymer* **2019**, *165*, 11–18. (b) Yue, T.-J.; Ren, B.-H.; Zhang, W.-J.; Lu, X.-B.; Ren, W.-M.; Darensbourg, D. J. *Angew. Chem. Int. Ed.* **2021**, *60*, 4315–4321. (c) Stephan, J.; Stühler, M. R.; Rupf, S. M.; Neale, S.; Plajer, A. J. *Cell. Rep. Phys. Sci*. **2023**, *4*, 101510.

(10) Selected examples: (a) Darensbourg, D. J.; Wang, Y. *Polym. Chem.* **2015**, *6*, 1768–1776. (b) Shaarani, F. W.; Bou, J. J. *Sci. Total Environ.* **2017**, *598*, 931–936. (c) Mo. W.; Zhuo, C.; Cao, H.; Liu, S.; Wang, X.; Wang, F. *Macromol. Chem. Phys.* **2022**, *223*, 2100403. (d) Sengoden, M.; Bhat, G. A.; Darensbourg, D. J. *Macromolecules* **2023**, *56*, 2362–2369. (e) Tang, S.; Suo, H.; Qu, R.; Tang, H.; Sun, M.; Qin, Y. *Polymers* **2023**, *15*, 748. (f) Mo, W.; Zhuo, C.; Liu, S.; Wang, X.; Wang, F.; Qin, Y. *Polym. Chem.* **2023**, *14*, 152–160.

(11) (a) Yu, B.; Zhao, Y.; Zhang, H.; Xu, J.; Hao, L.; Gao, X.; Liu, Z. *Chem. Commun*. **2014**, *50*, 2330–2333. (b) Yu, B.; Yang, Z.; Zhao, Y.; Hao, L.; Zhang, H.; Gao, X.; Han, B.; Liu, Z. *Chem. Eur. J*. **2016**, *22*, 1097–1102. (c) Anaby, A.; Feller, M.; Ben-David, Y.; Leitus, G.; Diskin-Posner, Y.; Shimon, L. J. W.; Milstein, D. *J. Am. Chem. Soc*. **2016**, *138*, 9941–9950. (d) Ren, X.; Zheng, Z.; Zhang, L.; Wang, Z.; Xia, C.; Ding, K. *Angew. Chem. Int. Ed*. **2017**, *56*, 310–313. (e) Liu, Z.; Yang, Z.; Yu, B.; Yu, X.; Zhang, H.; Zhao, Y.; Yang, P.; Liu, Z. *Org. Lett*. **2018**, *20*, 5130–

5134. (f) Murata, T.; Hiyoshi, M.; Ratanasak, M.; Hasegawa, J.; Ema, T. *Chem. Commun.* **2020**, *56*, 5783–5786.

(12) (a) Tani, Y.; Kuga, K.; Fujihara, T.; Terao, J.; Tsuji, Y. *Chem. Commun*. **2015**, *51*, 13020–13023. (b) Chen, X.-W.; Zhu, L.; Gui, Y.-Y.; Jing, K.; Jiang, Y.-X.; Bo, Z.-Y.; Lan, Y.; Li, J.; Yu, D.-G. *J. Am. Chem*. *Soc*. **2019**, *141*, 18825–18835. (c) Zhang, X.; Tian, X.; Shen, C.; Xia, C. He, L. *ChemCatChem* **2019**, *11*, 1986–1992. (d) Wang, M.-Y.; Jin, X.; Wang, X.; Xia, S.; Wang, Y.; Huang, S.; Li, Y.; He, L.-N.; Ma, X. *Angew. Chem. Int. Ed*. **2021**, *60*, 3984–3988. (e) Zhang, D.; Jarava-Barrera, C.; Bontemps, S. *ACS Catal.* **2021**, *11*, 4568–4575. (f) Béthegnies, A.; Escudié, Y.; Nuñez-Dallos, N.; Vendier, L.; Hurtado, J.; del Rosal, I.; Maron, L.; Bontemps, S. *ChemCatChem* **2019**, *11*, 760–765.

(13) (a) Jin, G.; Werncke, C. G.; Escudié, Y.; Sabo-Etienne, S.; Bontemps, S. *J. Am. Chem*. *Soc*. **2015**, *137*, 9563–9566. (b) Zhu, D.-Y.; Li, W.-D.; Yang, C. Chen, J.; Xia, J.-B. *Org. Lett.* **2018**, *20*, 3282–3285. (c) Rauch, M.; Strater, Z.; Parkin, G. *J. Am. Chem*. *Soc*. **2019**, *141*, 17754–17762.

(14) (a) Li, Y.; Yan, T.; Junge, K.; Beller, M. *Angew. Chem. Int. Ed.* **2014**, *53*, 10476–10480. (b) Zhu, D.-Y.; Fang, L.; Han, H.; Wang, Y.; Xia, J.-B. *Org. Lett*. **2017**, *19*, 4259–4262. (c) Zhao, Y.; Guo, X.; Ding, X.; Zhou, Z.; Li, M.; Feng, N.; Gao, B.; Lu, X.; Liu, Y.; You, J. *Org. Lett.* **2020**, *22*, 8326−8331. (d) Zhao, Y.; Liu, X.; Zheng, L.; Du, Y.; Shi, X.; Liu, Y.; Yan, Z.; You, J.; Jiang, Y. *J. Org. Chem.* **2020**, *85*, 912–923. (e) Zhao, Y.; Guo, X.; Du, Y.; Shi, X.; Yan, S.; Liu, Y.; You, J. *Org. Biomol. Chem.* **2020**, *18*, 6881–6888. (f) Li, W.-D.; Chen, J.; Zhu, D.-Y.; Xia, J.-B. *Chin. J. Chem*. **2021**, *39*, 614–620. (g)Takaishi, E.; Nishimura, R.; Toda, Y.; Morishita, H.; Ema, T. *Org. Lett.* **2023**, *25*, 1370–1374.

Chapter 2

Terpolymerizations of Cyclohexene Oxide, CO_2, and Isocyanates or Isothiocyanates

2.1 Abstract

The terpolymerizations of epoxide, CO_2, and isocyanates or isothiocyanates were achieved for the first time by using bifunctional Al^{III} porphyrins with quaternary ammonium bromides as catalysts. The terpolymerization of cyclohexene oxide (CHO), CO_2 (2 MPa), and aryl isothiocyanates produced poly(carbonate–thioimidocarbonate)s with gradient character in composition, and the ratio of the polythioimidocarbonate to the polycarbonate units in the terpolymers could be controlled by the CO_2 pressure. A block copolymer, poly(carbonate–*b*–thioimidocarbonate), was also synthesized in a one-pot two-step manner. On the other hand, the terpolymerization of CHO, CO_2 (1 atm), and aryl isocyanates furnished poly(carbonate–urethane)s with random sequences. Poly(carbonate–thioimidocarbonate)s underwent partial degradation upon acid treatment or UV irradiation to give polycarbonates, while poly(carbonate–urethane)s were stable under the same conditions.

2.2 Introduction

The ring-opening copolymerization (ROCOP) of epoxides and carbon dioxide (CO_2) for the synthesis of aliphatic polycarbonates is a green and sustainable synthetic technology with 100% atom economy, and it has been intensively studied since the first report in 1969.[1–3] On the other hand, the terpolymerization of epoxides, CO_2, and comonomers, such as lactones,[4] lactides,[5] cyclic acid anhydrides,[6] and heteroallenes,[7,8] is an effective strategy for the development of new CO_2-based polymers (Scheme 1a). The thermal, optical, mechanical, or degradation properties can be added or tuned by incorporating new polymer backbones derived from the comonomers at the expense of the CO_2 content. The scope of comonomers and the tunability of the physical properties are important factors in the terpolymerizations. Heteroallenes used as comonomers have been limited to SO_2 and COS,[7,8] which are gases to be carefully used, while isocyanates or isothiocyanates have never been used to prepare CO_2-based polymers despite the commercial availability, good reactivity, and tunability with substituents.[9] The terpolymerizations of epoxides, CO_2, and isocyanates or isothiocyanates may open up a new way for the development of novel CO_2-based polymers.

In 2020, two groups independently achieved the first epoxide/isocyanate ROCOP (without CO_2) to obtain new polyurethanes (PUs) with tertiary carbamate linkages,[10a,b] which are almost inaccessible via the conventional synthetic method with diisocyanates and diols. There are only several reports on this type of ROCOP partly because of the difficulty in using highly reactive isocyanates,[10] which

readily trimerize into isocyanurates.[11] On the other hand, the epoxide/isothiocyanate ROCOP for the synthesis of poly(thioimidocarbonate)s (PTICs) was reported by three groups independently in 2021, and strong bases were used to activate isothiocyanates with poor reactivity as compared with isocyanates.[12] These pioneering works suggest that the terpolymerizations of epoxides, CO_2, and isocyanates or isothiocyanates might be difficult to achieve especially with a single catalyst because the ideal reaction conditions for the epoxide/CO_2 ROCOPs are quite different from those for the epoxide/iso(thio)cyanate ROCOPs.

Previously, bifunctional Mg^{II} or Zn^{II} porphyrin catalysts showed high activity for the synthesis of cyclic carbonates from epoxides and CO_2,[13] while bifunctional Al^{III} porphyrin catalysts **1** promoted the ROCOP of epoxides and CO_2 efficiently to produce polycarbonates (Scheme 1b).[14,15] The cooperative actions of the metal center and the quaternary ammonium halides led to the high activity and selectivity in both cases.[16] More recently, we have also succeeded in the selective conversions of oxetanes and CO_2 into trimethylene carbonates or poly(trimethylene carbonate)s with **1d**.[17] We envisioned that isocyanates or isothiocyanates could be used as comonomers in our catalytic system. Here we report the terpolymerizations of epoxide, CO_2, and isocyanates or isothiocyanates for the first time (Scheme 1c). The terpolymerization of cyclohexene oxide (CHO), CO_2 (2 MPa), and aryl isothiocyanates produced poly(carbonate–thioimidocarbonate)s with gradient character, while that of CHO, CO_2 (1 atm), and aryl isocyanates afforded poly(carbonate–urethane)s with random sequences. The former underwent partial degradation upon acid treatment or UV irradiation to give polycarbonates, while the latter was stable under the same conditions.

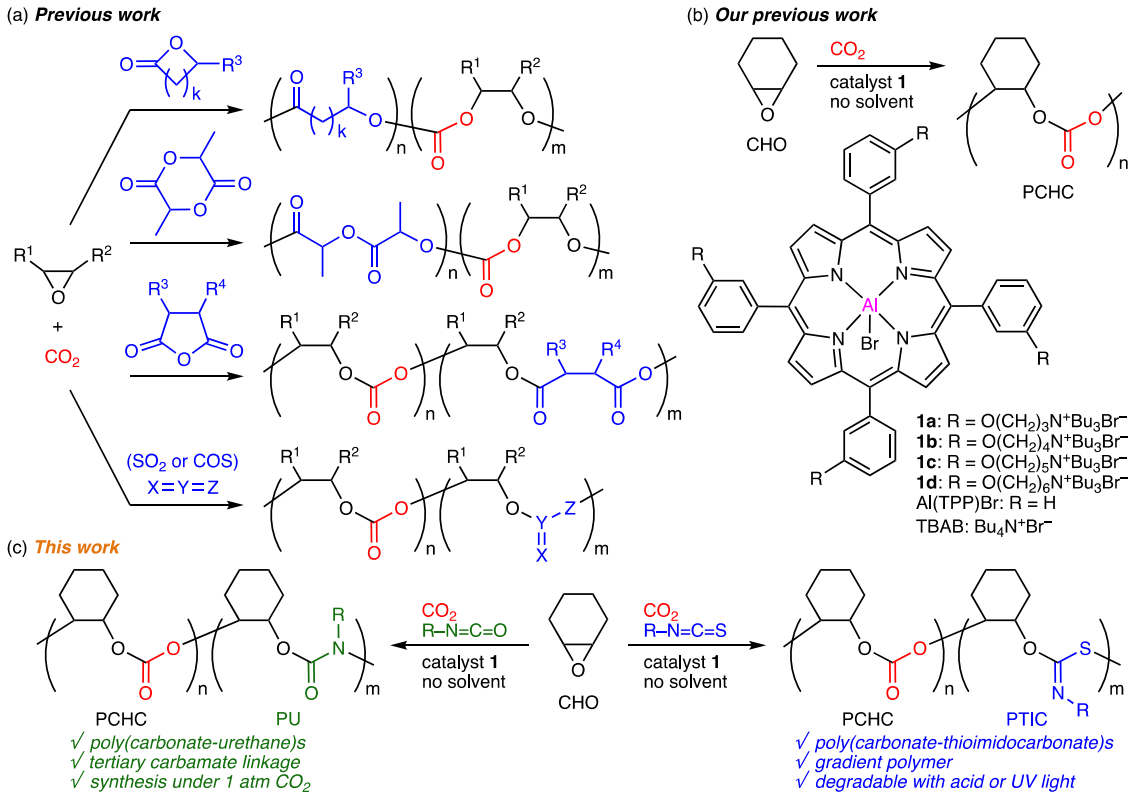

Scheme 1. (a) Previous work on terpolymerization of epoxides, CO_2, and comonomers. (b) Our previous work. (c) This work.

2.3 Results and Discussion

We investigated the terpolymerization of CHO, CO_2 (2 MPa), and phenyl isothiocyanate (**2a**) with **1b**, which showed the highest activity for the ROCOP of CHO and CO_2.[15] As a result, terpolymer **3a** containing the poly(cyclohexene carbonate) (PCHC) and PTIC units were successfully obtained at 90 °C (Table 1, entry 1).

Table 1. Terpolymerization of CHO, CO_2, and **2** with **1b**.[a]

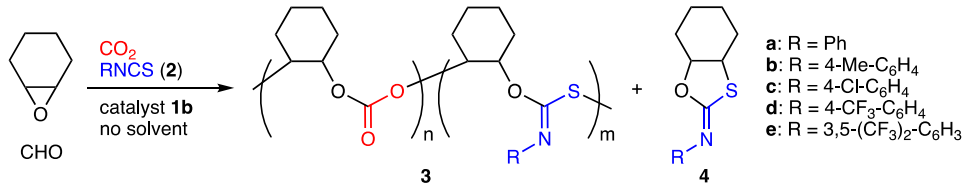

			conv.[c] (%)				**3**		**4**
entry	**2**	S/C[b]	CHO	**2**	TON[c]	n:m[d]	M_n[e] (kg mol^{-1})	PDI[e]	yield[c] (%)
1	**2a**	6250	94	75	5400	4:1	83/34	1.1/1.1	6
2	**2a**	20000	93	46	12400	5:1	164/63	1.0/1.3	3
3[f]	**2a**	20000	83	71	15600	3:1	167/55	1.1/1.3	7
4[g]	**2a**	20000	80	85	9000	2:1	85/22	1.1/1.4	10
5	**2a**	40000	87	30	31600	8:1	183/57	1.1/1.5	3
6	**2b**	40000	89	39	29600	9:1	121/41	1.1/1.4	0
7	**2c**	40000	90	71	27600	3:1	74/25	1.1/1.3	0
8	**2d**	40000	91	77	23500	4:1	132/45	1.1/1.4	0
9	**2e**	40000	80	>99	33100	2:1	164/59	1.1/1.2	0

[a] Reaction conditions: CHO (12.5 mmol), **2** (3.1 mmol), **1b** (quantity indicated above), CO_2 (2.0 MPa), 90 °C, 24 h, in an autoclave. [b] Ratio of CHO to **1b**. [c] Determined by ^{1}H NMR analysis of the crude reaction mixture. TON for the formation of **3**. The yields of **4** were calculated based on **2**. [d] Determined by ^{1}H NMR analysis of the purified polymer. [e] Determined by SEC analysis of the purified polymer using THF as an eluent and polystyrene as a molecular-weight standard. Peaks had bimodal shapes. [f] CO_2 (1.0 MPa). [g] CO_2 (0.5 MPa).

3a was isolated by reprecipitation (chloroform/methanol) and characterized by ^{1}H NMR spectroscopy; the broad signals for the methine group of the PCHC unit appeared at 4.6 ppm, and those for the PTIC unit were observed at 6.6–7.4 ppm (Figure S6a). Size-exclusion chromatography (SEC) indicated that **3a** had high molecular weights with a bimodal distribution (Figure S6c). Bimodal molecular weight distributions are often observed for copolymerizations of epoxides and CO_2, and higher-molecular-weight polymers are twice as large as lower-molecular-weight polymers.[14] In the present terpolymerization, interestingly, the former was more than twice as large as the latter. The IR spectrum showed two strong absorptions at 1624 and 1759 cm^{-1} corresponding to the C=N and C=O stretching vibrations, respectively (Figure S6d). The MALDI-TOF mass spectrum of **3a** showed two *m*/*z* intervals of 142 and 233 corresponding to the PCHC and PTIC units,

respectively (Figure S8). The formation of terpolymers rather than blends was also confirmed by diffusion-ordered spectroscopy (DOSY) (Figure S7). Furthermore, we also synthesized a model compound to confirm the structure of **3a**, and the NMR and IR spectra showed good similarities between **3a** and the model compound (Figure S13).

Table 2. Optimization of reaction conditions for terpolymerization of CHO, CO_2, and **2a** with **1b**.

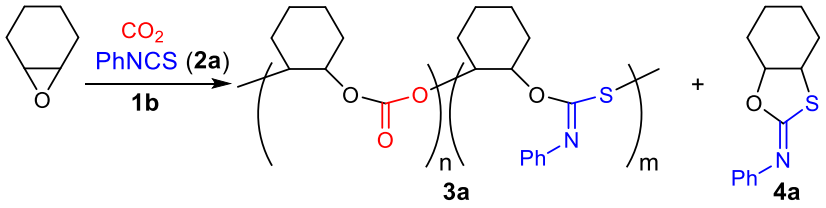

			conv.[b] (%)				**3a**		**4a**
entry[a]	*T* (°C)	CHO/**2a**	CHO	**2a**	TON[b]	n:m[b]	M_n[c] (kg mol^{-1})	PDI[c]	yield[b] (%)
1	80	5	91	61	5700	5:1	71/28	1.1/1.2	0
2	90	5	79	87	4600	3:1	45/16	1.1/1.3	5
3	100	5	92	85	5700	4:1	38	1.5	9
4	90	4	94	75	5400	3:1	73/26	1.1/1.3	6
5	90	3	98	67	5400	3:1	80/29	1.1/1.3	3
6	90	2	99	40	5800	4:1	109/39	1.1/1.3	2

[a] Reaction conditions: CHO (12.5 mmol), **2a** (quantity indicated above), **1b** (S/C = 6250 for CHO), CO_2 (2.0 MPa), 24 h, in an autoclave. [b] Determined by ^{1}H NMR analysis of the crude reaction mixture. TON for the formation of **3a**. [c] Determined by SEC analysis of the crude reaction mixture using THF as an eluent and polystyrene as a molecular-weight standard.

The reaction conditions were optimized. Higher temperature promoted the formation of byproduct **4a**, while lower temperature resulted in a lower conversion of **2a**; 90 °C was optimal (Table 2, entries 1–3). When the molar ratio of CHO to **2a** was set to 4:1, both the molecular weight of the polymer and the conversion of **2a** were high (entries 2, 4–6). When the amount of catalyst **1b** decreased from 0.016 to 0.0025 mol% (S/C = 40000), turnover numbers (TONs) increased from 5400 to 31600 to give high-molecular-weight polymers, and both the conversion of **2a** and the PTIC content (n:m) decreased (Table 1, entries 1, 2, 5). Interestingly, lower CO_2 pressure led to a higher PTIC content (entries 2–4). These results suggest that although the formation of the PTIC unit is slower than that of the PCHC unit, the former becomes favorable as CO_2 is consumed. This trend is consistent with the electrophilicity parameters reported for heteroallenes; isothiocyanates are less electrophilic than CO_2.[18] The linker length of catalysts **1** had a significant effect on the catalytic activity, and **1b** exhibited the best result (Table 3, entries 1–4). We consider that catalysts **1c** and **1d** have longer linkers that may hinder the polymer elongation owing to steric bulkiness, while catalyst **1a** has shorter linkers that cannot assist well the ring-opening of CHO and/or the insertion of CO_2 or **2a**. In sharp

contrast, a binary catalytic system composed of Al(TPP)Br and tetrabutylammonium bromide (TBAB) showed little or no activity for the PTIC formation under otherwise the same conditions (entry 5), which clearly demonstrates the importance of cooperative catalysis with bifunctional catalyst **1b**.[13–17]

Table 3. Screening of catalysts for the terpolymerization of CHO, CO_2, and **2a**.

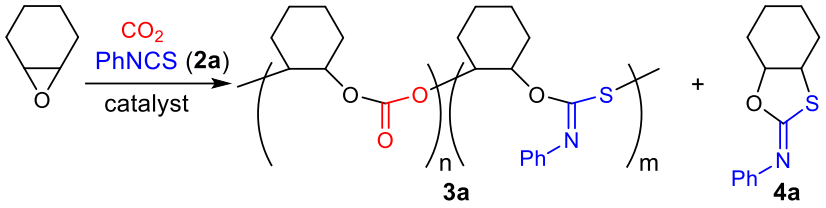

		conv.[b] (%)				**3a**		**4a**
entry[a]	catalyst	CHO	**2a**	TON[b]	n:m[c]	M_n[d] (kg mol^{-1})	PDI[d]	yield[b] (%)
1	**1a**	82	5	17100	>20:1	121/59	1.0/1.1	0
2	**1b**	87	30	31600	8:1	183/57	1.1/1.5	3
3	**1c**	90	5	23600	20:1	104/44	1.1/1.2	0
4	**1d**	82	11	28000	10:1	78	1.5	0
5[e]	Al(TPP)Br	30	0	600	N.D.	<1.0[f]	–[f]	0

[a] Reaction conditions: CHO (12.5 mmol), **2a** (3.1 mmol), catalyst (S/C = 40000 for CHO), CO_2 (2.0 MPa), 90 °C, 24 h, in an autoclave. [b] Determined by ^{1}H NMR analysis of the crude reaction mixture. TON for the formation of **3a**. [c] Determined by ^{1}H NMR analysis of the purified polymer. [d] Determined by SEC analysis of the purified polymer using THF as an eluent and polystyrene as a molecular-weight standard. [e] Tetrabutylammonium bromide (4 equiv relative to Al(TPP)Br) was added. [f] Crude reaction mixtures were analyzed.

The scope of aryl isothiocyanates **2** was explored under the optimized conditions with **1b**. Isothiocyanate **2b** with the methyl group at the *para* position was modestly incorporated to form terpolymer **3b** (Table 1, entry 6). In contrast, isothiocyanates **2c**–**e** with electron-withdrawing groups showed much higher reactivity, and terpolymers **3c**–**e** with higher PTIC contents were successfully obtained (entries 7–9).

We next examined the reactivity of aryl isocyanates **5**. In view of the facile conversion of **5a** into isocyanurate **9a**, we employed a syringe-pump for the slow dropwise addition of **5a** via syringe under atmospheric CO_2 pressure (balloon), which allowed us to optimize the reaction conditions for the terpolymerization of CHO, CO_2, and **5a** (Table 4). Terpolymer **6a** containing both the PCHC and PU units was obtained most efficiently with a catalyst loading of 0.016 mol% (S/C = 6250) (entries 1–3). The formation of byproduct **9a** was minimal at 90 °C, although the formation of cyclohexene carbonate (**7**) and 2-oxazolidone **8a** was suppressed at 80–100 °C (entries 2, 4, 5). A faster dropwise addition of **5a** resulted in the formation of a significant amount of **9a** (entry 6). The use of 10 equiv

of CHO relative to **5a** was better than that of 5 or 15 equiv of CHO (entries 2, 7, 8). The linker length of **1** had a crucial effect on the catalytic activity; **1b** was the best catalyst (Table 5, entries 1–4). In sharp contrast, a binary catalytic system composed of Al(TPP)Br and TBAB showed poor polymerization activity (entry 5), which demonstrates the advantage of bifunctional catalyst **1b**.

Table 4. Optimization of reaction conditions for the terpolymerization of CHO, CO_2, and **5a** with **1b**.

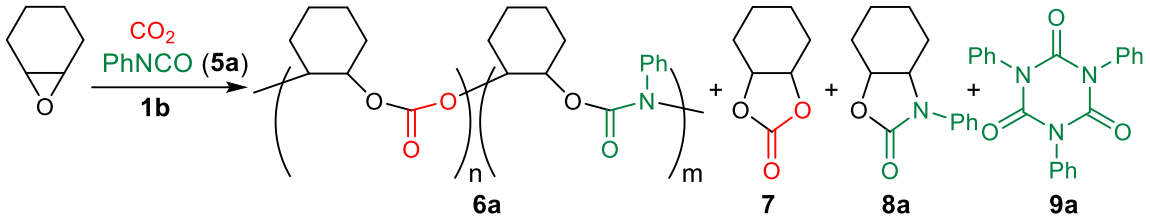

			conv.[c] (%)				**6a**		byproduct[c] (%)		
entry[a]	S/C[b]	*T* (°C)	CHO	**5a**	TON[c]	n:m[d]	M_n[e] (kg mol^{-1})	PDI[e]	**7**	**8a**	**9a**
1	10000	90	53	>99	1500	N.D.[f]	1.4[g]	1.4[g]	1	0	52
2	6250	90	81	>99	3200	6:1	7.1	1.4	3	0	8
3	3000	90	85	>99	1900	6:1	7.3	1.3	4	0	7
4	6250	80	79	>99	3600	5:1	6.0	1.3	3	0	14
5	6250	100	85	>99	3400	6:1	6.4	1.2	4	0	15
6[h]	6250	90	35	>99	1100	N.D.[f]	1.1[g]	1.5[g]	0	0	75
7[i]	6250	90	46	>99	1200	N.D.[f]	2.6[g]	1.3[g]	0	0	66
8[j]	6250	90	79	>99	3300	8:1	7.2	1.5	3	0	18

[a] A mixture of CHO (1.2 mmol) and **5a** (1.2 mmol) was added dropwise to a mixture of CHO (11.2 mmol) and **1b** (quantity indicated above) at 15 μL/h with a syringe-pump under CO_2 (1 atm, balloon) at 90 °C, and the mixture was stirred at 90 °C for 2 h. [b] Ratio of CHO to **1b**. [c] Determined by ^{1}H NMR analysis of the crude reaction mixture. TON for the formation of **6a**. [d] Determined by ^{1}H NMR analysis of the purified polymer. [e] Determined by SEC analysis of the purified polymer using THF as an eluent and polystyrene as a molecular-weight standard. [f] The PCHC/PU ratio was not determined due to the low molecular weight of polymers or the considerable formation of byproduct **9a**. [g] The crude reaction mixture was analyzed. [h] Addition at 24 μL/h. [i] CHO = 4.8 mmol instead of 11.2 mmol. [j] CHO = 16.8 mmol instead of 11.2 mmol.

Pure terpolymer **6a** was obtained by reprecipitation (chloroform/methanol), and **6a** was characterized by ^{1}H NMR spectroscopy (Figure S20a). In addition to the broad signals at 4.6 ppm for the methine group of the PCHC unit, broad signals appeared at 6.9–7.5 ppm, which clearly indicates the incorporation of **5a**. The ^{13}C NMR spectrum showed the signals for the carbonyl groups of the PCHC and PU units at 153–154 ppm (Figure S20b). The IR spectrum showed two peaks for the C=O stretching vibrations of the PU and PCHC units at 1707 and 1749 cm^{-1}, respectively (Figure S20d). The structure of **6a** was also analyzed by MALDI-TOF mass spectroscopy (Figure S22a); *m*/*z* intervals of 142 and 217 corresponding to the PCHC and PU units, respectively, were observed.

DOSY also supported the formation of **6a** (Figure S21). The analysis of hydrolysis products as well as the comparison of the NMR spectra between **6a** and a model compound also supported the existence of the PCHC and PU units (Figures S26 and S27).

Table 5. Screening of catalysts for the terpolymerization of CHO, CO_2, and **5a**.

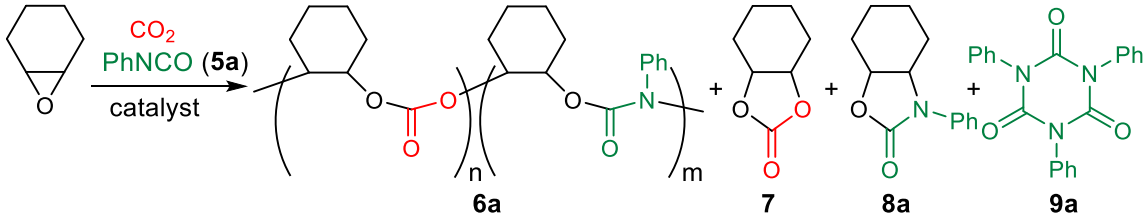

		conv.[b] (%)				**6a**		byproduct[b] (%)		
entry[a]	catalyst	CHO	**5a**	TON[b]	n:m[c]	M_n[d] (kg mol^{-1})	PDI[d]	**7**	**8a**	**9a**
1	**1a**	57	>99	1400	N.D.[e]	3.7	1.3	0	2	82
2	**1b**	81	>99	3200	6:1	7.1[f]	1.4[f]	3	0	8
3	**1c**	63	>99	2600	N.D.[e]	2.5	1.5	2	1	21
4	**1d**	50	>99	1500	N.D.[e]	1.0	1.4	2	0	48
5[g]	Al(TPP)Br	35	>99	100	N.D.[e]	<1.0	–	0	0	91

[a] A mixture of CHO (1.2 mmol) and **5a** (1.2 mmol) was added dropwise to a mixture of CHO (11.2 mmol) and catalyst (S/C = 6250 for CHO) at 15 μL/h with a syringe-pump under CO_2 (1 atm, balloon) at 90 °C, and the mixture was stirred at 90 °C for 2 h. [b] Determined by ^{1}H NMR analysis of the crude reaction mixture. TON for the formation of **6a**. [c] Determined by ^{1}H NMR analysis of the purified polymer. [d] Determined by SEC analysis of crude reaction mixtures using THF as an eluent and polystyrene as a molecular-weight standard. [e] The PCHC/PU ratio was not determined due to the low molecular weight of polymers or the formation of a large amount of byproduct **9a**. [f] The purified polymer was analyzed. [g] TBAB (4 equiv of Al(TPP)Br) was added.

The scope of aryl isocyanates **5** was examined (Table 6). Isocyanate **5b** with the methyl group at the *para* position was incorporated into terpolymer **6b** accompanied with **9b**. 4-Chlorophenyl isocyanate (**5c**) was successfully used to make **6c**, while 4-(trifluoromethyl)phenyl isocyanate (**5d**) led to the formation of **6d** with a larger molecular weight; byproduct **8d** seems to result from the backbiting of the highly electrophilic carbonyl group of the PU unit by the adjacent terminal alkoxide ion. We also challenged the quaterpolymerizations of CHO, CO_2, **2c** or **2d**, and **5c** (Scheme 2, Figures S28–S33). A mixture of **5c** and CHO was added dropwise with the syringe-pump to a mixture of CHO, **2c** or **2d**, and **1b** under CO_2 (1 atm); as a result, quaterpolymers **10a** with a M_n of 4.7 kg/mol and **10b** with a M_n of 4.5 kg/mol were produced with the quantitative conversions of the comonomers (**2c**, **2d**, and **5c**). NMR, DOSY, IR, and mass spectra of the purified polymers indicated that the PCHC, PTIC, and PU units were contained in the polymer chains. When alkyl isocyanates were used instead of aryl isocyanates, the corresponding terpolymers **6** could not be obtained efficiently (data not shown). This is partly due to the rapid formation of the corresponding isocyanurates **9**.

Table 6. Terpolymerization of CHO, CO_2, and **5** with **1b**.[a]

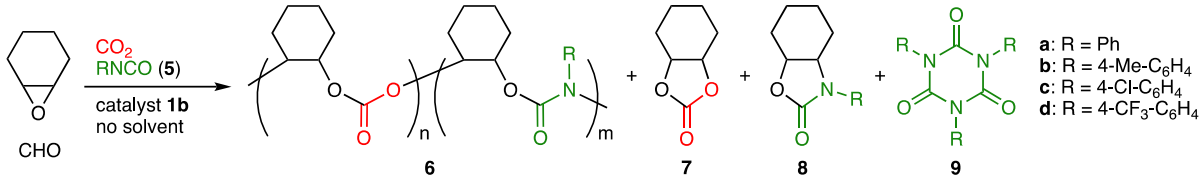

		conv.[b] (%)				6		byproduct[b] (%)		
entry	5	CHO	5	TON[b]	n:m[c]	M_n[d] (kg mol^{-1})	PDI[d]	7	8	9
1	**5a**	81	>99	3200	6:1	7.1	1.4	3	0	8
2	**5b**	85	>99	1900	2:1	4.2	1.4	1	0	29
3[e]	**5c**	79	>99	3100	3:1	7.4	1.5	3	0	2
4[e]	**5d**	80	>99	4200	9:1	14	1.3	4	8	12

[a] A mixture of CHO (1.2 mmol) and **5** (1.2 mmol) was added dropwise to a mixture of CHO (11.2 mmol) and **1b** (S/C = 6250 for CHO, 0.016 mol%) at 15 μL/h with a syringe-pump under CO_2 (1 atm, balloon) at 90 °C, and the mixture was then stirred at 90 °C for 2 h. [b] Determined by ^{1}H NMR analysis of the crude reaction mixture. TON for the formation of **6**. The yields of **7** were calculated based on CHO, and those of **8** and **9** were calculated based on **5**. [c] Determined by ^{1}H NMR analysis of the purified polymer. [d] Determined by SEC analysis of the purified polymer using THF as an eluent and polystyrene as a molecular-weight standard. [e] Addition at 24 μL/h.

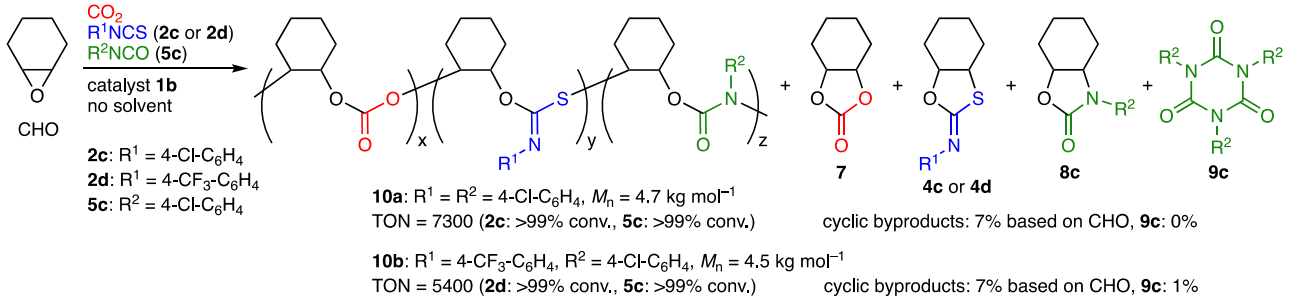

Scheme 2. Quaterpolymerizations of CHO, CO_2, **2c** or **2d**, and **5c**.

Recently, degradable polymers have attracted much attention from the viewpoint of the promotion of chemical recycling and the mitigation of plastic pollution.[19] Although sulfur-containing polymers are known to be susceptible to UV light or chemicals,[19a] there are no reports on the degradability of PTICs to our knowledge. We envisioned that terpolymers **3** containing the PTIC unit might be degradable upon acid treatment or UV light irradiation. To our delight, **3** did undergo partial degradation by acid exposure or UV irradiation (Figures 1a–c). Reprecipitation (chloroform/methanol) of the degradation mixtures and spectroscopic characterizations indicated that pure PCHCs were formed by the selective degradation of the PTIC linkages in both cases (Figures S35 and S39). Interestingly, Figures 1b–c strongly suggests that terpolymers **3** have gradient character

in composition (ratio of the PTIC to PCHC units);[20] **3c**–**e** with electron-withdrawing groups showed larger decrease in molecular weight upon acid treatment or UV light irradiation than **3a** and **3b**. Accordingly, kinetic studies indicated that **2d** was converted into the terpolymers faster than **2a** (Figure S14). For comparison, block copolymer PCHC-*b*-PTIC (**3e'**) was synthesized in a one-pot two-step manner, which was confirmed to exhibit the selective degradation of the PTIC moiety (Figures 1d–e and S42–S44), while copolymer PTIC that was synthesized from CHO and **2e** and purified in a similar manner was completely degraded (Figure S49). In sharp contrast, both PCHC and terpolymer **6a** showed little or no degradability under the same conditions, which indicates that the PCHC and PU linkages are more robust (Figures S37 and S41).

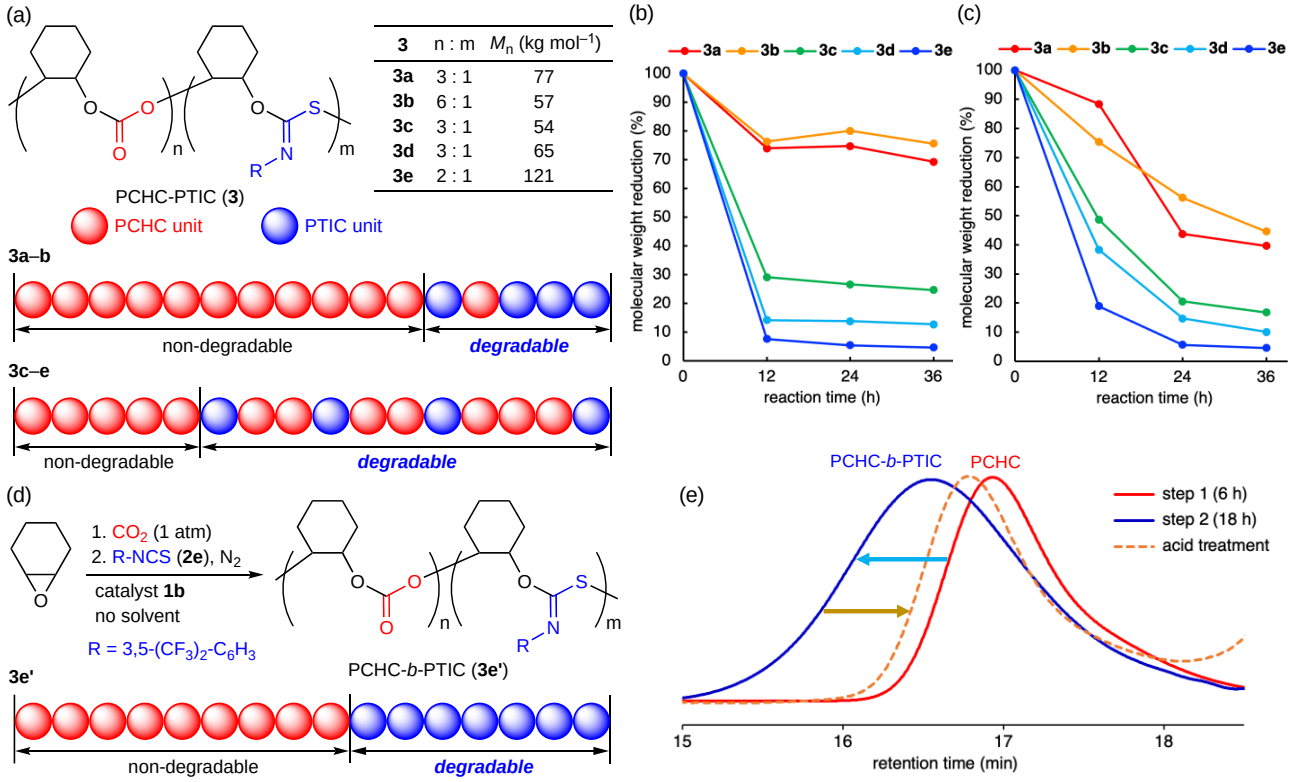

Figure 1. (a) Illustration of gradient character of **3**. The molecular weights of **3** are average values for two peaks in SEC charts. Degradation of **3** upon (b) acid treatment and (c) UV irradiation. (d) One-pot two-step synthesis of block copolymer **3e'**. (e) Synthesis and partial degradation of **3e'** monitored by SEC.

Plausible catalytic cycles for the **1b**-catalyzed polymerizations of CHO, CO_2, and isothiocyanates/isocyanates are shown in Scheme 3. The nucleophilic attack of the counter anion on CHO activated by the Al center of **1b** makes a new PCHC/PTIC/PU linkage, generating the alkoxide intermediate shown in the center. The subsequent insertion of CO_2/isothiocyanate/isocyanate into the Al–O bond gives the carbonate/thioimidocarbonate/imidocarbonate anion, which then forms an ion pair with the quaternary ammonium ion of **1b** upon CHO coordination. The S and N atoms of the thioimidocarbonate and carbamate anions, respectively, are more nucleophilic because the negatively

charged atom with less electronegativity is more labile, which is the key determinant for the selective formation of the PTIC or PU linkage. In the PTIC cycle, the reaction of the alkoxide anion with isothiocyanate **2** is considered to be the rate-determining step, judging from the substituent effect of **2** on the ratio of the PTIC to PCHC units (Table 1), degradation behaviors with gradient character (Figure 1), and kinetic studies (Figure S14). In the PU cycle, the PU linkage formation may be the rate-determining step, although the situation is complicated owing to the side reactions such as the formation of **9**. Cyclic byproducts **7**, **4**, and **8** are formed by the backbiting of the terminal alkoxide ions just after the construction of the PCHC, PTIC, and PU linkages, respectively.

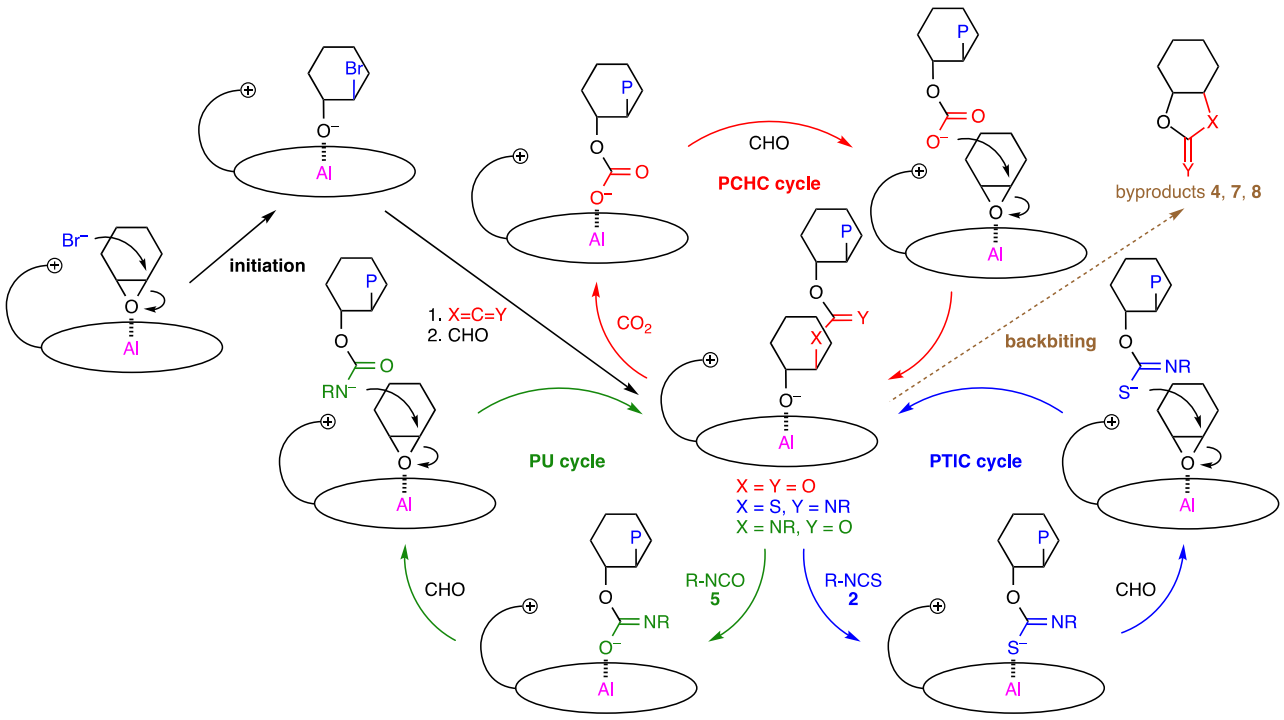

Scheme 3. Plausible catalytic cycles, where P simply represents a part of a polymer chain that may differ in each step.

The molecular weights of terpolymers **6** and quaterpolymers **10** synthesized at 1 atm CO_2 pressure (Table 2 and Scheme 2) were much smaller than those of terpolymers **3** synthesized at 2.0 MPa CO_2 pressure (Table 1). In the synthesis of **6** and **10**, isocyanates **5** were added dropwise to minimize the formation of byproducts **9**. It is likely that **6** and **10** growing at 1 atm CO_2 pressure have the alkoxide anions at the ends, which may experience backbiting and protonation. In contrast, **3** growing at the high CO_2 pressure can undergo the rapid addition of CO_2 to the alkoxide anions to form the carbonate anions, which leads to the smooth ring-opening of CHO rather than backbiting or protonation. If **5** could be added dropwise at the high CO_2 pressure, **6** and **10** with higher molecular weights would be obtained.

2.4 Conclusions

We have achieved terpolymerizations of epoxide, CO_2, and isocyanates or isothiocyanates to synthesize new terpolymers for the first time. These terpolymerizations are fascinating because the reactions can proceed with 100% atom economy if no cyclic byproducts are formed. Herein, CHO was used as an epoxide because of the excellent physical properties of the resulting polycarbonates,[15] while aryl iso(thio)cyanates were used because of the controllable reactivities. The terpolymerization of CHO, CO_2, and isothiocyanates produced poly(carbonate–thioimidocarbonate)s showing degradability for acids and UV light. The ratio of the PTIC to PCHC units in the terpolymers could be controlled by the CO_2 pressure, and the terpolymers had gradient character in composition. A block copolymer, poly(carbonate–*b*–thioimidocarbonate), was also synthesized in a one-pot two-step manner. On the other hand, the terpolymerization of CHO, CO_2, and isocyanates yielded poly(carbonate–urethane)s; the slow addition of isocyanates under atmospheric CO_2 pressure suppressed the formation of cyclic byproducts and enabled the formation of terpolymers with random sequences. It should be noted that all the terpolymerizations were catalyzed by a single catalyst, bifunctional Al^{III} porphyrin **1b**, which demonstrates that cooperative catalysis with the metal center and the tethered quaternary ammonium salts is effective for the conversions of the monomers with different reactivities into the terpolymers. The results reported here will be useful for the design and creation of environmentally benign polymers. Further studies on the application of the polymers and the creation of new CO_2-based polymers are currently underway in our group.

2.5 Experimental Section

[A] General methods.

Instrumentation. NMR spectra were measured on a JEOL ECS400 or ECZ600 spectrometer, and chemical shifts are reported as the delta scale in ppm using an internal reference (δ = 7.26 ppm ($CDCl_3$) or 2.50 ppm (DMSO-d_6) for ^{1}H NMR and δ = 77.16 ppm ($CDCl_3$) for ^{13}C NMR). DOSY was measured with 16 gradient increments using a ledbpgp2s sequence. Size-exclusion chromatography (SEC) was carried out with Shodex KF-804L columns (ϕ 8 mm × 30 cm × 2) using THF as an eluent at 1 mL/min at 40 °C, and molecular weights were calibrated with standard polystyrene samples. IR spectra were recorded on a Shimadzu IRAffinity-1 spectrophotometer. Matrix-assisted laser desorption/ionization time-of-flight (MALDI-TOF) mass spectrometry was measured on a Shimadzu MALDI-8020, while atmospheric pressure chemical ionization (APCI) mass spectrometry was measured on a Thermo Fisher Scientific LTQ Orbitrap XL Hybrid Ion Trap-Orbitrap Mass Spectrometer. High-resolution double-focusing mass spectrometry was measured on a JEOL JMS-700N. The stainless steel autoclave reactors were heated on a EYELA ChemiStation PPV-CTRL1. UV irradiation experiments were done in a quartz cell under N_2 atmosphere with an Asahi Spectra REX-250 fitted with a Hg lamp (250 W).

Materials. Catalysts **1** were prepared according to the reported procedures.[15] Cyclohexene oxide (CHO) was distilled from CaH_2. Aryl isothiocyanates **2** were dried over CaH_2 and distilled under vacuum, while aryl isocyanates **5** were distilled under vacuum. Other reagents were purchased and used without further purification unless otherwise specified. THF containing BHT (250 ppm) as a stabilizer was used as an eluent in SEC, while THF containing no stabilizers was used as solvent in the experiments to test the degradability of polymers upon acid treatment or UV irradiation. Column chromatography on silica gel was performed with BW-127 ZH (Fuji Silysia, 100–270 mesh), while column chromatography on alumina was done with alumina 019-08295 (FUJIFILM Wako Pure Chemical Corporation, 200 mesh).

[B] Terpolymerization of CHO, CO_2, and aryl isothiocyanates.

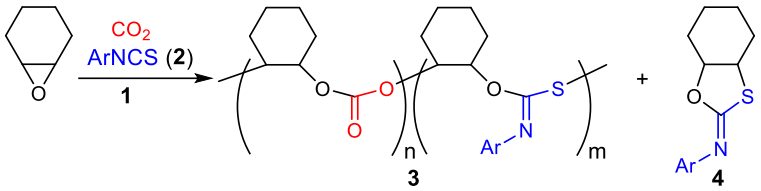

General procedure. Catalyst **1** (amount indicated in the Tables) and a magnetic stirring bar were put in a glass test tube, which was then put in a 50-mL stainless steel autoclave (preheated at 150 °C for a few hours and cooled down), and the reactor was dried under vacuum at 80 °C overnight. The autoclave was put in a glovebox (purge type) under N_2 atmosphere, and aryl isothiocyanate **2** (amount indicated in the Tables) and CHO (amount indicated in the Tables) were added via syringes. The autoclave was closed, and it was taken out from the glovebox and pressurized with CO_2 (2.0 MPa). The mixture was stirred at a constant temperature for a reaction time. The reactor was then cooled in a water bath for 10 min, and excess CO_2 was released carefully in a draft chamber. The reaction mixture was diluted with $CDCl_3$ for ^1H NMR analysis, and dimethyl sulfoxide (DMSO, 50 mg, 0.64 mmol) was added as an internal standard to determine the conversion of CHO, the TON of catalyst **1**, and the amount of byproduct **4**. Aryl isothiocyanate **2** remaining in the reaction mixture was quantified by the ^1H NMR analysis of the $CDCl_3$ solution to which cyclohexylamine was added to convert **2** into the corresponding thiourea in the NMR tube. Terpolymer **3** was isolated by adding the reaction mixture diluted with chloroform (ca. 5 mL) dropwise to methanol (ca. 200 mL) followed by filtration and vacuum drying. The ratio of the PCHC to PTIC units and molecular weights were determined by ^1H NMR and SEC analysis, respectively.

The ratio of the PCHC to PTIC units. The ratio of the PCHC to PTIC units was determined by the ^{1}H NMR spectrum of a crude reaction mixture or a purified polymer. In the case of the crude reaction mixture, the PTIC unit was quantified by the integration of the signals for the aromatic protons (6.5–7.8 ppm) subtracted by that for the aromatic protons of **2** and **4**; the amount of **2** was estimated from the corresponding thiourea formed in the same NMR tube upon addition of cyclohexylamine, while that of **4** was determined by the integration of the signal for methine proton **e** (for example, Figure S1). The PCHC unit was quantified by the integration of the signals at 3.2–5.6 ppm subtracted by that estimated for the PTIC unit and that for **4**. PCHC : PTIC (n : m) = (the integration of the signals for the PCHC unit divided by 2) : (the integration of the signals for the PTIC unit divided by the number of the aromatic protons). In the case of the purified polymer, the PTIC unit was quantified simply by the integration of the signals for the aromatic protons (for example, Figure S6a), while the PCHC unit was quantified by the integration of the signals at 3.2–5.6 ppm subtracted by that estimated for the PTIC unit. The ratio of the PCHC to PTIC units (n : m) was calculated as described for the crude reaction mixture.

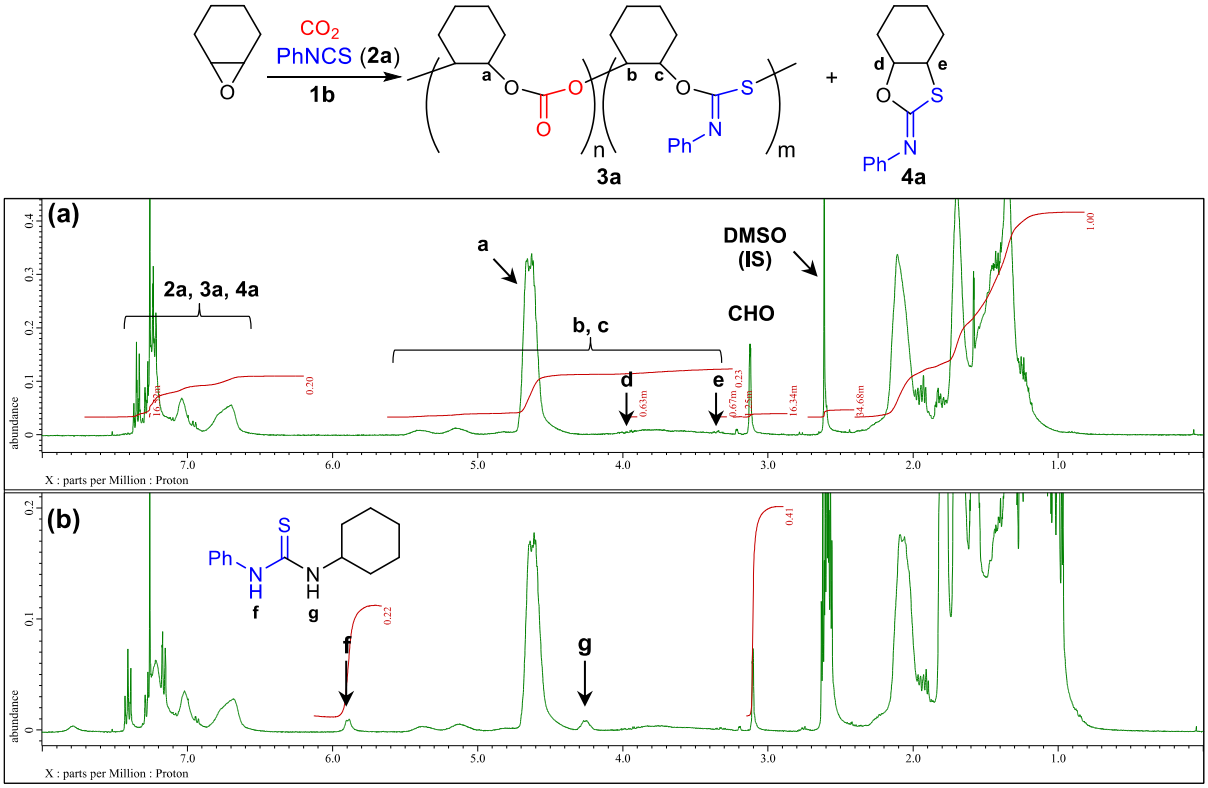

Figure S1. ^{1}H NMR spectra ($CDCl_3$) of crude reaction mixtures (a) after terpolymerization and (b) after the addition of cyclohexylamine (Table 1, entry 1).

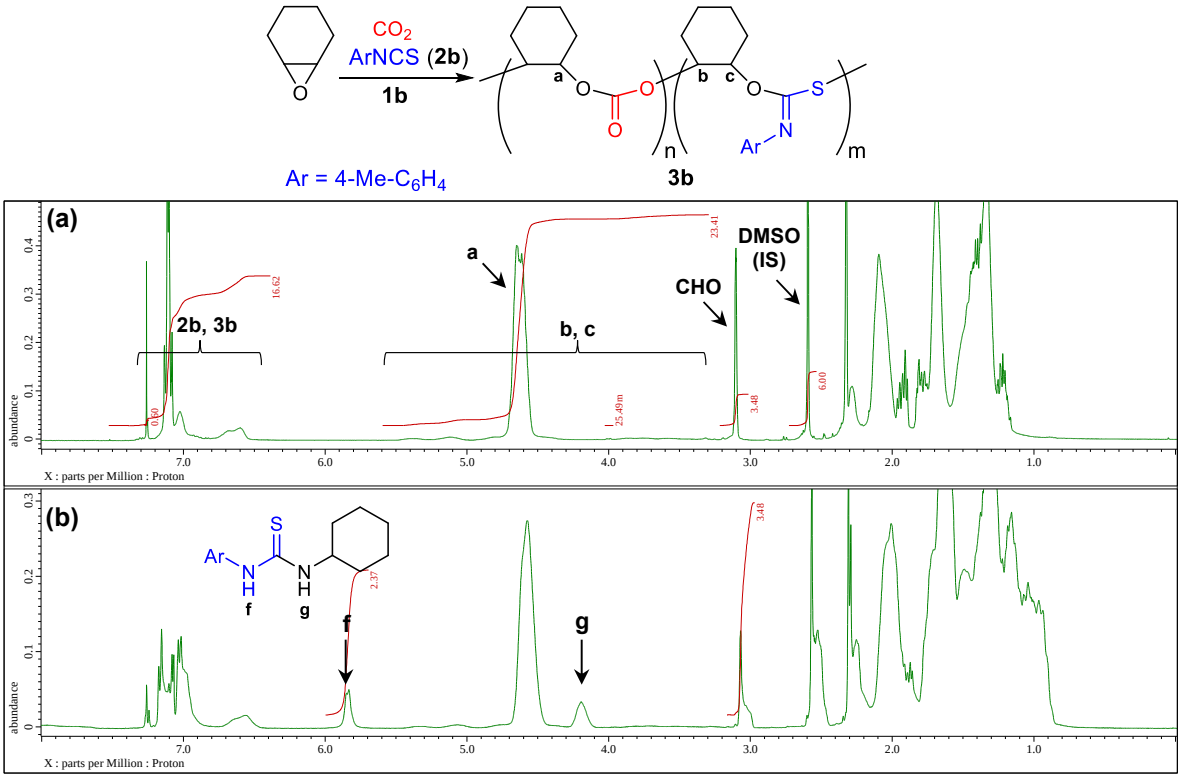

Figure S2. ^{1}H NMR spectra ($CDCl_3$) of the crude reaction mixtures (a) after terpolymerization and (b) after the addition of cyclohexylamine (Table 1, entry 6).

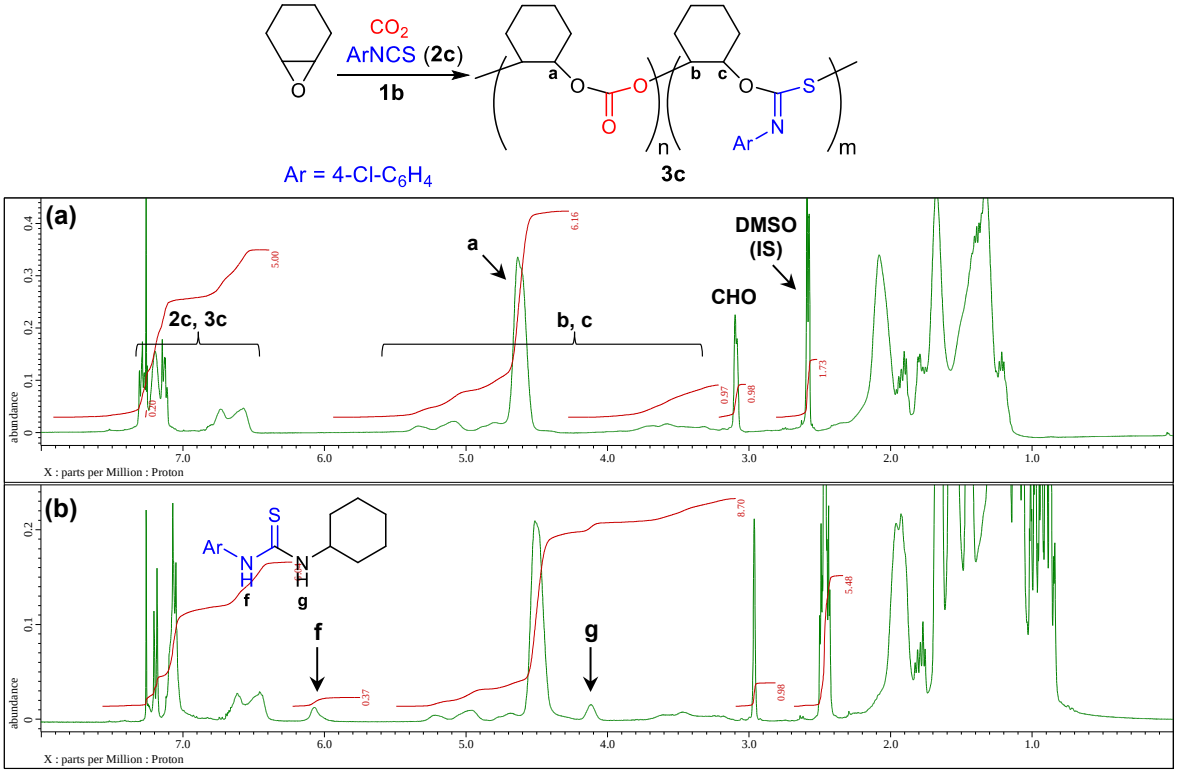

Figure S3. ^{1}H NMR spectra ($CDCl_3$) of the crude reaction mixtures (a) after terpolymerization and (b) after the addition of cyclohexylamine (Table 1, entry 7).

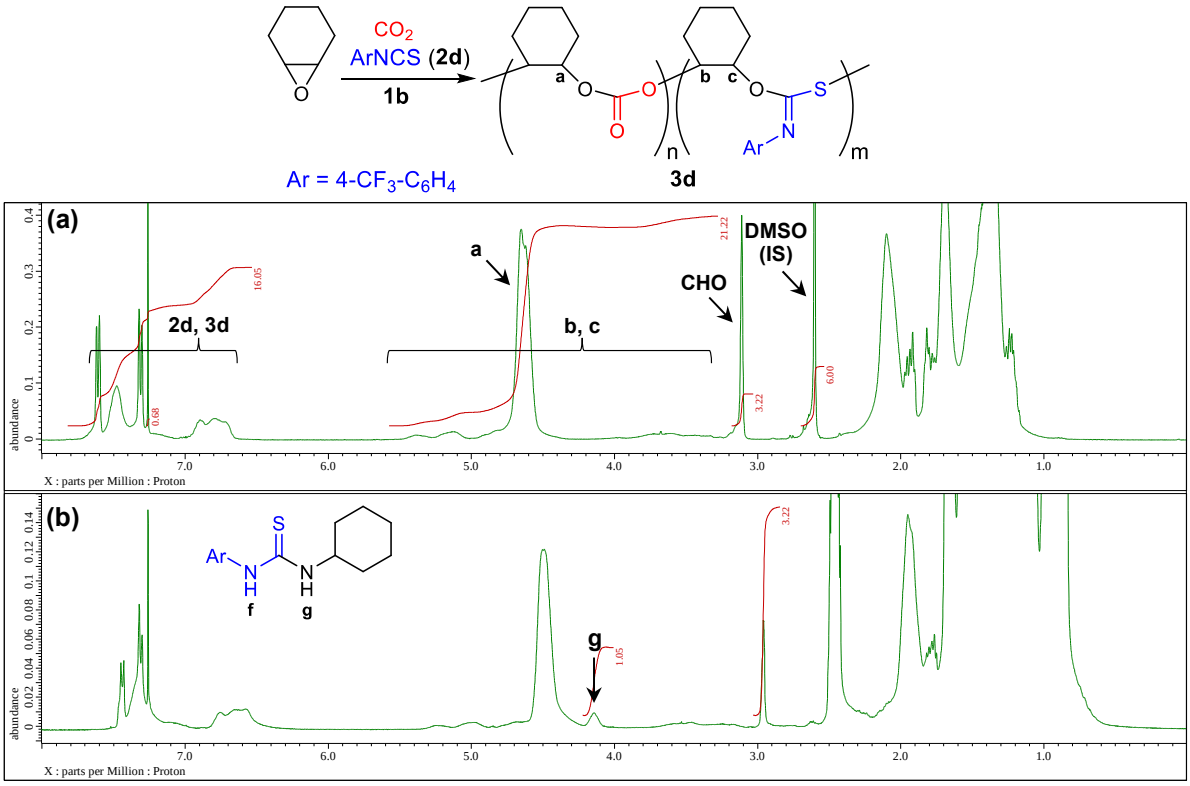

Figure S4. ^{1}H NMR spectra ($CDCl_3$) of the crude reaction mixtures (a) after terpolymerization and (b) after the addition of cyclohexylamine (Table 1, entry 8).

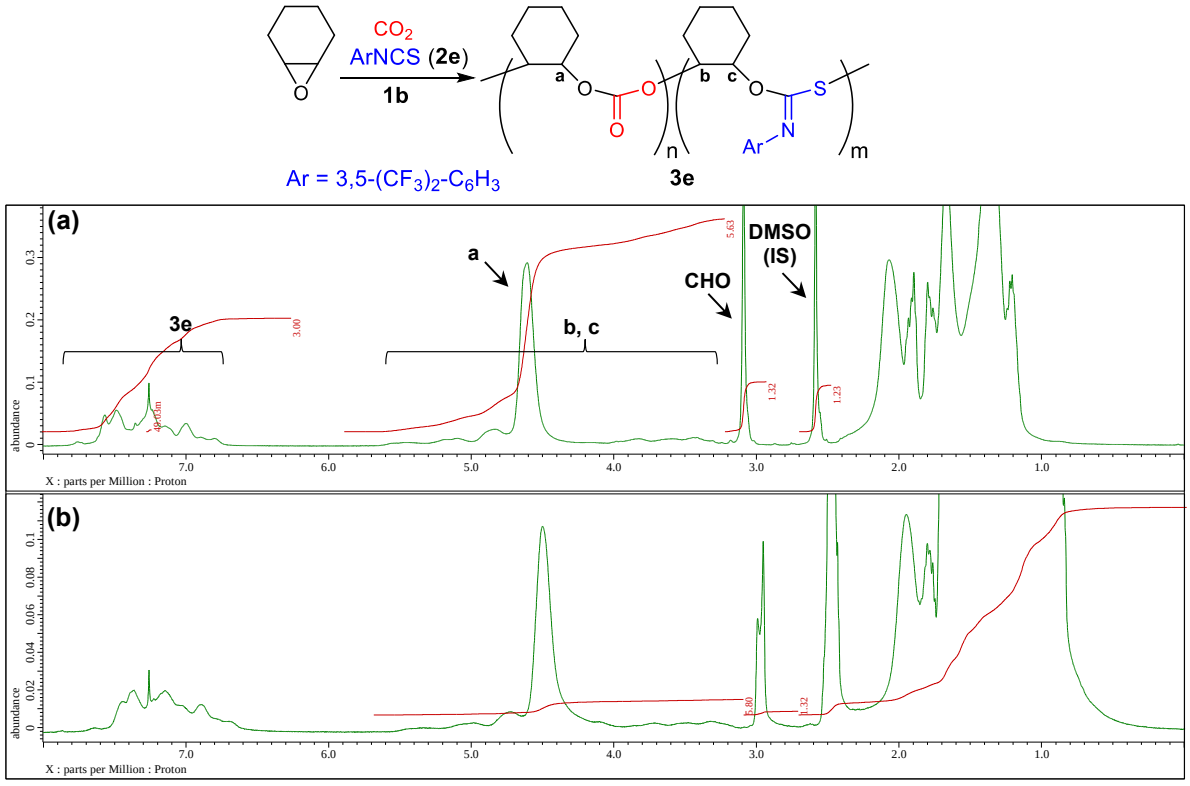

Figure S5. ^{1}H NMR spectra ($CDCl_3$) of the crude reaction mixtures (a) after terpolymerization and (b) after the addition of cyclohexylamine (Table 1, entry 9).

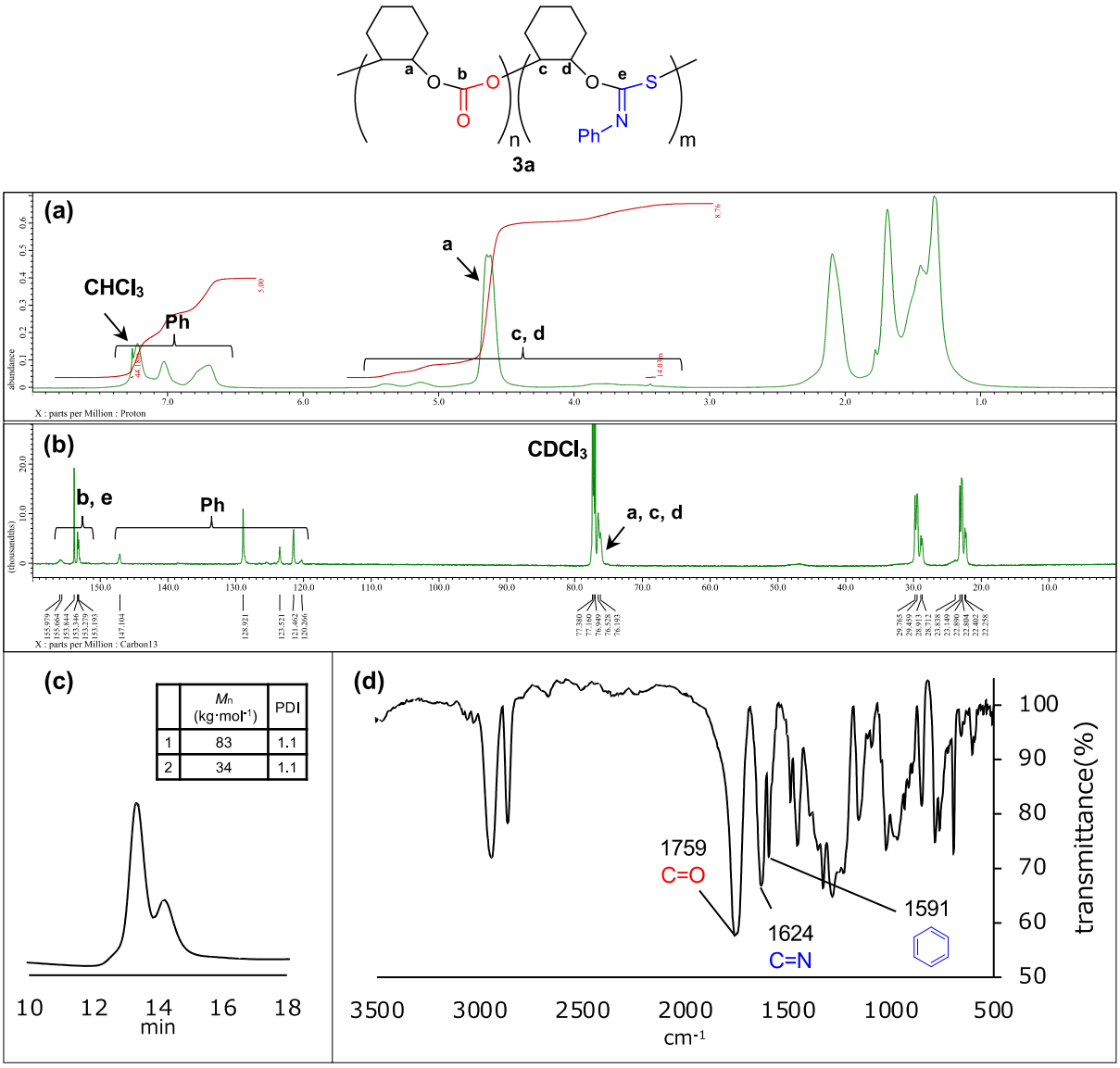

Figure S6. (a) ^{1}H NMR spectrum ($CDCl_3$), (b) ^{13}C NMR spectrum ($CDCl_3$), (c) SEC chart, and (d) IR spectrum of purified polymer **3a** (Table 1, entry 1).

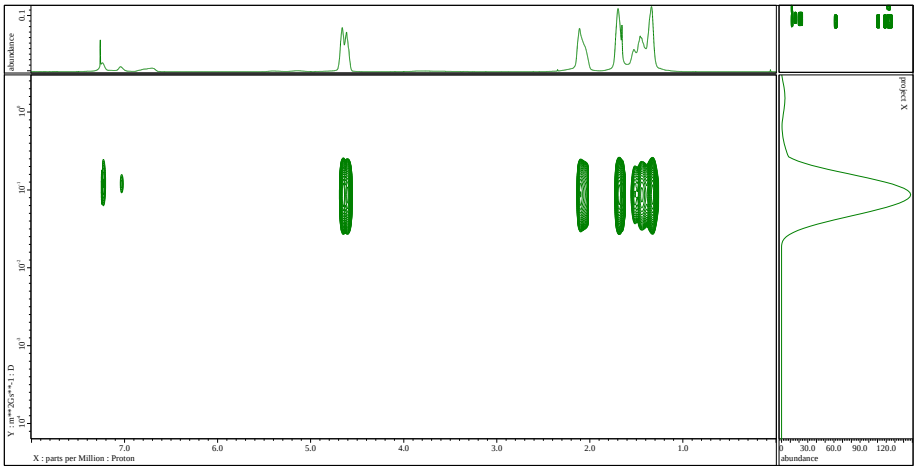

Figure S7. DOSY spectrum ($CDCl_3$) of purified polymer **3a**.

MALDI-TOF mass spectrum of terpolymer 3a. Terpolymer **3a** for the measurement of MALDI-TOF mass spectrometry was obtained according to the following procedure. Catalyst **1b** (2.07 mg, 1.00 μmol, 0.016 mol%), CHO (606 mg, 6.17 mmol), and **2a** (170 mg, 1.26 mmol) were put in a glass test tube, which was then put in a 50-mL stainless steel autoclave. The autoclave was pressurized with CO_2 (0.5 MPa), and the mixture was stirred at 90 °C for 20 h. The reactor was then cooled in a water bath for 10 min, and excess CO_2 was released carefully. The terpolymer was isolated by adding the reaction mixture diluted with chloroform dropwise to methanol followed by filtration and vacuum drying.

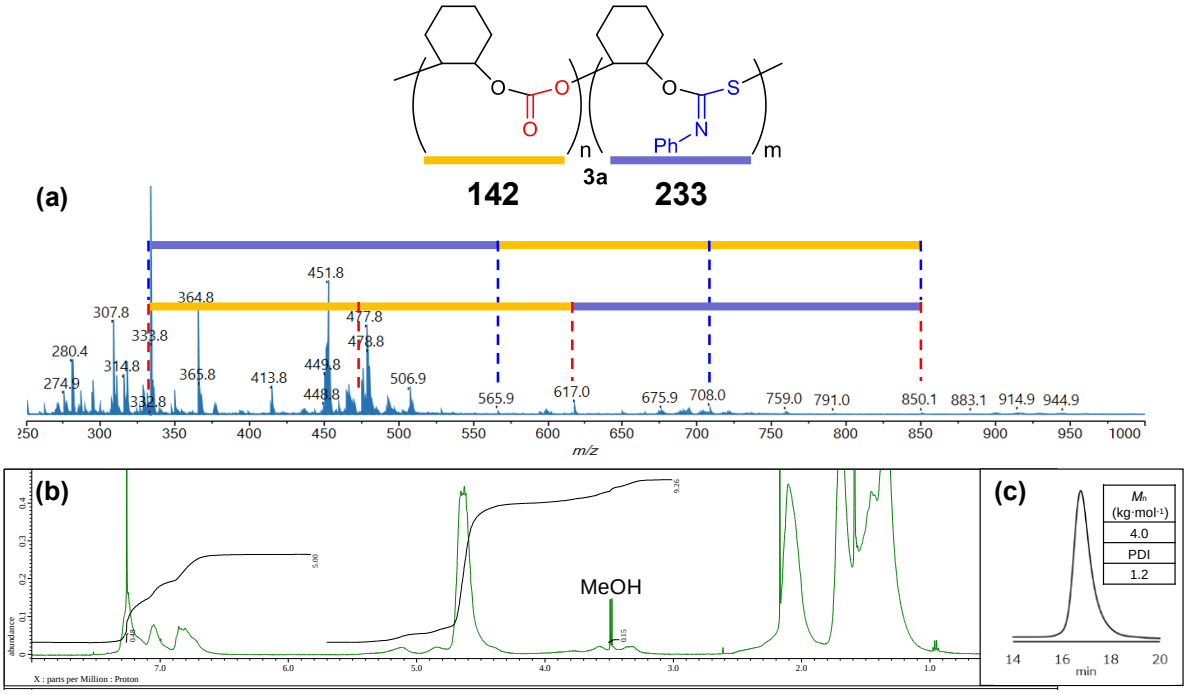

Figure S8. (a) MALDI-TOF mass spectrum, (b) ^1H NMR spectrum ($CDCl_3$), and (c) SEC chart of terpolymer **3a**.

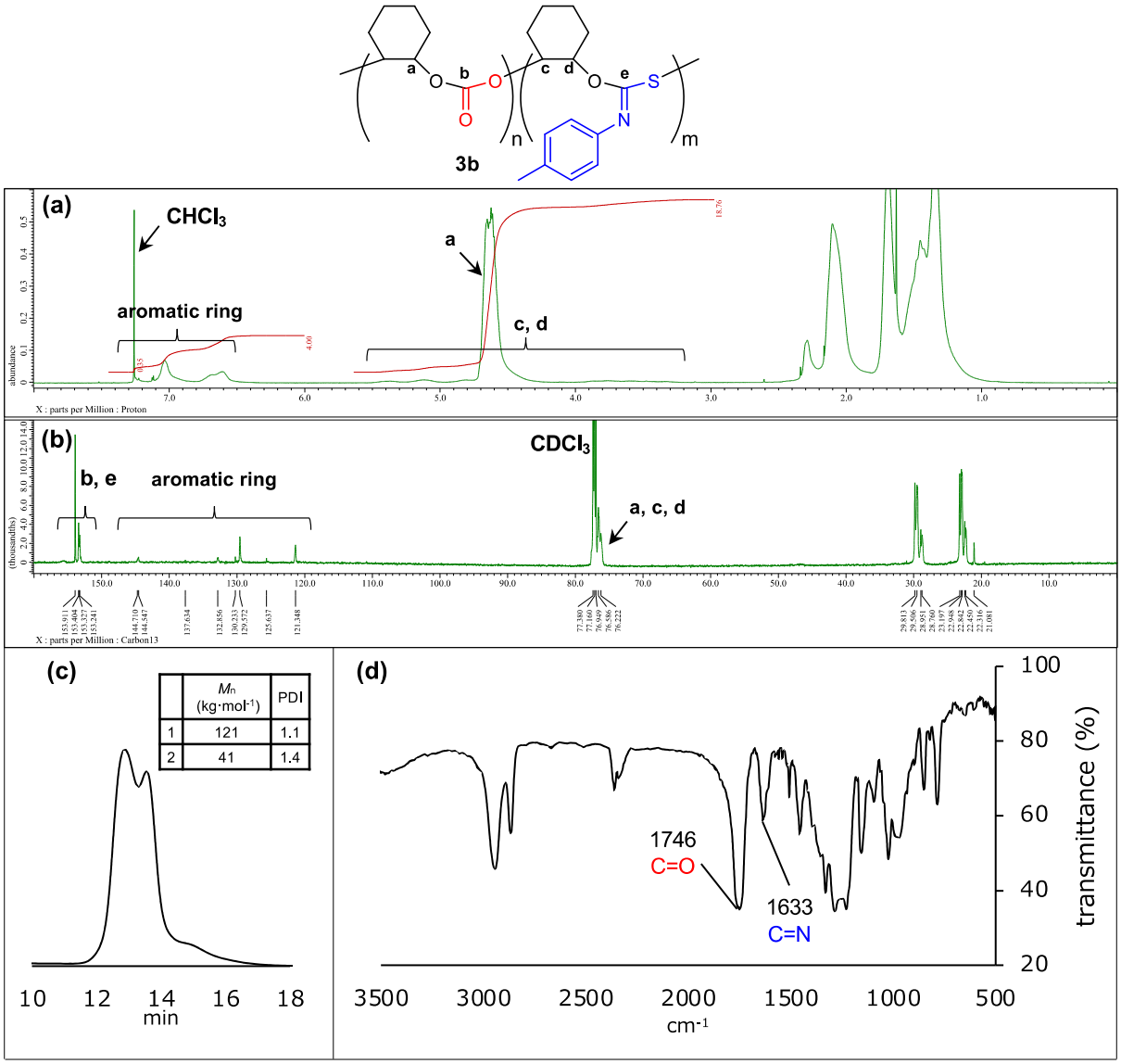

Figure S9. (a) ^{1}H NMR spectrum ($CDCl_3$), (b) ^{13}C NMR spectrum ($CDCl_3$), (c) SEC chart, and (d) IR spectrum of purified polymer **3b** (Table 1, entry 6).

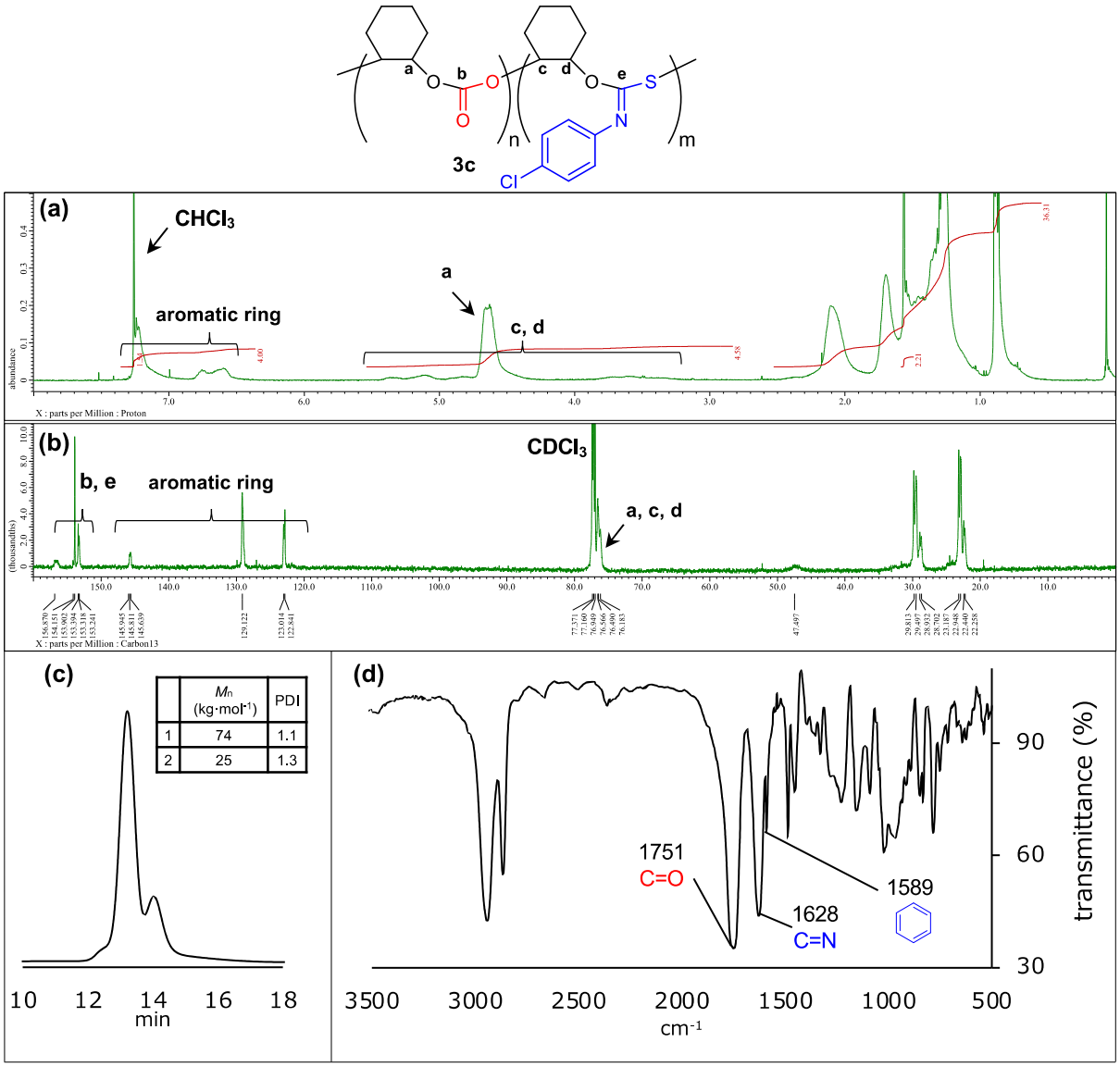

Figure S10. (a) ^{1}H NMR spectrum ($CDCl_3$), (b) ^{13}C NMR spectrum ($CDCl_3$), (c) SEC chart, and (d) IR spectrum of purified polymer **3c** (Table 1, entry 7).

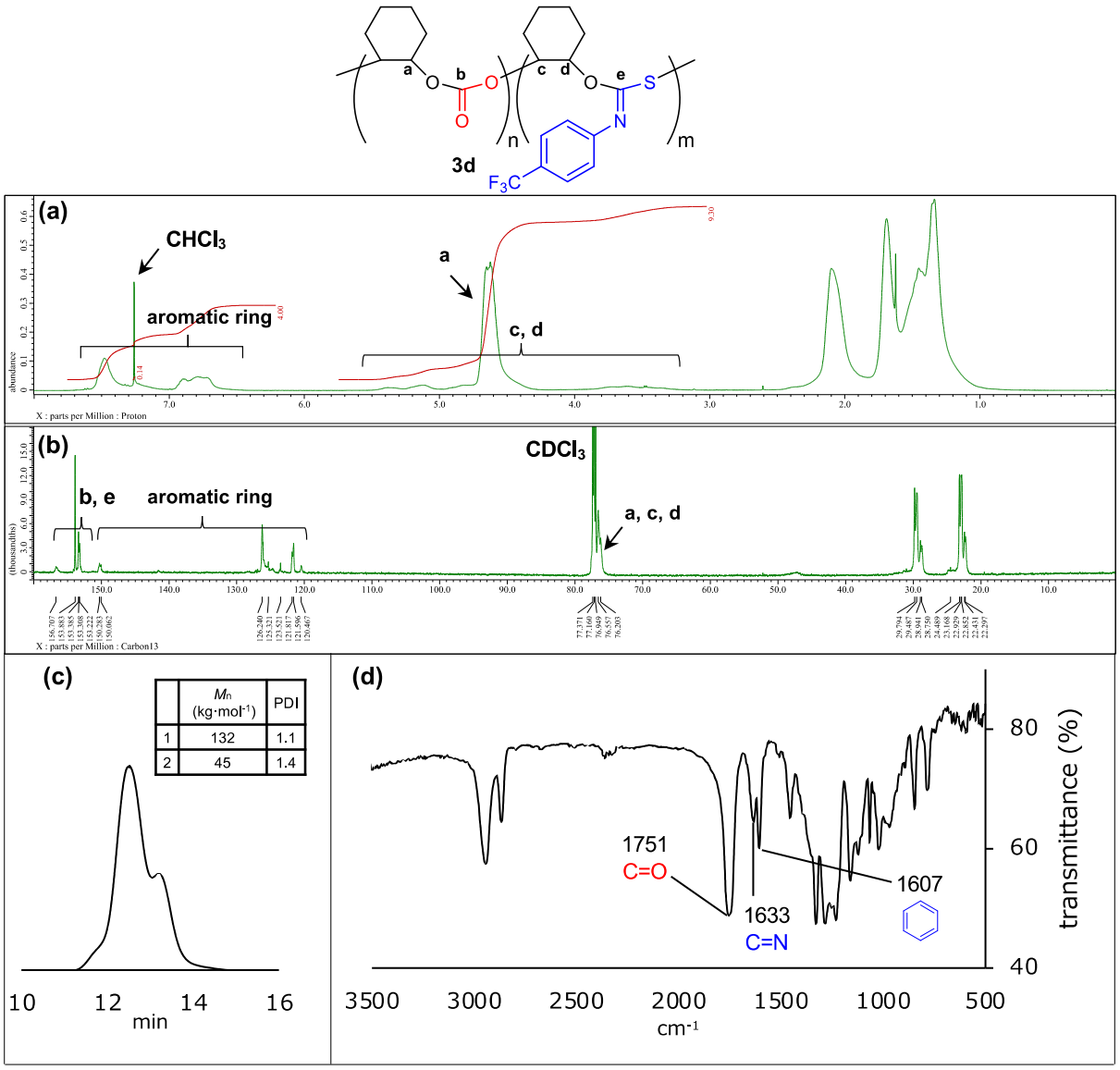

Figure S11. (a) ^{1}H NMR spectrum ($CDCl_3$), (b) ^{13}C NMR spectrum ($CDCl_3$), (c) SEC chart, and (d) IR spectrum of purified polymer **3d** (Table 1, entry 8).

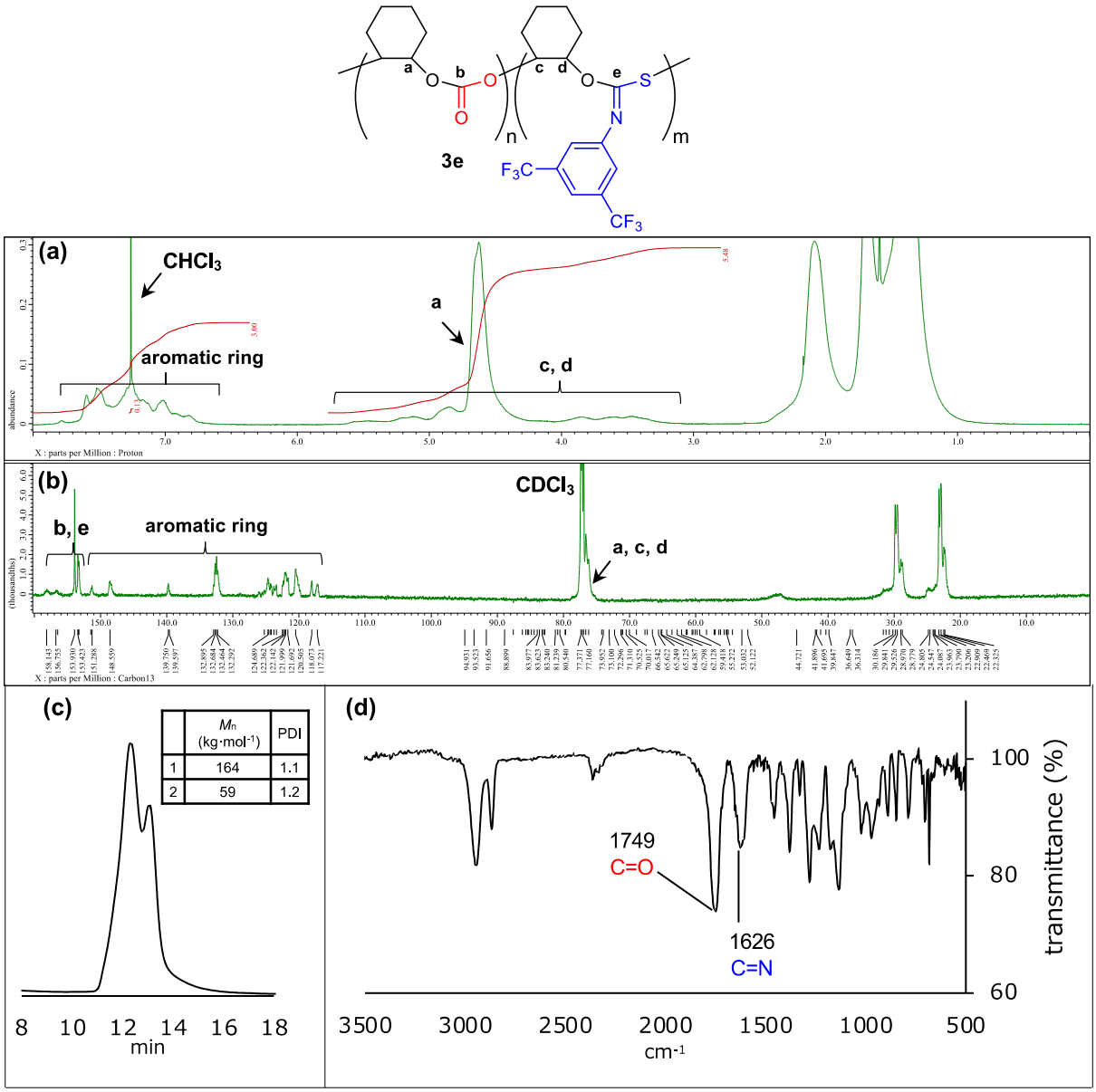

Figure S12. (a) ^{1}H NMR spectrum ($CDCl_3$), (b) ^{13}C NMR spectrum ($CDCl_3$), (c) SEC chart, and (d) IR spectrum of purified polymer **3e** (Table 1, entry 9).

Characterization of 4a. Byproduct **4a** was isolated from the reaction mixture of the terpolymerization of CHO, CO_2, and **2a** by means of silica gel column chromatography (hexane/EtOAc = 7/3).

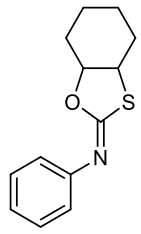

4a

White solid; mp 88–92 °C; ^{1}H NMR ($CDCl_3$, 400 MHz) δ 1.34–1.70 (m, 4H), 1.87 (d, J = 12.3 Hz, 1H), 1.96 (d, J = 14.6 Hz, 1H), 2.13 (d, J = 8.7 Hz, 1H), 2.36 (dd, J = 3.9, 12.1 Hz, 1H), 3.34 (dt, J = 3.7, 11.4 Hz, 1H), 3.94 (dt, J = 4.0, 11.2 Hz, 1H), 6.96 (d, J = 7.3 Hz, 2H), 7.10 (t, J = 7.3 Hz, 1H), 7.31 (t, J = 7.8 Hz, 2H); ^{13}C NMR ($CDCl_3$, 100 MHz) δ 23.9, 25.2, 28.8, 29.7, 52.9, 87.3, 121.4, 124.3, 129.2, 149.0, 163.0; IR (KBr) 2938, 2864, 1645, 1589, 1483, 1447, 1362, 1265, 1213, 1206, 1150, 1103, 1087, 1042, 1026, 972, 881, 766, 692, 675, 637, 600, 579 cm^{-1}; HRMS (EI) calcd for $C_{13}H_{15}NOS$ 233.0874, found 233.0874 (M^+).

[C] Synthesis and characterization of a model compound for terpolymer 3a.

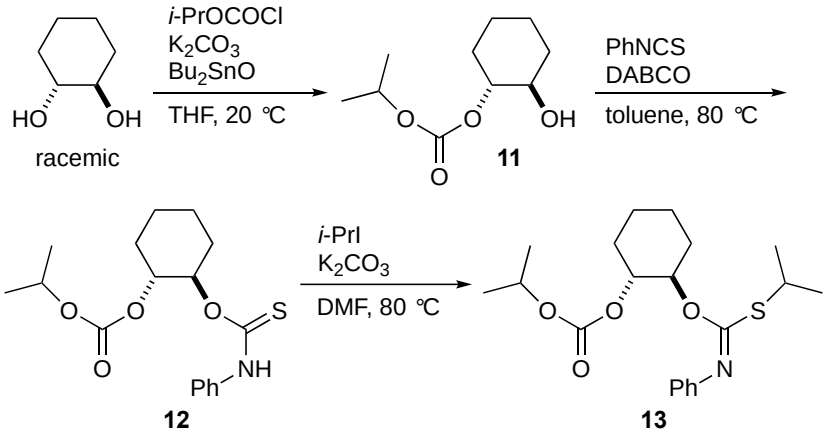

Synthesis of 11. *trans*-1,2-Cyclohexanediol (234 mg, 2.01 mmol), K_2CO_3 (336 mg, 2.43 mmol), and Bu_2SnO (5.2 mg, 0.021 mmol) were put in a flask (25 mL), and the mixture was dried under vacuum at room temperature for 2 h. Dry THF (4.0 mL) and isopropyl chloroformate (468 µL, 4.12 mmol) were added at 20 °C under N_2, and the mixture was stirred at 20 °C for 20 h. The mixture was diluted with EtOAc, washed with water, and dried over Na_2SO_4. Purification by silica gel column chromatography (hexane/EtOAc = 3/1) followed by alumina column chromatography (hexane/EtOAc = 3/1) gave **11** as a colorless oil (382 mg, 1.89 mmol, 94%). ^{1}H NMR ($CDCl_3$, 400 MHz) δ 1.14–1.40 (m, 10H), 1.67–1.73 (m, 2H), 1.99–2.14 (m, 2H), 2.49 (s, 1H), 3.50–3.60 (m, 1H), 4.35–4.43 (m, 1H), 4.82–4.90 (m, 1H); ^{13}C NMR ($CDCl_3$, 100 MHz) δ 21.9, 23.8, 23.9, 30.0, 32.9, 72.1, 72.6, 81.8, 154.7; IR (neat) 3445, 2982, 2940, 2864, 1740, 1456, 1375, 1261, 1094, 995, 916, 831, 791 cm^{-1}; HRMS (FAB) calcd for $C_{10}H_{19}O_4$ 203.1283, found 203.1283 ([M + H]$^+$).

Synthesis of 12. To a solution of **11** (818 mg, 4.04 mmol) and DABCO (456 mg, 4.07 mmol) in dry toluene (4.0 mL) was added phenyl isothiocyanate (1.46 mL, 12.3 mmol) under N_2, and the mixture was stirred at 80 °C for 48 h. The mixture was diluted with EtOAc, washed with water, and dried over Na_2SO_4. Purification by silica gel column chromatography (hexane/EtOAc = 8/1) gave **12** as a white

solid (625 mg, 1.85 mmol, 46%). mp 137–142 °C; ^{1}H NMR ($CDCl_3$, 400 MHz, 40 °C) δ 1.20–1.58 (m, 10H), 1.72–1.78 (m, 2H), 2.09–2.16 (m, 1H), 2.40 (s, 1H), 4.68–4.89 (m, 2H), 5.42–5.48 (m, 1H), 7.14–7.37 (m, 5H), 8.16 (s, 1H); ^{13}C NMR ($CDCl_3$, 150 MHz, 40 °C) δ 21.8, 21.9, 23.2, 23.4, 29.8, 30.2, 72.1, 76.7, 82.1, 122.0, 125.7, 129.1, 137.2, 154.3, 187.9; IR (KBr) 3231, 3075, 2945, 1732, 1597, 1553, 1495, 1414, 1360, 1302, 1267, 1213, 1188, 1094, 1034, 1001, 793, 748 cm^{-1}; HRMS (EI) calcd for $C_{17}H_{23}NO_4S$ 337.1348, found 337.1344 (M^+).

Synthesis of 13. Compound **12** (339 mg, 1.01 mmol) and K_2CO_3 (280 mg, 2.03 mmol) were put in a flask (25 mL), and the mixture was dried under vacuum at room temperature for 2 h. Dry DMF (1.0 mL) and 2-iodopropane (312 µL, 3.14 mmol) were added under N_2, and the mixture was stirred at 80 °C for 4 h. The mixture was diluted with EtOAc, washed with water, and dried over Na_2SO_4. Purification by silica gel column chromatography (hexane/EtOAc = 12/1) gave **13** as a slightly yellow solid (360 mg, 0.950 mmol, 94%). mp 50–52 °C; ^{1}H NMR ($CDCl_3$, 600 MHz) δ 1.25–1.33 (m, 12H), 1.35–1.62 (m, 4H), 1.74–1.78 (m, 2H), 2.12–2.15 (m, 1H), 2.49–2.51 (m, 1H), 3.59–3.65 (m, 1H), 4.83–4.92 (m, 2H), 5.12–5.16 (m, 1H), 6.85–6.86 (m, 2H), 7.05 (t, J = 7.6 Hz, 1H), 7.28 (t, J = 7.8 Hz, 2H); ^{13}C NMR ($CDCl_3$, 150 MHz) δ 21.90, 21.93, 23.4, 23.6, 23.8, 24.0, 29.6, 30.4, 36.2, 72.0, 77.3, 121.6, 123.6, 129.0, 147.5, 154.4, 157.2; IR (KBr) 2980, 2941, 2866, 1740, 1626, 1595, 1489, 1454, 1385, 1366, 1267, 1163, 1094, 1024, 982, 912, 766, 696 cm^{-1}; HRMS (EI) calcd for $C_{20}H_{29}NO_4S$ 379.1817, found 379.1817 (M^+).

Comparison of ^{1}H NMR spectra of 3a and model compound 13.

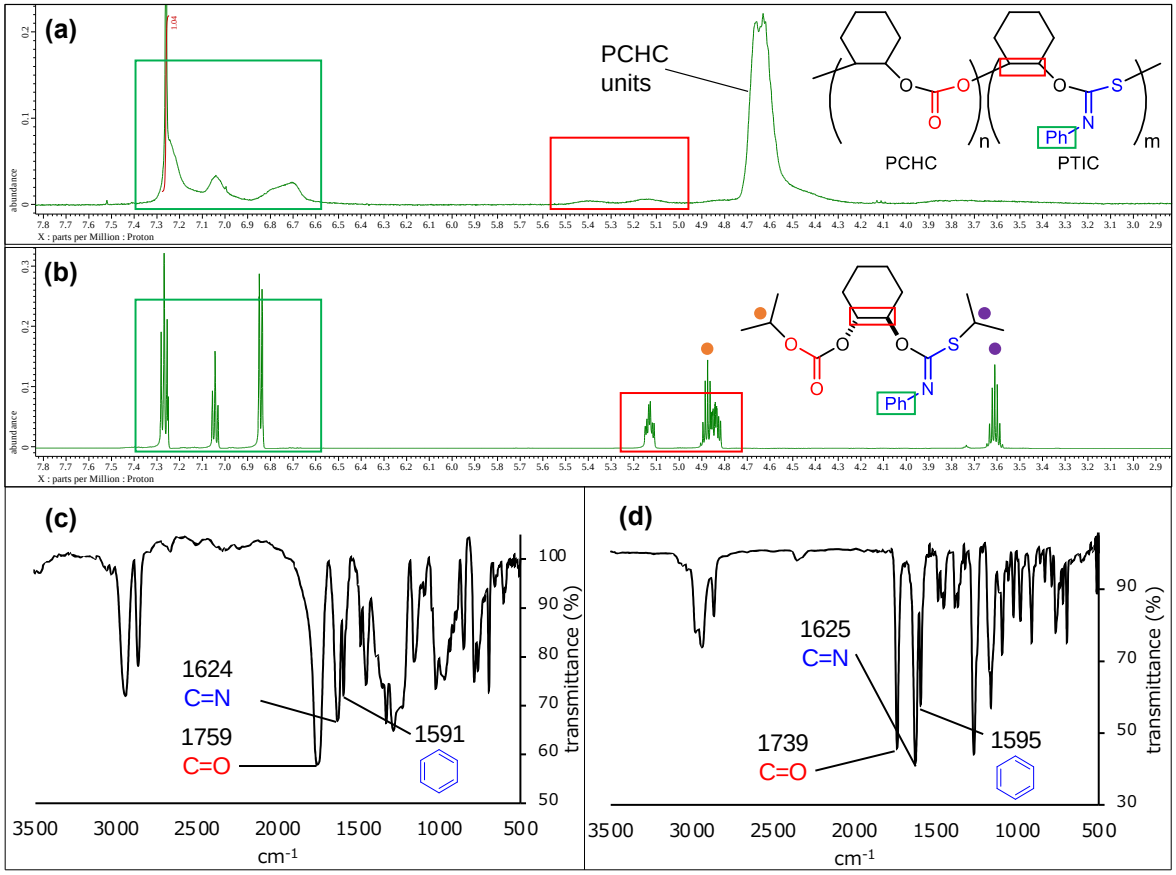

Figure S13. ^{1}H NMR spectra ($CDCl_3$) of (a) purified terpolymer **3a** and (b) model compound **13**. IR spectra of (c) purified terpolymer **3a** and (d) model compound **13**.

[D] Kinetic studies.

The time courses of the terpolymerizations of CHO (12.5 mmol), CO_2 (2.0 MPa), and **2a** or **2d** (3.1 mmol) with **1b** (S/C = 40000 for CHO) were monitored. The reaction mixture was diluted with $CDCl_3$, and the conversion of CHO and the amount of polymers were determined by ^1H NMR analysis. The conversion of **2** was determined by the ^1H NMR analysis of the $CDCl_3$ solution that was treated with cyclohexylamine to convert **2** into the corresponding thiourea in the NMR tube.

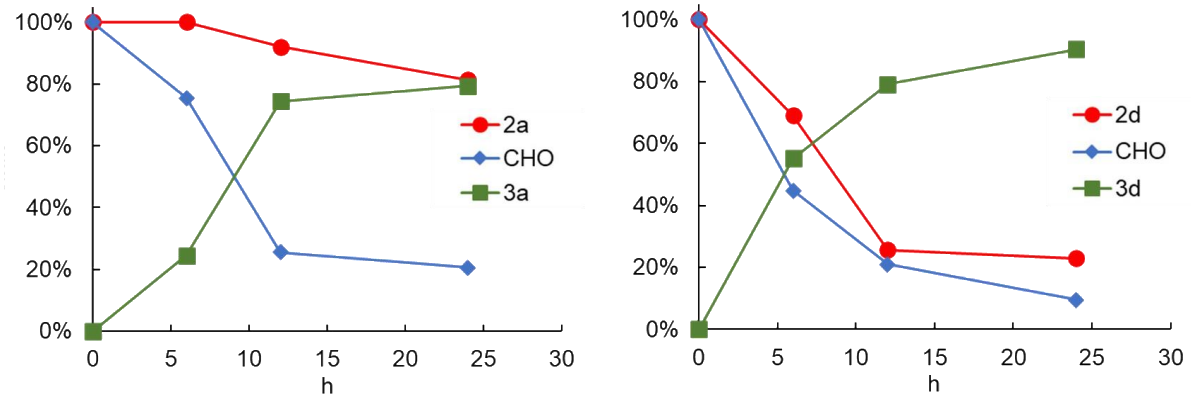

Figure S14. Plots of the conversions and the yields in the terpolymerizations of CHO, CO_2, and **2a** or **2d**.

[E] Terpolymerization of CHO, CO_2, and aryl isocyanates.

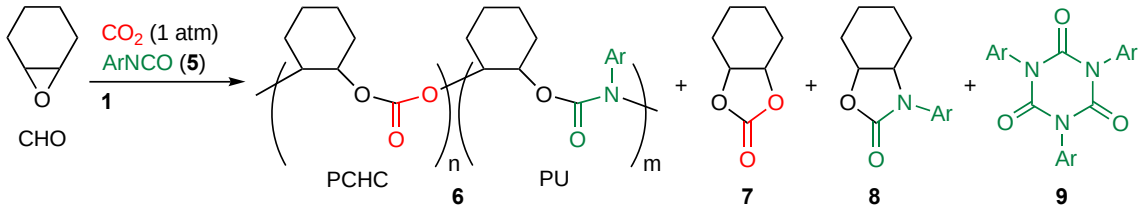

General procedure. Catalyst **1** (amount indicated in the Tables) and a magnetic stirring bar were put in a Schlenk flask (30 mL), and the flask was dried under vacuum at 80 °C overnight. The flask was put in a glovebox (purge type) under N_2 atmosphere, and CHO (amount indicated in the Tables) was added via syringe. The flask was taken out from the glovebox. A CO_2 balloon (1 atm, approximately 2.8 L) was attached to the flask, and the flask was quickly evacuated and filled with CO_2. A mixture of **5** (amount indicated in the Tables) and CHO (amount indicated in the Tables) was added dropwise via syringe at a constant rate with a syringe-pump to the mixture of CHO and **1** at a constant temperature under CO_2, and the mixture was further stirred for 2 h. The reaction mixture was cooled to room temperature and diluted with $CDCl_3$ for ^1H NMR analysis, and mesitylene (50 mg, 0.42 mmol) was added as an internal standard to determine the conversion of CHO, TON, and the amounts of byproducts **7**,[21] **8**,[22] and **9**[23]. The conversion of **5** was determined by the ^1H NMR analysis of the $CDCl_3$ solution that was treated with cyclohexylamine at room temperature to convert **5** into the corresponding urea in the NMR tube. Terpolymer **6** was isolated by adding the reaction mixture diluted with chloroform (ca. 2.5 mL) dropwise to methanol (ca. 150 mL) followed by filtration and vacuum drying. The ratio of the PCHC to PU units and the molecular weight were determined by ^1H NMR and SEC analysis of the isolated terpolymer, respectively.

The ratio of the PCHC to PU units. The ratio of the PCHC to PU units was determined by the ^{1}H NMR spectrum of a purified polymer. The PU unit was quantified simply by the integration of the signals for the aromatic protons (for example, Figure S20a), while the PCHC unit was quantified by the integration of the signals at 3.2–5.2 ppm subtracted by that for the PU unit. The ratio of the PCHC to PTIC units (n : m) was calculated as follows: PCHC : PU (n : m) = (the integration of the signals for the PCHC units divided by 2) : (the integration of the signals for the PU units divided by the number of aromatic protons).

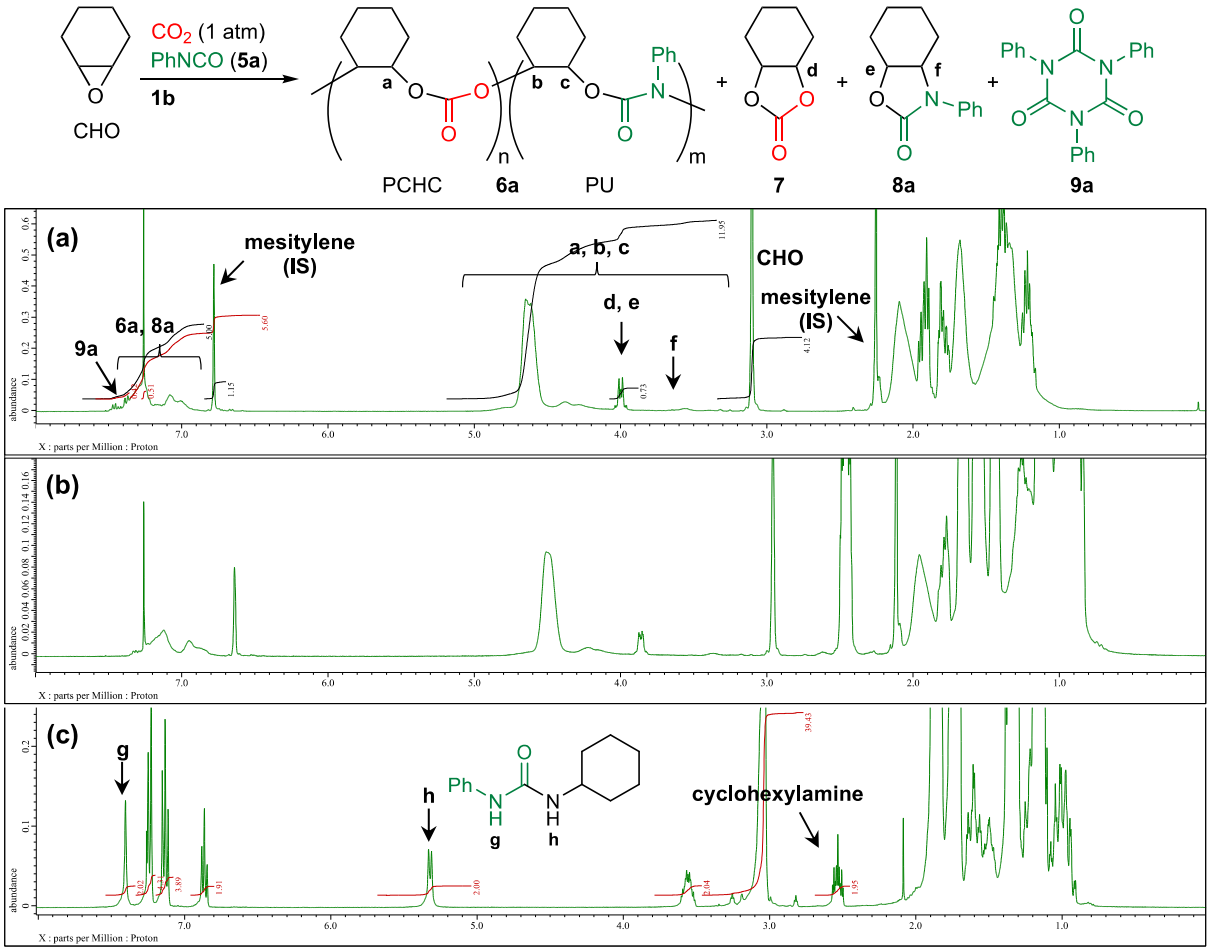

Figure S15. ^{1}H NMR spectra ($CDCl_3$) of the crude reaction mixture (a) after terpolymerization and (b) after the addition of cyclohexylamine (Table 2, entry 1). (c) An example of the ^{1}H NMR spectrum of a mixture of CHO, **5a**, and cyclohexylamine in $CDCl_3$.

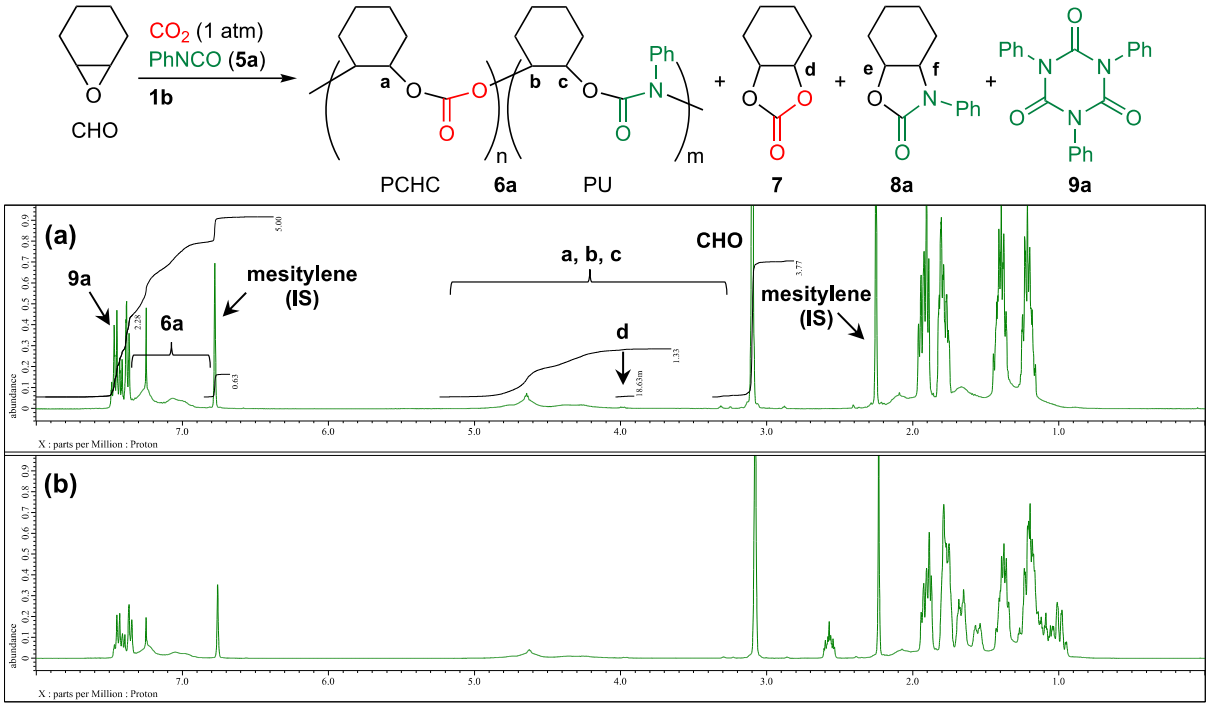

Figure S16. ^{1}H NMR spectra ($CDCl_3$) of the crude reaction mixture (a) after terpolymerization and (b) after the addition of cyclohexylamine (Table S3, entry 7).

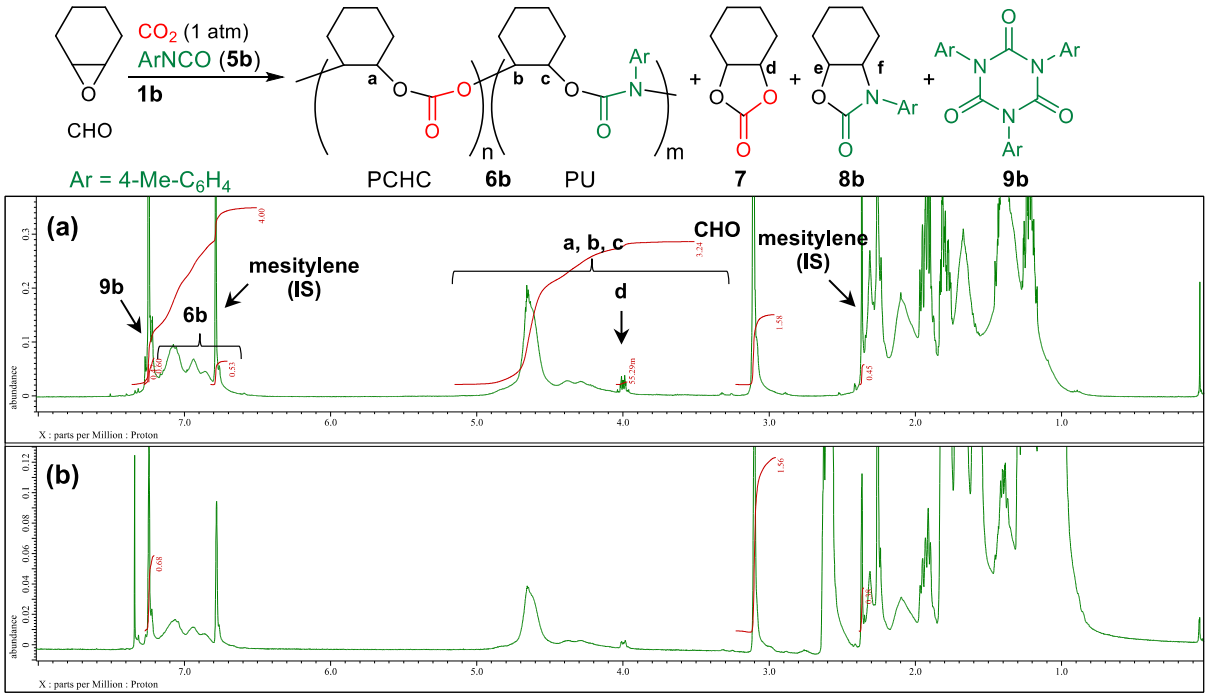

Figure S17. ^{1}H NMR spectra ($CDCl_3$) of the crude reaction mixture (a) after terpolymerization and (b) after the addition of cyclohexylamine (Table 2, entry 2).

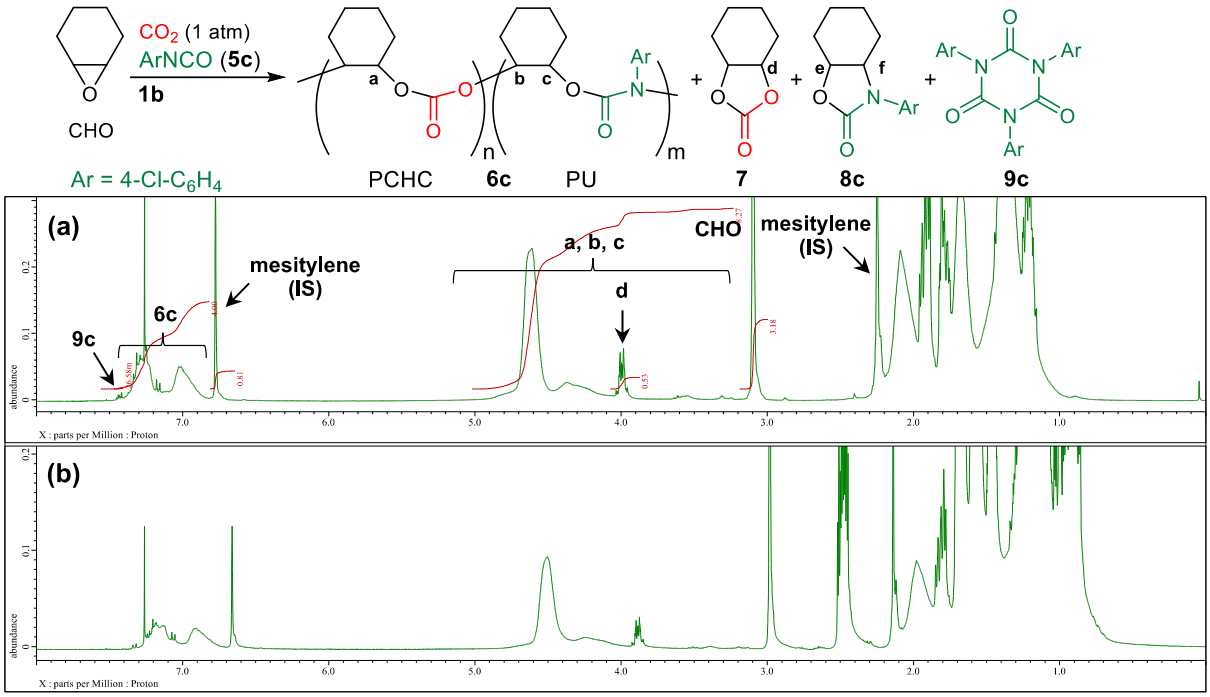

Figure S18. ^{1}H NMR spectra ($CDCl_3$) of the crude reaction mixture (a) after terpolymerization and (b) after the addition of cyclohexylamine (Table 2, entry 3).

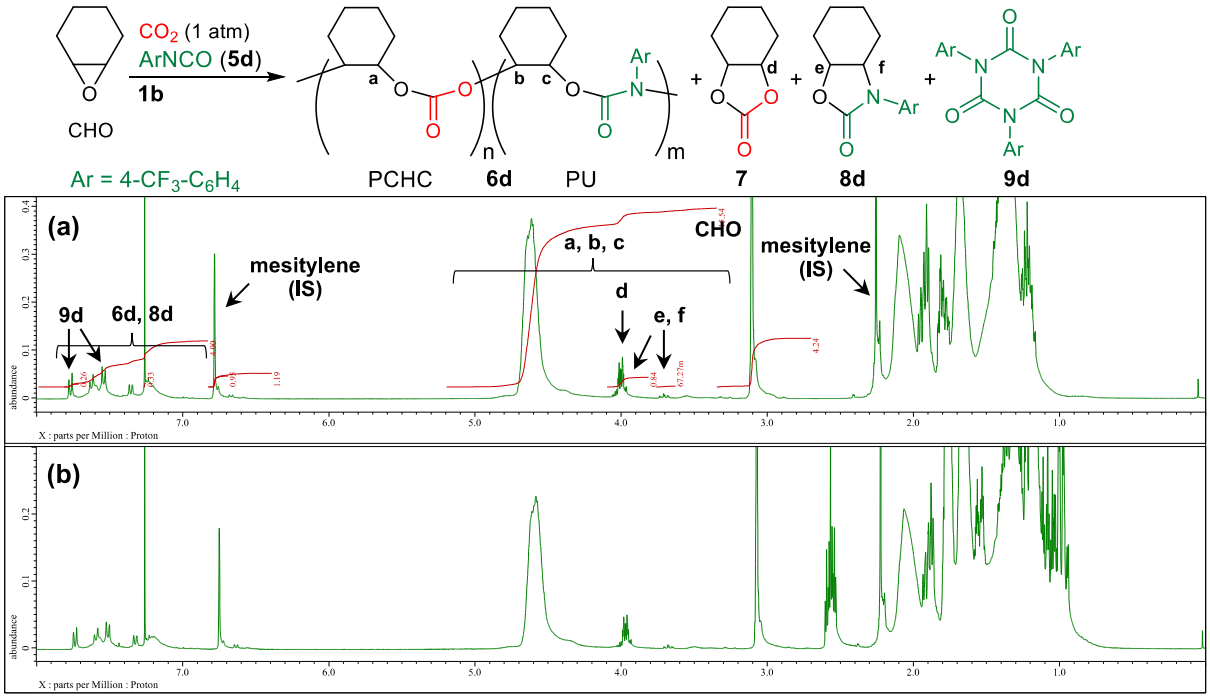

Figure S19. ^{1}H NMR spectra ($CDCl_3$) of the crude reaction mixture (a) after terpolymerization and (b) after the addition of cyclohexylamine (Table 2, entry 4).

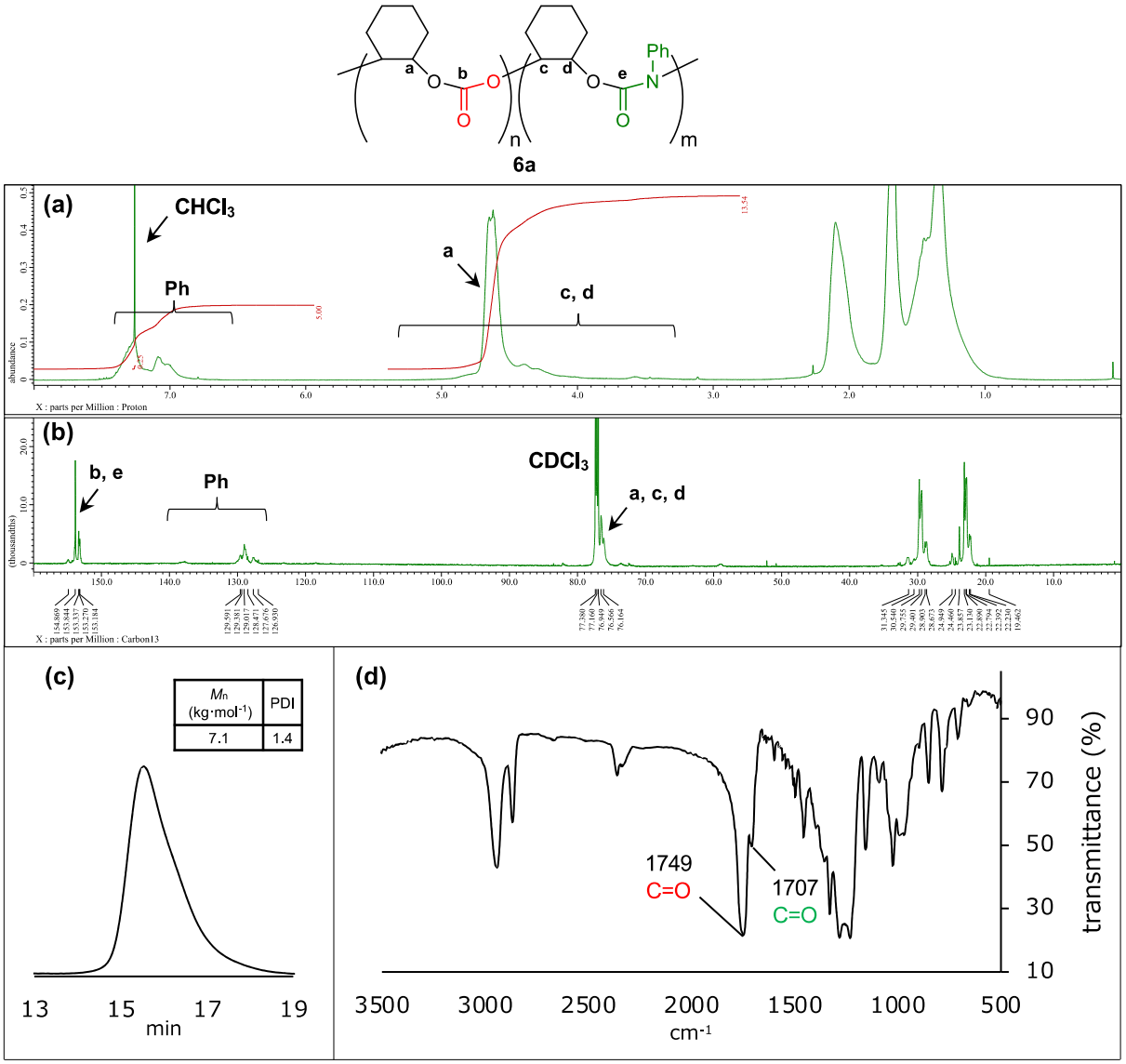

Figure S20. (a) ^{1}H NMR spectrum ($CDCl_3$), (b) ^{13}C NMR spectrum ($CDCl_3$), (c) SEC chart, and (d) IR spectrum of purified polymer **6a** (Table 2, entry 1).

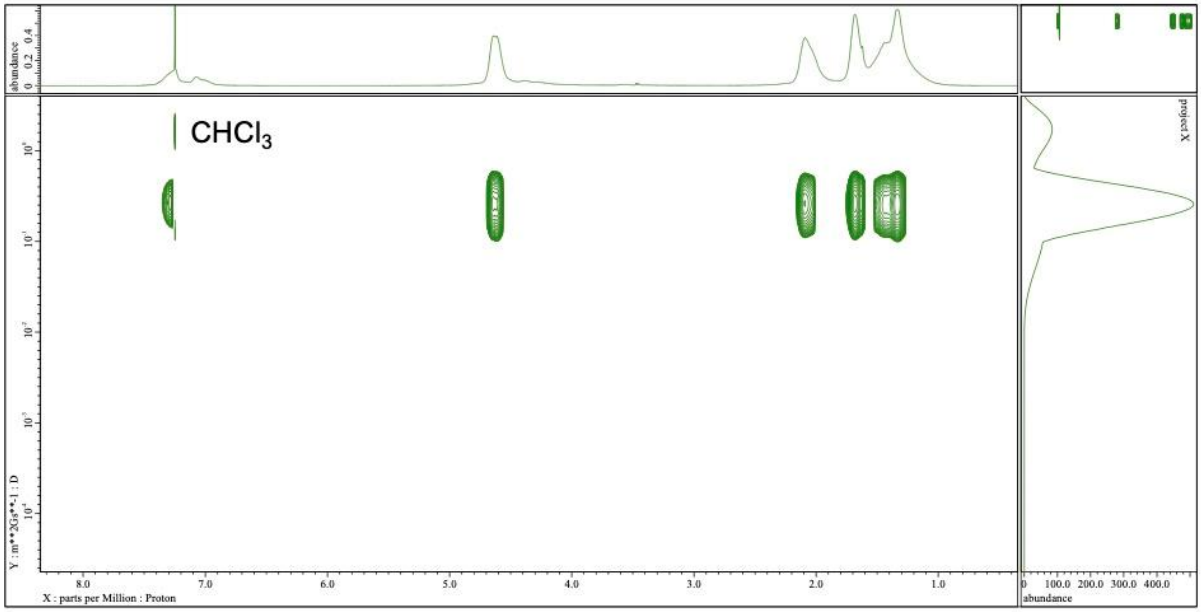

Figure S21. DOSY spectrum ($CDCl_3$) of purified polymer **6a**.

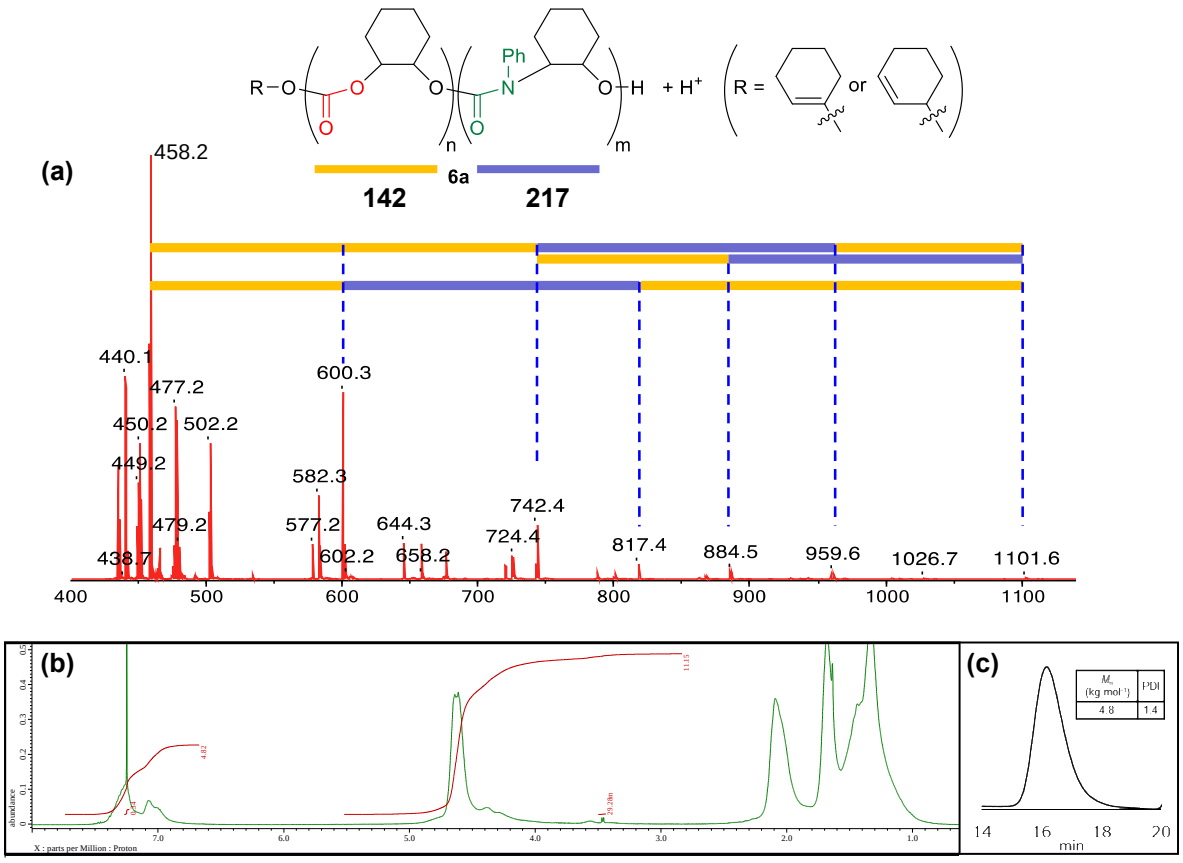

Figure S22. (a) MALDI-TOF mass spectrum, (b) ^1H NMR spectrum ($CDCl_3$), and (c) SEC chart of terpolymer **6a**.

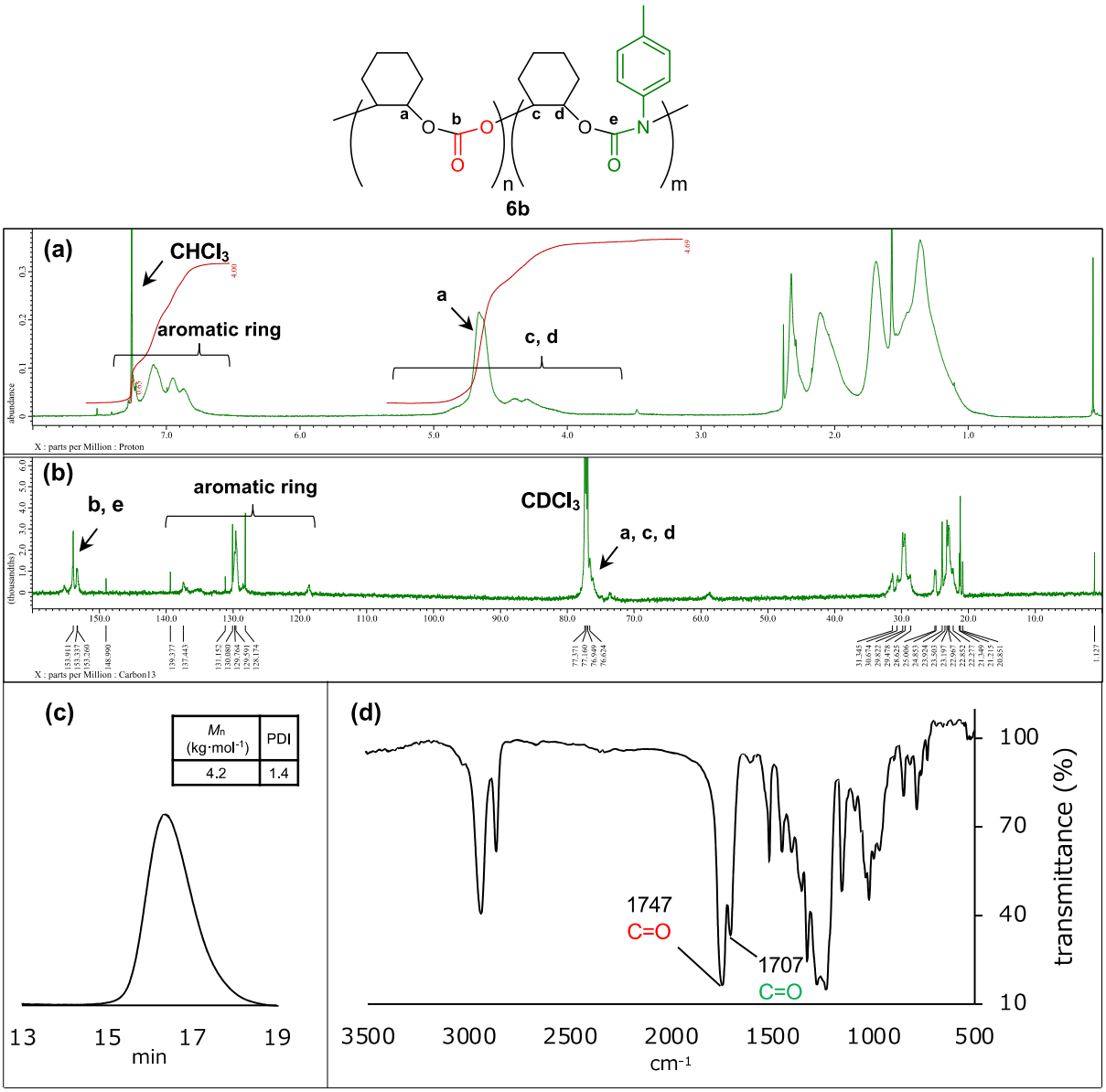

Figure S23. (a) ^{1}H NMR spectrum ($CDCl_3$), (b) ^{13}C NMR spectrum ($CDCl_3$), (c) SEC chart, and (d) IR spectrum of purified polymer **6b** (Table 2, entry 2).

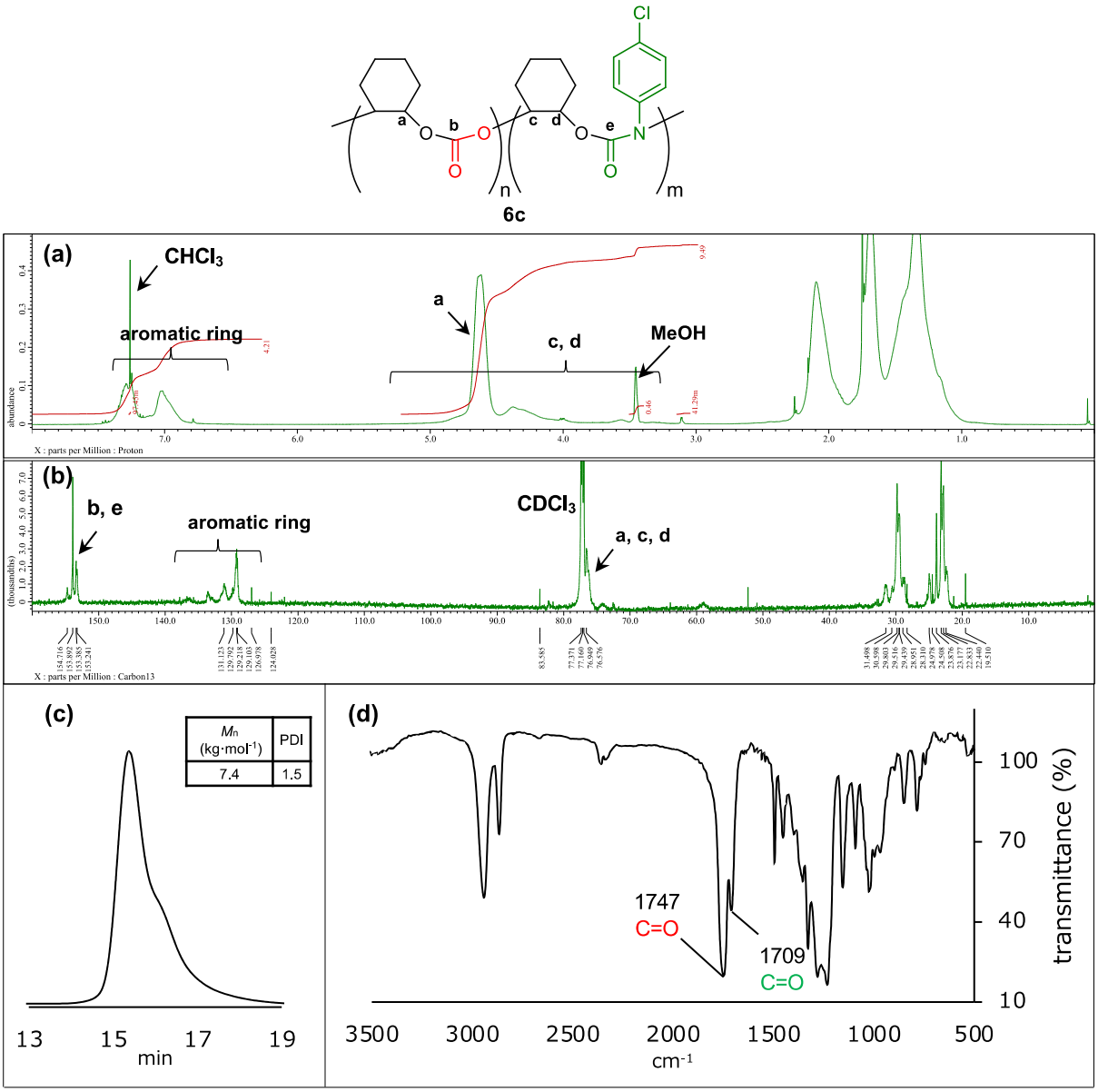

Figure S24. (a) ^{1}H NMR spectrum ($CDCl_3$), (b) ^{13}C NMR spectrum ($CDCl_3$), (c) SEC chart, and (d) IR spectrum of purified polymer **6c** (Table 2, entry 3).

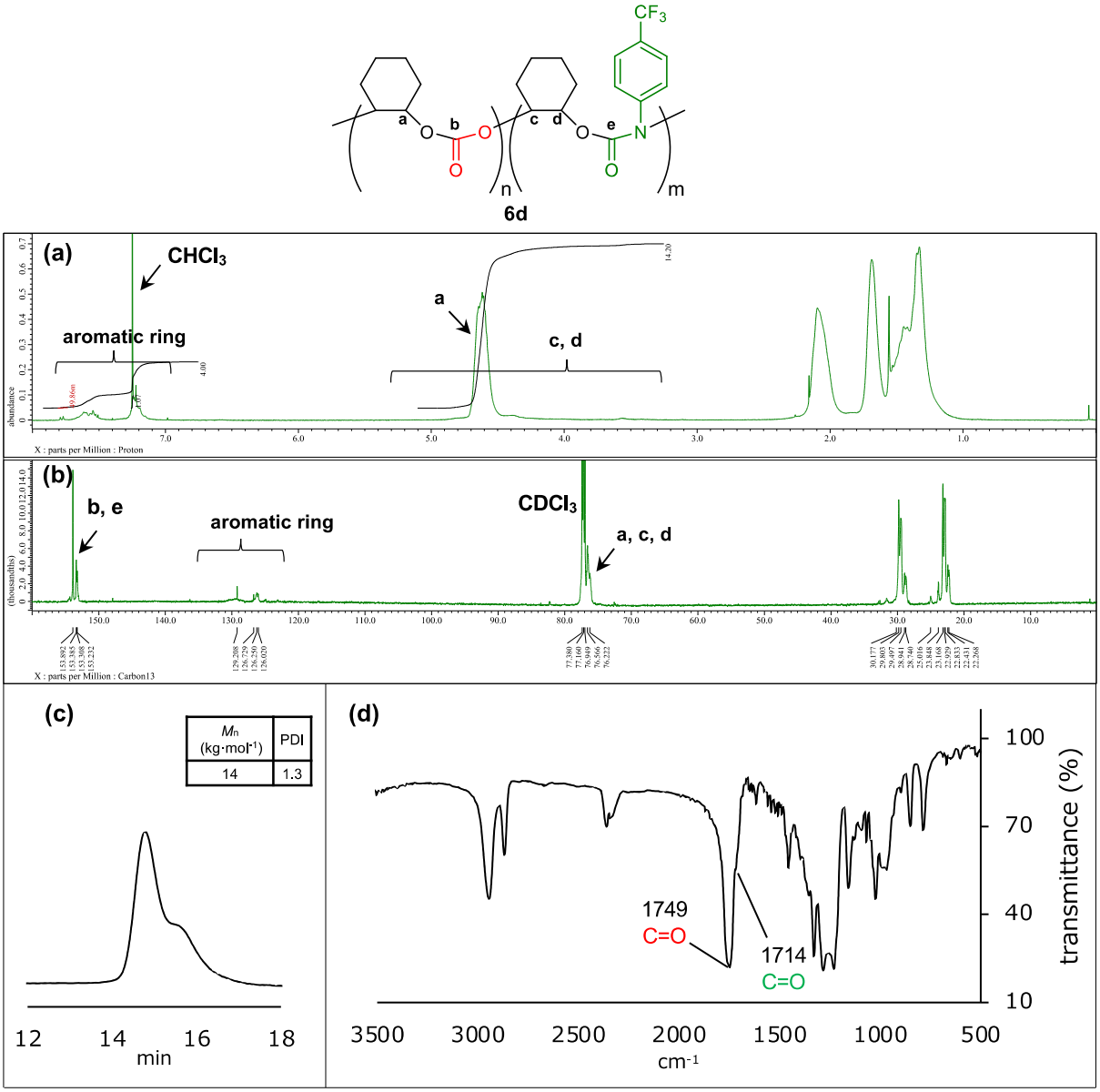

Figure S25. (a) ^{1}H NMR spectrum ($CDCl_3$), (b) ^{13}C NMR spectrum ($CDCl_3$), (c) SEC chart, and (d) IR spectrum of purified polymer **6d** (Table 2, entry 4).

Hydrolysis experiments. To confirm the existence of the PU unit, hydrolysis experiments were conducted according to the procedure reported by Adriaenssens.[10a] A solution of purified terpolymer **6a** (approximately 10 mg) and 2.0 M KOH in D_2O (0.1 g) in DMSO-d_6 in an NMR tube was heated at 90 °C for 15 h in an oil bath. ^{1}H NMR spectrum is shown in Figure S26. It is reported in the above reference that the hydrolysis of the polyallophanate linkage gives amino alcohol **B**, aniline (**C**), and cyclic urea **D**. In the present case, **C** and **D** were not detected at all, which revealed the absence of the polyallophanate linkage.

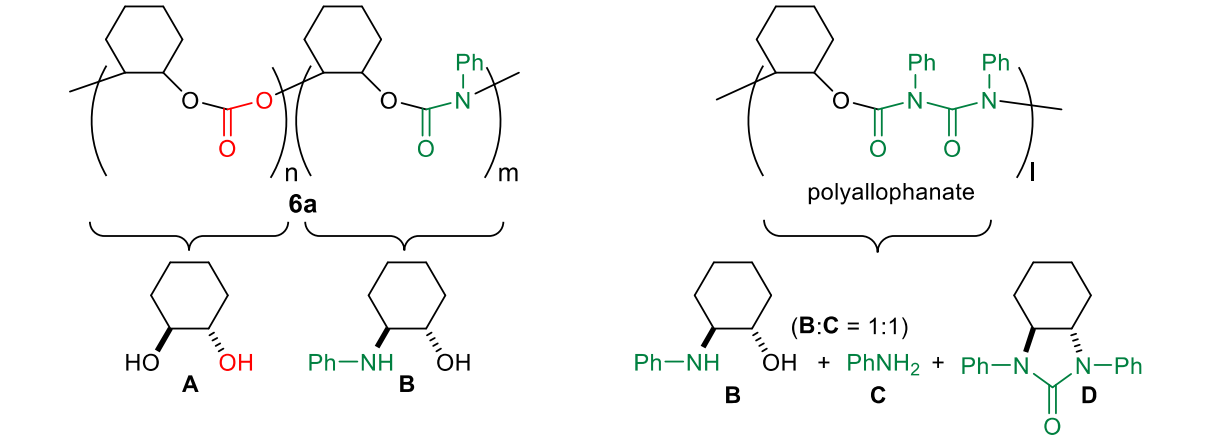

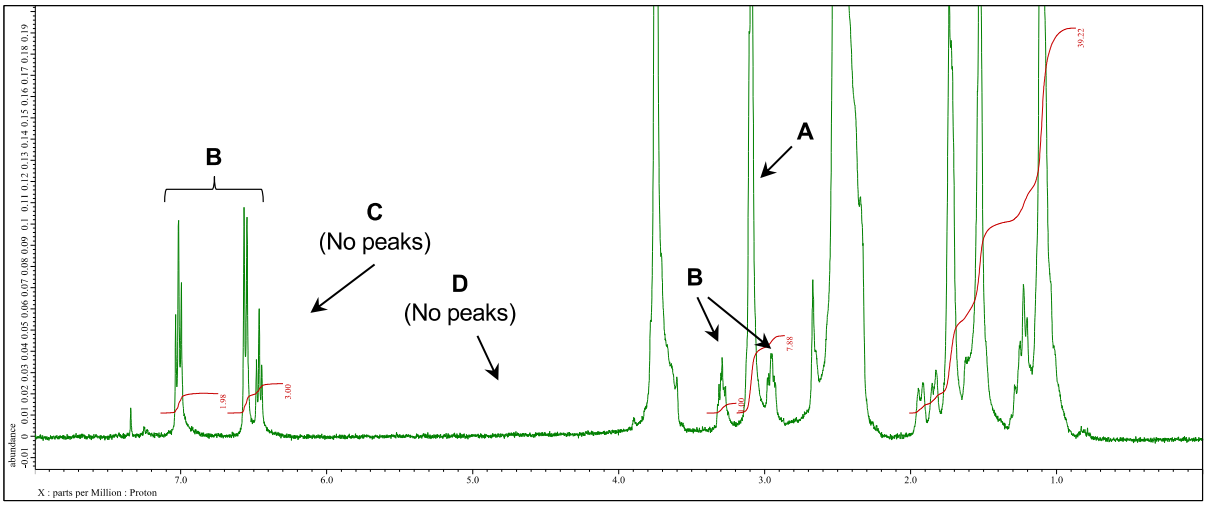

Figure S26. ^{1}H NMR spectrum after the hydrolysis of purified polymer **6a**.

[F] Synthesis and characterization of model compounds for terpolymer 6a.

Amino alcohol **14** was prepared and characterized according to the literature.[24]

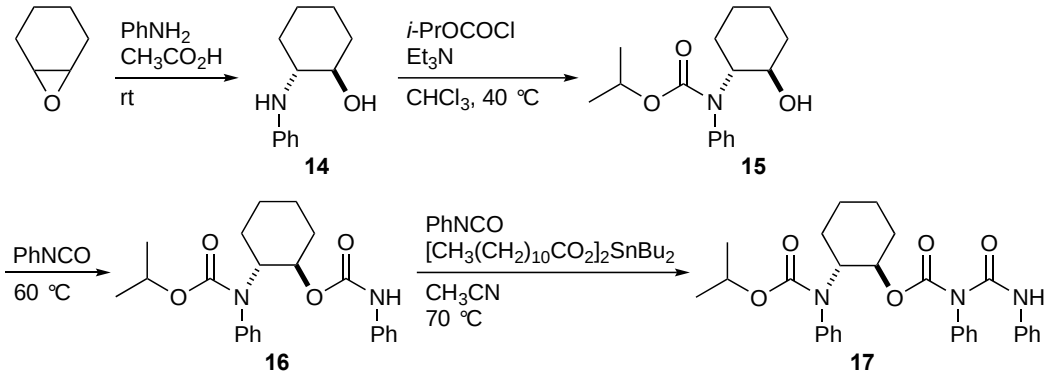

Synthesis of 15. Amino alcohol **14** (500 mg, 2.62 mmol) was put in a flask (25 mL), and it was dried under vacuum at room temperature for 3 h. After the addition of Et_3N (0.35 mL, 2.6 mmol) and dry $CHCl_3$ (2.0 mL) under N_2, isopropyl chloroformate (1.0 mL, 8.8 mmol) was added dropwise at 40 °C, and the reaction mixture was stirred at 40 °C for 4 h. The mixture was diluted with EtOAc, washed with water, and dried over Na_2SO_4. Purification by silica gel column chromatography (hexane/EtOAc = 5/1) gave **15** as a white solid (436 mg, 1.57 mmol, 60%). mp 84–87 °C; ^{1}H NMR ($CDCl_3$, 400 MHz, 50 °C) δ 1.00–1.41 (m, 10H), 1.60–1.69 (m, 2H), 1.83–1.90 (m, 1H), 2.04–2.11 (m, 1H), 2.28 (d, J = 6.0 Hz, 1H), 3.38–3.46 (m, 1H), 4.03–4.09 (m, 1H), 4.87–4.96 (m, 1H), 7.10–7.36 (m, 5H); ^{13}C NMR ($CDCl_3$, 150 MHz, 40 °C) δ 21.96, 22.01, 24.4, 25.4, 30.5, 35.5, 63.0, 69.1, 71.6, 127.4, 128.6, 130.0, 139.0, 157.1; IR (KBr) 3443, 2988, 2951, 2934, 2859, 1690, 1655, 1597, 1495, 1452, 1408, 1364, 1308, 1261, 1184, 1148, 1109, 1072, 1053, 1034, 1016, 999, 957, 866, 785, 768 cm^{-1}; HRMS (FAB) calcd for $C_{16}H_{24}NO_3$ 278.1756, found 278.1756 ([M + H]$^+$).

Synthesis of 16. Alcohol **15** (525 mg, 1.90 mmol) was put in a Schlenk flask (25 mL), and it was dried under vacuum at 40 °C for 2 h. To the flask under N_2 was added phenyl isocyanate (1.16 g, 9.74 mmol) via syringe, and the mixture was stirred at 60 °C for 2 h. Residual phenyl isocyanate was removed by vacuum distillation at 100 °C, and purification by silica gel column chromatography (hexane/EtOAc = 3/1) gave **16** as a white solid (324 mg, 0.817 mmol, 43%). mp 121–125 °C; ^{1}H NMR ($CDCl_3$, 400 MHz, 60 °C) δ 1.07–1.45 (m, 10H), 1.67–1.75 (m, 2H), 1.95 (br s, 1H), 2.23 (d, J = 10.5 Hz, 1H), 4.34 (br s, 1H), 4.65–4.69 (m, 1H), 4.87–4.94 (m, 1H), 6.61 (br s, 1H), 7.03–7.39 (m, 10H); ^{13}C NMR ($CDCl_3$, 150 MHz, 50 °C) δ 22.1, 24.1, 25.3, 29.9, 31.0, 32.2, 59.9, 69.1, 74.4, 118.9, 123.5, 127.5, 128.9, 129.2, 129.8, 138.3, 139.1, 153.1, 156.1; IR (KBr) 3298, 3063, 2980, 2934, 2860, 1732, 1699, 1682, 1601, 1541, 1501, 1445, 1404, 1373, 1312, 1223, 1109, 1082, 1061, 1042, 1030, 756, 706, 692 cm^{-1}; HRMS (FAB) calcd for $C_{23}H_{29}N_2O_4$ 397.2127, found 397.2127 ([M + H]$^+$).

Synthesis of 17. Compound **16** (130 mg, 0.327 mmol) was put in a Schlenk flask (25 mL), and it was dried under vacuum at 60 °C for 2 h. To the flask under N_2 was added phenyl isocyanate (408 mg, 3.43 mmol), dibutyltin dilaurate (216 mg, 0.342 mmol), and CH_3CN (1.0 mL) via syringes. The mixture was stirred at 70 °C for 4 h. Residual phenyl isocyanate and CH_3CN were removed by

vacuum distillation at 100 °C, and purification by alumina column chromatography (hexane/EtOAc = 6/1) gave **17** as a white solid (42.9 mg, 0.083 mmol, 25%). mp 57–61 °C; ^{1}H NMR ($CDCl_3$, 400 MHz, 50 °C) δ 1.12–1.33 (m, 10H), 1.69 (d, J = 7.3 Hz, 2H), 1.91–1.94 (m, 1H), 2.21–2.23 (m, 1H), 3.67 (br s, 1H), 4.85–4.94 (m, 1H), 5.08 (br s, 1H), 6.84 (d, J = 6.4 Hz, 2H), 7.06–7.10 (m, 1H), 7.17–7.33 (m, 7H), 7.36–7.46 (m, 3H), 7.48–7.57 (m, 2H), 10.9 (s, 1H); ^{13}C NMR ($CDCl_3$, 150 MHz, 50 °C) δ 22.0, 22.1, 24.0, 25.0, 30.1, 31.8, 62.3, 68.9, 76.6, 120.2, 124.1, 127.0, 128.3, 128.7, 128.9, 129.0, 129.1, 129.2, 137.3, 138.1, 141.0, 151.7, 154.8, 155.5; IR (KBr) 3285, 2978, 2938, 2862, 1732, 1697, 1593, 1545, 1493, 1449, 1375, 1329, 1304, 1269, 1234, 1179, 1155, 1109, 1078, 1007, 989, 756, 737, 694, 669 cm^{-1}; HRMS (FAB) calcd for $C_{30}H_{34}N_3O_5$ 516.2498, found 516.2498 ([M + H]$^{+}$).

Comparison of the ^{1}H NMR spectrum of terpolymer 6a and those of model compounds 16 and 17.

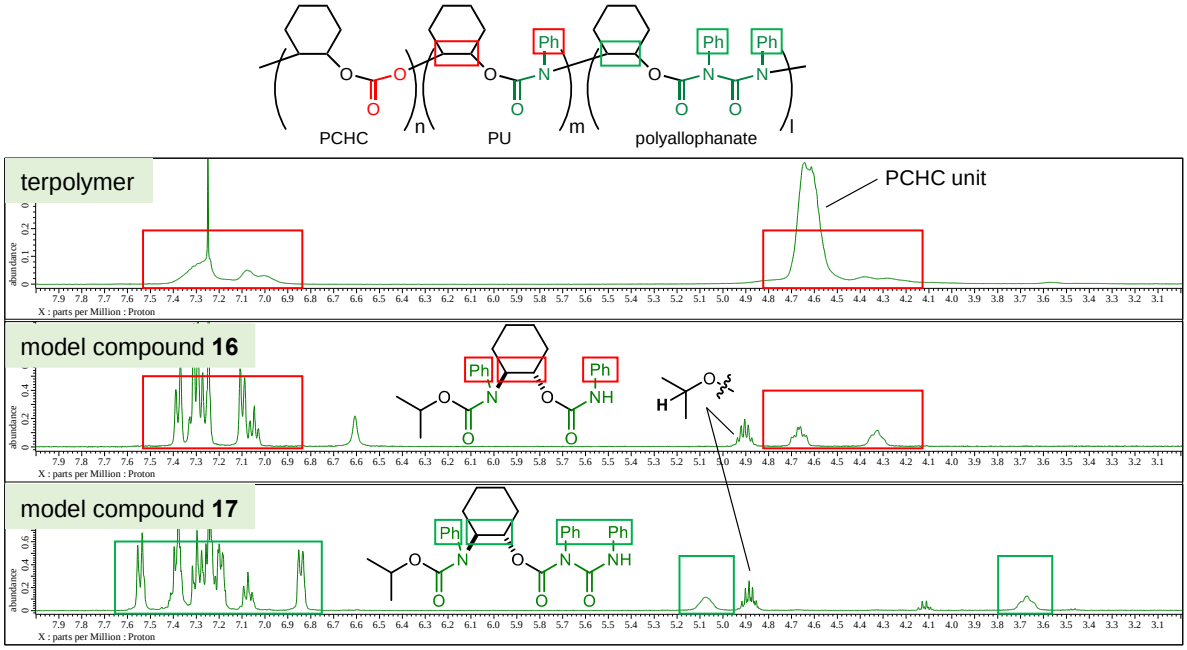

Figure S27. ^{1}H NMR spectra ($CDCl_3$) of purified terpolymer **6a** and model compounds **16** and **17**.

[G] Quaterpolymerization of CHO, CO_2, aryl isothiocyanates, and aryl isocyanates.

(a) Quaterpolymerization of CHO, CO_2, 2c, and 5c.

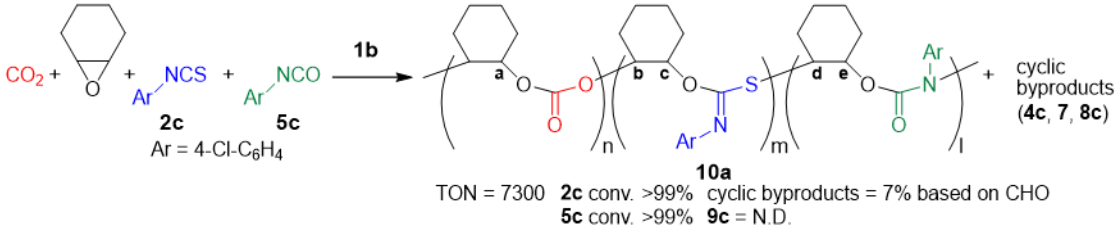

Catalyst **1b** (2.09 mg, 1.01 μmol, S/C = 12000 for CHO) was put in a Schlenk flask (30 mL) equipped with a magnetic stirrer, and it was dried at 80 °C under vacuum overnight. The flask was put in a glovebox (purge type) under N_2 atmosphere, and CHO (1.10 g, 11.2 mmol) and **2c** (0.42 g, 2.4 mmol) were added. The flask was taken out from the glovebox. A CO_2 balloon (1 atm) was attached to the flask, and the flask was quickly evacuated and filled with CO_2. A mixture of **5c** (0.19 g, 1.2 mmol) and CHO (0.12 g, 1.2 mmol) was added dropwise via syringe with a syringe-pump over 13 h to the mixture of CHO, **2c**, and **1b** at 90 °C under CO_2 (1 atm, balloon). The reaction mixture was cooled to room temperature and diluted with $CDCl_3$ for ^1H NMR analysis. The conversion of CHO, TON, and the amounts of cyclic byproducts were determined by using DMSO (41 mg, 0.53 mmol) as an internal standard. The conversions of **2c** and **5c** were determined by the ^1H NMR analysis of the $CDCl_3$ solution that was treated with cyclohexylamine at room temperature to convert **2c** and **5c** into the corresponding thiourea and urea, respectively, in the NMR tube. The quaterpolymer **10a** was isolated by adding the reaction mixture diluted with chloroform dropwise to methanol followed by filtration and vacuum drying.

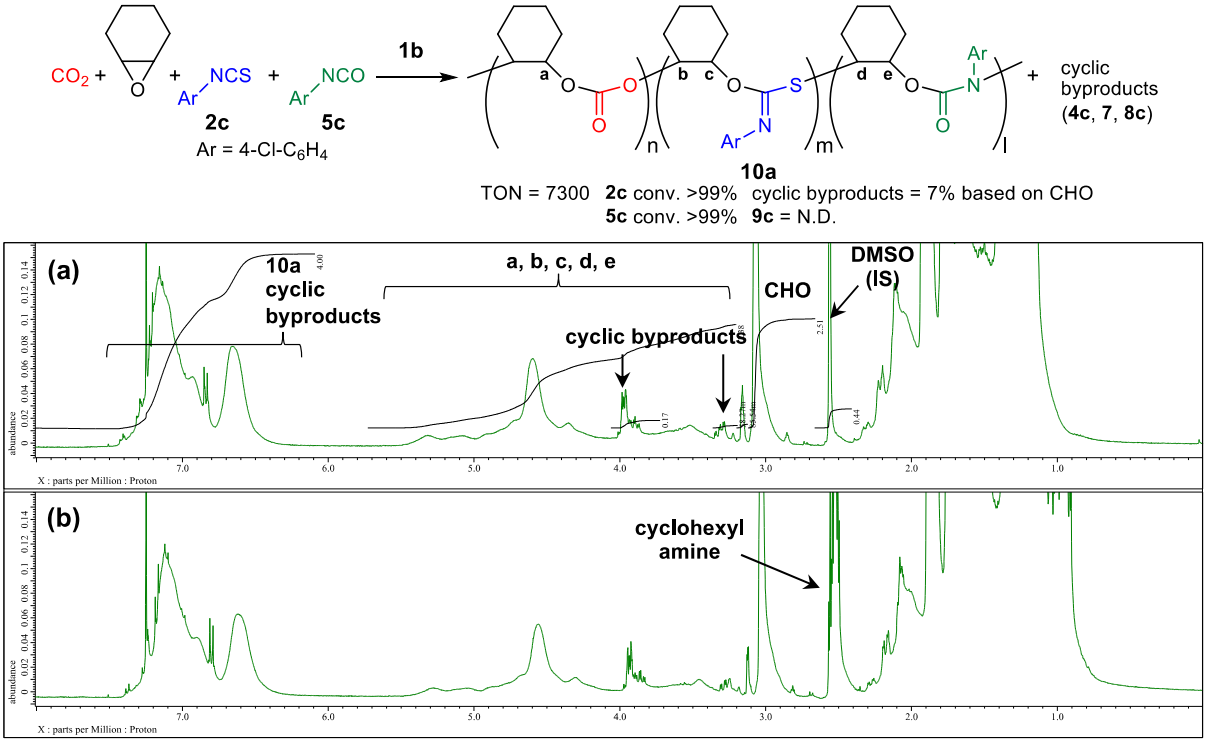

Figure S28. ^1H NMR spectra ($CDCl_3$) of the crude reaction mixture (a) after quaterpolymerization and (b) after the addition of cyclohexylamine.

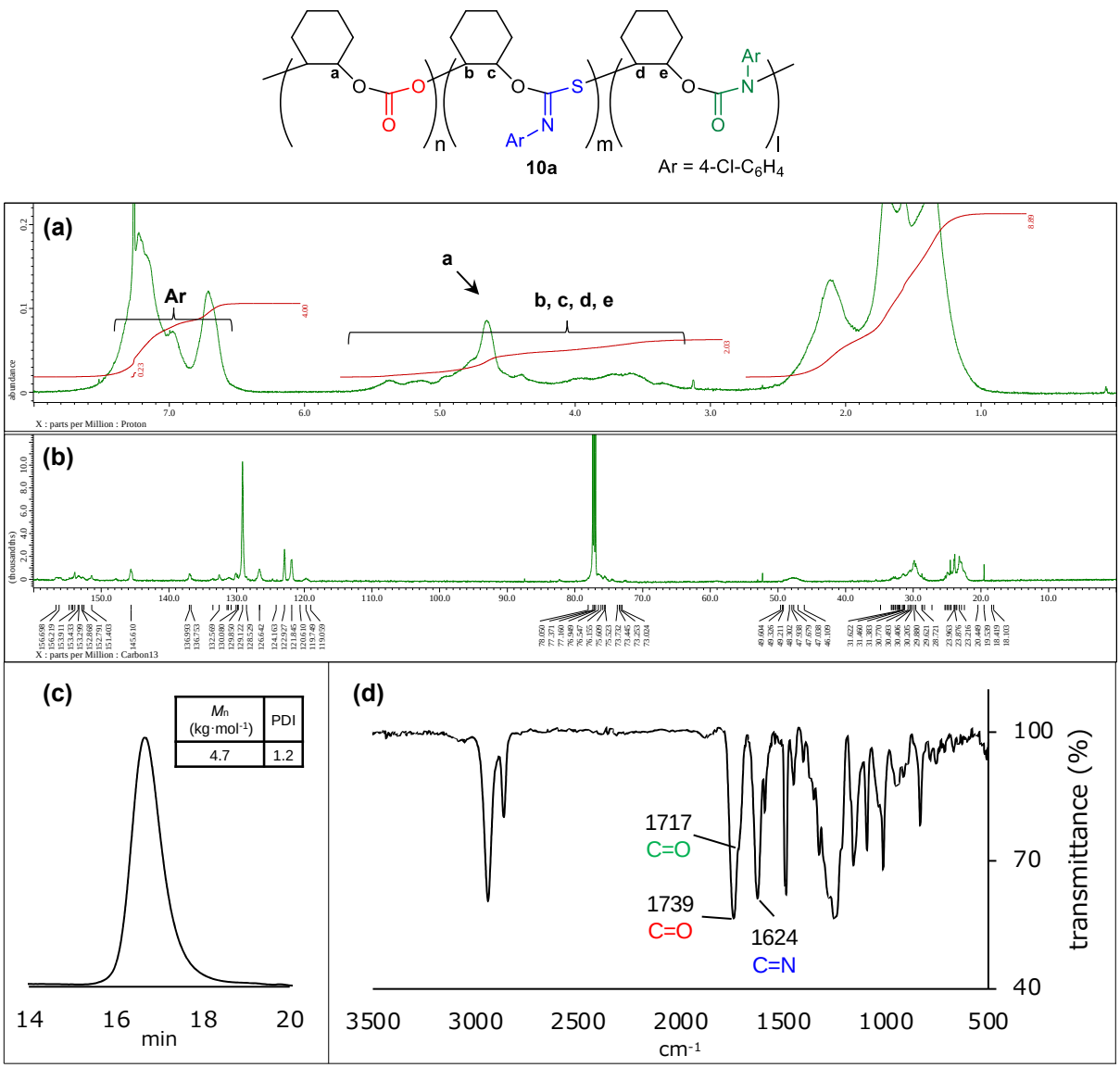

Figure S29. (a) ^{1}H NMR spectra ($CDCl_3$), (b) ^{13}C NMR spectra ($CDCl_3$), (c) SEC chart, and (d) IR spectrum of purified polymer **10a**.

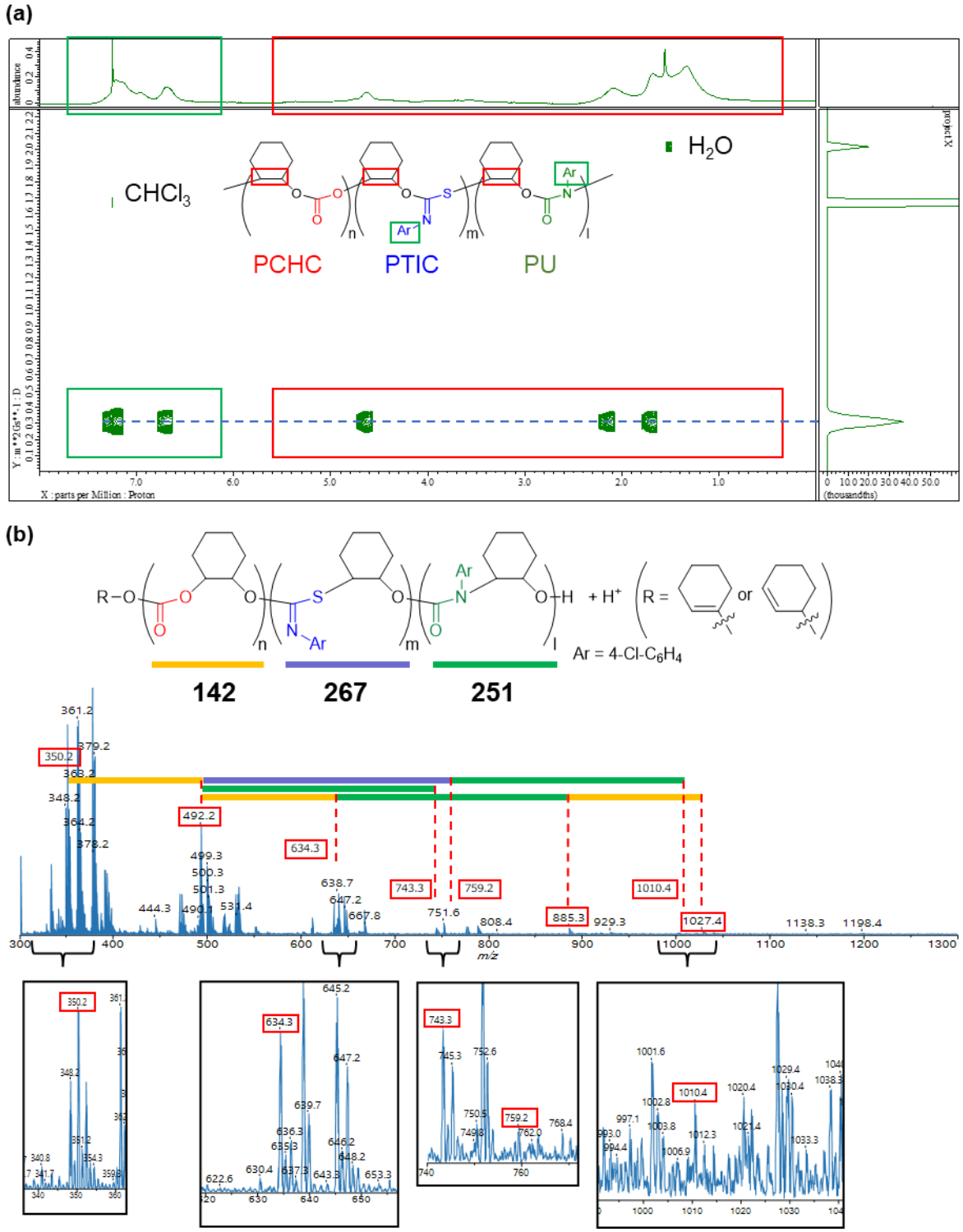

Figure S30. (a) DOSY spectrum ($CDCl_3$) of purified polymer **10a**. (b) MALDI-TOF mass spectrum of polymer **10a**.

(b) Quaterpolymerization of CHO, CO_2, 2d, and 5c.

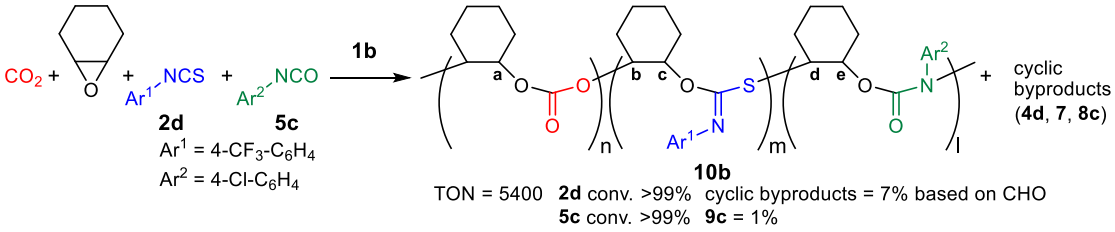

Catalyst **1b** (2.09 mg, 1.01 μmol, S/C = 12000 for CHO) was put in a Schlenk flask (30 mL) equipped with a magnetic stirrer, and it was dried at 90 °C under vacuum overnight. The flask was put in a glovebox (purge type) under N_2 atmosphere, and CHO (1.09 g, 11.2 mmol) and **2d** (0.50 g, 2.5 mmol) were added. The flask was taken out from the glovebox. A CO_2 balloon (1 atm) was attached to the flask, and the flask was quickly evacuated and filled with CO_2. A mixture of **5c** (0.20 g, 1.3 mmol) and CHO (0.12 g, 1.2 mmol) was added dropwise via syringe with a syringe-pump over 21 h to the mixture of CHO, **2d**, and **1b** at 90 °C under CO_2 (1 atm, balloon). The reaction mixture was cooled to room temperature and diluted with $CDCl_3$ for ^1H NMR analysis. The conversion of CHO, TON, and the amounts of cyclic byproducts were determined by using DMSO (56 mg, 0.72 mmol) as an internal standard. The conversions of **2d** and **5c** were determined by the ^1H NMR analysis of the $CDCl_3$ solution that was treated with cyclohexylamine at room temperature to convert **2d** and **5c** into the corresponding thiourea and urea, respectively, in the NMR tube. The quaterpolymer **10b** was isolated by adding the reaction mixture diluted with chloroform dropwise to methanol followed by filtration and vacuum drying.

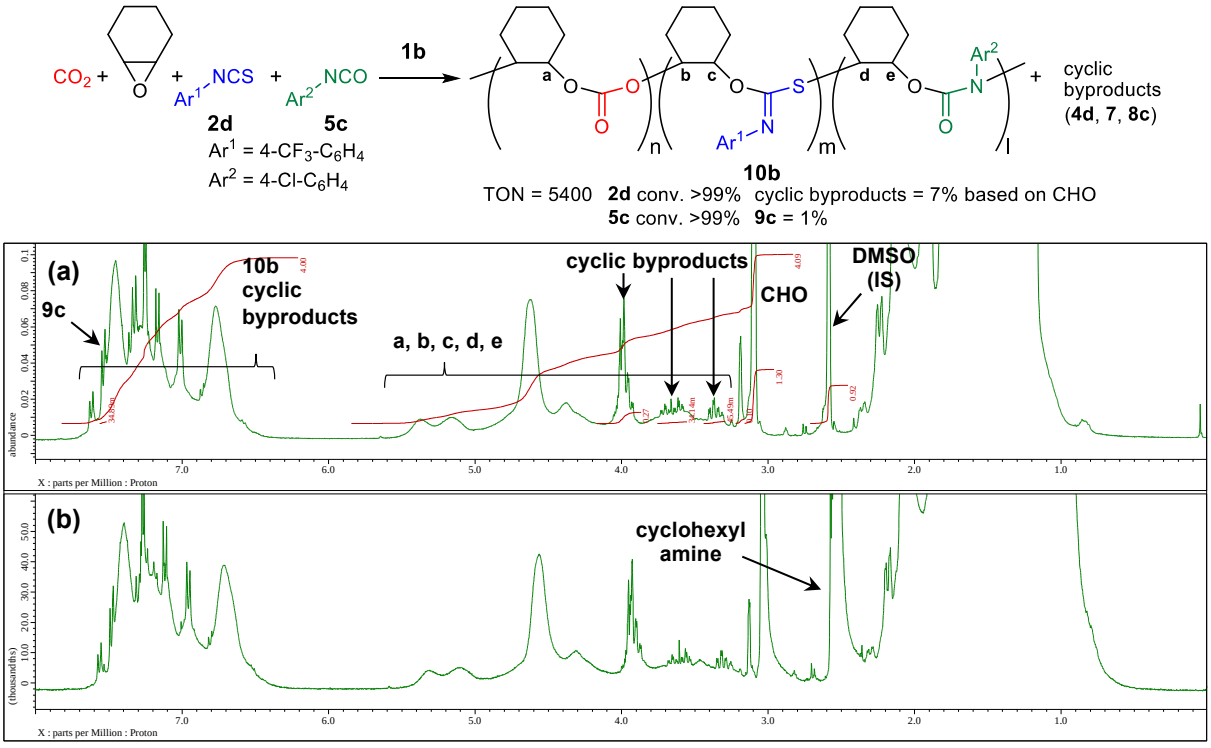

Figure S31. ^1H NMR spectra ($CDCl_3$) of the crude reaction mixture (a) after quaterpolymerization and (b) after the addition of cyclohexylamine.

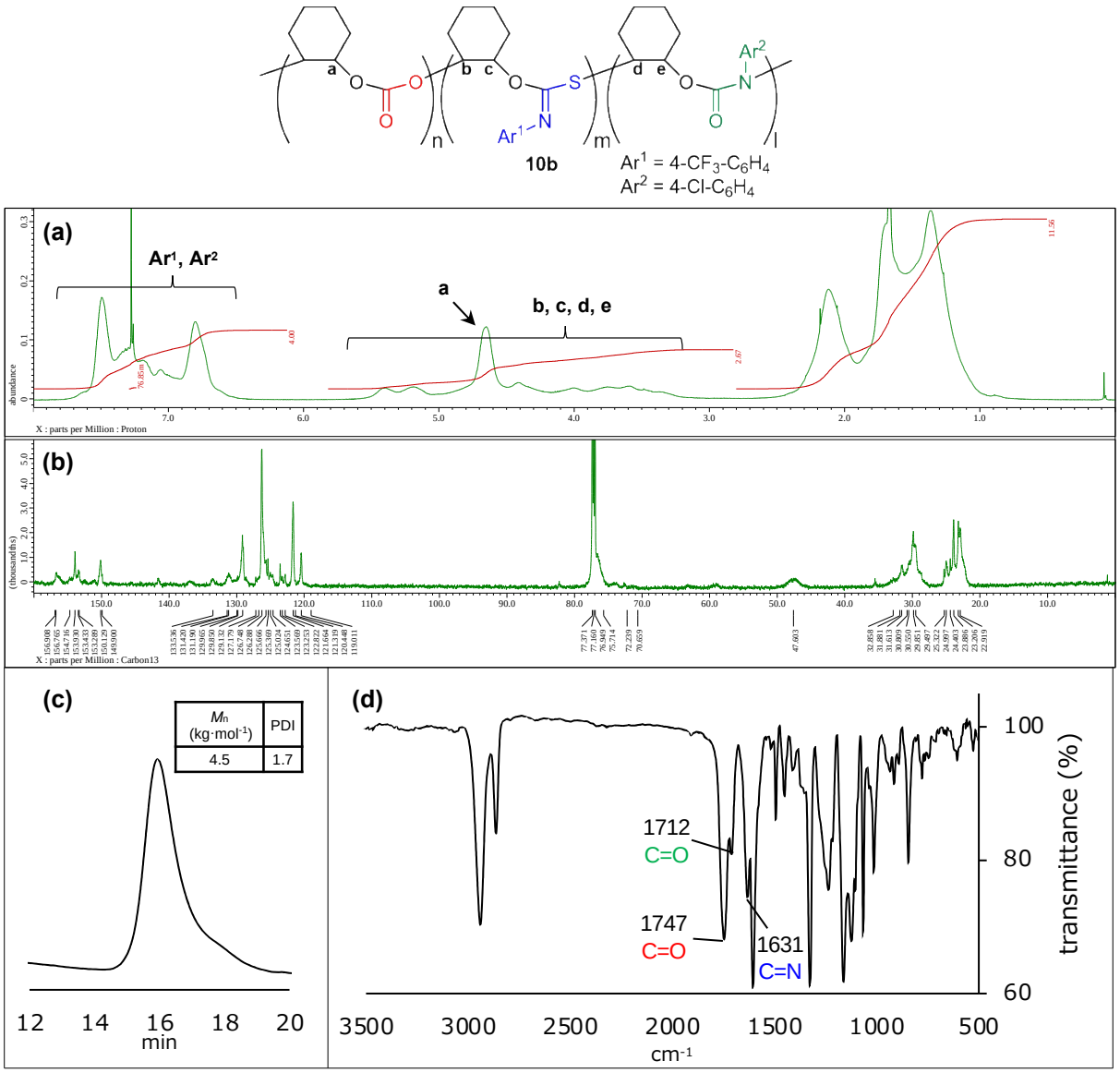

Figure S32. (a) ^{1}H NMR spectra ($CDCl_3$), (b) ^{13}C NMR spectra ($CDCl_3$), (c) SEC chart, and (d) IR spectrum of purified polymer **10b**.

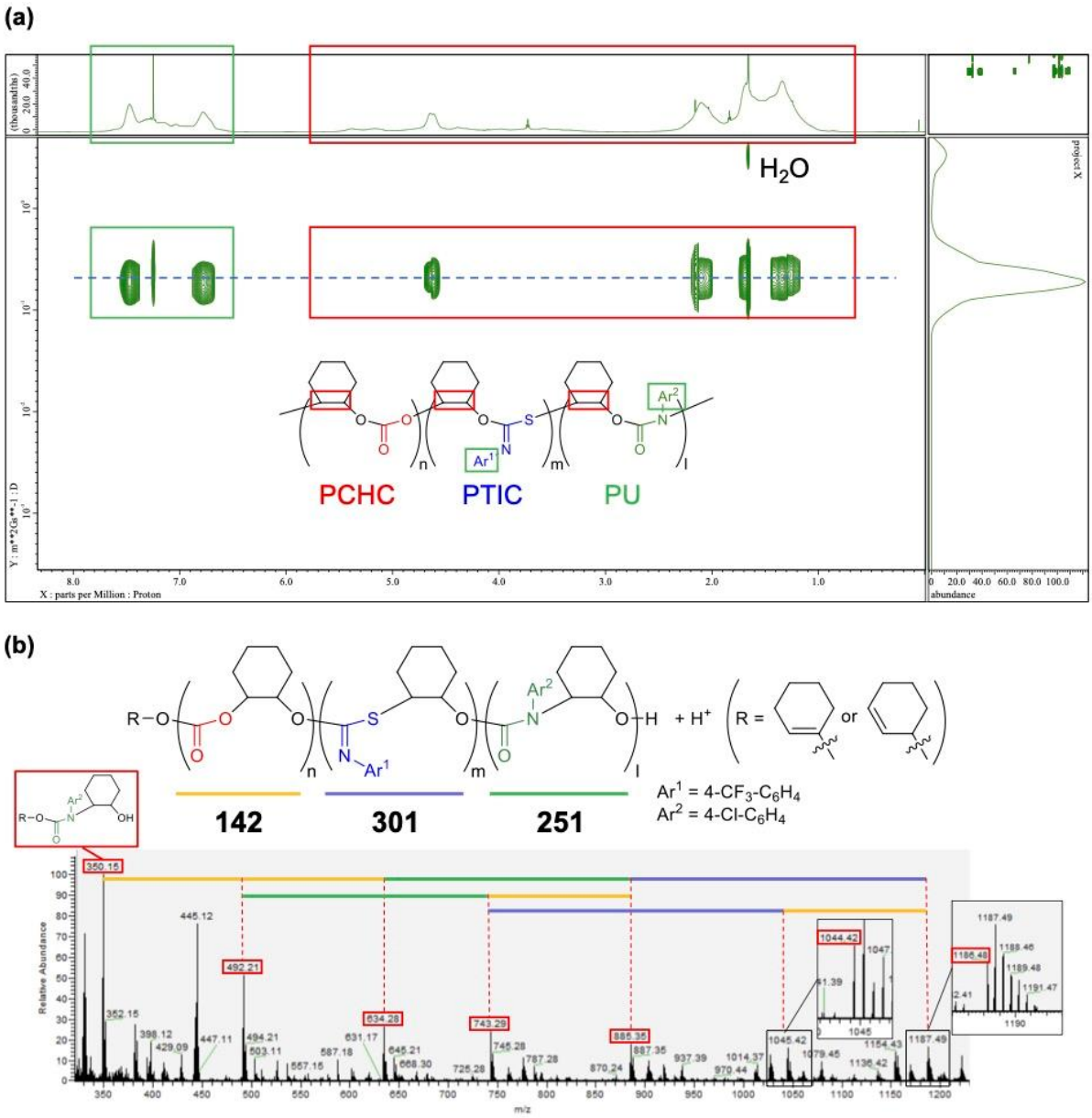

Figure S33. (a) DOSY spectrum ($CDCl_3$) of purified polymer **10b**. (b) APCI mass spectrum of polymer **10b**.

[H] Degradation of polymers by acid treatment or UV irradiation.

General procedure for acid treatment. Purified polymer (30 mg), THF (1 mL), and conc. HCl (35%, five drops, 0.15 g) were put in a flask (10 mL), and the mixture was stirred at room temperature for reaction time indicated in Figure 1b. The mixture was evaporated and diluted with $CDCl_3$ for ^1H NMR analysis or with THF for SEC analysis (Figures S34, S36, and S37). The residual polymer was isolated by adding the reaction mixture diluted with chloroform dropwise to methanol followed by filtration and vacuum drying. The purified polymer was analyzed by ^1H NMR spectroscopy and SEC, which indicated that the purified polymer consisted of only the PCHC unit (Figure S35).

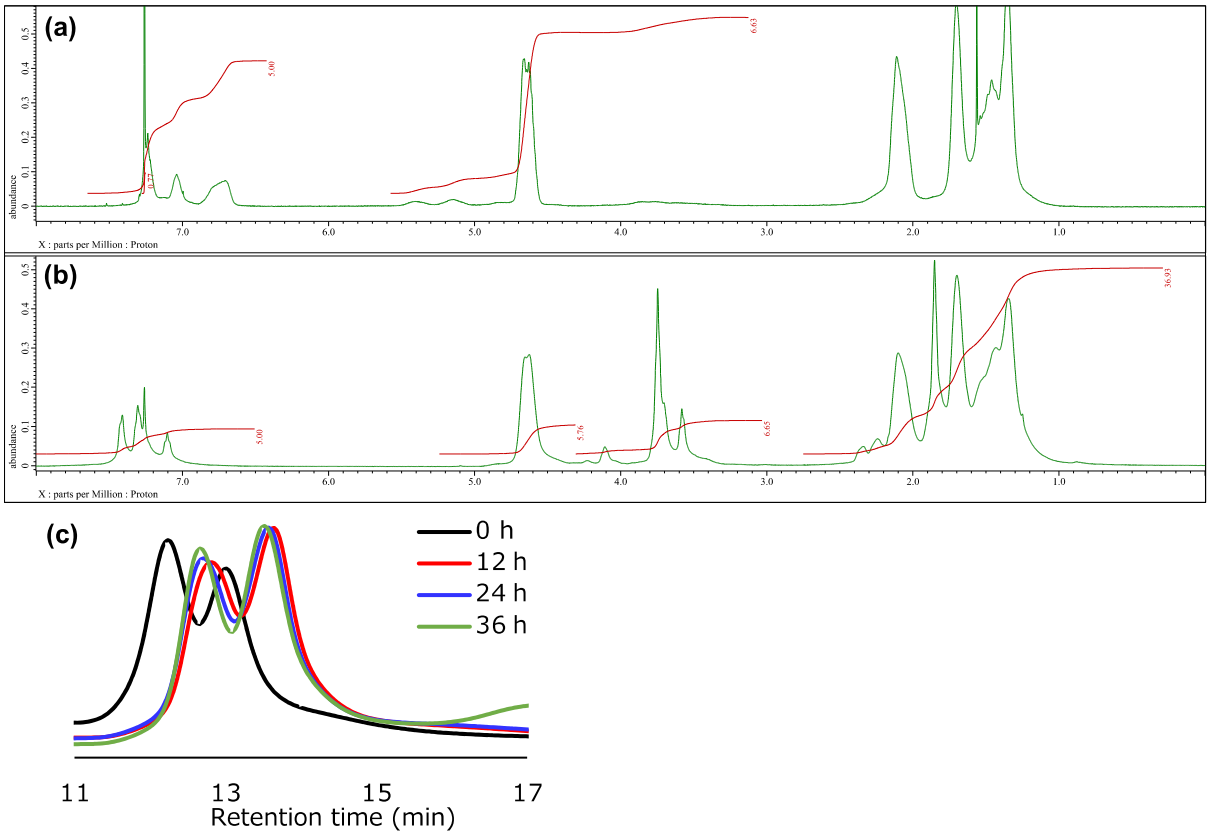

Figure S34. ^1H NMR spectra ($CDCl_3$) of (a) terpolymer **3a** and (b) the reaction mixture after acid treatment of **3a**. (c) SEC charts during the acid treatment of **3a**.

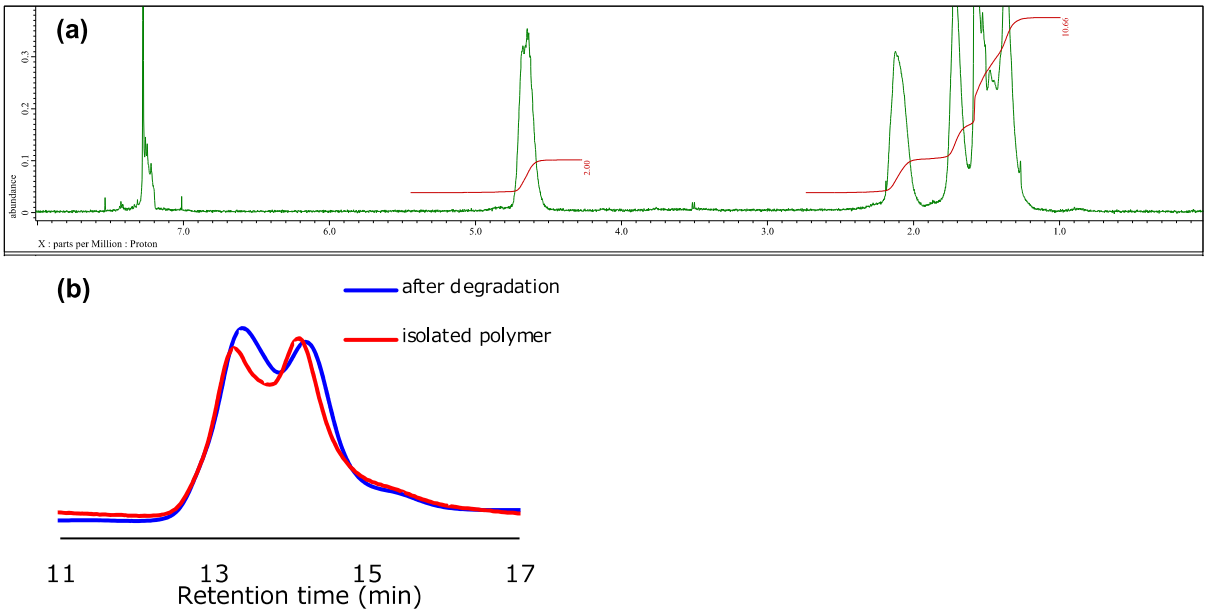

Figure S35. (a) ^{1}H NMR spectrum ($CDCl_3$) of the polymer isolated from the mixture after the acid treatment of **3a**. (b) SEC charts of the mixture after the acid treatment of **3a** and the polymer isolated from the mixture after the acid treatment of **3a**.

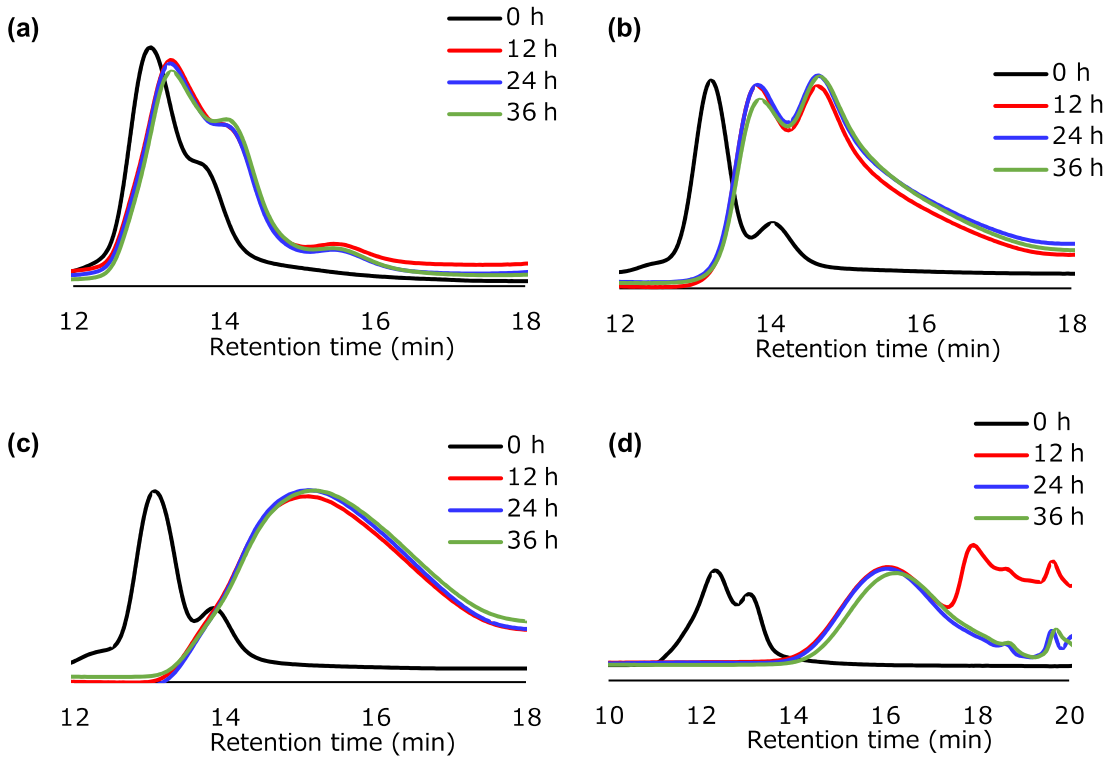

Figure S36. SEC charts during the acid treatment of (a) **3b**, (b) **3c**, (c) **3d**, and (d) **3e**.

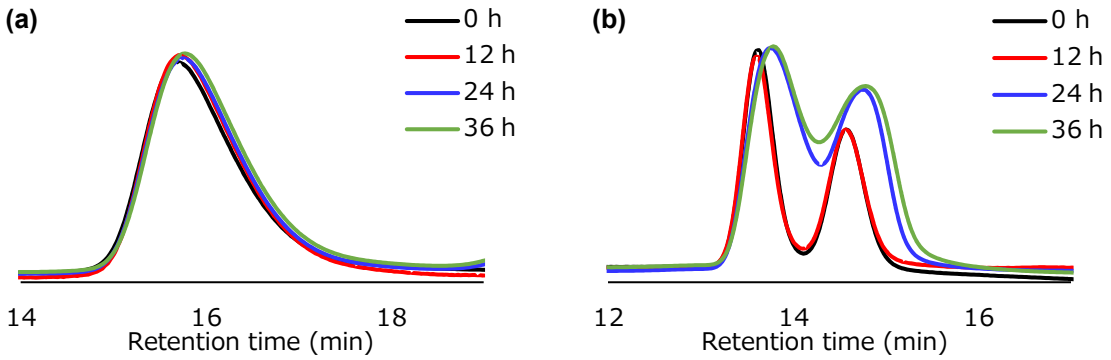

Figure S37. SEC charts during the acid treatment of (a) **6a** and (b) PCHC.

General procedure for UV irradiation. Purified polymer (30 mg) was dissolved in THF (1 mL) and irradiated with UV light for reaction time shown in Figure 1c. The reaction mixture was evaporated and diluted with $CDCl_3$ for ^1H NMR analysis or with THF for SEC analysis (Figures S38, S40, and S41). The residual polymer was isolated by adding the reaction mixture diluted with chloroform dropwise to methanol followed by filtration and vacuum drying. The purified polymer was analyzed by ^1H NMR spectroscopy and SEC, which indicated that the purified polymer consisted of only the PCHC unit (Figure S39).

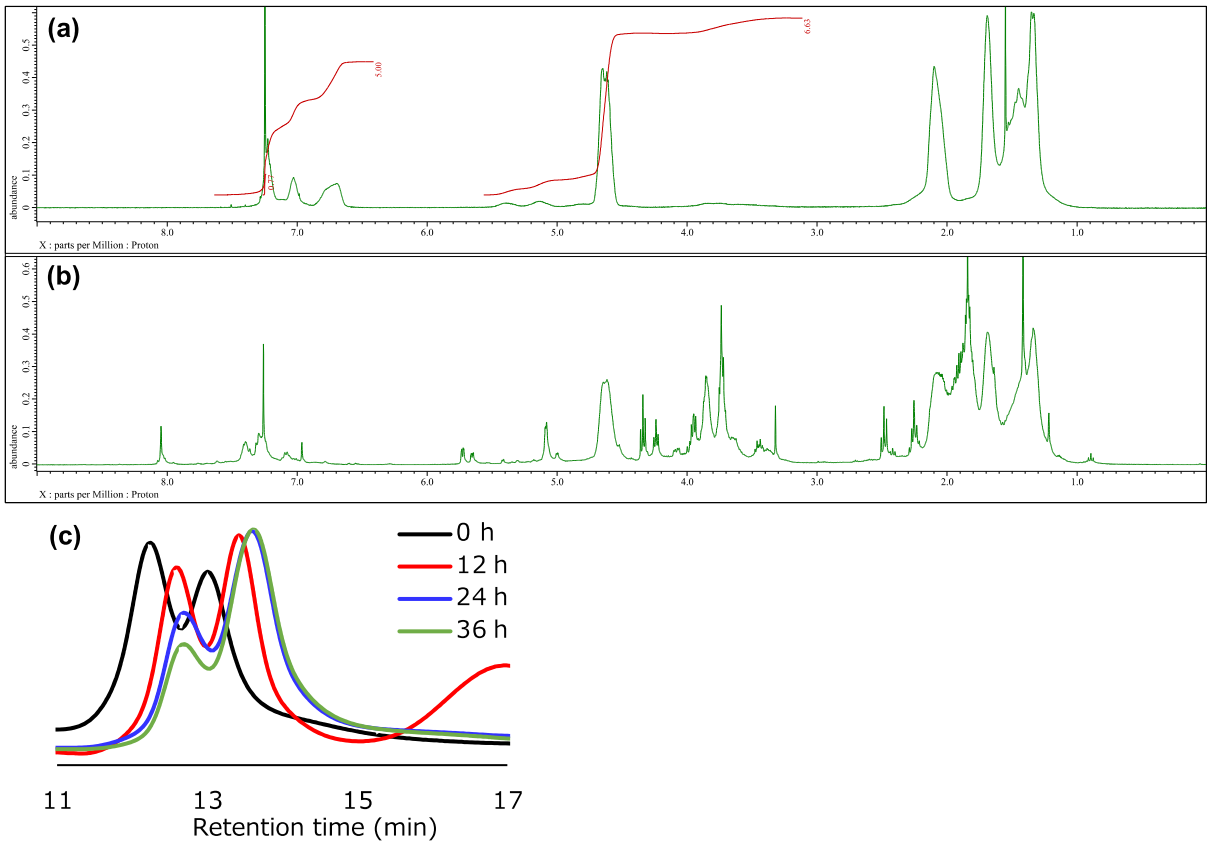

Figure S38. ^1H NMR spectra ($CDCl_3$) of (a) terpolymer **3a** and (b) the reaction mixture after UV irradiation of **3a**. (c) SEC charts during the UV irradiation of **3a**.

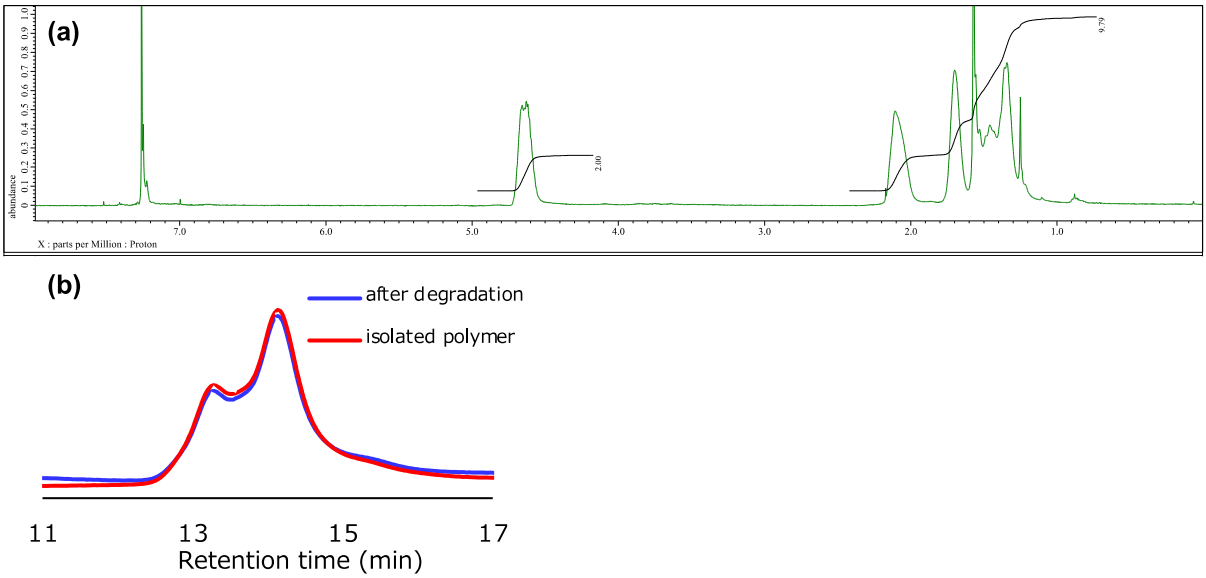

Figure S39. (a) ^{1}H NMR spectrum ($CDCl_3$) of the polymer isolated after the UV irradiation of **3a**. (b) SEC charts of the mixture after the UV irradiation of **3a** and the polymer isolated after the UV irradiation of **3a**.

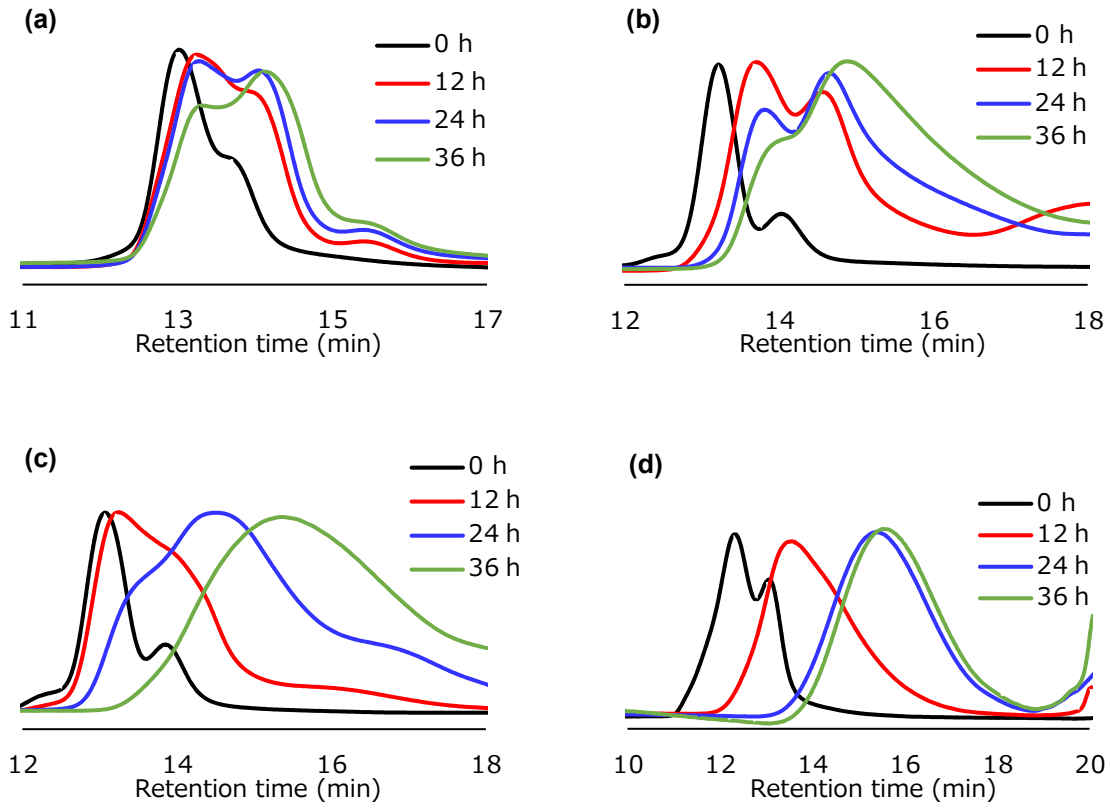

Figure S40. SEC charts during the UV irradiation of (a) **3b**, (b) **3c**, (c) **3d**, and (d) **3e**.

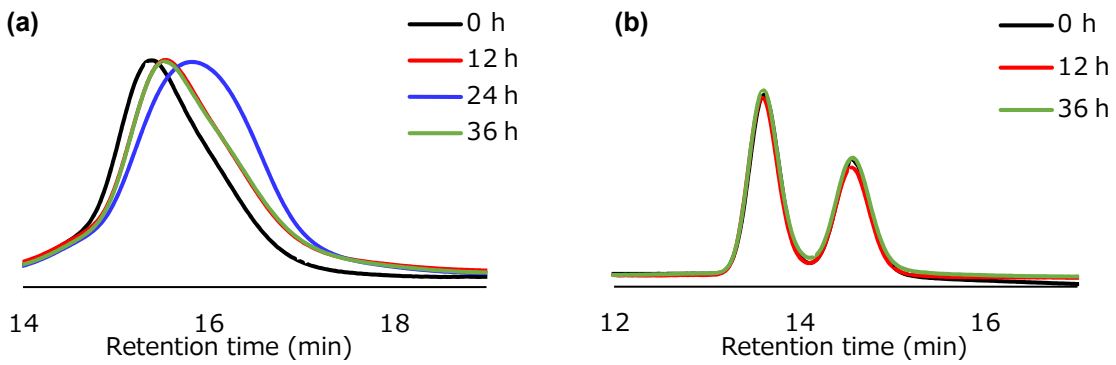

Figure S41. SEC charts during the UV irradiation of (a) **6a** and (b) PCHC.

[I] Synthesis and degradation of PCHC-*b*-PTIC and PTIC.

Two-step synthesis of block polymer PCHC-*b*-PTIC (3e').

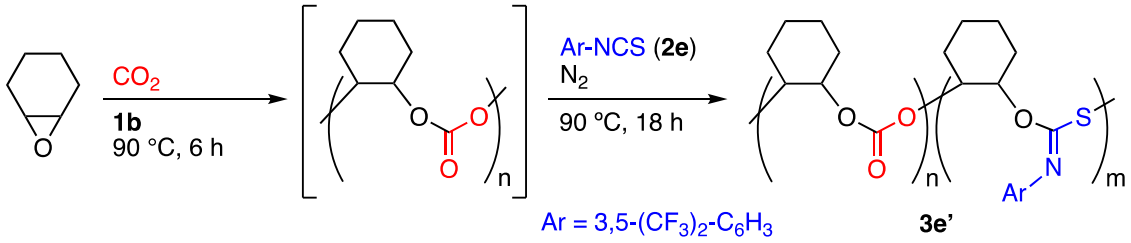

Catalyst **1b** (1.30 mg, 0.63 μmol, S/C = 20000 for CHO) and a magnetic stirring bar were put in a Schlenk flask (30 mL), and the flask was dried under vacuum at 90 °C overnight. The flask was put in a glovebox (purge type) under N_2 atmosphere, and CHO (1.22 g, 12.4 mmol) was added via syringe. The flask was taken out from the glovebox. A CO_2 balloon (1 atm, approximately 2.8 L) was attached to the flask, and the flask was quickly evacuated and filled with CO_2. The mixture was stirred at 90 °C for 6 h. After release of CO_2, a N_2 balloon was attached to the flask, and the flask was quickly evacuated and filled with N_2. Aryl isothiocyanate **2e** (839 mg, 3.1 mmol) was added via syringe. The mixture was stirred at 90 °C for 18 h. A small amount of reaction mixture was withdrawn by syringe at a time interval. After cooling to room temperature, the reaction mixture was diluted with $CDCl_3$, and DMSO (56.9 mg, 0.73 mmol) was added as an internal standard. The conversion of CHO was determined by ^{1}H NMR spectroscopy. Block polymer **3e'** was isolated by adding the reaction mixture diluted with chloroform dropwise to methanol followed by filtration and vacuum drying.

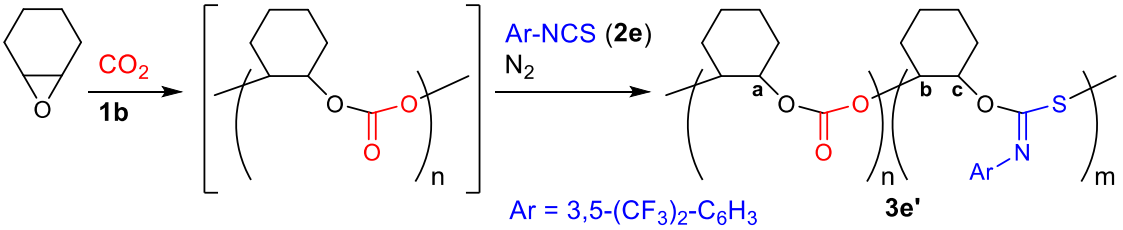

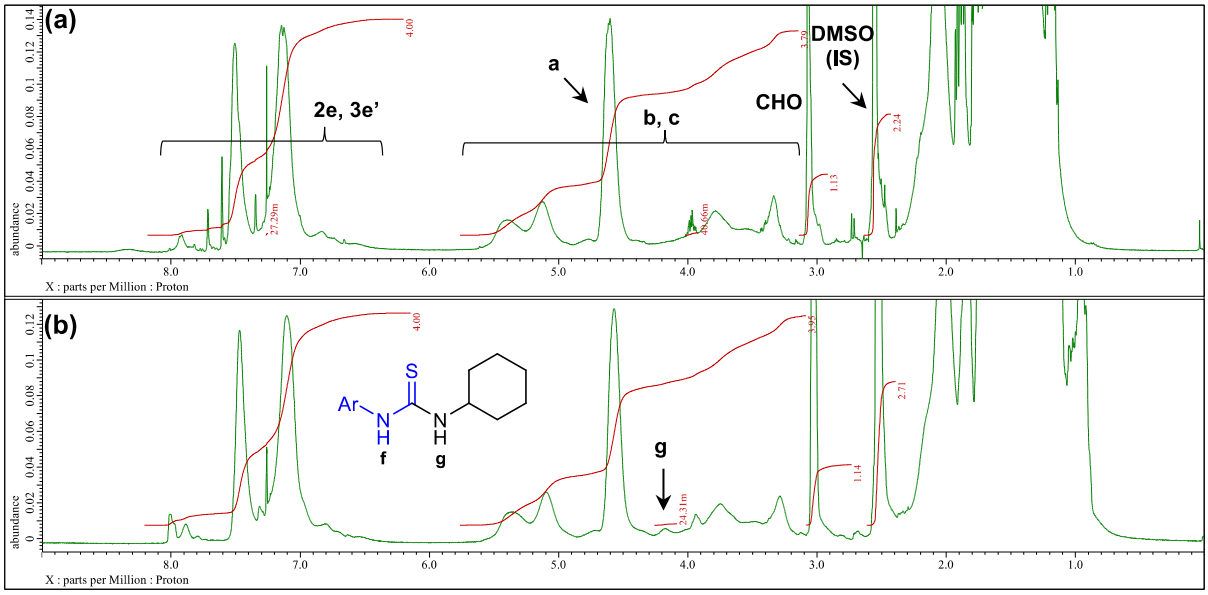

Figure S42. ^{1}H NMR spectra ($CDCl_3$) of the crude reaction mixtures (a) after block polymerization and (b) after the addition of cyclohexylamine (Figure 1d).

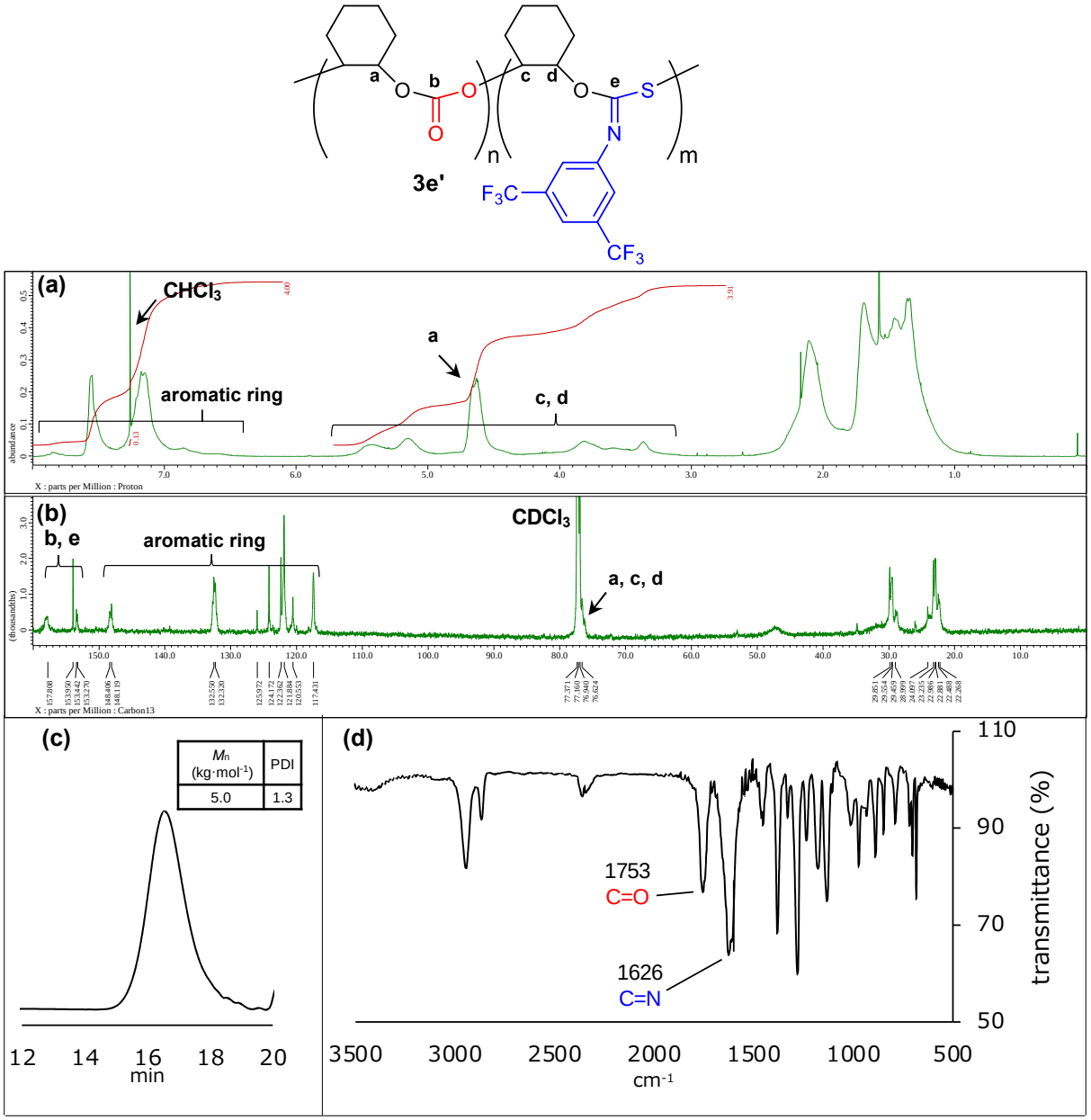

Figure S43. (a) ^{1}H NMR spectrum ($CDCl_3$), (b) ^{13}C NMR spectrum ($CDCl_3$), (c) SEC chart, and (d) IR spectrum of purified polymer **3e'** (Figure 1d).

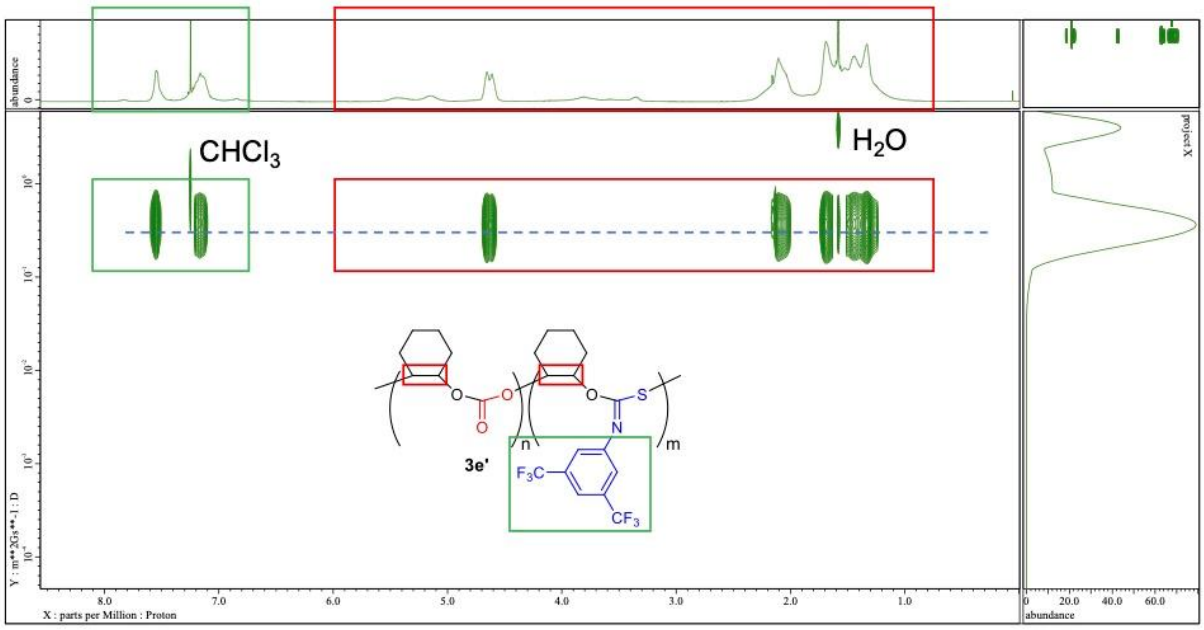

Figure S44. DOSY spectrum ($CDCl_3$) of purified polymer **3e'** (Figure 1d).

Synthesis of PTIC from CHO and isothiocyanate.

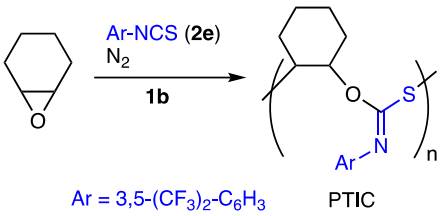

Catalyst **1b** (1.30 mg, 0.63 μmol, S/C = 20000 for CHO) and a magnetic stirring bar were put in a Schlenk flask (30 mL), and the flask was dried under vacuum at 90 °C overnight. The flask was put in a glovebox (purge type) under N_2 atmosphere, and CHO (1.22 g, 12.5 mmol) and aryl isothiocyanate **2e** (842 mg, 3.1 mmol) were added via syringes. A N_2 balloon (1 atm) was attached to the flask, and the flask was quickly evacuated and filled with N_2. The mixture was stirred at 90 °C for 24 h. The reaction mixture was cooled to room temperature and diluted with $CDCl_3$ for ^1H NMR analysis. The conversion of CHO, the TON of catalyst **1b**, and the amount of byproduct **4e** were determined by adding DMSO (54 mg, 0.69 mmol) as an internal standard. Aryl isothiocyanate **2e** remaining in the reaction mixture was quantified by the ^1H NMR analysis of the $CDCl_3$ solution to which cyclohexylamine was added to convert **2e** into the corresponding thiourea in the NMR tube. PTIC was isolated by adding the reaction mixture diluted with chloroform dropwise to methanol followed by filtration and vacuum drying.

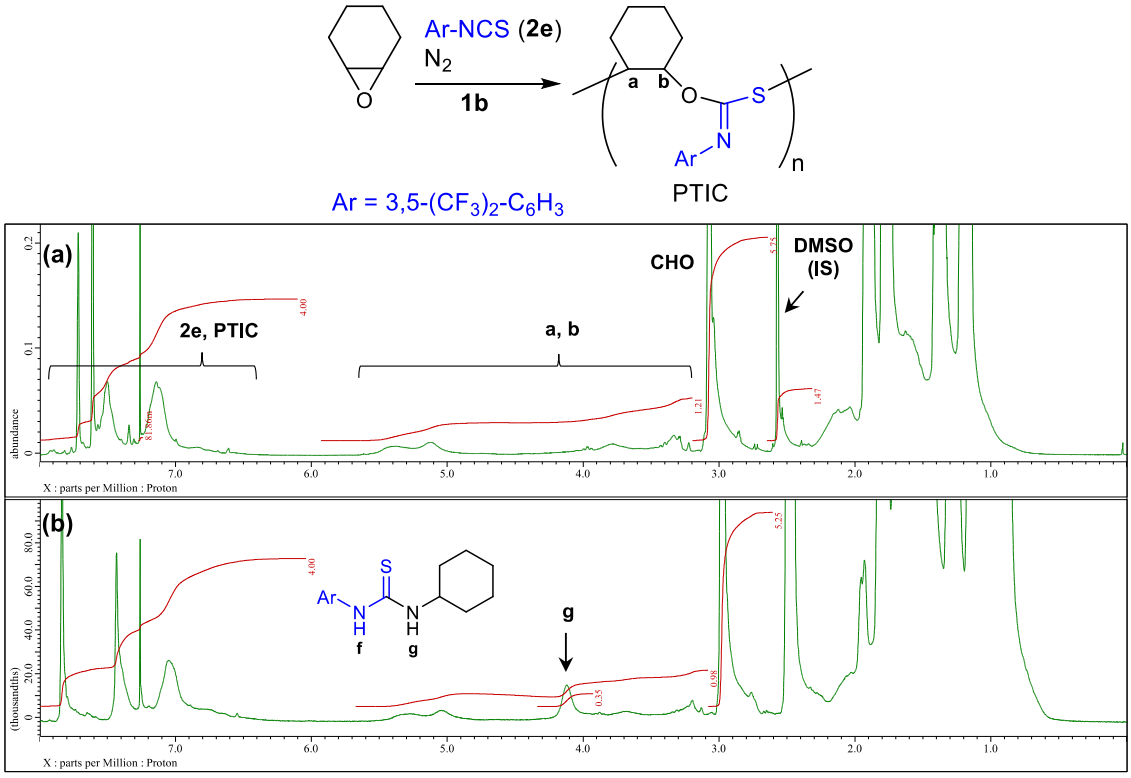

Figure S45. ^1H NMR spectra ($CDCl_3$) of the crude reaction mixtures (a) after polymerization and (b) after the addition of cyclohexylamine.

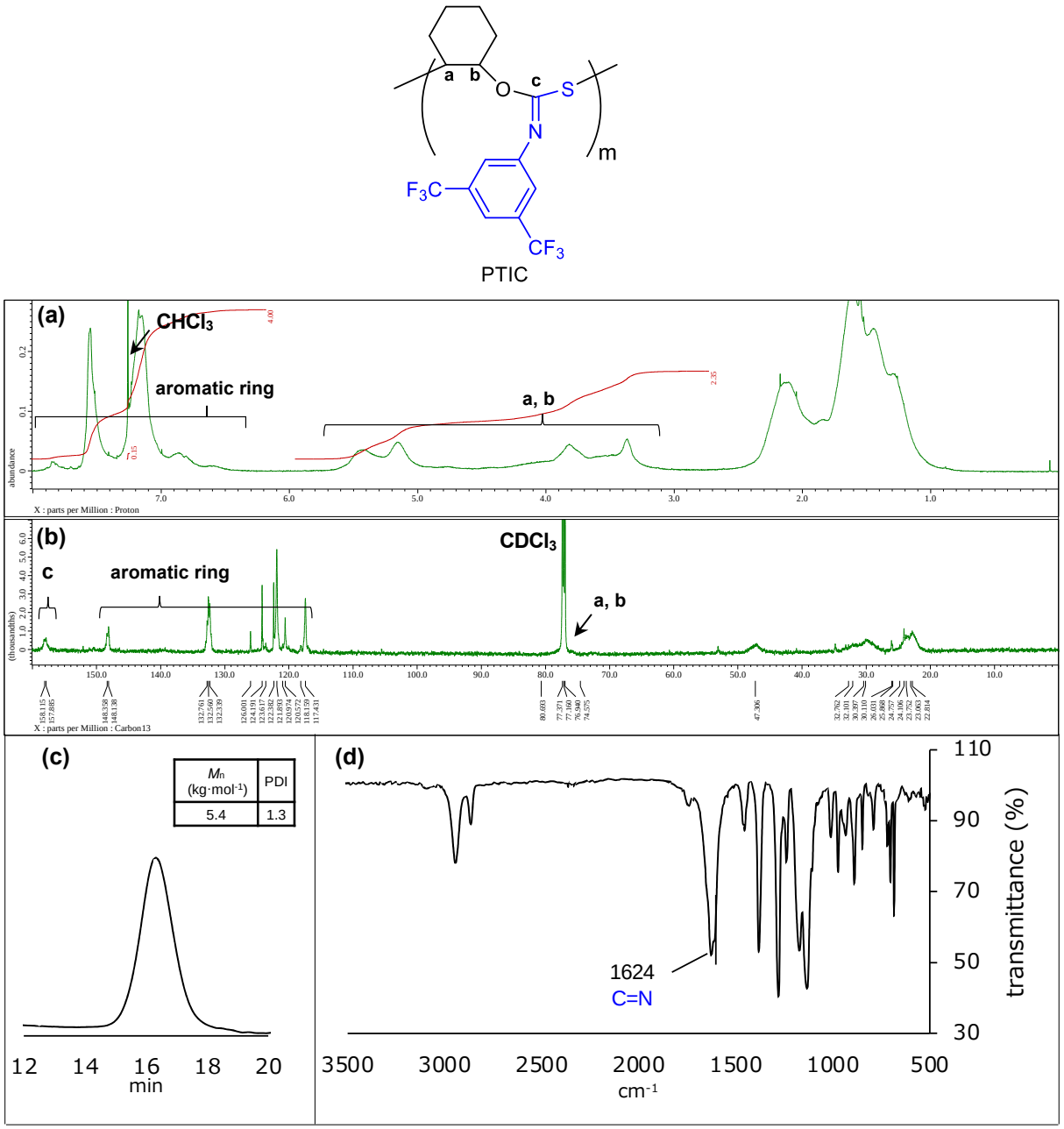

Figure S46. (a) ^{1}H NMR spectrum ($CDCl_3$), (b) ^{13}C NMR spectrum ($CDCl_3$), (c) SEC chart, and (d) IR spectrum of purified PTIC.

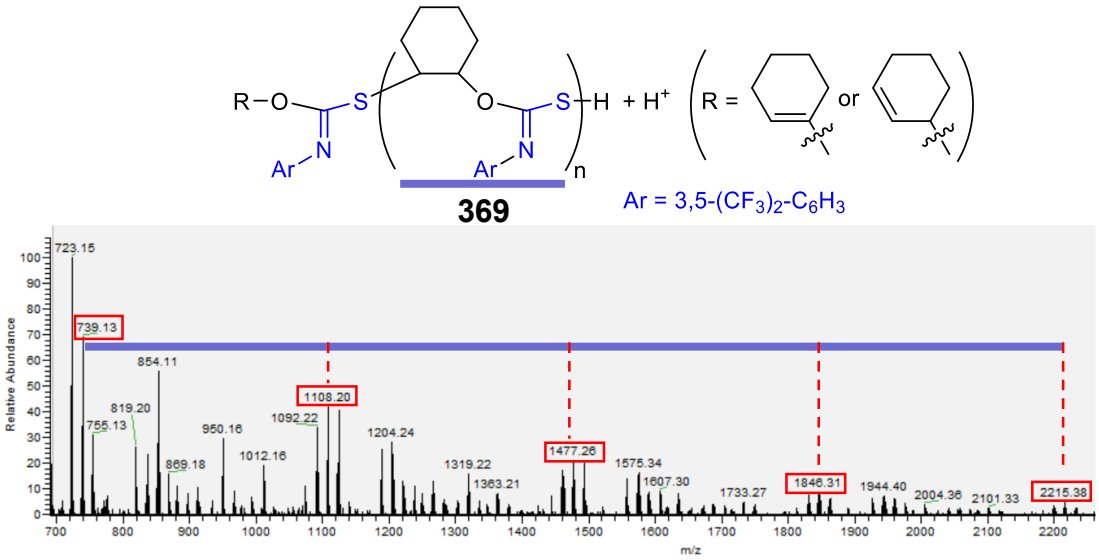

Figure S47. APCI mass spectrum of PTIC.

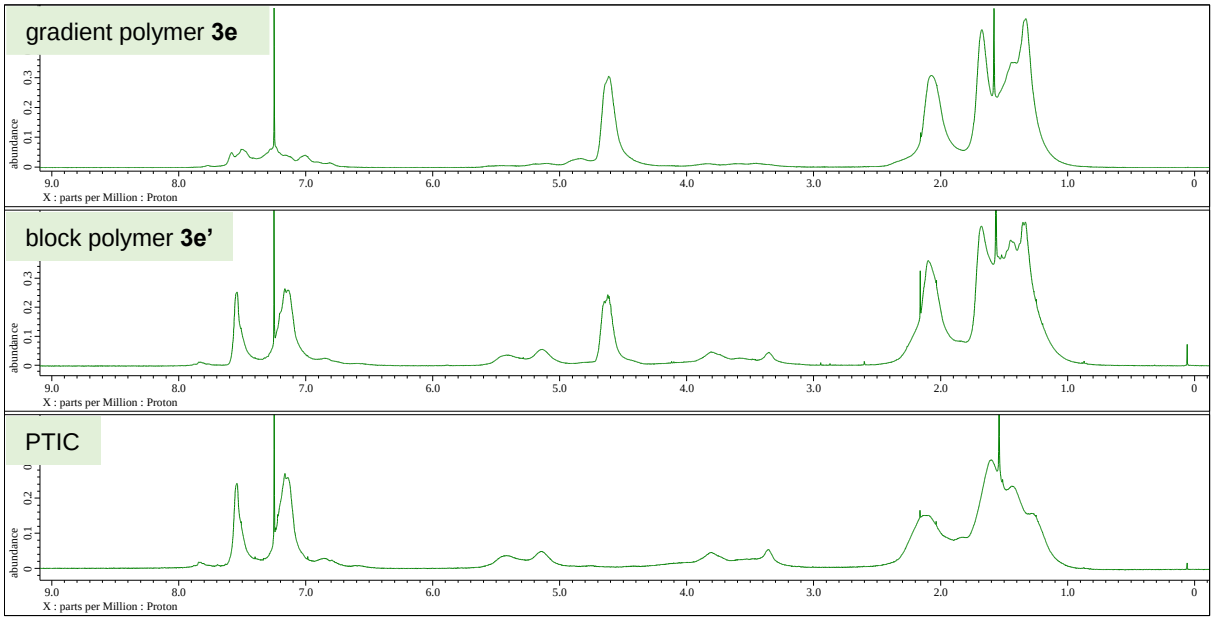

Figure S48. ^{1}H NMR spectra ($CDCl_3$) of purified gradient polymer **3e**, block polymer **3e'**, and PTIC.

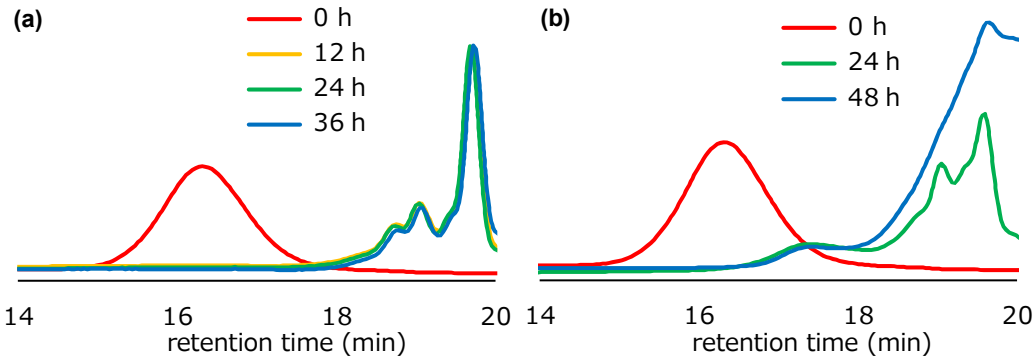

Figure S49. SEC charts during (a) the acid treatment and (b) the UV irradiation of purified PTIC.

2.5 References

(1) Recent reviews: (a) Wang, Y.; Darensbourg, D. J. *Coord. Chem. Rev.* **2018**, *372*, 85–100. (b) Kozak, C. M.; Ambrose, K.; Anderson, T. S. *Coord. Chem. Rev.* **2018**, *376*, 565–587. (c) Scharfenberg, M.; Hilf, J.; Frey, H. *Adv. Funct. Mater.* **2018**, *28*, 1704302. (d) Kamphuis, A. J.; Picchioni, F.; Pescarmona, P. P. *Green Chem.* **2019**, *21*, 406–448. (e) Paradiso, V.; Capaccio, V.; Lamparelli, D. H.; Capacchione, C. *Catalysts* **2020**, *10*, 825. (f) Huang, J.; Worch, J. C.; Dove, A. P.; Coulembier, O. *ChemSusChem* **2020**, *13*, 469–487. (g) Bhat, G. A.; Darensbourg, D. J. *Green Chem.* **2022**, *24*, 5007–5034. (h) Lidston, C. A. L.; Severson, S. M.; Abel, B. A.; Coates, G. W. *ACS Catal.* **2022**, *12*, 11037–11070.

(2) Recent examples: (a) Reiter, M.; Vagin, S.; Kronast, A.; Jandl, C.; Rieger, B. *Chem. Sci.* **2017**, *8*, 1876–1882. (b) Huang. Z.; Wang, Y.; Zhang, N.; Zhang, L.; Darensbourg, D. J. *Macromolecules* **2018**, *51*, 9122–9130. (c) Nagae, H.; Aoki, R.; Akutagawa, S.; Kleemann, J.; Tagawa, R.; Schindler, T.; Choi, G.; Spaniol, T. P.; Tsurugi, H.; Okuda, J.; Mashima, K. *Angew. Chem. Int. Ed.* **2018**, *57*, 2492–2496. (d) Duan, R.; Hu, C.; Sun, Z.; Zhang, H.; Pang, X.; Chen, X. *Green Chem.* **2019**, *21*, 4723–4731. (e) Patil, N. G.; Boopathi, S. K.; Alagi, P.; Hadjichristidis, N.; Gnanou, Y.; Feng, X. *Macromolecules* **2019**, *52*, 2431–2438. (f) Cao, H.; Qin, Y.; Zhuo, C.; Wang, X.; Wang, F. *ACS Catal.* **2019**, *9*, 8669–8676. (g) Asaba, H.; Iwasaki, T.; Hatazawa, M.; Deng, J.; Nagae, H.; Mashima, K.; Nozaki, K. *Inorg. Chem.* **2020**, *59*, 7928–7933. (h) Lindeboom, W.; Fraser, D. A. X.; Durr, C. B.; Williams, C. K. *Chem. Eur. J.* **2021**, *27*, 12224–12231. (i) Yang, G.-W.; Xu, C.-K.; Xie, R.; Zhang, Y.-Y.; Lu, C.; Qi, H.; Yang, L.; Wang, Y.; Wu, G.-P. *Nat. Synth.* **2022**, *1*, 892–901. (j) Li, Y.-N.; Yang, H.-H.; Lu, X.-B. *J. Polym. Sci.* **2022**, *60*, 2078–2085. (k) Zhang, R.; Kuang, Q.; Cao, H.; Liu, S.; Chen, X.; Wang, X.; Wang, F. *CCS Chem.* **2023**, *5*, 750–760.

(3) Inoue, S.; Koinuma, H.; Tsuruta, T. *J. Polym. Sci., Part B: Polym. Lett.* **1969**, *7*, 287–292.

(4) (a) Romain, C.; Williams, C. K. *Angew. Chem. Int. Ed.* **2014**, *53*, 1607–1610. (b) Paul, S.; Romain, C.; Shaw, J.; Williams, C. K. *Macromolecules* **2015**, *48*, 6047–6056. (c) Xu, Y.; Wang, S.; Lin, L.; Xiao, M.; Meng, Y. *Polym. Chem.* **2015**, *6*, 1533–1540. (d) Li, Y.; Hong, J.; Wei, R.; Zhang, Y.; Tong, Z.; Zhang, X.; Du, B.; Xu, J.; Fan, Z. *Chem. Sci.* **2015**, *6*, 1530–1536. (e) Kernbichl, S.; Reiter, M.; Adams, F.; Vagin, S.; Rieger, B. *J. Am. Chem. Soc.* **2017**, *139*, 6787–6790. (f) Kernbichl, S.; Reiter, M.; Mock, J.; Rieger, B. *Macromolecules* **2019**, *52*, 8476–8483. (g) Sulley, G. S.; Gregory, G. L.; Chen, T. T. D.; Carrodeguas, L. P.; Trott, G.; Santmarti, A.; Lee, K.-Y.; Terrill, N. J.; Williams, C. K. *J. Am. Chem. Soc.* **2020**, *142*, 4367–4378. (h) Yang, Z.; Hu, C.; Cui, F.; Pang, X.; Huang, Y.; Zhou, Y.; Chen, X. *Angew. Chem. Int. Ed.* **2022**, *61*, e202117533. (i) Zhou, Y.; Gao, Z.; Hu, C.; Meng, S.; Duan, R.; Sun, Z.; Pang, X. *Macromolecules* **2022**, *55*, 9951–9959.

(5) (a) Kröger, M.; Folli, C.; Walter, O.; Döring, M. *Adv. Synth. Catal.* **2006**, *348*, 1908–1918. (b) Liu, S.; Wang, J.; Huang, K.; Liu, Y.; Wu, W. *Polym. Bull.* **2011**, *66*, 327–340. (c) Gu, L.; Qin, Y.; Gao, Y.; Wang, X.; Wang, F. *Chin. J. Chem.* **2012**, *30*, 2121–2125. (d) Tang, L.; Luo, W.; Xiao, M.; Wang, S.; Meng, Y. *J. Polym. Sci., Part A: Polym. Chem.* **2015**, *53*, 1734–1741. (e)

Xie, D.; Yang, Z.; Wu, L.; Zhang, C.; Chisholm, M. H. *Polym. Int.* **2018**, *67*, 883–893. (f) Hu, C.; Duan, R.; Yang, S.; Pang, X.; Chen, X. *Macromolecules* **2018**, *51*, 4699–4704. (g) Li, X.; Hu, C.; Pang, X.; Duan, R.; Chen, X. *Catal. Sci. Technol.* **2018**, *8*, 6452–6457. (h) Duan, R.; Hu, C.; Sun, Z.; Zhang, H.; Pang, X.; Chen, X. *Green Chem.* **2019**, *21*, 4723–4731. (i) Liu, N.; Gu, C.; Chen, M.; Zhang, J.; Yang, W.; Zhan, A.; Zhang, K.; Lin, Q.; Zhu, L. *ChemistrySelect* **2020**, *5*, 2388–2394. (j) Chen, Y.; Wang, W.; Xie, D.; Wu, L.; Zhang, C. *J. Polym. Sci.* **2021**, *59*, 1528–1539. (k) Li, X.; Duan, R.-L.; Hu, C.-Y.; Pang, X.; Deng, M.-X. *Polym. Chem.* **2021**, *12*, 1700–1706. (l) Li, X.; Hu, C.-Y.; Duan, R.-L.; Liang, Z.-Z.; Pang, X.; Deng, M.-X. *Polym. Chem.* **2021**, *12*, 3124–3131. (m) Huang, Y.; Hu, C.; Pang, X.; Zhou, Y.; Duan, R.; Sun, Z.; Chen, X. *Angew. Chem. Int. Ed.* **2022**, *61*, e202202660.

(6) Recent reviews: (a) Liang, J.; Ye, S.; Wang, S.; Xiao, M.; Meng, Y. *Polym. J.* **2021**, *53*, 3–27. (b) Lamparelli, D. H.; Capacchione, C. *Catalysts* **2021**, *11*, 961.

(7) Zhi, Y.; Miao, Y.; Zhao, W.; Wang, J.; Zheng, Y.; Su, H.; Jia, Q.; Shan, S. *Polymer* **2019**, *165*, 11–18.

(8) Yue, T.-J.; Ren, B.-H.; Zhang, W.-J.; Lu, X.-B.; Ren, W.-M.; Darensbourg, D. J. *Angew. Chem. Int. Ed.* **2021**, *60*, 4315–4321.

(9) Plajer, A. J.; Williams, C. K. *Angew. Chem. Int. Ed.* **2022**, *61*, e202104495.

(10) (a) Jurrat, M.; Pointer-Gleadhill, B. J.; Ball, L. T.; Chapman, A.; Adriaenssens, L. *J. Am. Chem. Soc.* **2020**, *142*, 8136–8141. (b) Song, L.; Wei, W.; Farooq, M. A.; Xiong, H. *ACS Macro Lett.* **2020**, *9*, 1542–1546. (c) Jia, M.; Hadjichristidis, N.; Gnanou, Y.; Feng, X. *Angew. Chem. Int. Ed.* **2021**, *60*, 1593–1598. (d) Hu, C.; Chen, X.; Niu, M.; Zhang, Q.; Duan, R.; Pang, X. *Macromolecules* **2022**, *55*, 652–657. (e) Teng, Y.-Q.; Liu, Y.; Lu, X.-B. *Macromolecules* **2022**, *55*, 9074–9080.

(11) (a) Taguchi, Y.; Shibuya, I.; Yasumoto, M.; Tsuchiya, T.; Yonemoto, K. *Bull. Chem. Soc. Jpn.* **1990**, *63*, 3486–3489. (b) Nambu, Y.; Endo, T. *J. Org. Chem.* **1993**, *58*, 1932–1934.

(12) (a) Chen, C.; Gnanou, Y.; Feng, X. *Macromolecules* **2021**, *54*, 9474–9481. (b) Song, L.; Liu, M.; You, D.; Wei, W.; Xiong, H. *Macromolecules* **2021**, *54*, 10529–10536. (c) Lai, T.; Zhang, P.; Zhao, J.; Zhang, G. *Macromolecules* **2021**, *54*, 11113–11125. (d) Zhu, X.-F.; Lu, X.-Y.; Xu, C.-K.; Fang, Y.-B.; Yang, G.-W.; Li, W.; Wang, J.; Wu, G.-P. *Chin. J. Chem.* **2023**, *41*, 3311–3318.

(13) (a) Ema, T.; Miyazaki, Y.; Koyama, S.; Yano, Y.; Sakai, T. *Chem. Commun.* **2012**, *48*, 4489−4491. (b) Ema, T.; Miyazaki, Y.; Shimonishi, J.; Maeda, C.; Hasegawa, J. *J. Am. Chem. Soc.* **2014**, *136*, 15270−15279. (c) Maeda, C.; Taniguchi, T.; Ogawa, K.; Ema, T. *Angew. Chem. Int. Ed.* **2015**, *54*, 134−138. (d) Maeda, C.; Shimonishi, J.; Miyazaki, R.; Hasegawa, J.; Ema, T. *Chem. Eur. J.* **2016**, *22*, 6556−6563. (e) Maeda, C.; Sasaki, S.; Ema, T. *ChemCatChem* **2017**, *9*, 946−949.

(14) Deng, J.; Ratanasak, M.; Sako, Y.; Tokuda, H.; Maeda, C.; Hasegawa, J.; Nozaki, K.; Ema, T. *Chem. Sci.* **2020**, *11*, 5669–5675.

(15) Maeda, C.; Kawabata, K.; Niki, K.; Sako, Y.; Okihara, T.; Ema, T. *Polym. Chem.* **2023**, *14*,

4338–4343.

(16) (a) Hasegawa, J.; Miyazaki, R.; Maeda, C.; Ema, T. *Chem. Rec.* **2016**, *16*, 2260–2267. (b) Ema, T. *Bull. Chem. Soc. Jpn.* **2023**, *96*, 693–701.

(17) Maeda, C.; Inoue, H.; Ichiki, A.; Okihara, T.; Ema, T. *ACS Catal.* **2022**, *12*, 13042–13049.

(18) Li, Z.; Mayer, R. J.; Ofial, A. R.; Mayr, H. *J. Am. Chem. Soc.* **2020**, *142*, 8383–8402.

(19) Recent reviews: (a) Yue, T.-J.; Wang, L.-Y.; Ren, W.-M. *Polym. Chem.* **2021**, *12*, 6650–6666. (b) Uva, A.; Lin, A.; Babi, J.; Tran, H. *J. Chem. Technol. Biotechnol.* **2022**, *97*, 801–809. (c) Carboué, Q.; Fadlallah, S.; Lopez, M.; Allais, F. *Macromol. Rapid Commun.* **2022**, *43*, 2200254. (d) Dirauf, M.; Muljajew, I.; Weber, C.; Schubert, U. S. *Prog. Polym. Sci.* **2022**, *129*, 101547. (e) Hu, C.; Pang, X.; Chen, X. *Macromolecules* **2022**, *55*, 1879–1893.

(20) Selected review: Alam, M. M.; Jack, K. S.; Hill, D. J. T.; Whittaker, A. K.; Peng, H. *Eur. Polym. J.* **2019**, *116*, 394−414.

(21) Whiteoak, C. J.; Martin, E.; Escudero-Adán, E.; Kleij, A. W. *Adv. Synth. Catal.* **2013**, *355*, 2233–2239.

(22) Baba, A.; Seki, K.; Matsuda, H. *J. Org. Chem.* **1991**, *56*, 2684–2688.

(23) Li, C.; Zhao, W.; He, J.; Zhang, Y. *Chem. Commun.* **2019**, *55*, 12563–12566.

(24) Li, D.; Wang, J.; Yu, S.; Ye, S.; Zou, W.; Zhang, H.; Chen, J. *Chem. Commun.* **2020**, *56*, 2256–2259.

Chapter 3

One-Pot Synthesis of Enamines, Aldehydes, and Nitriles from CO_2

3.1 Abstract

Tetrabutylammonium acetate (TBAA) and $Cu(OAc)_2$ worked as a binary catalytic system for the solvent-free *N*-formylation of amines with CO_2 and $PhSiH_3$. This catalysis making C–H and C–N bonds with CO_2 was coupled with the C–C bond-forming reactions to achieve the one-pot synthesis of enamines, aldehydes, and nitriles. The X-ray crystal structure of a $Cu(OAc)_2$–TBAA complex was also revealed.

3.2 Introduction

Effective CO_2 utilization is essential for the creation of carbon-neutral societies, and CO_2 fixation plays a pivotal role in carbon-recycling technologies. Among them, reductive conversions of CO_2 have attracted considerable attention of chemists from the viewpoint of energy and sustainable organic synthesis.[1] In particular, deoxygenative CO_2 conversions making both C–H and C–C bonds can give value-added chemicals such as aldehydes,[2] alcohols,[3] alkenes,[4] and heterocyclic compounds,[5] and expanding the product diversity is desirable. Hydrosilanes are inexpensive and easy-to-use liquid reductants that are useful for CO_2 reduction because deoxygenative CO_2 conversions with hydrosilanes are thermodynamically favored by the formation of the strong Si–O bond.[6] The catalytic *N*-formylation of amines with CO_2 and hydrosilanes to give formamides is one of the most successful examples.[6–8]

One-pot reactions can reduce solvent, waste, time, labor, and cost by omitting the purification of intermediates and have great potential in sustainable organic synthesis (pot economy),[9] although conducting multiple reactions in a single reactor may decrease product yields because of detrimental interactions between reagents, solvents, and byproducts. Despite such challenging aspects, one-pot sequential reactions with CO_2 are fascinating,[3e,4a,5c–f,10] among which one-pot two-step reactions that involve a C–H bond-forming reaction to give bis(silyl)acetal or bis(boryl)acetal followed by a C–C bond-forming reaction have opened up new ways of reductive CO_2 fixation leading to various products.[3e,4a,5c–f]

On the other hand, silyl formates (HCO_2SiR_3) cannot be utilized directly for the synthesis of aldehydes or related compounds despite the importance of the formyl group.[8] We envisioned that a C–H bond-forming reaction via CO_2 hydrosilylation in the presence of amine and the subsequent robust C–C bond-forming reaction in a one-pot sequential manner could be a reliable synthetic method for various CO_2-derived compounds. As an initial proof of concept, we have demonstrated one-pot aldehyde synthesis via the solvent-free *N*-formylation of *N*,*O*-dimethylhydroxylamine with

CO_2 and $PhSiH_3$ in the presence of tetrabutylammonium acetate ($Bu_4N^+AcO^-$, TBAA) to give Weinreb formamide, Me(MeO)NCHO, followed by the C–C bond formation with Grignard reagents in THF (Scheme 1).[8] Although this one-pot strategy via formamides has good potential in the selective synthesis of diverse chemicals from CO_2, our preliminary experiments have indicated that the catalytic efficiency and selectivity in the first step needs to be enhanced to achieve other C–C bond-forming reactions in the second step because residual stuffs sometimes have a detrimental effect on the second step. Here we have found $Cu(OAc)_2$ as an effective co-catalyst for the TBAA-catalyzed *N*-formylation of amines with CO_2 (1 atm) and $PhSiH_3$ (1 equiv) under solvent-free conditions at 20 °C to cleanly produce various formamides. This solvent-free catalytic system enabled us to conduct various C–C bond-forming reactions such as the Peterson, Vilsmeier–Haack, and modified Vilsmeier–Haack reactions in the second step of one-pot reactions to synthesize enamines, aldehydes, and nitriles, respectively (Scheme 1).

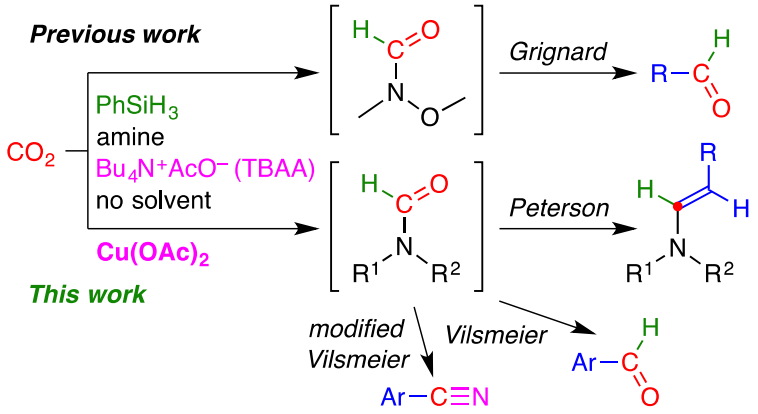

Scheme 1. One-pot strategy via formamides.

3.3 Result and Discussion

We screened potential co-catalysts (3 mol%) in the solvent-free *N*-formylation of *N*-methylaniline (**1a**) with CO_2 (1 atm) and $PhSiH_3$ (1 equiv) in the presence of 3 mol% TBAA (Table 1). As a result, $Cu(OAc)_2$ showed the highest yield (96%), while lower yields based on synergetic or inhibitory effects were observed for the other metal acetate salts (entries 1–9). In sharp contrast, other copper salts $CuCl_2$ and $CuBr_2$ quenched the reaction completely (entries 11–12), although $CuSO_4$ showed little or no effect on the yield (entry 10). CuOAc was less effective (entry 13). Clearly, the combination of TBAA and $Cu(OAc)_2$ was the best choice. Interestingly, the addition of TBAA was essential for the reaction (entries 14–15). Reducing the amounts of catalyst and co-catalyst to 1 mol% and 0.5 mol% gave **2a** in 98% and 91% yields, respectively (entries 16–17), and the yield was higher at 20 °C than at 30 °C (entries 16 and 18); entry 16 is optimal. This catalytic system is one of the rare examples of solvent-free *N*-formylation of amines with CO_2 using commercially available catalysts under mild conditions.[6–8]

Table 1. Solvent-free *N*-formylation of **1a**.[a]

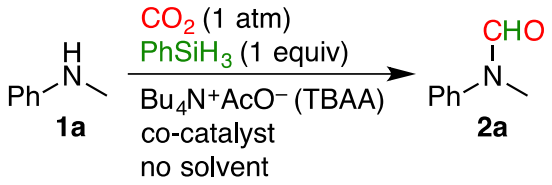

entry	catalyst	co-catalyst	yield (%)[b]
1	TBAA	–	82
2[c]	TBAA	$Mn(OAc)_2$	67
3	TBAA	$Fe(OAc)_2$	90
4[c]	TBAA	$Co(OAc)_2$	75
5[c]	TBAA	$Ni(OAc)_2$	63
6	TBAA	$Cu(OAc)_2$	96
7[d]	TBAA	$Zn(OAc)_2$	75
8	TBAA	$Pd(OAc)_2$	66
9	TBAA	AgOAc	90
10	TBAA	$CuSO_4$	78
11	TBAA	$CuCl_2$	0
12	TBAA	$CuBr_2$	0
13	TBAA	CuOAc	92
14	–	$Cu(OAc)_2$	0
15	–	CuOAc	0
16[e]	TBAA	$Cu(OAc)_2$	98
17[f]	TBAA	$Cu(OAc)_2$	91
18[e,g]	TBAA	$Cu(OAc)_2$	80

[a] Reaction conditions: **1a** (2.0 mmol), $PhSiH_3$ (2.0 mmol), CO_2 (1 atm, balloon), TBAA (3 mol%), co-catalyst (3 mol%), 20 °C, 18 h. [b] Determined by ^1H NMR using mesitylene as an internal standard. [c] A metal salt of tetrahydrate was used. [d] A metal salt of dihydrate was used. [e] TBAA (1 mol%), $Cu(OAc)_2$ (1 mol%). [f] TBAA (0.5 mol%), $Cu(OAc)_2$ (0.5 mol%). [g] 30 °C.

Substrate scope was examined with a catalyst loading of 1 mol% (Scheme 2). Various amines with electron-withdrawing or electron-donating groups were successfully converted into *N*-substituted formanilides **2a**–**e** in good to high isolated yields. Other *N*-substituted anilines **1f**–**h** were also tolerated, and the corresponding formanilides were successfully obtained. Although more bulky amine **1i** was poor substrates, *N*-benzylamines **1j**–**k** exhibited good reactivity to give formamides **2j**–**k**.

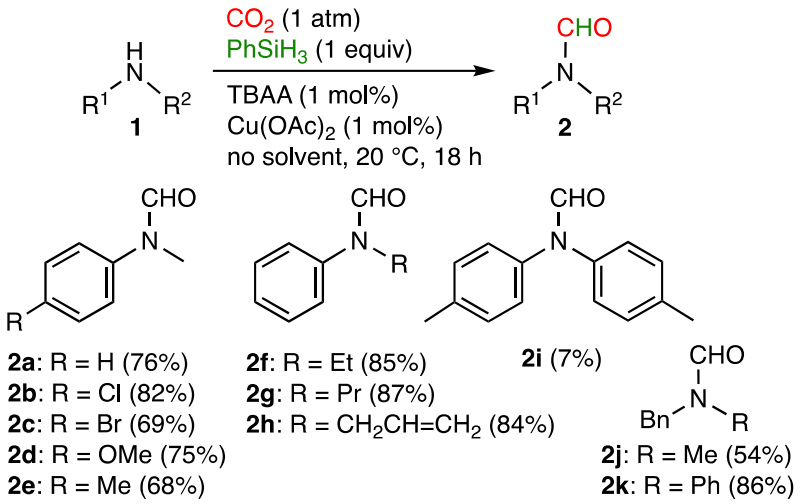

Scheme 2. Solvent-free *N*-formylation of amines.

Interestingly, the present solvent-free catalysis needs no ligand such as phosphines and NHCs in contrast to the previous reports on the copper-catalyzed hydrosilylation of CO_2 in organic solvent.[7c,11] To access the mechanistic aspect, the $Cu(OAc)_2$–TBAA complex crystallized from THF/Et_2O was subjected to X-ray diffraction analysis (Figure 1). The crystal contained two types of copper complexes; one is a self-assembled chain, where the $Cu_2(OAc)_4$ paddlewheel structures are interconnected by AcO^- accompanied by a tetrabutylammonium cation, and the other is a discrete dinuclear Cu(II) complex with hydroxide and acetate bridges; the hydroxide ion may come from TBAA although the accurate origin is unknown. We suppose that these complexes, which exist in equilibria, make the copper ions soluble in the neat liquid substrates without solvent, where amine **1** may also participate in the complex formation. Based on the crystal structure (Figure 1) and the previous reports,[11] a plausible reaction mechanism is shown in Scheme 3. The AcO^- ion reacts with $PhSiH_3$ to afford a copper hydride, which is a catalytically active species.[11] Our attempts to detect a copper hydride species by means of NMR spectroscopy were unsuccessful probably because of the polymeric nature of the catalytic system (Figure 1) as well as additional complex equilibria involving amine **1**. There is even a possibility of the formation of metal clusters or nanoparticles upon addition of $PhSiH_3$, for which TBAA is essential (Table 1, entries 6 and 14). The subsequent insertion of CO_2 into the Cu–H bond generates a copper formate, which reacts with $PhSiH_3$ to give a silyl formate with the regeneration of the copper hydride species. The silyl formate reacts with amines to give formamides. Although the previously reported catalytic cycle driven by TBAA alone, where TBA formate acts as a catalytically active species, may be predominant,[8] judging from the reaction yields (Table 1, entries 1 and 6), this copper-based catalysis is considered to be important for the complete and clean conversion of **1a** into **2a**.

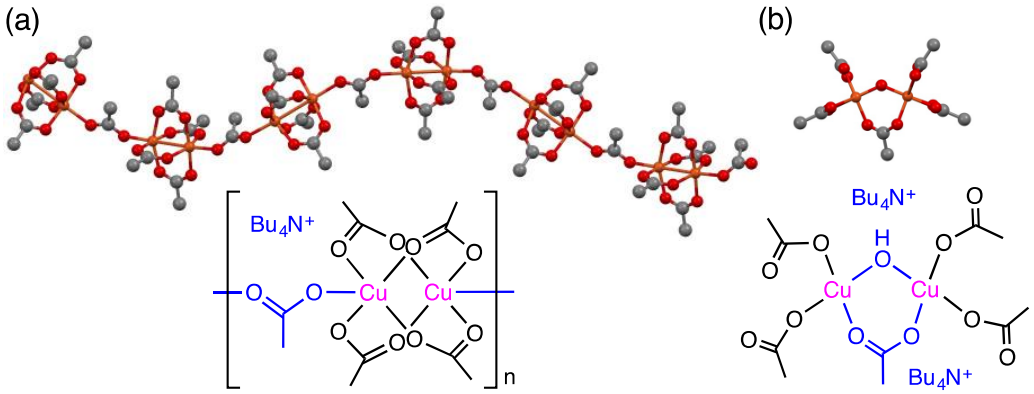

Figure 1. X-ray crystal structure of $Cu(OAc)_2$–TBAA complex (CCDC 2162064). (a) Coordination polymer moiety and (b) dinuclear Cu(II) complex moiety. Hydrogen atoms and counter cations are omitted for clarity.

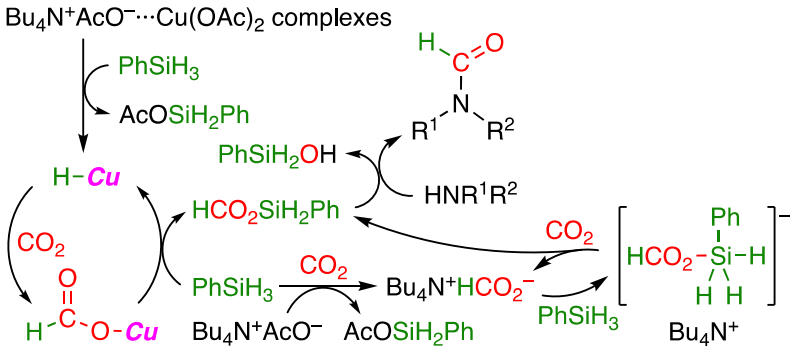

Scheme 3. Plausible reaction mechanism.

With the efficient solvent-free catalytic system for C–H bond formation with CO_2 in hand, we next searched for C–C bond-forming reactions that could be employed in the second step, where any solvent could be selected freely. The deoxygenative conversion of CO_2 into olefins is quite rare and challenging.[4] We envisioned that our solvent-free *N*-formylation system could be used for unprecedented olefination to synthesize enamines, which are useful intermediates for various compounds including heterocyclic compounds and pharmaceutical drugs.[12] In view of only a few successful conversions of *N*-formanilides into enamines,[13] we tested several olefination methods such as the Wittig, Reformatsky, and Peterson reactions of **2a** before the trial of a one-pot reaction. As a result, only the Peterson reaction gave an olefination product in a high yield. We therefore employed the Peterson reaction in the second step of the one-pot enamine synthesis from CO_2 (Scheme 4). After the solvent-free *N*-formylation of **1a** with CO_2 and $PhSiH_3$ in the presence of 1 mol% TBAA and $Cu(OAc)_2$, the reaction mixture was cooled to –40 °C, and a solution of lithium *N*,*N*-dimethyl-2-(trimethylsilyl)acetamide[14] in THF was added via a syringe. The solution was stirred for 30 min, and the reaction was quenched by saturated aqueous NH_4Cl. To our delight, the one-pot Peterson reaction successfully proceeded to give enamine **3a** in 69% yield. Interestingly, a mixture of *cis*/*trans*-enamines was produced before quenching, and the *cis*-isomer was completely converted into the

trans-isomer during silica gel column chromatography. *N*-Methylanilines **1b**–**e** with electron-withdrawing or electron-donating groups at the *para*-position were well tolerated, and the corresponding enamines **3b**–**e** were obtained in good yields. *N*-Substituted anilines **1f**–**h** were also smoothly converted into enamines **3f**–**h** in good yields while *N*,*N*-dialkylamine **1j**–**k** exhibited moderate reactivity.

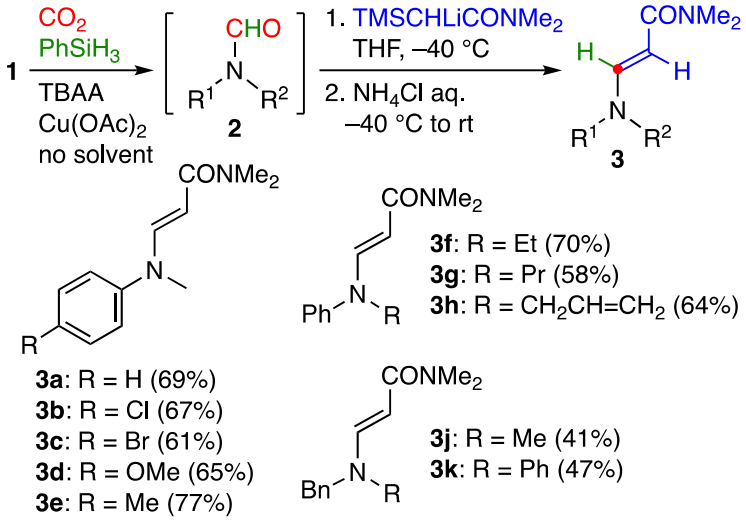

Scheme 4. One-pot synthesis of enamines.

Encouraged by these results, we further explored the scope of the one-pot strategy via formamides. The Vilsmeier–Haack reaction is an efficient method for the C–H transformation of electron-rich aromatics with $POCl_3$ and DMF or *N*-methylformanilide (**2a**) to the corresponding aromatic aldehydes.[15] We expected that the Vilsmeier–Haack reaction might be applicable to this system. After the solvent-free synthesis of **2a** from **1a**, $PhSiH_3$ and CO_2 in the presence of 1 mol% TBAA and $Cu(OAc)_2$, anthracene, *o*-dichlorobenzene, and $POCl_3$ were added, and the mixture was stirred at 90 °C for 4 h. After cooling to room temperature, the reaction was quenched and neutralized with saturated aqueous NaOAc to give 9-anthraldehyde (**4a**) in 70% NMR yield (Table S1). Interestingly, the NMR yield was enhanced to 85% when the amounts of TBAA and $Cu(OAc)_2$ were increased to 3 mol%. We consider that residual hydrosilane (Si–H bond) affected the Vilsmeier–Haack reaction. In addition, when only TBAA (3 mol%) was used as a catalyst, the NMR yield of **4a** was decreased to 63%, which indicates the important role of $Cu(OAc)_2$. Substrate scope was examined under the optimized conditions using 3 mol% of TBAA and $Cu(OAc)_2$ (Scheme 5). Aromatic aldehydes **4a**–**e** were obtained in good to high isolated yields. Heteroaromatic aldehydes **4f**–**h** were also obtained in moderate yields. Although 2-bromothiophene was converted into a mixture of aldehydes with a bromide or chloride substituent, the use of $POBr_3$ instead of $POCl_3$ furnished **4i** selectively in a high yield.

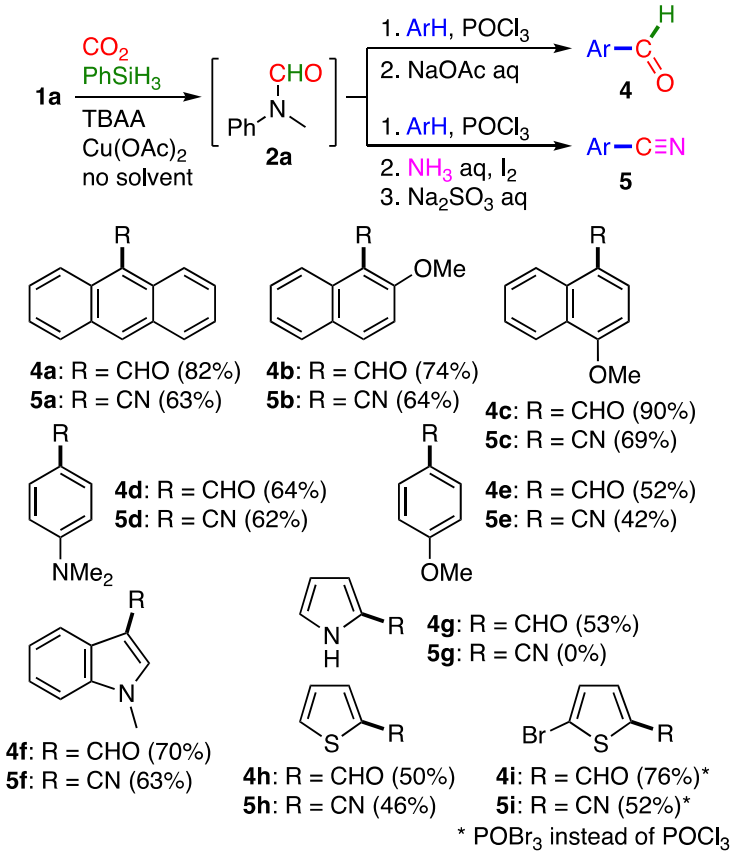

Scheme 5. One-pot synthesis of aldehydes and nitriles.

Aryl nitriles are an important class of compounds widely found in natural products, drugs, functional materials, and intermediates, which have driven organic chemists to develop a variety of synthetic methods.[16] To our knowledge, however, there are only two reports on nitrile synthesis from CO_2, where CO_2 and NH_3 (gas) were used as the CN sources while aryl or alkyl halides and transition metals were used as substrates and catalysts, respectively.[17] The nitrile synthesis from CO_2 and NH_3 is fascinating because the highly toxic cyanide ion is unnecessary. We turned our attention to the transformation of simple aromatics to aromatic nitriles via C–H bond activation using the modified Vilsmeier–Haack reaction.[18] This cyanation is easy and inexpensive because of the use of aqueous NH_3. We carried out the one-pot three-step synthesis of nitriles from CO_2 (Scheme 5). Various nitriles **5** including heteroaromatic nitriles **5f** and **5h**–**i** were obtained selectively in modest to good yields although 2-cyanopyrrole (**5g**) could not be prepared.

3.4 Conclusions

In summary, TBAA and $Cu(OAc)_2$ worked as an excellent binary catalytic system for the solvent-free *N*-formylation of amines with CO_2 and $PhSiH_3$ to give formamides, which were then converted into enamines, aldehydes, and nitriles in one pot. This is the first example of the Peterson and the Vilsmeier–Haack reactions using CO_2 as a C1 source, and the synthesis of enamines from CO_2 is unprecedented. Clean solvent-free C–H bond-forming catalysis in the first step was essential for the

efficient C–C bond-forming reaction in the second step. The one-pot strategy via formamides has great potential in the controlled synthesis of various CO_2-derived compounds.

3.5 Experimental Section

[A] General Methods.

NMR spectra were measured on a JEOL JNM-ECS400 spectrometer, and chemical shifts are reported as the delta scale in ppm using an internal reference (δ = 7.26 ppm ($CDCl_3$) for ^1H NMR and δ = 77.16 ppm ($CDCl_3$) for $^{13}C\{^1H\}$ NMR). IR spectra were recorded on a Shimadzu IRAffinity-1 spectrophotometer. Melting points were measured on a Yanaco melting point apparatus (uncorrected). High-resolution double-focusing mass spectrometry (HRMS) was measured on a JEOL JMS-700N. Column chromatography on silica gel was carried out using Fuji Silysia BW-127 ZH (100–270 mesh).

[B] *N*-formylation of Amines with CO_2 and Phenylsilane.

General Procedure. In a glovebox (purge type) under N_2 atmosphere, TBAA (6.0 mg, 0.020 mmol, 1 mol%) and $Cu(OAc)_2$ (3.6 mg, 0.020 mmol, 1 mol%) were put in a 30 mL Schlenk flask fitted with a rubber septum (solid amine **1d** or **1i** (2.0 mmol) was added in this step), and the flask was taken out from the glovebox. After the flask was evacuated and filled with CO_2 (balloon), the flask was put in a thermostatic bath at 20 °C. Amine **1** (2.0 mmol) and $PhSiH_3$ (250 μL, 2.0 mmol, stored over molecular sieves 3A) were added in this order via syringes. The mixture was stirred at 20 °C for 18 h. Purification by silica gel column chromatography (eluent shown below) gave formamide **2**.

***N*-Methylformanilide (2a).**[8] Eluent = hexane/EtOAc (3:1); 205 mg (1.52 mmol, 76% yield); Yellow oil; ^1H NMR ($CDCl_3$, 400 MHz) δ 8.48 (s, 1H), 7.42 (t, J = 7.9 Hz, 2H), 7.28 (t, J = 7.6 Hz, 1H), 7.18 (d, J = 7.4 Hz, 2H), 3.33 (s, 3H); $^{13}C\{^1H\}$ NMR ($CDCl_3$, 100 MHz) δ 162.3, 142.1, 129.6, 126.3, 122.3, 32.0.

***N*-(4-Chlorophenyl)-*N*-methylformamide (2b).**[8] Eluent = hexane/EtOAc (2:1); 276 mg (1.63 mmol, 82% yield); Off-white solid; mp 46.9–47.2 °C; ^1H NMR ($CDCl_3$, 400 MHz) δ 8.45 (s, 1H), 7.38 (d, J = 8.8 Hz, 2H), 7.11 (d, J = 8.8 Hz, 2H), 3.30 (s, 3H); $^{13}C\{^1H\}$ NMR ($CDCl_3$, 100 MHz) δ 162.1, 140.8, 132.1, 129.8, 123.6, 32.1.

***N*-(4-Bromophenyl)-*N*-methylformamide (2c).**[8] Eluent = hexane/EtOAc (3:1); 297 mg (1.39 mmol, 69% yield); White solid; mp 66.2–68.1 °C; ^1H NMR ($CDCl_3$, 400 MHz) δ 8.46 (s, 1H), 7.53 (d, J = 8.8 Hz, 2H), 7.06 (d, J = 8.6 Hz, 2H), 3.30 (s, 3H); $^{13}C\{^1H\}$ NMR ($CDCl_3$, 100 MHz) δ 162.0, 141.3, 132.8, 123.8, 119.8, 32.0.

***N*-(4-Methoxyphenyl)-*N*-methylformamide (2d).**[8] Eluent = hexane/EtOAc (1:1); 246 mg (1.49 mmol, 75% yield); Colorless oil; ^1H NMR ($CDCl_3$, 400 MHz) δ 8.32 (s, 1H), 7.08 (d, J = 8.8 Hz, 2H), 6.92 (d, J = 9.0 Hz, 2H), 3.81 (s, 3H), 3.26 (s, 3H); $^{13}C\{^1H\}$ NMR ($CDCl_3$, 100 MHz) δ 162.6, 158.4, 135.3, 124.8, 114.9, 55.7, 32.8.

***N*-Methyl-*N*-(4-methylphenyl)formamide (2e).**[8] Eluent = hexane/EtOAc (3:1); 202 mg (1.35 mmol, 68% yield); Colorless oil; ^1H NMR ($CDCl_3$, 400 MHz) δ 8.42 (s, 1H), 7.21 (d, J = 8.2 Hz, 2H), 7.06 (d, J = 8.2 Hz, 2H), 3.29 (s, 3H), 2.36 (s, 3H); $^{13}C\{^1H\}$ NMR ($CDCl_3$, 100 MHz) δ 162.2, 139.6, 136.2, 130.1, 122.4, 32.1, 20.8.

***N*-Ethyl-*N*-phenylformamide (2f).**[8] Eluent = hexane/EtOAc (3:1); 254 mg (1.70 mmol, 85% yield); Yellow oil; ^{1}H NMR ($CDCl_3$, 400 MHz) δ 8.35 (s, 1H), 7.41 (t, J = 7.8 Hz, 2H), 7.30 (t, J = 7.6 Hz, 1H), 7.17 (d, J = 7.6 Hz, 2H), 3.86 (q, J = 7.2 Hz, 2H), 1.16 (t, J = 7.2 Hz, 3H); ^{13}C{^{1}H} NMR ($CDCl_3$, 100 MHz) δ 161.8, 140.6, 129.4, 126.6, 124.0, 39.8, 12.8.

***N*-Phenyl-*N*-propylformamide (2g).**[8] Eluent = hexane/EtOAc (3:1); 285 mg (1.75 mmol, 87% yield); Colorless oil; ^{1}H NMR ($CDCl_3$, 400 MHz) δ 8.38 (s, 1H), 7.41 (t, J = 7.7 Hz, 2H), 7.30 (t, J = 7.4 Hz, 1H), 7.17 (d, J = 7.3 Hz, 2H), 3.78 (t, J = 7.6 Hz, 2H), 1.54–1.59 (m, 2H), 0.89 (t, J = 7.4 Hz, 3H); ^{13}C{^{1}H} NMR ($CDCl_3$, 100 MHz) δ 162.4, 141.0, 129.6, 126.8, 124.2, 46.5, 20.8, 11.2.

***N*-Allyl-*N*-phenylformamide (2h).**[8] Eluent = hexane/EtOAc (3:1); 270 mg (1.68 mmol, 84% yield); Yellow oil; ^{1}H NMR ($CDCl_3$, 400 MHz) δ 8.49 (s, 1H), 7.40 (t, J = 7.7 Hz, 2H), 7.28 (t, J = 7.4 Hz, 1H), 7.19 (d, J = 7.4 Hz, 2H), 5.80–5.90 (m, 1H), 5.16–5.22 (m, 2H), 4.42 (dt, J = 1.6, 3.1 Hz, 2H); ^{13}C{^{1}H} NMR ($CDCl_3$, 100 MHz) δ 161.9, 141.1, 132.5, 129.5, 126.6, 123.4, 117.6, 47.8.

***N*,*N*-Di(4-tolyl)formamide (2i).**[8] Eluent = hexane/EtOAc (4:1); 33.0 mg (0.146 mmol, 7% yield); Yellow solid; mp 126.1–126.9 °C; ^{1}H NMR ($CDCl_3$, 400 MHz) δ 8.62 (s, 1H), 7.15–7.20 (m, 6H), 7.05 (d, J = 8.5 Hz, 2H), 2.37 (s, 3H), 2.35 (s, 3H); ^{13}C{^{1}H} NMR ($CDCl_3$, 100 MHz) δ 161.9, 139.5, 137.3, 137.0, 136.8, 130.3, 129.9, 126.0, 125.1, 21.2, 21.1.

***N*-Benzyl-*N*-methylformamide (2j).**[8] Eluent = hexane/EtOAc (1:1); 162 mg (1.09 mmol, 54% yield); Colorless oil; ^{1}H NMR ($CDCl_3$, 400 MHz) (major rotamer) δ 8.29 (s, 1H), 7.19–7.39 (m, 5H), 4.39 (s, 2H), 2.78 (s, 3H); (minor rotamer) δ 8.16 (s, 1H), 7.19–7.39 (m, 5H), 4.52 (s, 2H), 2.84 (s, 3H); ^{13}C{^{1}H} NMR ($CDCl_3$, 100 MHz) δ 162.7, 162.5, 136.0, 135.7, 128.8, 128.6, 128.2, 128.0, 127.6, 127.3, 53.4, 47.6, 34.0, 29.3.

***N*-Benzyl-*N*-phenylformamide (2k).**[7g] Eluent = hexane/EtOAc (3:1); 365 mg (1.73 mmol, 86% yield); Yellow oil; ^{1}H NMR ($CDCl_3$, 400 MHz) δ 8.56 (s, 1H), 7.22–7.36 (m, 8H), 7.10 (d, J = 8.2 Hz, 2H), 5.00 (s, 2H); ^{13}C{^{1}H} NMR ($CDCl_3$, 100 MHz) δ 162.5, 141.0, 136.7, 129.6, 128.6, 127.9, 127.5, 126.9, 124.1, 48.9.

[C] One-Pot Enamine Synthesis from CO_2.

General Procedure. In a glovebox (purge type) under N_2 atmosphere, TBAA (6.0 mg, 0.020 mmol, 1 mol%) and $Cu(OAc)_2$ (3.6 mg, 0.020 mmol, 1 mol%) were put in a 30 mL Schlenk flask fitted with a rubber septum (solid amine **1d** or **1k** was added in this step), and the flask was taken out from the glovebox. After the flask was evacuated and filled with CO_2 (balloon), the flask was put in a thermostatic bath at 20 °C. Amine **1** (2.0 mmol) and $PhSiH_3$ (250 μL, 2.0 mmol, stored over molecular sieves 3A) were added in this order via syringes. The mixture was stirred at 20 °C for 18 h. This reaction mixture containing formamide **2** was used in the subsequent reaction without purification. The CO_2 balloon was replaced by a N_2 balloon, and dry THF (1 mL) was added. The reaction mixture was cooled to –40 °C, and a solution of lithium *N*,*N*-dimethyl-2-(trimethylsilyl)acetamide in THF (3.7 mL, 2.2 mmol) (Supporting Information) was added via syringe. After stirring at –40 °C for reaction time (typically 30 min), saturated aqueous NH_4Cl (5 mL) was added, and the mixture was warmed to room temperature. The product was extracted with EtOAc (10 mL × 3), and the organic

layers were combined, dried over Na_2SO_4, and concentrated. Purification by silica gel column chromatography (eluent = EtOAc except for **3k**) afforded enamine **3**.

(*E*)-*N*,*N*-Dimethyl-3-(*N*-methyl-*N*-phenylamino)-2-propenamide (3a).[19] Reaction time 30 min; 293 mg (1.44 mmol, 69% yield); White solid; mp 106–108 °C; ^{1}H NMR ($CDCl_3$, 400 MHz) δ 8.03 (d, J = 12.8 Hz, 1H), 7.30–7.34 (m, 2H), 7.12–7.15 (m, 2H), 7.07 (t, J = 7.3 Hz, 1H), 5.26 (d, J = 12.6 Hz, 1H), 3.25 (s, 3H), 3.05 (s, 6H); ^{13}C{^{1}H} NMR ($CDCl_3$, 100 MHz) δ 168.9, 147.2, 147.0, 129.4, 123.5, 119.5, 90.2, 36.6; IR (KBr) 1645 cm^{-1}; HRMS (EI) *m*/*z*: [M]$^+$ calcd for $C_{12}H_{16}N_2O$ 204.1263; found 204.1259.

(*E*)-3-[*N*-(4-Chlorophenyl)-*N*-methylamino]-*N*,*N*-dimethyl-2-propenamide (3b). Reaction time 30 min; 318 mg (1.33 mmol, 67% yield); White solid; mp 133–136 °C; ^{1}H NMR ($CDCl_3$, 400 MHz) δ 7.95 (d, J = 12.6 Hz, 1H), 7.28 (d, J = 9.1 Hz, 2H), 7.06 (d, J = 8.9 Hz, 2H), 5.29 (d, J = 12.7 Hz, 1H), 3.23 (s, 3H), 3.04 (s, 6H); ^{13}C{^{1}H} NMR ($CDCl_3$, 100 MHz) δ 168.7, 146.6, 145.6, 129.4, 128.7, 120.6, 91.0, 36.6; IR (KBr) 1651 cm^{-1}; HRMS (EI) *m*/*z*: [M]$^+$ calcd for $C_{12}H_{15}{}^{35}ClN_2O$ 238.0873; found 238.0868.

(*E*)-3-[*N*-(4-Bromophenyl)-*N*-methylamino]-*N*,*N*-dimethyl-2-propenamide (3c). Reaction time 30 min; 348 mg (1.24 mmol, 61% yield); White solid; mp 147–150 °C; ^{1}H NMR ($CDCl_3$, 400 MHz) δ 7.95 (d, J = 12.8 Hz, 1H), 7.42 (d, J = 9.1 Hz, 2H), 7.00 (d, J = 9.0 Hz, 2H), 5.30 (d, J = 12.8 Hz, 1H), 3.22 (s, 3H), 3.04 (s, 6H); ^{13}C{^{1}H} NMR ($CDCl_3$, 100 MHz) δ 168.6, 146.4, 146.0, 132.4, 120.9, 116.2, 91.2, 36.5; IR (KBr) 1651 cm^{-1}; HRMS (EI) *m*/*z*: [M]$^+$ calcd for $C_{12}H_{15}{}^{79}BrN_2O$ 282.0368; found 282.0367.

(*E*)-3-[*N*-(4-Methoxyphenyl)-*N*-methylamino]-*N*,*N*-dimethyl-2-propenamide (3d). Reaction time 30 min; 305 mg (1.31 mmol, 65% yield); White solid; mp 93–95 °C; ^{1}H NMR ($CDCl_3$, 400 MHz) δ 7.89 (d, J = 12.4 Hz, 1H), 7.06 (d, J = 8.9 Hz, 2H), 6.86 (d, J = 8.7 Hz, 2H), 5.15 (d, J = 12.6 Hz, 1H), 3.79 (s, 3H), 3.21 (s, 3H), 3.02 (s, 6H); ^{13}C{^{1}H} NMR ($CDCl_3$, 100 MHz) δ 169.0, 156.2, 148.0, 140.7, 121.6, 114.5, 88.7, 55.5, 37.5, 36.4 (br s); IR (KBr) 1651 cm^{-1}; HRMS (EI) *m*/*z*: [M]$^+$ calcd for $C_{13}H_{18}N_2O_2$ 234.1368; found 234.1367.

(*E*)-*N*,*N*-Dimethyl-3-[*N*-methyl-*N*-(4-tolyl)amino]-2-propenamide (3e). Reaction time 30 min; 344 mg (1.58 mmol, 77% yield); White solid; mp 121–124 °C; ^{1}H NMR ($CDCl_3$, 400 MHz) δ 7.98 (d, J = 12.8 Hz, 1H), 7.12 (d, J = 8.0 Hz, 2H), 7.03 (d, J = 8.5 Hz, 2H), 5.21 (d, J = 12.6 Hz, 1H), 3.23 (s, 3H), 3.04 (s, 6H), 2.31 (s, 3H); ^{13}C{^{1}H} NMR ($CDCl_3$, 100 MHz) δ 169.1, 147.5, 144.7, 133.3, 130.0, 119.7, 89.5, 36.9, 20.8; IR (KBr) 1651 cm^{-1}; HRMS (EI) *m*/*z*: [M]$^+$ calcd for $C_{13}H_{18}N_2O$ 218.1419; found 218.1419.

(*E*)-3-(*N*-Ethyl-*N*-phenylamino)-*N*,*N*-dimethyl-2-propenamide (3f). Reaction time 1 h; 305 mg (1.40 mmol, 70% yield); Colorless oil; ^{1}H NMR ($CDCl_3$, 400 MHz) δ 7.91 (d, J = 12.8 Hz, 1H), 7.31–7.35 (m, 2H), 7.07–7.15 (m, 3H), 5.28 (d, J = 12.8 Hz, 1H), 3.73 (q, J = 7.2 Hz, 2H), 3.02 (s, 6H), 1.26 (t, J = 7.2 Hz, 3H); ^{13}C{^{1}H} NMR ($CDCl_3$, 100 MHz) δ 169.1, 146.0, 145.7, 129.4, 123.8, 120.3, 89.4, 44.8, 36.5 (br s), 11.8; IR (neat) 1645 cm^{-1}; HRMS (EI) *m*/*z*: [M]$^+$ calcd for $C_{13}H_{18}N_2O$ 218.1419; found 218.1419.

(*E*)-*N*,*N*-Dimethyl-3-(*N*-phenyl-*N*-propylamino)-2-propenamide (3g). Reaction time 1 h; 277 mg (1.19 mmol, 58% yield); White solid; mp 38–44 °C; ^{1}H NMR ($CDCl_3$, 400 MHz) δ 7.90 (d, J = 12.9 Hz, 1H), 7.30–7.34 (m, 2H), 7.07–7.15 (m, 3H), 5.24 (d, J = 12.8 Hz, 1H), 3.59 (t, J = 7.6 Hz, 2H), 3.01 (s, 6H), 1.70 (sext, J = 7.5 Hz, 2H), 0.94 (t, J = 7.5 Hz, 3H); ^{13}C{^{1}H} NMR ($CDCl_3$, 100 MHz) δ 169.2, 147.0, 145.9, 129.5, 124.0, 120.9, 89.4, 52.3, 36.4 (br s), 20.1, 11.5; IR (KBr) 1645 cm^{-1}; HRMS (EI) *m*/*z*: [M]$^+$ calcd for $C_{14}H_{20}N_2O$ 232.1576; found 232.1574.

(*E*)-3-(*N*-Allyl-*N*-phenylamino)-*N*,*N*-dimethyl-2-propenamide (3h). Reaction time 1 h; 306 mg (1.33 mmol, 64% yield); Colorless oil; ^{1}H NMR ($CDCl_3$, 400 MHz) δ 8.02 (d, J = 12.8 Hz, 1H), 7.31 (t, J = 7.6 Hz, 2H), 7.05–7.17 (m, 3H), 5.84–5.91 (m, 1H), 5.19–5.29 (m, 3H), 4.27 (t, J = 2.2 Hz, 2H), 3.01 (s, 6H); ^{13}C{^{1}H} NMR ($CDCl_3$, 100 MHz) δ 168.9, 146.4, 145.7, 131.4, 129.4, 123.7, 119.6, 117.0, 91.0, 52.5, 36.8 (br s); IR (neat) 1647 cm^{-1}; HRMS (EI) *m*/*z*: [M]$^+$ calcd for $C_{14}H_{18}N_2O$ 230.1419; found 230.1419.

(*E*)-3-[*N*-Benzyl-*N*-methylamino]-*N*,*N*-dimethyl-2-propenamide (3j). Reaction time 30 min; 185 mg (0.85 mmol, 41% yield); Light yellow oil; ^{1}H NMR ($CDCl_3$, 400 MHz) δ 7.72 (d, J = 12.5 Hz, 1H), 7.28–7.35 (m, 3H), 7.19–7.20 (m, 2H), 4.90 (d, J = 12.5 Hz, 1H), 4.35 (s, 2H), 2.99 (s, 6H), 2.75 (s, 3H); ^{13}C{^{1}H} NMR ($CDCl_3$, 100 MHz) δ 169.5, 151.7, 136.9, 128.7, 127.6, 127.3, 84.5, 59.5 (br s), 36.6 (br s); IR (neat) 1639 cm^{-1}; HRMS (EI) *m*/*z*: [M]$^+$ calcd for $C_{13}H_{18}N_2O$ 218.1419; found 218.1419.

(*E*)-3-[*N*-Benzyl-*N*-phenylamino]-*N*,*N*-dimethyl-2-propenamide (3k). Reaction time 1 h; Eluent = hexane/EtOAc (1:1); 264 mg (0.94 mmol, 47% yield); White solid; mp 148–152 °C; ^{1}H NMR ($CDCl_3$, 400 MHz) δ 8.14 (d, J = 12.9 Hz, 1H), 7.28–7.35 (m, 5H), 7.06–7.26 (m, 5H), 5.21 (d, J = 12.9 Hz, 1H), 4.90 (s, 2H), 2.90 (s, 6H); ^{13}C{^{1}H} NMR ($CDCl_3$, 100 MHz) δ 168.8, 146.6, 145.8, 136.4, 129.6, 128.9, 127.4, 126.4, 123.8, 119.5, 91.9, 53.9; IR (KBr) 1647 cm^{-1}; HRMS (EI) *m*/*z*: [M]$^+$ calcd for $C_{18}H_{20}N_2O$ 280.1576; found 280.1573.

[D] One-Pot Aldehyde Synthesis from CO_2.

Synthetic Procedure. In a glovebox (purge type) under N_2 atmosphere, TBAA (18.1 mg, 0.060 mmol, 3 mol%) and $Cu(OAc)_2$ (10.9 mg, 0.060 mmol, 3 mol%) were put in a 30 mL Schlenk flask fitted with a rubber septum, and the flask was taken out from the glovebox. After the flask was evacuated and filled with CO_2 (balloon), the flask was put in a thermostatic bath at 20 °C. *N*-Methylaniline (**1a**) (220 μL, 2.0 mmol, stored over molecular sieves 3A) and $PhSiH_3$ (250 μL, 2.0 mmol, stored over molecular sieves 3A) were added in this order via syringes. The mixture was stirred at 20 °C for 18 h. This reaction mixture containing *N*-methylformanilide (**2a**) was used in the subsequent reaction without purification. The CO_2 balloon was removed, and a reflux condenser and a drying tube containing $CaCl_2$ were attached. Aromatic substrate (1.0 mmol), *o*-dichlorobenzene (0.4 mL, for the synthesis of **4a**–**b**) or 1,2-dichloroethane (0.4 mL, for the synthesis of **4g** and **4i**) or no solvent (for the synthesis of **4c**–**f** and **4h**), and $POCl_3$ (0.4 mL, 4.3 mmol) were added, and the mixture was stirred at 90 °C for 4 h (for the synthesis of **4a**–**f**) or at 25 °C for 19 h (for the synthesis of **4g**–**i**) in a draft chamber. The reaction was quenched and neutralized with saturated aqueous NaOAc or $NaHCO_3$ at room temperature, and the mixture was stirred for 30 min. The product was extracted

with CH_2Cl_2 (10 mL × 3), and the organic layers were combined, washed with brine (10 mL × 1), and dried over $MgSO_4$. Purification by silica gel column chromatography (eluent shown below) gave aldehyde **4**.

9-Anthraldehyde (4a).[15a] Eluent = hexane/EtOAc (20:1); 170 mg (0.824 mmol, 82% yield); Yellow solid; mp 104–107 °C; ^{1}H NMR ($CDCl_3$, 400 MHz) δ 11.55 (s, 1H), 9.01 (d, J = 9.1 Hz, 2H), 8.73 (s, 1H), 8.09 (d, J = 8.7 Hz, 2H), 7.68–7.72 (m, 2H), 7.57 (t, J = 7.3 Hz, 2H); ^{13}C{^{1}H} NMR ($CDCl_3$, 100 MHz) δ 193.2, 135.4, 132.3, 131.2, 129.4, 129.3, 125.9, 124.9, 123.7; IR (KBr) 1666 cm^{-1}.

2-Methoxy-1-naphthaldehyde (4b).[15a] Eluent = hexane/EtOAc (10:1); 139 mg (0.747 mmol, 74% yield); Light yellow solid; mp 82–84 °C; ^{1}H NMR ($CDCl_3$, 400 MHz) δ 10.91 (s, 1H), 9.28 (d, J = 8.8 Hz, 1H), 8.07 (d, J = 9.2 Hz, 1H), 7.78 (d, J = 8.2 Hz, 1H), 7.63 (t, J = 7.9 Hz, 1H), 7.42 (t, J = 7.5 Hz, 1H), 7.31 (d, J = 9.2 Hz, 1H), 4.07 (s, 3H); ^{13}C{^{1}H} NMR ($CDCl_3$, 100 MHz) δ 192.2, 164.1, 137.7, 131.7, 130.0, 128.6, 128.4, 125.1, 124.9, 116.7, 112.7, 56.7; IR (KBr) 1666 cm^{-1}.

4-Methoxy-1-naphthaldehyde (4c).[15a] Eluent = hexane/EtOAc (10:1); 172 mg (0.924 mmol, 90% yield); Light yellow oil; ^{1}H NMR ($CDCl_3$, 400 MHz) δ 10.17 (s, 1H), 9.30 (d, J = 8.6 Hz, 1H), 8.30 (d, J = 7.9 Hz, 1H), 7.85 (d, J = 8.0 Hz, 1H), 7.66–7.70 (m, 1H), 7.53–7.57 (m, 1H), 6.85 (d, J = 8.0 Hz, 1H), 4.05 (s, 3H); ^{13}C{^{1}H} NMR ($CDCl_3$, 100 MHz) δ 192.4, 160.9, 139.8, 131.9, 129.6, 126.4, 125.5, 125.0, 124.9, 122.4, 103.0, 56.0; IR (neat) 1687 cm^{-1}.

4-(Dimethylamino)benzaldehyde (4d).[15a] Eluent = hexane/EtOAc (15:1); 98 mg (0.66 mmol, 64% yield); Light yellow solid; mp 72–73 °C; ^{1}H NMR ($CDCl_3$, 400 MHz) δ 9.76 (s, 1H), 7.75 (d, J = 9.0 Hz, 2H), 6.75 (d, J = 9.0 Hz, 2H), 3.10 (s, 6H); ^{13}C{^{1}H} NMR ($CDCl_3$, 100 MHz) δ 190.5, 154.4, 132.1, 125.5, 111.3, 40.3; IR (KBr) 1662 cm^{-1}.

4-Methoxybenzaldehyde (4e).[15a] Eluent = hexane/EtOAc (5:1); 73 mg (0.53 mmol, 52% yield); Brown oil; ^{1}H NMR ($CDCl_3$, 400 MHz) δ 9.89 (s, 1H), 7.84 (d, J = 8.6 Hz, 2H), 7.01 (d, J = 8.7 Hz, 2H), 3.89 (s, 3H); ^{13}C{^{1}H} NMR ($CDCl_3$, 100 MHz) δ 190.9, 164.7, 132.1, 130.0, 114.4, 55.7; IR (neat) 1685 cm^{-1}.

3-Formyl-1-methylindole (4f).[15a] Eluent = hexane/EtOAc (3:1); 116 mg (0.729 mmol, 70% yield); Yellow solid; mp 61–64 °C; ^{1}H NMR ($CDCl_3$, 400 MHz) δ 9.93 (s, 1H), 8.29 (dd, J = 3.1, 5.6 Hz, 1H), 7.60 (s, 1H), 7.29–7.34 (m, 3H), 3.81 (s, 3H); ^{13}C{^{1}H} NMR ($CDCl_3$, 100 MHz) δ 33.7, 110.0, 118.0, 122.0, 123.0, 124.1, 125.3, 137.9, 139.4, 184.5; IR (KBr) 1643 cm^{-1}.

2-Formylpyrrole (4g).[15a] Eluent = hexane/EtOAc (10:1); 51 mg (0.54 mmol, 53% yield); Light yellow solid; mp 40–42 °C; ^{1}H NMR ($CDCl_3$, 400 MHz) δ 9.54 (s, 1H), 9.31 (br s, 1H), 7.11–7.12 (m, 1H), 6.98–7.00 (m, 1H), 6.35–6.37 (m, 1H); ^{13}C{^{1}H} NMR ($CDCl_3$, 100 MHz) δ 179.5, 133.0, 126.6, 121.5, 111.5; IR (KBr) 1651 cm^{-1}.

2-Formylthiophene (4h).[8] Eluent = hexane/EtOAc (10:1); 57 mg (0.51 mmol, 50% yield); Light yellow oil; ^{1}H NMR ($CDCl_3$, 400 MHz) δ 9.96 (s, 1H), 7.77–7.79 (m, 2H), 7.21–7.23 (m, 1H); ^{13}C{^{1}H} NMR ($CDCl_3$, 100 MHz) δ 183.1, 144.2, 136.4, 135.3, 128.4; IR (neat) 1670 cm^{-1}.

2-Bromo-5-formylthiophene (4i).[15a] The synthetic procedure described above was modified as follows. $POBr_3$ (1.15 g, 4.01 mmol) was used instead of $POCl_3$. Column chromatography was done

with Aluminium oxide 90 active neutral (Merck, 1.01077.1000) (eluent = hexane/EtOAc (30:1)); 149 mg (0.780 mmol, 76% yield); Yellow oil; ^{1}H NMR ($CDCl_3$, 400 MHz) δ 9.78 (s, 1H), 7.52 (d, J = 3.8 Hz, 1H), 7.20 (d, J = 4.2 Hz, 1H); ^{13}C{^{1}H} NMR ($CDCl_3$, 100 MHz) δ 181.9, 145.3, 136.7, 131.6, 125.1; IR (neat) 1664 cm^{-1}.

[E] One-Pot Nitrile Synthesis from CO_2.

Synthetic Procedure. In a glovebox (purge type) under N_2 atmosphere, TBAA (18.1 mg, 0.060 mmol, 3 mol%) and $Cu(OAc)_2$ (10.9 mg, 0.060 mmol, 3 mol%) were put in a 30 mL Schlenk flask fitted with a rubber septum, and the flask was taken out from the glovebox. After the flask was evacuated and filled with CO_2 (balloon), the flask was put in a thermostatic bath at 20 °C. *N*-Methylaniline (**1a**) (220 μL, 2.0 mmol, stored over molecular sieves 3A) and $PhSiH_3$ (250 μL, 2.0 mmol, stored over molecular sieves 3A) were added in this order via syringes. The mixture was stirred at 20 °C for 18 h. This reaction mixture containing **2a** was used in the subsequent reaction without purification. The CO_2 balloon was replaced by a N_2 balloon. Aromatic substrate (1.0 mmol), *o*-dichlorobenzene (0.4 mL), and $POCl_3$ (0.4 mL, 4.3 mmol) were added, and the mixture was stirred at 90 °C for 4 h (for the synthesis of **5a**–**f**) or at 25 °C for 19 h (for the synthesis of **5h**–**i**) in a draft chamber. After cooling in an ice bath, I_2 (2.03 g, 8.0 mmol) and aqueous NH_3 (28%, 10 mL) were carefully added with vigorous stirring. (Caution! Use a shield in case of bumping.) The mixture was stirred at room temperature for 2 h and quenched with saturated aqueous Na_2SO_3 (15 mL). The product was extracted with $CHCl_3$ (20 mL × 3), and the organic layers were combined, washed with 10% HCl (30 mL), and dried over Na_2SO_4. The mixture was concentrated, and the residue, dissolved in EtOAc, was passed through a short pad of silica gel (eluent = EtOAc). Purification by silica gel column chromatography (eluent shown below) gave nitrile **5**.

9-Cyanoanthracene (5a).[18b] Eluent = hexane/EtOAc (20:1); 128 mg (0.630 mmol, 63% yield); Yellow solid; mp 176–178 °C; ^{1}H NMR ($CDCl_3$, 400 MHz) δ 8.70 (s, 1H), 8.44 (d, J = 8.8 Hz, 2H), 8.09 (d, J = 8.5 Hz, 2H), 7.73 (t, J = 7.8 Hz, 2H), 7.60 (t, J = 7.6 Hz, 2H); ^{13}C{^{1}H} NMR ($CDCl_3$, 100 MHz) δ 133.4, 132.9, 130.7, 129.090, 129.089, 126.5, 125.4, 117.4, 105.5; IR (KBr) 2212 cm^{-1}.

1-Cyano-2-methoxynaphthalene (5b).[18b] Eluent = hexane/EtOAc (10:1); 118 mg (0.644 mmol, 64% yield); Orange solid; mp 93–95 °C; ^{1}H NMR ($CDCl_3$, 400 MHz) δ 8.10 (d, J = 8.7 Hz, 1H), 8.05 (d, J = 9.2 Hz, 1H), 7.84 (d, J = 8.3 Hz, 1H), 7.65 (t, J = 7.7 Hz, 1H), 7.46 (t, J = 7.6 Hz, 1H), 7.28 (d, J = 8.0 Hz, 1H), 4.08 (s, 3H); ^{13}C{^{1}H} NMR ($CDCl_3$, 100 MHz) δ 161.7, 135.1, 133.6, 129.2, 128.6, 128.0, 125.1, 124.1, 115.8, 112.1, 95.2, 56.7; IR (KBr) 2210 cm^{-1}.

1-Cyano-4-methoxynaphthalene (5c).[18b] Eluent = hexane/EtOAc (10:1); 130 mg (0.710 mmol, 69% yield); Light orange solid; mp 100–103 °C; ^{1}H NMR ($CDCl_3$, 400 MHz) δ 8.32 (d, J = 8.6 Hz, 1H), 8.17 (d, J = 8.3 Hz, 1H), 7.87 (d, J = 8.1 Hz, 1H), 7.70 (t, J = 7.6 Hz, 1H), 7.59 (t, J = 7.7 Hz, 1H), 6.84 (d, J = 8.1 Hz, 1H), 4.07 (s, 3H); ^{13}C{^{1}H} NMR ($CDCl_3$, 100 MHz) δ 159.5, 134.2, 133.6, 129.1, 126.9, 125.3, 125.1, 122.9, 118.6, 103.5, 102.0, 56.1; IR (KBr) 2210 cm^{-1}.

4-(*N*,*N*-Dimethylamino)benzonitrile (5d).[18b] Eluent = hexane/EtOAc (10:1); 94 mg (0.643 mmol, 62% yield); Orange solid; mp 72–74 °C; ^{1}H NMR ($CDCl_3$, 400 MHz) δ 7.42 (d, J = 8.9 Hz, 2H), 6.61

(d, J = 9.0 Hz, 2H), 3.01 (s, 6H); $^{13}C\{^{1}H\}$ NMR ($CDCl_3$, 100 MHz) δ 152.5, 133.3, 120.8, 111.4, 97.1, 39.9; IR (KBr) 2210 cm^{-1}.

4-Methoxybenzonitrile (5e).[18b] Eluent = hexane/EtOAc (10:1); 57 mg (0.43 mmol, 42% yield); Orange solid; mp 50–52 °C; ^{1}H NMR ($CDCl_3$, 400 MHz) δ 7.59 (d, J = 8.9 Hz, 2H), 6.96 (d, J = 8.8 Hz, 2H), 3.86 (s, 3H); $^{13}C\{^{1}H\}$ NMR ($CDCl_3$, 100 MHz) δ 163.0, 134.1, 119.4, 114.9, 104.1, 55.7; IR (KBr) 2218 cm^{-1}.

3-Cyano-1-methylindole (5f).[18b] Eluent = hexane/EtOAc (3:1); 103 mg (0.659 mmol, 63% yield); Brown oil; ^{1}H NMR ($CDCl_3$, 400 MHz) δ 7.77 (d, J = 7.8 Hz, 1H), 7.57 (s, 1H), 7.29–7.41 (m, 3H), 3.86 (s, 3H); $^{13}C\{^{1}H\}$ NMR ($CDCl_3$, 100 MHz) δ 136.1, 135.7, 127.9, 124.0, 122.3, 120.0, 116.1, 110.5, 85.6, 33.8; IR (neat) 2218 cm^{-1}.

2-Cyanothiophene (5h).[18b] The synthetic procedure described above was modified as follows. After addition of $POCl_3$ (0.4 mL, 4.3 mmol) without solvent, the mixture was stirred at 25 °C for 30 min, and thiophene (80 μL, 1.0 mmol) was then added. The mixture was stirred at 25 °C for 19 h, and 1,2-dichloroethane (0.4 mL) was added before addition of I_2 and aqueous NH_3. Alumina (Wako) was used instead of silica gel for short column chromatography, and the product was purified by bulb-to-bulb distillation (oven 100 °C, 3.5 Pa); 50 mg (0.46 mmol, 46% yield); Slightly yellow oil; ^{1}H NMR ($CDCl_3$, 400 MHz) δ 7.65 (d, J = 3.1 Hz, 1H), 7.61 (d, J = 5.0 Hz, 1H), 7.14 (t, J = 4.4 Hz, 1H); $^{13}C\{^{1}H\}$ NMR ($CDCl_3$, 100 MHz) δ 137.6, 132.7, 127.8, 114.4, 110.0; IR (neat) 2222 cm^{-1}.

2-Bromo-5-cyanothiophene (5i).[20] The synthetic procedure described above was modified as follows. 1,2-Dichloroethane (1.0 mL) and $POBr_3$ (2.29 g, 8.00 mmol) were added instead of *o*-dichlorobenzene and $POCl_3$, respectively, after which the mixture was stirred at 25 °C for 30 min, and 2-bromothiophene (100 μL, 1.0 mmol) was then added. Column chromatography was done with alumina (Wako) (eluent = hexane/EtOAc (20:1)); 100 mg (0.53 mmol, 52% yield); Light yellow oil; ^{1}H NMR ($CDCl_3$, 400 MHz) δ 7.39 (d, J = 4.3 Hz, 1H), 7.10 (d, J = 3.7 Hz, 1H); $^{13}C\{^{1}H\}$ NMR ($CDCl_3$, 100 MHz) δ 138.1, 130.8, 120.3, 113.3, 111.5; IR (neat) 2222 cm^{-1}.

3.6 References

(1) Recent reviews: (a) Jiang, X.; Nie, X.; Guo, X.; Song, C.; Chen, J. G. *Chem. Rev.* **2020**, *120*, 7984–8034. (b) Zhang, Y.; Zhang, T.; Das, S. *Green Chem.* **2020**, *22*, 1800–1820. (c) Modak, A.; Bhanja, P.; Dutta, S.; Chowdhury, B.; Bhaumik, A. *Green Chem.* **2020**, *22*, 4002–4033. (d) Sable, D. A.; Vadagaonkar, K. S.; Kapdi, A. R.; Bhanage, B. M. *Org. Biomol. Chem.* **2021**, *19*, 5725–5757.

(2) (a) Yu, B.; Zhao, Y.; Zhang, H.; Xu, J.; Hao, L.; Gao, X.; Liu, Z. *Chem. Commun.* **2014**, *50*, 2330–2333. (b) Anaby, A.; Feller, M.; Ben-David, Y.; Leitus, G.; Diskin-Posner, Y.; Shimon, L. J. W.; Milstein, D. *J. Am. Chem. Soc.* **2016**, *138*, 9941–9950. (c) Yu, B.; Yang, Z.; Zhao, Y.; Hao, L.; Zhang, H.; Gao, X.; Han, B.; Liu, Z. *Chem. Eur. J.* **2016**, *22*, 1097–1102. (d) Ren, X.; Zheng, Z.; Zhang, L.; Wang, Z.; Xia, C.; Ding, K. *Angew. Chem. Int. Ed.* **2017**, *56*, 310–313. (e) Liu, Z.; Yang, Z.; Yu, B.; Yu, X.; Zhang, H.; Zhao, Y.; Yang, P.; Liu, Z. *Org. Lett.* **2018**, *20*, 5130–5134.

(3) (a) Tani, Y.; Kuga, K.; Fujihara, T.; Terao, J.; Tsuji, Y. *Chem. Commun.* **2015**, *51*, 13020–13023. (b) Chen, X.-W.; Zhu, L.; Gui, Y.-Y.; Jing, K.; Jiang, Y.-X.; Bo, Z.-Y.; Lan, Y.; Li, J.; Yu, D.-G. *J. Am. Chem. Soc.* **2019**, *141*, 18825–18835. (c) Zhang, X.; Tian, X.; Shen, C.; Xia, C.; He, L. *ChemCatChem* **2019**, *11*, 1986–1992. (d) Wang, M.-Y.; Jin, X.; Wang, X.; Xia, S.; Wang, Y.; Huang, S.; Li, Y.; He, L.-N.; Ma, X. *Angew. Chem. Int. Ed.* **2021**, *60*, 3984–3988. (e) Zhang, D.; Jarava-Barrera, C.; Bontemps, S. *ACS Catal.* **2021**, *11*, 4568–4575.

(4) (a) Jin, G.; Werncke, C. G.; Escudié, Y.; Sabo-Etienne, S.; Bontemps, S. *J. Am. Chem. Soc.* **2015**, *137*, 9563–9566. (b) Zhu, D.-Y.; Li, W.-D.; Yang, C.; Chen, J.; Xia, J.-B. *Org. Lett.* **2018**, *20*, 3282–3285. (c) Rauch, M.; Strater, Z.; Parkin, G. *J. Am. Chem. Soc.* **2019**, *141*, 17754–17762.

(5) (a) Li, Y.; Yan, T.; Junge, K.; Beller, M. *Angew. Chem. Int. Ed.* **2014**, *53*, 10476–10480. (b) Zhu, D.-Y.; Fang, L.; Han, H.; Wang, Y.; Xia, J.-B. *Org. Lett*. **2017**, *19*, 4259–4262. (c) Béthegnies, A.; Escudié, Y.; Nuñez-Dallos, N.; Vendier, L.; Hurtado, J.; del Rosal, I.; Maron, L.; Bontemps, S. *ChemCatChem* **2019**, *11*, 760–765. (d) Zhao, Y.; Guo, X.; Ding, X.; Zhou, Z.; Li, M.; Feng, N.; Gao, B.; Lu, X.; Liu, Y.; You, J. *Org. Lett.* **2020**, *22*, 8326–8331. (e) Zhao, Y.; Liu, X.; Zheng, L.; Du, Y.; Shi, X.; Liu, Y.; Yan, Z.; You, J.; Jiang, Y. *J. Org. Chem.* **2020**, *85*, 912–923. (f) Zhao, Y.; Guo, X.; Du, Y.; Shi, X.; Yan, S.; Liu, Y.; You, J. *Org. Biomol. Chem.* **2020**, *18*, 6881–6888. (g) Takaishi, K.; Kosugi, H.; Nishimura, R.; Yamada, Y.; Ema, T. *Chem. Commun.* **2021**, *57*, 8083–8086. (h) Li, W.-D.; Chen, J.; Zhu, D.-Y.; Xia, J.-B. *Chin. J. Chem*. **2021**, *39*, 614–620. (i) Murata, T.; Hiyoshi, M.; Maekawa, S.; Saiki, Y.; Ratanasak, M.; Hasegawa, J.; Ema, T. *Green Chem.* **2022**, *24*, 2385–2390.

(6) Recent reviews: (a) Li, Z.; Yu, Z.; Luo, X.; Li, C.; Wu, H.; Zhao, W.; Li, H.; Yang, S. *RSC Adv.* **2020**, *10*, 33972–34005. (b) Pramudita, R. A.; Motokura, K. *ChemSusChem* **2021**, *14*, 281–292.

(7) (a) Das Neves Gomes, C.; Jacquet, O.; Villiers, C.; Thuéry, P.; Ephritikhine, M.; Cantat, T. *Angew. Chem. Int. Ed.* **2012**, *51*, 187–190. (b) Jacquet, O.; Das Neves Gomes, C.; Ephritikhine, M.; Cantat, T. *J. Am. Chem. Soc.* **2012**, *134*, 2934–2937. (c) Motokura, K.; Takahashi, N.; Kashiwame, D.; Yamaguchi, S.; Miyaji, A.; Baba, T. *Catal. Sci. Technol.* **2013**, *3*, 2392–2396. (d) Luo, R.; Lin, X.; Chen, Y.; Zhang, W.; Zhou, X.; Ji, H. *ChemSusChem* **2017**, *10*, 1224–1232. (e) Li, X.-Y.; Zheng, S.-S.; Liu, X.-F.; Yang, Z.-W.; Tan, T.-Y.; Yu, A.; He, L.-N. *ACS Sustainable Chem. Eng.* **2018**, *6*, 8130–8135. (f) Takaishi, K.; Nath, B. D.; Yamada, Y.; Kosugi, H.; Ema, T. *Angew. Chem. Int. Ed.* **2019**, *58*, 9984–9988. (g) Jiang, X.; Huang, Z.; Makha, M.; Du, C.-X.; Zhao, D.; Wang, F.; Li, Y. *Green Chem.* **2020**, *22*, 5317–5324. (h) Zhang, Q.; Lin, X.-T.; Fukaya, N.; Fujitani, T.; Sato, K.; Choi, J.-C. *Green Chem.* **2020**, *22*, 8414–8422. (i) Wang, P.; He, Q.; Zhang, H.; Sun, Q.; Cheng, Y.; Gan, T.; He, X.; Ji, H. *Catal. Commun.* **2021**, *149*, 106195.

(8) Murata, T.; Hiyoshi, M.; Ratanasak, M.; Hasegawa, J.; Ema, T. *Chem. Commun.* **2020**, *56*, 5783–5786.

(9) Hayashi, Y. *Chem. Sci.* **2016**, *7*, 866–880.

(10) Nogi, K.; Fujihara, T.; Terao, J.; Tsuji, Y. *J. Am. Chem. Soc.* **2016**, *138*, 5547–5550.

(11) (a) Motokura, K.; Kashiwame, D.; Miyaji, A.; Baba, T. *Org. Lett.* **2012**, *14*, 2642–2645. (b) Zhang, L.; Cheng, J.; Hou, Z. *Chem. Commun.* **2013**, *49*, 4782–4784. (c) Li, X.-D.; Xia, S.-M.; Chen, K.-H.; Liu, X.-F.; Li, H.-R.; He, L.-N. *Green Chem.* **2018**, *20*, 4853–4858.

(12) (a) Toh, K. K.; Sanjaya, S.; Sahnoun, S.; Chong, S. Y.; Chiba, S. *Org. Lett.* **2012**, *14*, 2290–2292. (b) Suri, M.; Jousseaume, T.; Neumann, J. J.; Glorius, F. *Green Chem.* **2012**, *14*, 2193–2196. (c) Ke, J.; He, C.; Liu, H.; Li, M.; Lei, A. *Chem. Commun.* **2013**, *49*, 7549–7551. (d) Wan, J.-P.; Jing, Y.; Hu, C.; Sheng, S. *J. Org. Chem.* **2016**, *81*, 6826–6831.

(13) Taneda, H.; Inamoto, K.; Kondo, Y. *Chem. Commun.* **2014**, *50*, 6523–6525.

(14) (a) Woodbury, R. P.; Rathke, M. W. *J. Org. Chem.* **1978**, *43*, 881–884. (b) Woodbury, R. P.; Rathke, M. W. *J. Org. Chem.* **1978**, *43*, 1947–1949.

(15) (a) Jones, G.; Stanforth, S. P. *Org. React.* **1997**, *49*, 1–330. (b) Jones, G.; Stanforth, S. P. *Org. React.* **2000**, 56, 355–659.

(16) Yan, G.; Zhang, Y.; Wang, J. *Adv. Synth. Catal.* **2017**, *359*, 4068–4105.

(17) (a) Wang, H.; Dong, Y.; Zheng, C.; Sandoval, C. A.; Wang, X.; Makha, M.; Li, Y. *Chem* **2018**, *4*, 2883–2893. (b) Dong, Y.; Yang, P.; Zhao, S.; Li, Y. *Nat. Commun.* **2020**, *11*, 4096.

(18) (a) Ushijima, S.; Togo, H. *Synlett* **2010**, 1067–1070. (b) Ushijima, S.; Moriyama, K.; Togo, H. *Tetrahedron* **2012**, *68*, 4588–4595.

(19) Chen, X. Y.; Zhang, L.; Tang, Y.; Yuan, S.; Zhu, B.; Chen, G.; Cheng, X. *Synlett* **2020**, *31*, 878–882.

(20) Augustine, J. K.; Bombrun, A.; Atta, R. N. *Synlett* **2011**, 2223–2227.

Chapter 4

One-Pot Synthesis of Aldehydes or Alcohols from CO_2

4.1 Abstract

The solvent-free *N*-formylation of 2-(methylamino)pyridine (**1a**) with CO_2 and phenylsilane was catalyzed by $Cu(OAc)_2$ alone to give *N*-methyl-*N*-(2-pyridyl)formamide (**2a**) called Comins–Meyers formamide. The X-ray crystallographic analysis of a $Cu(OAc)_2$–**1a** complex revealed a paddle-wheel structure consisting of two copper ions bridged by four acetate ions with two molecules of **1a** on both axial sites, which suggested (i) the improved solubility of the copper ion and (ii) the enhanced nucleophilicity of the acetate ion for the activation of phenylsilane. ^{1}H NMR spectra of benzene-d_6 solutions containing $Cu(OAc)_2$, **1a**, and phenylsilane showed a singlet signal at 2.62 ppm, which was assigned to a catalytically active Cu–H species, and this signal disappeared upon exposure to CO_2, which led to the formation of **2a**. Formamide **2a** synthesized from **1a** via the copper-catalyzed hydrosilylation of CO_2 under solvent-free conditions was directly subjected to the Grignard reactions in THF for the one-pot synthesis of aldehydes or alcohols. On the other hand, silyl formates prepared from CO_2 and phenylsilane using tetrabutylammonium acetate (TBAA) as an organocatalyst were also found to be good precursors of alcohols.

4.2 Introduction

Carbon dioxide (CO_2) is an abundant, inexpensive, and renewable C1 resource as well as a greenhouse gas giving a severe damage on the Earth. Effective and efficient CO_2 utilization is becoming more and more important from the viewpoint of sustainability, and CO_2 fixation is a key molecular technology for realizing carbon-neutral societies.[1] A variety of CO_2 transformations have been studied,[2] such as C–H bond-forming reactions producing C_1 compounds such as formic acid and methanol,[3] C–C bond-forming reactions giving carboxylic acids,[4] and C–O bond-forming reactions with epoxides to afford cyclic carbonates or polycarbonates.[5,6] In addition, CO_2 fixation reactions making both C–H and C–C bonds can produce aldehydes,[7] alcohols,[8] alkenes,[9] and heterocycles.[10] Reductive CO_2 fixation with amines makes both C–H and C–N bonds.[11] Hydrosilanes are useful reductants for CO_2 reduction because of moderate reactivity yet stability under air, and the reactions of CO_2 with hydrosilanes give reactive intermediates such as silyl formates and bis(silyl)acetals that can be used to make various compounds.[12] For example, amines undergo *N*-formylation in the presence of CO_2 and hydrosilane, which is catalyzed by organocatalysts and metal complex catalysts.[13]

One-pot reactions, which involve multi-step reactions in one flask, attract much attention of chemists because solvents, wastes, costs, and time can be saved by omitting the isolation procedures

of intermediate products (pot economy).[14] Several one-pot reactions with CO_2 have been reported.[15,16] In view of the difficulty of using CO_2-derived silyl formates as a formyl source, we have previously developed the one-pot two-step synthesis of aldehydes via Weinreb formamide prepared from CO_2 using tetrabutylammonium acetate (TBAA) as a catalyst under solvent-free conditions (Scheme 1a).[16] However, *N*,*O*-dimethylhydroxylamine must be freshly prepared by distillation after the neutralization of its HCl salt, and it is quite volatile (bp 43 °C). On the other hand, Comins and Meyers have reported that the reaction of *N*-methyl-*N*-(2-pyridyl)formamide (**2a**) with a Grignard reagent gives a six-membered Mg^{2+} chelate complex, which affords aldehyde upon hydrolysis, and that the reaction of **2a** with two equivalent of a Grignard reagent with heating furnishes alcohol.[17] Here we report the solvent-free synthesis of Comins–Meyers formamide **2a** from 2-(methylamino)pyridine (**1a**), CO_2, and $PhSiH_3$ and the subsequent one-pot reactions with Grignard reagents for the selective synthesis of aldehydes or alcohols (Scheme 1b). In the conversion of **1a** into **2a**, $Cu(OAc)_2$ was the best catalyst, and a specific mechanism of solvent-free catalysis has been proposed on the basis of the X-ray crystal structure of a $Cu(OAc)_2$–**1a** complex. ^1H NMR spectra have detected a singlet signal (2.62 ppm) assigned to a copper(I) hydride (Cu–H) species, which is considered to be a catalytically active species for CO_2 reduction. We have also confirmed that silyl formates prepared from CO_2 and $PhSiH_3$ using TBAA as an organocatalyst serve as good precursors of alcohols.

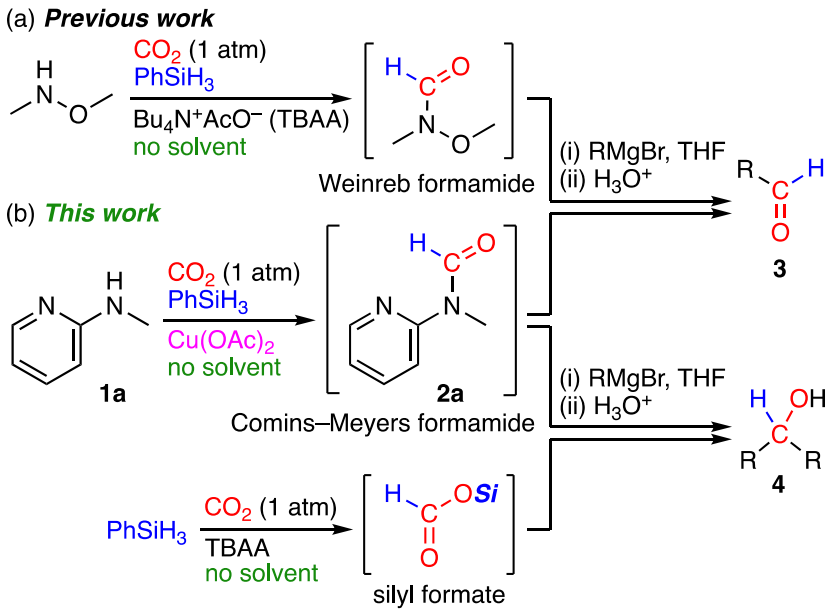

Scheme 1. (a) One-pot two-step synthesis of aldehydes from CO_2. (b) Outline of this work.

4.3 Result and Discussion

We searched for a catalyst suitable for the solvent-free synthesis of formamide **2a** from **1a** and CO_2 (1 atm, balloon) in the presence of hydrosilane at ambient temperature (Table 1). When TBAA (3 mol%) was used, **2a** was obtained in 63% yield (entry 1). The addition of $Cu(OAc)_2$ as a co-catalyst elevated the yield to 85% (entry 2). The use of $Cu(OAc)_2$ alone unexpectedly afforded **2a** in 98% yield (entry 3), while no formation of **2a** was confirmed without catalyst (entry 4). The former result sharply contrasts with our previous report that the use of both TBAA and $Cu(OAc)_2$ was more productive for the *N*-formylation of *N*-methylaniline than the single use of TBAA or $Cu(OAc)_2$.[18] Other metal acetate salts were screened to find that $Mn(OAc)_2$, $Fe(OAc)_2$, $Ni(OAc)_2$, $Pd(OAc)_2$, and AgOAc had little or no ability to produce **2a** (entries 5, 6, 8, 10, and 11). $Co(OAc)_2$ and $Zn(OAc)_2$ gave **2a** in low and modest yields, respectively (entries 7 and 9). When CuOAc was employed, the yield decreased slightly to 90%, while other copper salts showed much lower catalytic activities (entries 12–19); $Cu(OAc)_2$ and CuOAc were found to be excellent. When the amounts of $Cu(OAc)_2$ and CuOAc were decreased to 2 mol%, **2a** was obtained in 83% and 75% yield, respectively (entries 20 and 21), which indicates that the use of 3 mol% $Cu(OAc)_2$ is the best choice. The lower yields were observed at 30 and 40 °C (entries 22 and 23); 20 °C is the best temperature. Other hydrosilanes were screened to confirm that $PhSiH_3$ was the most reactive (entries 3 and 24–27).

Table 1. Solvent-free *N*-formylation of **1**.[a]

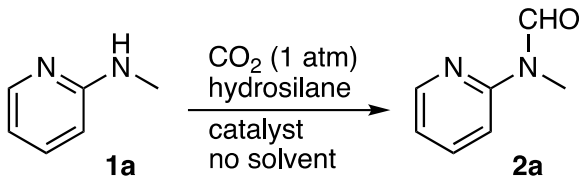

1a **2a**

entry	hydrosilane	catalyst	*T* (°C)	yield (%)[b]
1	$PhSiH_3$	TBAA	20	63
2	$PhSiH_3$	TBAA + $Cu(OAc)_2$	20	85
3	$PhSiH_3$	$Cu(OAc)_2$	20	**98**
4	$PhSiH_3$	–	20	0
5[c]	$PhSiH_3$	$Mn(OAc)_2$	20	0
6	$PhSiH_3$	$Fe(OAc)_2$	20	trace
7[c]	$PhSiH_3$	$Co(OAc)_2$	20	11
8[c]	$PhSiH_3$	$Ni(OAc)_2$	20	0
9[d]	$PhSiH_3$	$Zn(OAc)_2$	20	49
10	$PhSiH_3$	$Pd(OAc)_2$	20	0
11	$PhSiH_3$	AgOAc	20	trace
12	$PhSiH_3$	$CuSO_4$	20	30
13	$PhSiH_3$	$CuCl_2$	20	0
14	$PhSiH_3$	$CuBr_2$	20	0
15	$PhSiH_3$	CuO	20	25
16	$PhSiH_3$	CuCl	20	18
17	$PhSiH_3$	CuBr	20	22
18	$PhSiH_3$	CuI	20	22
19	$PhSiH_3$	CuOAc	20	90
20[e]	$PhSiH_3$	$Cu(OAc)_2$	20	83
21[e]	$PhSiH_3$	CuOAc	20	75
22	$PhSiH_3$	$Cu(OAc)_2$	30	83
23	$PhSiH_3$	$Cu(OAc)_2$	40	83
24	$PhMe_2SiH$	$Cu(OAc)_2$	60	25
25	Ph_2MeSiH	$Cu(OAc)_2$	60	36
26	Ph_2SiH_2	$Cu(OAc)_2$	60	25
27[f]	PMHS	$Cu(OAc)_2$	30	11

[a] Reaction conditions: **1** (2.0 mmol), hydrosilane (2.0 mmol), CO_2 (1 atm, balloon), catalyst (3 mol%), 18 h. [b] Determined by ^1H NMR using mesitylene as an internal standard. [c] A metal salt of tetrahydrate was used. [d] A metal salt of dihydrate was used. [e] A catalyst loading of 2 mol%. [f] PMHS (400 μL, Si–H: 6 mmol)

The effect of the position and number of the nitrogen atom in the aromatic ring on the reactivity of secondary amines was investigated (Scheme 2). Under the standard conditions, **2a** was synthesized and isolated in 80% yield. The *meta* isomer **2b** and the *para* isomer **2c** were obtained in 53 and 42% yields, respectively. The pyrimidine-containing amine **1d** was formylated to give **2d** in 32% yield. Interestingly, *N*-methylaniline (**1e**), containing no nitrogen atom in the aromatic ring, showed no reactivity at all.[18] To elucidate the catalytic behavior of $Cu(OAc)_2$ for **1a**, a single crystal prepared from a solution of $Cu(OAc)_2$ and **1a** in MeOH/Et_2O was subjected to X-ray diffraction analysis

(Figure 1). The paddle-wheel structure consisting of two copper ions bridged by four acetate ions is flanked by two molecules of **1a**, where the pyridine ring is coordinated to the copper ion while the amino group is hydrogen-bonded with the oxygen atom of the acetate bridge. We consider that $Cu(OAc)_2$ can dissolve into liquid substrates without solvent because of this type of complex formation.

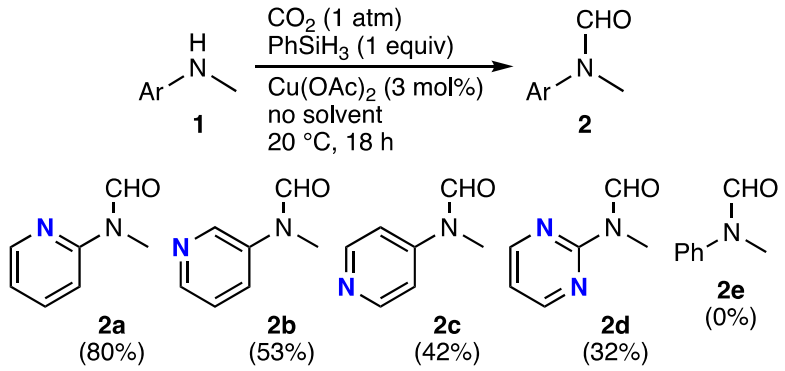

Scheme 2. Influence of the aryl group on reactivity.

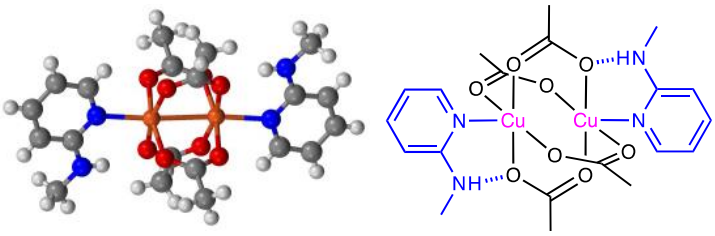

Figure 1. X-ray crystal structure of $Cu(OAc)_2$–**1a** complex (CCDC 2189185).

A plausible reaction mechanism is shown in Scheme 3, where **1a** plays a pivotal role in the synthesis of **2a**. The ligation (electron donation) of the pyridyl moiety of **1a** to the copper ion promotes the dissociation of the acetate ion, which attacks the silicon atom of $PhSiH_3$ to generate a Cu–H species. The subsequent CO_2 insertion affords a HCO_2–Cu species, and this formate ion in turn attacks $PhSiH_3$ to generate a silyl formate with the regeneration of the Cu–H species. The resulting silyl formate reacts with **1a** to give **2a**. This final step can be accelerated by the metal coordination of the pyridyl nitrogen atom of **1a** and the carbonyl oxygen atom of the silyl formate, despite the poor nucleophilicity of the amino group of **1a** with the electron-withdrawing pyridyl group. This proximity effect as well as the paddle-wheel complexation that favors the dissolution of $Cu(OAc)_2$ in the neat substrates and the formation of the ion pair (Scheme 3) makes **1a** the most reactive amine (Scheme 2).

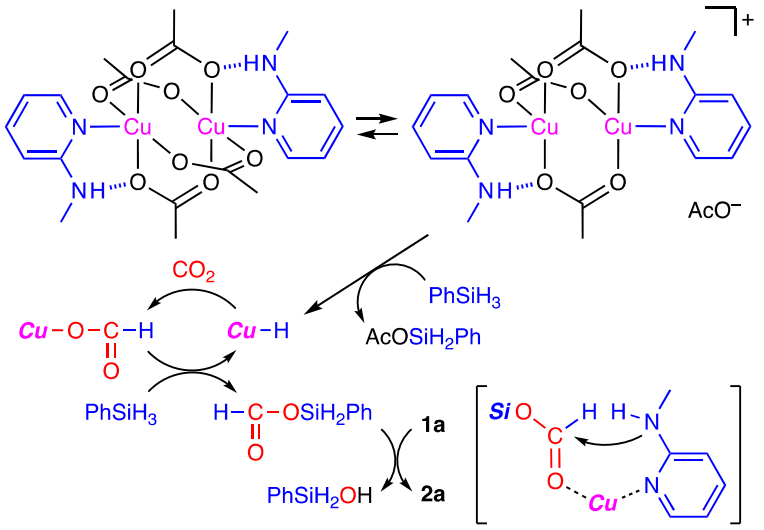

Scheme 3. Plausible reaction mechanism.

We performed NMR experiments to detect a copper(I) hydride (Cu–H) species. To a mixture of $Cu(OAc)_2$ (0.05 mmol) and **1a** (0.2 mmol) in benzene-d_6 (1.0 mL) at 20 °C under N_2 in a Schlenk flask was added $PhSiH_3$ (1.0 mmol, 20 equiv) via a syringe. The solution was stirred at 20 °C for 3 h, and ^1H NMR spectrum was measured (Figure 2b). The signals for the methyl group of **1a** were slightly shifted downfield, and importantly, a singlet signal appeared at 2.62 ppm, which was assigned to a Cu–H species. This signal disappeared upon exposure to CO_2 (1 atm, balloon), and the reaction at 20 °C for additional 48 h gave **2a** (Figure 2c), which was isolated by silica gel column chromatography in 76% yield. This chemical shift (2.62 ppm) is reasonable as compared with those reported for Cu–H species with ligands such as phosphines and *N*-heterocyclic carbenes (NHCs).[19] It is interesting to note that there are several minor singlet signals around the signal at 2.62 ppm (Figure 2b), which suggests that a few Cu–H species with different structures might also coexist.

The time course of the formation of the Cu–H species at 30 °C under otherwise the same conditions was monitored, and the signal at 2.62 ppm was intensified slowly over several hours (Figure 3a). This signal almost disappeared after CO_2 bubbling for 15 min (Figure 3b). When this sample was left at 30 °C for 3 h without CO_2 bubbling, the signal at 2.62 ppm increased. This signal on/off process could be repeated several times. These results suggest that the Cu–H species reacts rapidly with CO_2 to give the copper–formate species (HCO_2–Cu), which reacts with $PhSiH_3$ more slowly to regenerate the Cu–H species together with the formation of silyl formates after stopping CO_2 bubbling. Because an excess amount (20 equiv) of $PhSiH_3$ was present, this procedure could be repeated. Figure 3b also confirms the late formation of **2a**. The NMR detection of Cu–H species without phosphine or NHC ligands is quite rare.[19]

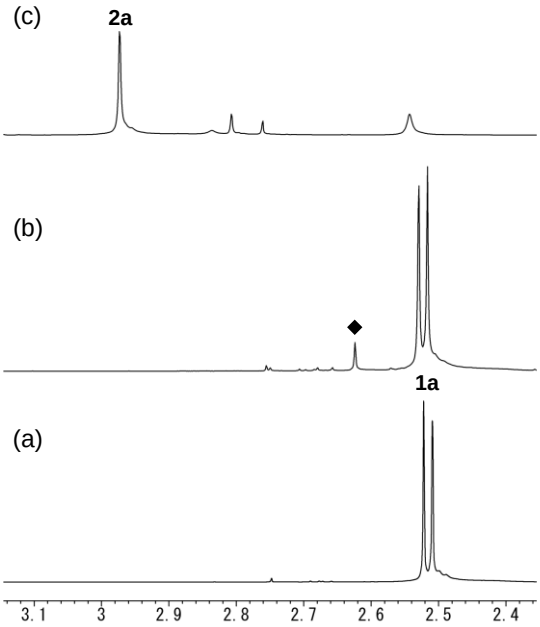

Figure 2. ^{1}H NMR spectra of (a) **1a** in benzene-d_6 and (b) a mixture of $Cu(OAc)_2$ (0.05 mmol), **1a** (0.2 mmol), and $PhSiH_3$ (1.0 mmol) in benzene-d_6 (1.0 mL) after stirring at 20 °C for 3 h. (c) The latter solution was exposed to CO_2 at 20 °C for 48 h. The signal designated with the filled diamond is assigned to a Cu–H species.

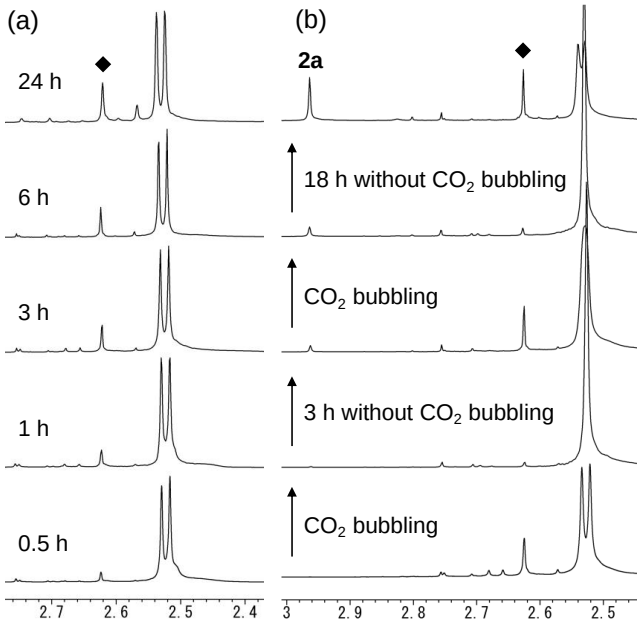

Figure 3. ^{1}H NMR spectra of benzene-d_6 solutions containing $Cu(OAc)_2$ (0.05 mmol), **1a** (0.2 mmol), and $PhSiH_3$ (1.0 mmol), where the filled diamond is assigned to a Cu–H species. (a) Time course at 30 °C. (b) The effects of CO_2 bubbling at 30 °C for 15 min and no CO_2 bubbling.

We performed the one-pot synthesis of aldehydes **3** from CO_2 (Scheme 4). Comins–Meyers formamide **2a** was prepared from **1a**, CO_2, and $PhSiH_3$ under the optimized conditions, and the CO_2 balloon was replaced by a N_2 balloon. A Grignard reagent (2 equiv) was carefully added at 0 °C, and the mixture was stirred for 2 h. The reaction was carefully quenched with aqueous NH_4Cl or HCl,

and purification by silica gel column chromatography gave aldehyde **3**. Aromatic aldehydes such as naphthaldehyde **3a** and benzaldehydes **3b**–**e** were obtained in good yields. Heteroaromatic aldehyde **3f**, alkynylaldehyde **3g**, and aliphatic aldehyde **3h** were obtained in moderate yields.

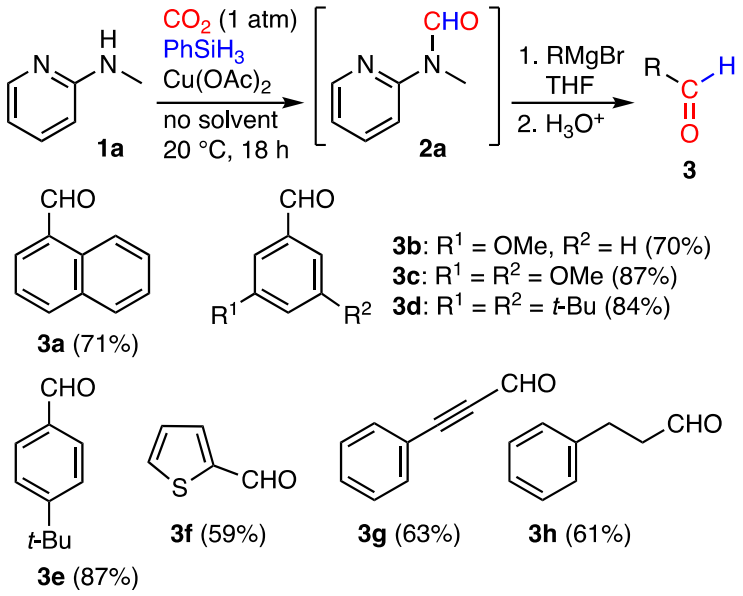

Scheme 4. Scope of one-pot aldehyde synthesis.

We also conducted the one-pot synthesis of alcohols **4** from CO_2 (Scheme 5). After the careful addition of a Grignard reagent (1 equiv) at 0 °C, the reaction mixture was stirred for 10 min, and the Grignard reagent (2 equiv) was further added. The mixture was then heated at 65 °C for 3 h. After cooling, aqueous HCl was carefully added to quench the reaction. As a result, diphenylmethanol (**4a**) was synthesized in excellent yield (95%), and other diarylmethanols **4b**–**f** were also obtained in high yields. The thiophene-containing alcohol **4g** and aliphatic alcohol **4h** were isolated in good yields.

Although both aldehydes and alcohols can be selectively synthesized by using Comins–Meyers formamide **2a**, to the best of our knowledge, there are no examples of the synthesis of alcohols from the Weinreb formamide. The reactivities of Comins–Meyers and Weinreb formamides toward PhMgBr (3 equiv) were compared (Scheme 6). Alcohol **4a** was obtained via Comins–Meyers formamide in 95%, where a trace amount of benzaldehyde and no residual **2a** were detected (Scheme 6a). Next, the Weinreb formamide was prepared according to the procedure reported by us,[16] and PhMgBr was added in the same way to give benzaldehyde in 72% and **4a** in 29% (Scheme 6b). Benzaldehyde and **4a** were obtained from pure Weinreb formamide in 80% and 10% yields, respectively (Scheme 6c). Clearly, the Weinreb formamide is unsuitable for the synthesis of alcohols, which is probably due to the poor leaving ability of the *N*,*O*-dimethylhydroxylamine moiety.

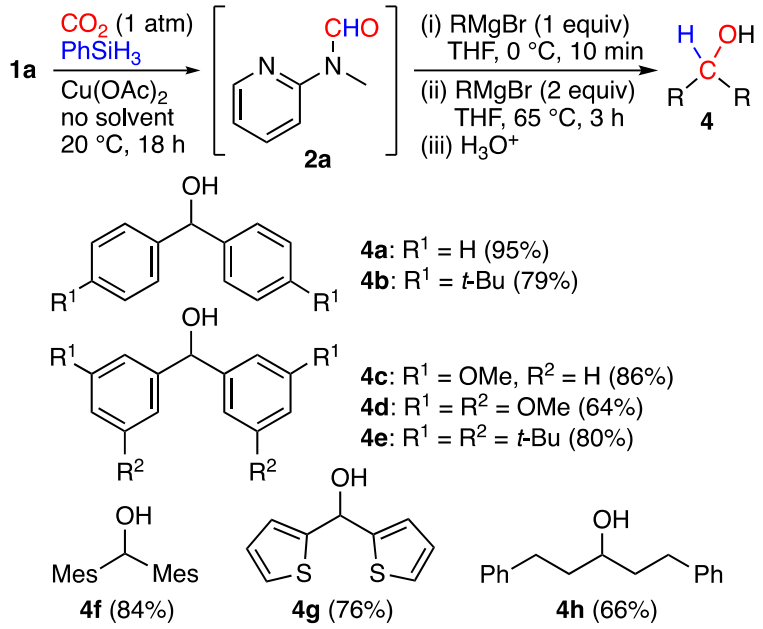

Scheme 5. Scope of one-pot alcohol synthesis.

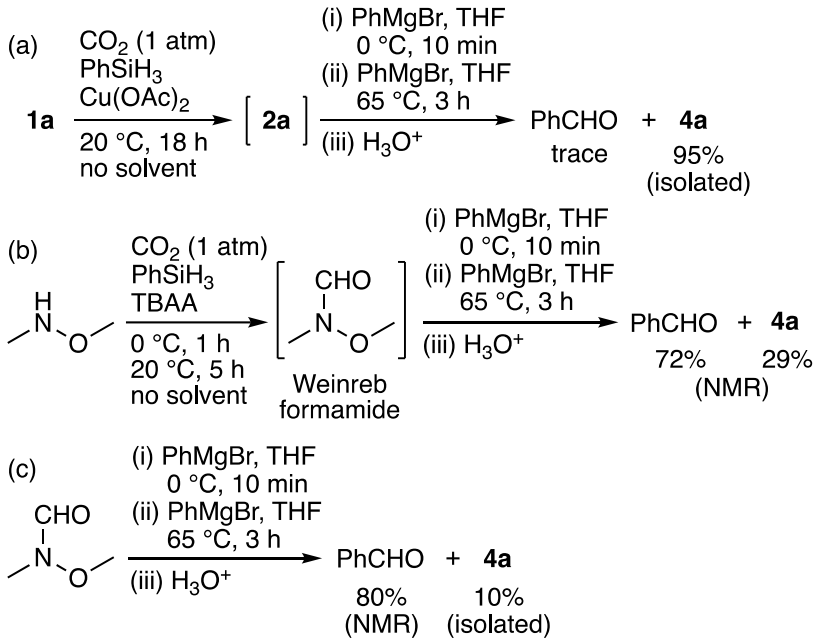

Scheme 6. Synthesis of **4a** via Comins–Meyers or Weinreb formamide.

Mizuno and co-workers have previously synthesized HCO_2SiMe_2Ph from CO_2 and $PhMe_2SiH$, and the reaction of this silyl formate with PhMgBr gave alcohol **4a**.[20] Although only one example has been reported, this work has opened up a new way of reductive CO_2 fixation. Here we employed $PhSiH_3$ and $PhMe_2SiH$ for comparison in the TBAA-catalyzed hydrosilylation of CO_2 under solvent-free conditions, and the corresponding silyl formates were allowed to react with PhMgBr in THF. As a result, **4a** was synthesized from $PhMe_2SiH$ in 32% yield (Scheme 7), while **4a** was synthesized from $PhSiH_3$ in 81% yield (Scheme 8), which clearly indicates that the latter is a promising method

for alcohol synthesis. The substrate scope was examined, and all the products could be obtained in satisfactory yields (Scheme 8). Although these reactions via silyl formates were slightly less productive than those via Comins–Meyers formamide **2a**, the former is fascinating in terms of atom efficiency.

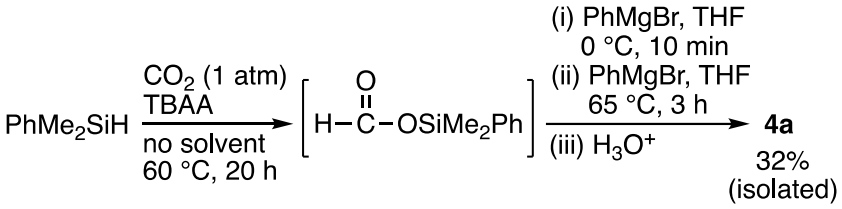

Scheme 7. One-pot synthesis of **4a** with $PhMe_2SiH$.

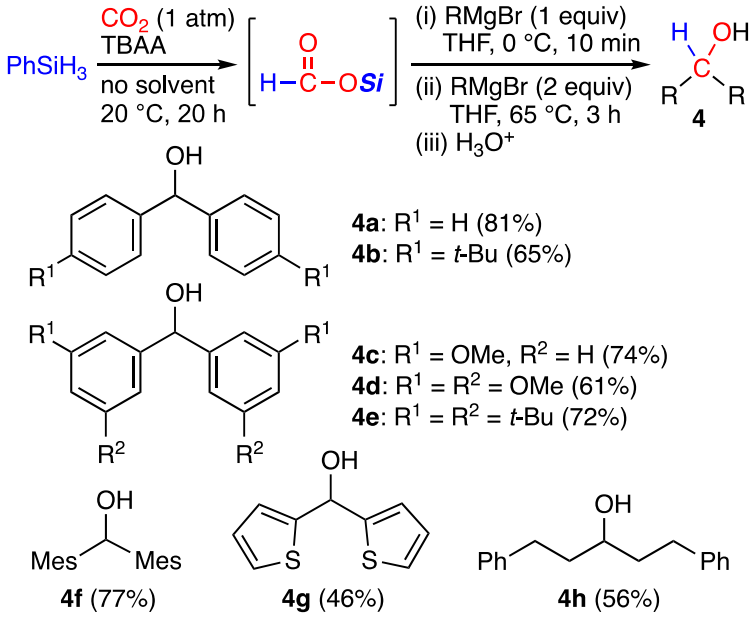

Scheme 8. One-pot alcohol synthesis via silyl formate.

Furthermore, we also investigated whether aldehydes could be directly synthesized via silyl formates (Scheme 9). After the synthesis of silyl formates from CO_2 and $PhSiH_3$ using TBAA as a catalyst under solvent-free conditions,[16] a less amount of PhMgBr (1 equiv) was added to suppress the formation of **4a**. After the workup procedure, **4a** was detected in 18% NMR yield, whereas only a trace amount of benzaldehyde was detected. Even when a smaller amount of PhMgBr (0.5 equiv) was added, we observed almost no formation of benzaldehyde. This is probably because benzaldehyde, generated *in situ*, is much more reactive than silyl formates.

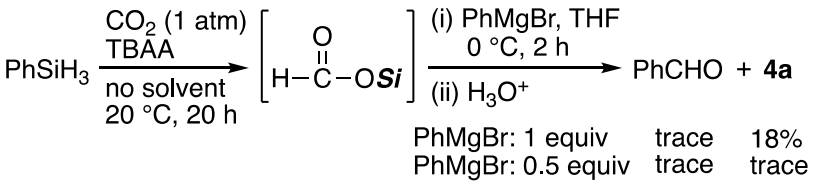

Scheme 9. One-pot aldehyde synthesis via silyl formate.

4.4 Conclusions

In summary, we have found a specific catalyst, $Cu(OAc)_2$, for the solvent-free *N*-formylation of **1a** with CO_2 and $PhSiH_3$ to give Comins–Meyers formamide **2a**. The X-ray crystal structure of a $Cu(OAc)_2$–**1a** complex suggested that the ligation of the pyridyl moiety of **1a** to the copper ion of the paddle-wheel structure plays an important role in the improvement of the solubility of the copper ion in the mixture of liquid substrates, the enhancement of the nucleophilicity of the acetate ion, and the acceleration of the *N*-formylation of **1a** by the proximity effect. ^{1}H NMR spectra detected a singlet signal (2.62 ppm) assigned to a Cu–H species, which is considered to be a catalytically active species in the hydrosilylation of CO_2. The resulting **2a** was subjected to the one-pot Grignard reaction to selectively synthesize aldehydes or alcohols. On the other hand, silyl formates prepared from CO_2 and $PhSiH_3$ were good alternative intermediates for alcohols, although they could not be converted into aldehydes. Further work is under way in our group for the catalytic conversions of CO_2 into a variety of functional groups useful for organic synthesis.

4.5 Experimental Section

[A] General Methods. NMR spectra were measured on a JEOL JNM-ECS400 spectrometer, and chemical shifts are reported as the delta scale in ppm using an internal reference (7.26 ppm ($CDCl_3$) or 7.16 ppm (C_6D_6) for ^{1}H NMR and 77.16 ppm ($CDCl_3$) for $^{13}C\{^1H\}$ NMR). Melting points were measured on a Yanaco melting point apparatus (uncorrected). Column chromatography was carried out using Fuji Silysia BW-127 ZH (100–270 mesh). Grignard reagents (RMgBr, 1 M) for the synthesis of **3a**–**f**, **3h**, and **4** were freshly prepared by the dropwise addition of RBr to Mg turnings (1.1 equiv) in dry THF at ambient temperature, and that for the synthesis of **3g** was freshly prepared by the dropwise addition of the ethynylbenzene to a suspension of EtMgBr (1 M, 1.1 equiv) in dry THF in an ice bath followed by heating at 55 °C for 2 h.

[B] Synthesis of formamides 2 with CO_2.

General procedure. In a glovebox (purge type) under N_2 atmosphere, $Cu(OAc)_2$ (10.9 mg, 0.060 mmol, 3 mol%) was put in a 30 mL Schlenk flask fitted with a rubber septum (solid amine **1c** or **1d** (2.0 mmol) was added in this step), and the flask was taken out from the glovebox. After the flask was evacuated and filled with CO_2 (balloon), the flask was put in a thermostatic bath at 20 °C. Amine **1a** or **1b** (2.0 mmol, stored over molecular sieves 3A) and $PhSiH_3$ (250 μL, 2.0 mmol, stored over molecular sieves 3A) were added in this order via syringes. The mixture was stirred at 20 °C for 18 h. Purification by silica gel column chromatography (eluent shown below) gave formamide **2**.

***N*-Methyl-*N*-(2-pyridyl)formamide (2a).**[131]

Eluent = hexane/EtOAc (3:1); 220 mg (1.61 mmol, 80% yield); Colorless oil; ^{1}H NMR ($CDCl_3$, 400 MHz) δ 9.31 (s, 1H), 8.35 (dd, J = 1.2, 4.8 Hz, 1H), 7.68–7.72 (m, 1H), 7.07–7.10 (m, 1H), 6.98 (d, J = 8.2 Hz, 1H), 3.30 (s, 3H); $^{13}C\{^1H\}$ NMR ($CDCl_3$, 100 MHz) δ 162.3, 154.1, 148.6, 138.6, 120.2, 111.6, 28.9; HRMS (EI) calcd for $C_7H_8N_2O$ 136.0637, found 136.0636 (M^+).

***N*-Methyl-*N*-(3-pyridyl)formamide (2b).**[131]

Eluent = hexane/EtOAc/MeOH (10:10:1); 144 mg (1.06 mmol, 53% yield); Yellow oil; ^{1}H NMR ($CDCl_3$, 400 MHz) δ 8.53 (s, 2H), 8.49 (s, 1H), 7.51–7.53 (m, 1H), 7.35–7.39 (m, 1H), 3.34 (s, 3H); $^{13}C\{^{1}H\}$ NMR ($CDCl_3$, 100 MHz) δ 161.8, 147.8, 143.8, 138.7, 129.5, 124.2, 32.0; HRMS (EI) calcd for $C_7H_8N_2O$ 136.0637, found 136.0637 (M^+).

***N*-Methyl-*N*-(4-pyridyl)formamide (2c).**[131]

Eluent = hexane/EtOAc/MeOH (5:5:1); 113 mg (0.830 mmol, 42% yield); White solid; mp 75–76 °C; ^{1}H NMR ($CDCl_3$, 400 MHz) δ 8.82 (s, 1H), 8.59 (s, 2H), 7.10–7.11 (m, 2H), 3.34 (s, 3H); $^{13}C\{^{1}H\}$ NMR ($CDCl_3$, 100 MHz) δ 161.3, 151.3, 149.0, 113.8, 30.3; HRMS (EI) calcd for $C_7H_8N_2O$ 136.0637, found 136.0637 (M^+).

***N*-Methyl-*N*-(2-pyrimidinyl)formamide (2d).**[21]

Eluent = hexane/EtOAc (5:1); 88 mg (0.64 mmol, 32% yield); White solid; mp 73–75 °C; ^{1}H NMR ($CDCl_3$, 400 MHz) δ 9.88 (s, 1H), 8.57 (d, J = 4.8 Hz, 2H), 7.05 (t, J = 4.8 Hz, 1H), 3.39 (s, 3H); $^{13}C\{^{1}H\}$ NMR ($CDCl_3$, 100 MHz) δ 163.4, 159.4, 158.1, 116.9, 27.8; HRMS (EI) calcd for $C_6H_7N_3O$ 137.0589, found 137.0589 (M^+).

[C] One-pot aldehyde synthesis with CO_2.

General procedure. In a glovebox (purge type) under N_2 atmosphere, $Cu(OAc)_2$ (10.9 mg, 0.060 mmol, 3 mol%) was put in a 30 mL Schlenk flask fitted with a rubber septum, and the flask was taken out from the glovebox. After the flask was evacuated and filled with CO_2 (balloon), the flask was put in a thermostatic bath at 20 °C. Amine **1a** (210 μL, 2.0 mmol, stored over molecular sieves 3A) and $PhSiH_3$ (250 μL, 2.0 mmol, stored over molecular sieves 3A) were added in this order via syringes. The mixture was stirred at 20 °C for 18 h. This reaction mixture containing formamide **2a** was used in the following reaction without purification. The CO_2 balloon was replaced by a N_2 balloon, and the reaction mixture was cooled in an ice bath, and a suspension of a Grignard reagent (RMgBr, 1 M, 2 equiv) in dry THF (4 mL) was added. The mixture was stirred at 0 °C for 2 h, and the reaction was quenched and neutralized with saturated aqueous NH_4Cl or 3% HCl. The product was extracted with Et_2O (10 mL × 3), and the organic layers were combined and dried over $MgSO_4$. Purification by silica gel column chromatography (eluent shown below) gave aldehyde **3**.

1-Naphthaldehyde (3a).[16]

Eluent = hexane/EtOAc (20:1); 223 mg (1.42 mmol, 71% yield); Light yellow oil; ^{1}H NMR ($CDCl_3$, 400 MHz) δ 10.41 (s, 1H), 9.26 (d, J = 7.7 Hz, 1H), 8.11 (d, J = 8.2 Hz, 1H), 8.00 (dd, J = 1.3, 7.0 Hz, 1H), 7.93 (d, J = 8.2 Hz, 1H), 7.58–7.72 (m, 3H); $^{13}C\{^{1}H\}$ NMR ($CDCl_3$, 100 MHz) δ 193.7, 136.8, 135.5, 133.9, 131.6, 130.7, 129.2, 128.6, 127.1, 125.0.

3-Methoxybenzaldehyde (3b).[16]

Eluent = hexane/EtOAc (30:1); 191 mg (1.40 mmol, 70% yield); Light yellow oil; ^{1}H NMR ($CDCl_3$, 400 MHz) δ 9.98 (s, 1H), 7.44–7.46 (m, 2H), 7.39 (d, J = 2.0 Hz, 1H), 7.17–7.19 (m, 1H), 3.87 (s, 3H); $^{13}C\{^1H\}$ NMR ($CDCl_3$, 100 MHz) δ 192.3, 160.3, 137.9, 130.2, 123.7, 121.7, 112.1, 55.6.

3,5-Dimethoxybenzaldehyde (3c).[16]

Eluent = hexane/EtOAc (20:1); 290 mg (1.74 mmol, 87% yield); White solid; mp 43 °C; ^{1}H NMR ($CDCl_3$, 400 MHz) δ 9.91 (s, 1H), 7.02 (d, J = 2.3 Hz, 2H), 6.71 (t, J = 2.3 Hz, 1H), 3.85 (s, 6H); $^{13}C\{^1H\}$ NMR ($CDCl_3$, 100 MHz) δ 192.1, 161.4, 138.5, 107.34, 107.27, 55.8.

3,5-Di-*tert*-butylbenzaldehyde (3d).[22]

Eluent = hexane/EtOAc (30:1); 366 mg (1.68 mmol, 84% yield); White solid; mp 87–88 °C; ^{1}H NMR ($CDCl_3$, 400 MHz) δ 10.01 (s, 1H), 7.71–7.73 (m, 3H), 1.37 (s, 18H); $^{13}C\{^1H\}$ NMR ($CDCl_3$, 100 MHz) δ 193.4, 152.0, 136.3, 129.1, 124.3, 35.1, 31.5.

4-*tert*-Butylbenzaldehyde (3e).[23]

Eluent = hexane/EtOAc (30:1); 281 mg (1.73 mmol, 87% yield); Light yellow oil; ^{1}H NMR ($CDCl_3$, 400 MHz) δ 9.98 (s, 1H), 7.82 (d, J = 8.5 Hz, 2H), 7.55 (d, J = 8.3 Hz, 2H), 1.35 (s, 9H); $^{13}C\{^1H\}$ NMR ($CDCl_3$, 100 MHz) δ 192.2, 158.6, 134.2, 129.8, 126.1, 35.5, 31.2.

Thiophene-2-carbaldehyde (3f).[16]

Eluent = hexane/EtOAc (10:1); 132 mg (1.18 mmol, 59% yield); Orange oil; ^{1}H NMR ($CDCl_3$, 400 MHz) δ 9.95 (s, 1H), 7.75–7.80 (m, 2H), 7.21–7.23 (m, 1H); $^{13}C\{^1H\}$ NMR ($CDCl_3$, 100 MHz) δ 183.2, 144.2, 136.5, 135.3, 128.4.

3-Phenyl-2-propynal (3g).[16]

Eluent = hexane/EtOAc (10:1); 164 mg (1.26 mmol, 63% yield); Light yellow oil; ^{1}H NMR ($CDCl_3$, 400 MHz) δ 9.42 (s, 1H), 7.59–7.62 (m, 2H), 7.47–7.51 (m, 1H), 7.38–7.42 (m, 2H); $^{13}C\{^1H\}$ NMR ($CDCl_3$, 100 MHz) δ 177.0, 133.4, 131.4, 128.9, 119.5, 95.3, 88.5.

3-Phenylpropanal (3h).[16]

Eluent = hexane/EtOAc (10:1); 165 mg (1.23 mmol, 61% yield); Yellow oil; ^{1}H NMR ($CDCl_3$, 400 MHz) δ 9.83 (t, J = 1.4 Hz, 1H), 7.30 (t, J = 7.4 Hz, 2H), 7.19–7.23 (m, 3H), 2.97 (t, J = 7.6 Hz, 2H), 2.77–2.81 (m, 2H); $^{13}C\{^1H\}$ NMR ($CDCl_3$, 100 MHz) δ 201.7, 140.4, 128.7, 128.4, 126.4, 45.3, 28.2.

[D] One-pot alcohol synthesis with CO_2.

General procedure. In a glovebox (purge type) under N_2 atmosphere, $Cu(OAc)_2$ (10.9 mg, 0.060 mmol, 3 mol%) was put in a 30 mL Schlenk flask fitted with a rubber septum, and the flask was taken out from the glovebox. After the flask was evacuated and filled with CO_2 (balloon), the flask was put in a thermostatic bath at 20 °C. Amine **1a** (210 μL, 2.0 mmol, stored over molecular sieves 3A) and $PhSiH_3$ (250 μL, 2.0 mmol, stored over molecular sieves 3A) were added in this order via syringes. The mixture was stirred at 20 °C for 18 h. This reaction mixture containing formamide **2a** was used in the following reaction without purification. A reflux condenser was attached, and the CO_2 balloon was replaced by a N_2 balloon. The reaction mixture was cooled in an ice bath. A suspension of a Grignard reagent (RMgBr, 1 M, 1 equiv) in dry THF (2 mL) was added, and the mixture was stirred at 0 °C for 10 min. The Grignard reagent (RMgBr, 1 M, 2 equiv) in dry THF (4 mL) was further

added, and the reaction mixture was heated at reflux for 3 h. After cooling to rt, the reaction was quenched and neutralized with 10% HCl. The product was extracted with Et_2O (10 mL × 3), and the organic layers were combined and dried over $MgSO_4$. Purification by silica gel column chromatography (eluent shown below) gave alcohol **4**.

Diphenylmethanol (4a).[24]

Eluent = hexane/EtOAc (10:1); 350 mg (1.90 mmol, 95% yield); White solid; mp 62–63 °C; ^{1}H NMR ($CDCl_3$, 400 MHz) δ 7.31–7.39 (m, 8H), 7.24–7.28 (m, 2H), 5.85 (d, J = 3.4 Hz, 1H), 2.22 (d, J = 3.6 Hz, 1H); ^{13}C{^{1}H} NMR ($CDCl_3$, 100 MHz) δ 143.9, 128.7, 127.7, 126.7, 76.4.

Bis(4-*tert*-butylphenyl)methanol (4b).[25]

Eluent = hexane/EtOAc (15:1); 469 mg (1.58 mmol, 79% yield); White solid; mp 104–105 °C; ^{1}H NMR ($CDCl_3$, 400 MHz) δ 7.31–7.38 (m, 8H), 5.81 (d, J = 2.9 Hz, 1H), 2.16 (d, J = 3.3 Hz, 1H), 1.31 (s, 18H); ^{13}C{^{1}H} NMR ($CDCl_3$, 100 MHz) δ 150.5, 141.1, 126.4, 125.5, 76.1, 34.6, 31.5.

Bis(3-methoxyphenyl)methanol (4c).[26]

Eluent = hexane/EtOAc (5:1); 419 mg (1.72 mmol, 86% yield); Colorless oil; ^{1}H NMR ($CDCl_3$, 400 MHz) δ 7.23–7.27 (m, 2H), 6.95–6.96 (m, 4H), 6.79–6.82 (m, 2H), 5.79 (d, J = 3.6 Hz, 1H), 3.79 (s, 6H), 2.20 (d, J = 3.6 Hz, 1H); ^{13}C{^{1}H} NMR ($CDCl_3$, 100 MHz) δ 159.9, 145.4, 129.7, 119.0, 113.2, 112.2, 76.2, 55.4.

Bis(3,5-dimethoxyphenyl)methanol (4d).[27]

Eluent = hexane/EtOAc (3:1); 387 mg (1.27 mmol, 64% yield); White solid; mp 121–122 °C; ^{1}H NMR ($CDCl_3$, 400 MHz) δ 6.55 (t, J = 2.2 Hz, 4H), 6.36 (t, J = 2.3 Hz, 2H), 5.68 (s, 1H), 3.77 (s, 12H), 2.20 (s, 1H); ^{13}C{^{1}H} NMR ($CDCl_3$, 100 MHz) δ 161.0, 146.1, 104.6, 99.6, 76.4, 55.5.

Bis(3,5-di-*tert*-butylphenyl)methanol (4e).[25]

Eluent = hexane/EtOAc (30:1); 652 mg (1.60 mmol, 80% yield); White solid; mp 143–144 °C; ^{1}H NMR ($CDCl_3$, 400 MHz) δ 7.33 (t, J = 1.7 Hz, 2H), 7.26 (s, 4H), 5.84 (s, 1H), 2.22 (s, 1H), 1.31 (s, 36H); ^{13}C{^{1}H} NMR ($CDCl_3$, 100 MHz) δ 150.9, 143.1, 121.6, 121.2, 77.7, 35.0, 31.6.

Bis(2,4,6-trimethylphenyl)methanol (4f).[28]

Eluent = hexane/EtOAc (20:1); 450 mg (1.68 mmol, 84% yield); White solid; mp 148–150 °C; ^{1}H NMR ($CDCl_3$, 400 MHz) δ 6.79 (s, 4H), 6.35 (d, J = 4.8 Hz, 1H), 2.25 (s, 6H), 2.20 (s, 12H), 1.72 (d, J = 4.9 Hz, 1H); ^{13}C{^{1}H} NMR ($CDCl_3$, 100 MHz) δ 136.7, 130.7, 73.5, 21.3, 20.8.

Bis(2-thienyl)methanol (4g).[29]

Eluent = hexane/EtOAc (10:1); 298 mg (1.52 mmol, 76% yield); Light yellow solid; mp 50–52 °C; ^{1}H NMR ($CDCl_3$, 400 MHz) δ 7.30 (dd, J = 1.3, 5.0 Hz, 2H), 7.03 (d, J = 3.6 Hz, 2H), 6.96–6.99 (m, 2H), 6.32 (d, J = 4.4 Hz, 1H), 2.56 (d, J = 4.4 Hz, 1H); ^{13}C{^{1}H} NMR ($CDCl_3$, 100 MHz) δ 147.2, 126.8, 125.7, 125.2, 68.7.

1,5-Diphenyl-3-pentanol (4h).[30]

Eluent = hexane/EtOAc (5:1); 318 mg (1.32 mmol, 66% yield); Colorless solid; mp 38–39 °C; ^{1}H NMR ($CDCl_3$, 400 MHz) δ 7.25–7.31 (m, 4H), 7.18–7.20 (m, 6H), 3.63–3.71 (m, 1H), 2.75–2.83 (m, 2H), 2.63–2.71 (m, 2H), 1.73–1.88 (m, 4H), 1.37 (d, J = 4.6 Hz, 1H); ^{13}C{^{1}H} NMR ($CDCl_3$, 100 MHz) δ 142.2, 128.56, 128.54, 126.0, 70.9, 39.3, 32.2.

[E] One-pot alcohol synthesis with CO_2 and phenylsilane via silyl formate.

General procedure. In a glovebox (purge type) under N_2 atmosphere, TBAA (18.1 mg, 0.060 mmol, 3 mol%) was put in a 30 mL Schlenk flask fitted with a rubber septum, and the flask was taken out from the glovebox. After the flask was evacuated and filled with CO_2 (balloon), the flask was put in a thermostatic bath at 20 °C. $PhSiH_3$ (250 μL, 2.0 mmol, stored over molecular sieves 3A) was added via a syringe. The mixture was stirred at 20 °C for 20 h. This reaction mixture containing silyl formate was used in the following reaction without purification. A reflux condenser was attached, and the CO_2 balloon was replaced by a N_2 balloon. The reaction mixture was cooled in an ice bath. A suspension of a Grignard reagent (RMgBr, 1 M, 1 equiv) in dry THF (2 mL) was added, and the mixture was stirred at 0 °C for 10 min. The Grignard reagent (RMgBr, 1 M, 2 equiv) in dry THF (4 mL) was further added, and the reaction mixture was heated at reflux for 3 h. After cooling to rt, the reaction was quenched and neutralized with 10% HCl. The product was extracted with Et_2O (10 mL × 3), and the organic layers were combined and dried over $MgSO_4$. Purification by silica gel column chromatography gave alcohol **4**.

Diphenylmethanol (4a). 300 mg (1.62 mmol, 81% yield).

Bis(4-*tert*-butylphenyl)methanol (4b). 388 mg (1.31 mmol, 65% yield).

Bis(3-methoxyphenyl)methanol (4c). 360 mg (1.47 mmol, 74% yield).

Bis(3,5-dimethoxyphenyl)methanol (4d). 369 mg (1.21 mmol, 61% yield).

Bis(3,5-di-*tert*-butylphenyl)methanol (4e). 586 mg (1.43 mmol, 72% yield).

Bis(2,4,6-trimethylphenyl)methanol (4f). 412 mg (1.54 mmol, 77% yield).

Bis(2-thienyl)methanol (4g). 182 mg (0.929 mmol, 46% yield).

1,5-Diphenyl-3-pentanol (4h). 269 mg (1.12 mmol, 56% yield).

[F] Detection of Cu–H species by means of ^{1}H NMR spectroscopy.

(a) NMR experiments for Figure 2. In a glovebox (purge type) under N_2 atmosphere, $Cu(OAc)_2$ (9.1 mg, 0.050 mmol), benzene-d_6 (1.0 mL), and amine **1a** (21 μL, 0.2 mmol) were put in a 30 mL Schlenk flask fitted with a rubber septum, and the flask was taken out from the glovebox. The flask was put in a thermostatic bath at 20 °C, and $PhSiH_3$ (125 μL, 1.0 mmol, stored over molecular sieves 3A) was added via a syringe. The mixture was stirred at 20 °C for 3 h, and ^{1}H NMR spectrum was measured (Figure 2b). The solution was exposed to CO_2 (balloon), stirred at 20 °C for 48 h, and ^{1}H NMR spectrum was then measured (Figure 2c). Purification by silica gel column chromatography afforded formamide **2a**. 20.6 mg (0.151 mmol, 76% yield); Colorless oil; ^{1}H NMR (C_6D_6, 400 MHz) δ 9.44 (s, 1H), 8.05 (d, J = 4.6 Hz, 1H), 6.85–6.89 (m, 1H), 6.39–6.42 (m, 1H), 6.04 (d, J = 8.3 Hz, 1H), 2.96 (s, 3H).

(b) NMR experiments for Figure 3a. In a glovebox (purge type) under N_2 atmosphere, $Cu(OAc)_2$ (9.1 mg, 0.050 mmol), benzene-d_6 (1.0 mL), and amine **1a** (21 μL, 0.2 mmol) were put in a 30 mL Schlenk flask fitted with a rubber septum, and the flask was taken out from the glovebox. The flask was put in a thermostatic bath at 30 °C, and $PhSiH_3$ (125 μL, 1.0 mmol, stored over molecular sieves 3A) was added via a syringe. The mixture was stirred at 30 °C, and the progress of the reaction was monitored by ^{1}H NMR spectra.

(c) NMR experiments for Figure 3b. In a glovebox (purge type) under N_2 atmosphere, $Cu(OAc)_2$ (9.1 mg, 0.050 mmol), benzene-d_6 (1.0 mL), and amine **1a** (21 μL, 0.2 mmol) were put in a 30 mL Schlenk flask fitted with a rubber septum, and the flask was taken out from the glovebox. The flask was put in a thermostatic bath at 30 °C, and $PhSiH_3$ (125 μL, 1.0 mmol, stored over molecular sieves 3A) was added via a syringe. The mixture was stirred at 30 °C for 3 h, and ^1H NMR spectrum was measured; See the bottom spectrum. This solution in the NMR tube was then bubbled with a CO_2 gas for 15 min, and ^1H NMR spectrum was measured. This NMR tube was incubated at 30 °C for 3 h, and ^1H NMR spectrum was measured. This solution in the NMR tube was again bubbled with a CO_2 gas for 15 min, and ^1H NMR spectrum was measured. This NMR tube was incubated at 30 °C for 18 h, and ^1H NMR spectrum was measured.

4.6 References

(1) Mustafa, A.; Lougou, B. G.; Shuai, Y.; Wang, Z.; Tan, H. *J. Energy Chem.* **2020**, *49*, 96–123.

(2) (a) Modak, A.; Bhanja, P.; Dutta, S.; Chowdhury, B.; Bhaumik, A. *Green Chem.* **2020**, *22*, 4002–4033. (b) Sable, D. A.; Vadagaonkar, K. S.; Kapdi, A. R.; Bhanage, B. M. *Org. Biomol. Chem.* **2021**, *19*, 5725–5757.

(3) (a) Jiang, X.; Nie, X.; Guo, X.; Song, C.; Chen, J. G. *Chem. Rev.* **2020**, *120*, 7984–8034. (b) Zhang, Y.; Zhang, T.; Das, S. *Green Chem.* **2020**, *22*, 1800–1820.

(4) (a) Tortajada, A.; Juliá-Hernández, F.; Börjesson, M.; Moragas, T.; Martin, R. *Angew. Chem. Int. Ed.* **2018**, *57*, 15948–15982. (b) Nozaki, K. *Bull. Chem. Soc. Jpn.* **2021**, *94*, 984–988.

(5) Shaikh, R. R.; Pornpraprom, S.; D'Elia, V. *ACS Catal.* **2018**, *8*, 419–450.

(6) Kamphuis, A. J.; Picchioni, F.; Pescarmona, P. P. *Green Chem.* **2019**, *21*, 406–448.

(7) (a) Yu, B.; Zhao, Y.; Zhang, H.; Xu, J.; Hao, L.; Gao, X.; Liu, Z. *Chem. Commun.* **2014**, *50*, 2330–2333. (b) Yu, B.; Yang, Z.; Zhao, Y.; Hao, L.; Zhang, H.; Gao, X.; Han, B.; Liu, Z. An *Chem. Eur. J.* **2016**, *22*, 1097–1102. (c) Ren, X.; Zheng, Z.; Zhang, L.; Wang, Z.; Xia, C.; Ding, K. *Angew. Chem. Int. Ed.* **2017**, *56*, 310–313. (d) Liu, Z.; Yang, Z.; Yu, B.; Yu, X.; Zhang, H.; Zhao, Y.; Yang, P.; Liu, Z. *Org. Lett.* **2018**, *20*, 5130–5134.

(8) (a) Tani, Y.; Kuga, K.; Fujihara, T.; Terao, J.; Tsuji, Y. *Chem. Commun.* **2015**, *51*, 13020–13023. (b) Chen, X.-W.; Zhu, L.; Gui, Y.-Y.; Jing, K.; Jiang, Y.-X.; Bo, Z.-Y.; Lan, Y.; Li, J.; Yu, D.-G. *J. Am. Chem. Soc.* **2019**, *141*, 18825–18835. (c) Zhang, X.; Tian, X.; Shen, C.; Xia, C.; He, L. *ChemCatChem* **2019**, *11*, 1986–1992. (d) Wang, M.-Y.; Jin, X.; Wang, X.; Xia, S.; Wang, Y.; Huang, S.; Li, Y.; He, L.-N.; Ma, X. *Angew. Chem. Int. Ed.* **2021**, *60*, 3984–3988.

(9) Zhu, D.-Y.; Li, W.-D.; Yang, C.; Chen, J.; Xia, J.-B. *Org. Lett.* **2018**, *20*, 3282–3285.

(10) (a) Li, Y.; Yan, T.; Junge, K.; Beller, M. *Angew. Chem. Int. Ed.* **2014**, *53*, 10476–10480. (b) Zhu, D.-Y.; Fang, L.; Han, H.; Wang, Y.; Xia, J.-B. *Org. Lett*. **2017**, *19*, 4259–4262. (c) Takaishi, K.; Kosugi, H.; Nishimura, R.; Yamada, Y.; Ema, T. *Chem. Commun.* **2021**, *57*, 8083–8086. (d) Li, W.-D.; Chen, J.; Zhu, D.-Y.; Xia, J.-B. *Chin. J. Chem*. **2021**, *39*, 614–620. (e) Xiang, S.; Fan, W.; Zhang, W.; Li, Y.; Guo, S.; Huang, D. *Green Chem.* **2021**, *23*, 7950–7955. (f) Murata, T.; Hiyoshi, M.; Maekawa, S.; Saiki, Y.; Ratanasak, M.; Hasegawa, J.; Ema, T. *Green Chem.* **2022**, *24*, 2385–

2390. (g) Ratanasak, M.; Murata, T.; Adachi, T.; Hasegawa, J.; Ema, T. *Chem. Eur. J.* **2022**, *28*, e202202210.

(11) (a) Tlili, A.; Blondiaux, E.; Frogneux, X.; Cantat, T. *Green Chem.* **2015**, *17*, 157–168. (b) Li, Z.; Yu, Z.; Luo, X.; Li, C.; Wu, H.; Zhao, W.; Li, H.; Yang, S. *RSC Adv.* **2020**, *10*, 33972–34005. (c) Pramudita, R. A.; Motokura, K. *ChemSusChem* **2021**, *14*, 281–292.

(12) (a) Riduan, S. N.; Zhang, Y.; Ying, J. Y. *Angew. Chem. Int. Ed.* **2009**, *48*, 3322–3325. (b) Rauch, M.; Parkin, G. *J. Am. Chem. Soc*. **2017**, *139*, 18162–18165. (c) Rauch, M.; Strater, Z.; Parkin, G. *J. Am. Chem. Soc.* **2019**, *141*, 17754–17762. (d) Cramer, H. H.; Chatterjee, B.; Weyhermüller, T.; Werlé, C.; Leitner, W. *Angew. Chem. Int. Ed.* **2020**, *59*, 15674–15681. (e) Ritter, F.; Spaniol, T. P.; Douair, I.; Maron, L.; Okuda, J. *Angew. Chem. Int. Ed.* **2020**, *59*, 23335–23342.

(13) (a) Das Neves Gomes, C.; Jacquet, O.; Villiers, C.; Thuéry, P.; Ephritikhine, M.; Cantat, T. A *Angew. Chem. Int. Ed.* **2012**, *51*, 187–190. (b) Jacquet, O.; Das Neves Gomes, C.; Ephritikhine, M.; Cantat, T. *J. Am. Chem. Soc.* **2012**, *134*, 2934–2937. (c) Motokura, K.; Takahashi, N.; Kashiwame, D.; Yamaguchi, S.; Miyaji, A.; Baba, T. *Catal. Sci. Technol.* **2013**, *3*, 2392–2396. (d) Hulla, M.; Bobbink, F. D.; Das, S.; Dyson, P. J. *ChemCatChem* **2016**, *8*, 3338–3342. (e) Lv, H.; Xing, Q.; Yue, C.; Lei, Z.; Li, F. *Chem. Commun.* **2016**, *52*, 6545–6548. (f) Luo, R.; Lin, X.; Chen, Y.; Zhang, W.; Zhou, X.; Ji, H. *ChemSusChem* **2017**, *10*, 1224–1232. (g) Hulla, M.; Laurenczy, G.; Dyson, P. J. *ACS Catal.* **2018**, *8*, 10619–10630. (h) Li, G.; Chen, J.; Zhu, D.-Y.; Chen, Y.; Xia, J.-B. *Adv. Synth. Catal.* **2018**, *360*, 2364–2369. (i) Li, W.-D.; Zhu, D.-Y.; Li, G.; Chen, J.; Xia, J.-B. *Adv. Synth. Catal*. **2019**, *361*, 5098–5104. (j) Hulla, M.; Ortiz, D.; Katsyuba, S.; Vasilyev, D.; Dyson, P. J. *Chem. Eur. J.* **2019**, *25*, 11074–11079. (k) Takaishi, K.; Nath, B. D.; Yamada, Y.; Kosugi, H.; Ema, T. *Angew. Chem. Int. Ed.* **2019**, *58*, 9984–9988. (l) Jiang, X.; Huang, Z.; Makha, M.; Du, C.-X.; Zhao, D.; Wang, F.; Li, Y. *Green Chem.* **2020**, *22*, 5317–5324. (m) Zhang, Q.; Lin, X.-T.; Fukaya, N.; Fujitani, T.; Sato, K.; Choi, J.-C. *Green Chem.* **2020**, *22*, 8414–8422. (n) Sarkar, D.; Weetman, C.; Dutta, S.; Schubert, E.; Jandl, C.; Koley, D.; Inoue, S. *J. Am. Chem. Soc.* **2020**, *142*, 15403–15411. (o) Wang, P.; He, Q.; Zhang, H.; Sun, Q.; Cheng, Y.; Gan, T.; He, X.; Ji, H. *Catal. Commun.* **2021**, *149*, 106195.

(14) Hayashi, Y. *Chem. Sci.* **2016**, *7*, 866–880.

(15) (a) Jin, G.; Werncke, C. G.; Escudié, Y.; Sabo-Etienne, S.; Bontemps, S. *J. Am. Chem. Soc.* **2015**, *137*, 9563–9566. (b) Nogi, K.; Fujihara, T.; Terao, J.; Tsuji, Y. *J. Am. Chem. Soc.* **2016**, *138*, 5547–5550. (c) Béthegnies, A.; Escudié, Y.; Nuñez-Dallos, N.; Vendier, L.; Hurtado, J.; del Rosal, I.; Maron, L.; Bontemps, S. *ChemCatChem* **2019**, *11*, 760–765. (d) Zhao, Y.; Guo, X.; Ding, X.; Zhou, Z.; Li, M.; Feng, N.; Gao, B.; Lu, X.; Liu, Y.; You, J. *Org. Lett.* **2020**, *22*, 8326–8331. (e) Zhao, Y.; Liu, X.; Zheng, L.; Du, Y.; Shi, X.; Liu, Y.; Yan, Z.; You, J.; Jiang, Y. *J. Org. Chem.* **2020**, *85*, 912–923. (f) Zhao, Y.; Guo, X.; Du, Y.; Shi, X.; Yan, S.; Liu, Y.; You, J. *Org. Biomol. Chem.* **2020**, *18*, 6881–6888. (g) Zhang, D.; Jarava-Barrera, C.; Bontemps, S. *ACS Catal.* **2021**, *11*, 4568–4575.

(16) Murata, T.; Hiyoshi, M.; Ratanasak, M.; Hasegawa, J.; Ema, T. *Chem. Commun.* **2020**, *56*, 5783–5786.

(17) (a) Comins, D.; Meyers, A. I. *Synthesis* **1978**, 403–404. (b) Meyers, A. I.; Comins, D. L. *Tetrahedron Lett.* **1978**, *52*, 5179–5182. (c) Comins, D. L.; Dernell, W. *Tetrahedron Lett.* **1981**, *22*, 1085–1088.

(18) Nakaoka, K.; Guo, C.; Saiki, Y.; Furukawa, S.; Ema, T. *J. Org. Chem.* **2023**, *88*, 15444–15451.

(19) NMR detection of Cu–H species. (a) Mankad, N. P.; Laitar, D. S.; Sadighi, J. P. *Organometallics* **2004**, *23*, 3369–3371. (b) Lipshutz, B. H.; Frieman, B. A. *Angew. Chem. Int. Ed.* **2005**, *44*, 6345–6348. (c) Fujihara, T.; Xu, T.; Semba, K.; Terao, J.; Tsuji, Y. *Angew. Chem. Int. Ed.* **2011**, *50*, 523–527. (d) Lv, H.; Cai, Y.-B.; Zhang, J.-L. *Angew. Chem. Int. Ed.* **2013**, *52*, 3203–3207. (e) Motokura, K.; Kashiwame, D.; Takahashi, N.; Miyaji, A.; Baba, T. *Chem. Eur. J.* **2013**, *19*, 10030–10037. (f) Nguyen, T.-A. D.; Goldsmith, B. R.; Zaman, H. T.; Wu, G.; Peters, B.; Hayton, T. W. *Chem. Eur. J.* **2015**, *21*, 5341–5344.

(20) Itagaki, S.; Yamaguchi, K.; Mizuno, N. *J. Mol. Catal. A: Chem.* **2013**, *366*, 347–352.

(21) Amaratunga, W.; Fréchet, J. M. J. *Tetrahedron Lett.* **1983**, *24*, 1143–1146.

(22) Zehnder, D. W.; Smithrud, D. B. *Org. Lett.* **2001**, *3,* 2485–2487.

(23) Lee, K.; Maleczka, R. E., Jr. *Org. Lett.* **2006**, *8,* 1887–1888.

(24) Ni, S.; El Remaily, M. A. E. A. A. A.; Franzén, J. *Adv. Synth. Catal*. **2018**, *360*, 4197–4204.

(25) Zhang, Y.-D.; Li, X.-Y.; Mo, Q.-K.; Shi, W.-B.; Zhao, J.-B.; Zhu, S.-F. *Angew. Chem. Int. Ed.* **2022**, *61*, e202208473.

(26) Presset, M.; Paul, J.; Cherif, G. N.; Ratnam, N.; Laloi, N.; Léonel, E.; Gosmini, C.; Le Gall, E. *Chem. Eur. J.* **2019**, *25*, 4491–4495.

(27) Kabro, A.; Roisnel, T.; Fischmeister, C.; Bruneau, C. *Chem. Eur. J.* **2010**, *16*, 12255–12261.

(28) Tanner, D. D.; Yang, C. M. *J. Org. Chem.* **1993**, *58*, 5907–5914.

(29) Plajer, A. J.; Ahrens, L.; Wieteck, M.; Lustosa, D. M.; Babaahmadi, R.; Yates, B.; Ariafard, A.; Rudolph, M.; Rominger, F.; Hashmi, A. S. K. *Chem. Eur. J.* **2018**, *24*, 10766–10772.

(30) Zhang, Q.-C.; Wu, F.-T.; Hao, H.-M.; Xu, H.; Zhao, H.-X.; Long, L.-S.; Huang, R.-B.; Zheng, L.-S. *Angew. Chem. Int. Ed.* **2013**, *52*, 12602–12605.

Chapter 5

Grand Summary

This thesis describes both non-reductive and reductive conversions of CO_2 into useful chemical products such as poly(carbonate–urethane)s, poly(carbonate–thioimidocarbonate)s, *N*-formamides, enamines, aldehydes, nitriles, and alcohols.

In the study of non-reductive transformations of CO_2, we have achieved the terpolymerizations of CHO, CO_2, and isothiocyanates or isocyanates for the first time using bifunctional Al^{III} porphyrin catalysts with quaternary ammonium bromides under solvent-free conditions (Scheme 1). The terpolymerizations of CHO, CO_2, and isothiocyanates gave poly(carbonate–thioimidocarbonate)s showing degradability for acids and UV light. The ratio of the PTIC to PCHC units in the terpolymer could be controlled by the CO_2 pressure and substituents on isothiocyanates. Gradient terpolymers and block polymers could be synthesized in a one-step manner and a one-pot two-step manner, respectively. On the other hand, the terpolymerizations of CHO, CO_2, and isocyanates gave poly(carbonate–urethane)s with tertiary carbamate linkages under atmospheric CO_2 pressure. The slow addition of isocyanates suppressed the formation of isocyanurates, cyclic trimeric byproducts. The terpolymers showed little or no degradability for acids and UV light unlike poly(carbonate–thioimidocarbonate)s, which indicates that the PCHC and PU linkages are more robust. These results were described in Chapter 2.

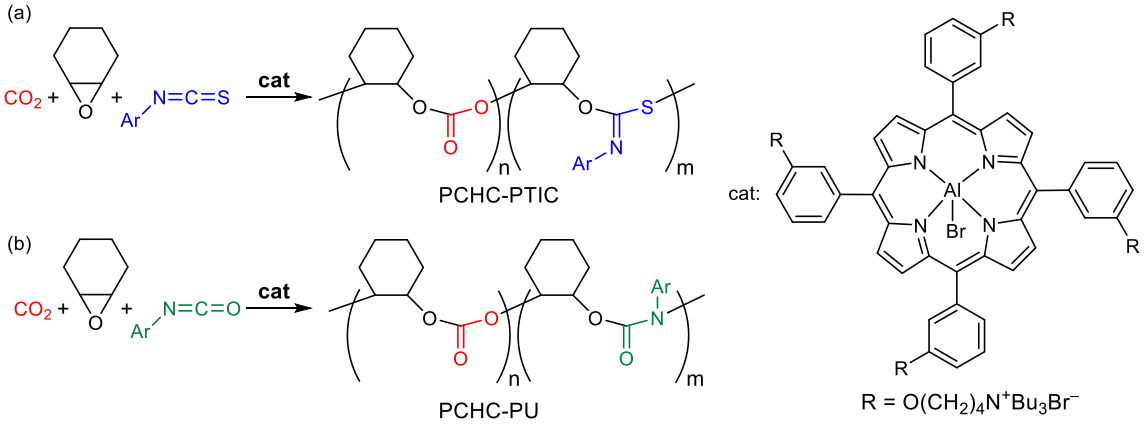

Scheme 1. Summary of Chapter 2.

We have also achieved two types of solvent-free *N*-formylation of amines with CO_2 and $PhSiH_3$ as reductive conversions of CO_2 (Scheme 2). One involves a binary catalyst system composed of TBAA and $Cu(OAc)_2$, which was used to synthesize various formamides. This solvent-free catalytic system enabled us to conduct various C–C bond-forming reactions of formamides such as the Peterson, Vilsmeier–Haack, and modified Vilsmeier–Haack reactions in the second step of one-pot reactions to synthesize enamines, aldehydes, and nitriles, respectively (Scheme 2a). These results are described in Chapter 3. The other involves the *N*-formylation of 2-(methylamino)pyridine with CO_2 and $PhSiH_3$

catalyzed by $Cu(OAc)_2$ alone to give Comins–Meyers formamide. The X-ray crystal structure of a $Cu(OAc)_2$–2-(methylamino)pyridine complex suggested that the ligation of the pyridyl moiety of 2-(methylamino)pyridine to the copper ion of the paddle-wheel structure plays an important role in the improvement of the solubility of the copper ion in the mixture of liquid substrates and the enhancement of the nucleophilicity of the acetate ion. The resulting Comins–Meyers formamide was subjected to the one-pot Grignard reaction to selectively synthesize aldehydes or alcohols (Scheme 2b). These results are described in Chapter 4.

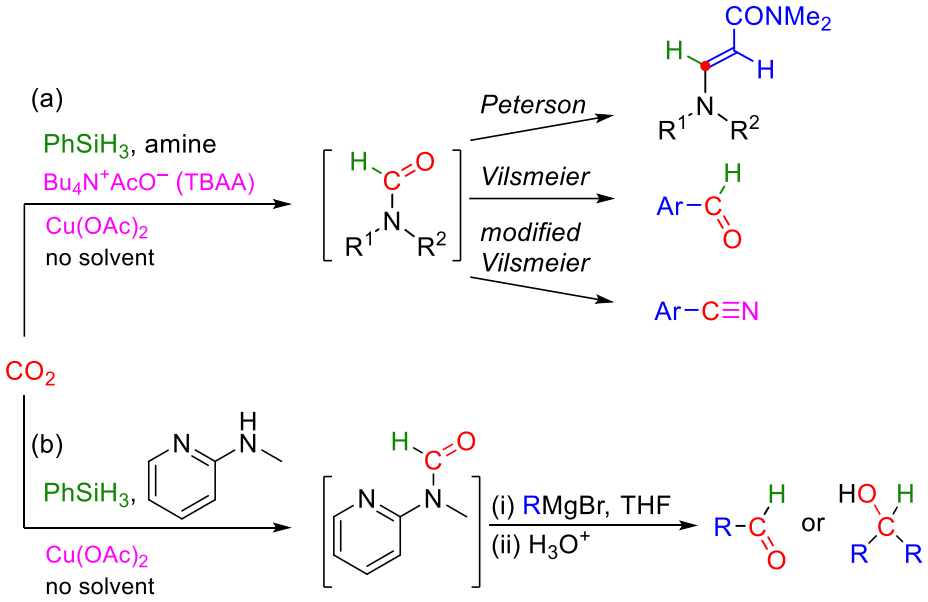

Scheme 2. Summary of Chapters 3 and 4.

In conclusion, we have achieved the non-reductive conversions of CO_2 to poly(carbonate–thioimidocarbonate)s and poly(carbonate–urethane)s using bifunctional Al^{III} porphyrin catalyst with quaternary ammonium bromides. We have also carried out the reductive conversions of CO_2 to enamines, aldehydes, nitriles, and alcohols via the solvent-free *N*-formylation of amines with CO_2 and $PhSiH_3$ using $Cu(OAc)_2$ as a catalyst. These methods will contribute to the development of CO_2 utilization.

List of Publications

1. Terpolymerizations of Cyclohexene Oxide, CO_2, and Isocyanates or Isothiocyanates for the Synthesis of Poly(carbonate–urethane)s or Poly(carbonate–thioimidocarbonate)s.
   Nakaoka, K.; Muranaka, S.; Yamamoto, I.; Ema, T. *Polym. Chem.* **2024**, *15*, 707–713.

2. Synthesis of Enamines, Aldehydes, and Nitriles from CO_2: Scope of the One-Pot Strategy via Formamides.
   Nakaoka, K.; Guo, C.; Saiki, Y.; Furukawa, S.; Ema, T. *J. Org. Chem.* **2023**, *88*, 15444–15451.

3. One-Pot Synthesis of Aldehydes or Alcohols from CO_2 via Formamides or Silyl Formates.
   Yang, F.; Saiki, Y.; Nakaoka, K.; Ema, T. *Adv. Synth. Catal.* **2023**, *365*, 877–883.

List of Oral/Poster Presentations

1. Catalytic terpolymerization of CO_2, epoxides, and heteroallenes (2).
   Koichi Nakaoka, Satoshi Muranaka, Io Yamamoto, Chihiro Maeda, Kazuto Takaishi, and Tadashi Ema
   Conference: The 103rd CSJ Annual Meeting, Chiba (March, 2023)
   Type of Presentation: Oral

2. Terpolymerization of epoxides, CO_2, and iso(thio)cyanates for the synthesis of poly(carbonate–urethane)s or poly(carbonate–thioimidocarbonate)s.
   Koichi Nakaoka, Satoshi Muranaka, Io Yamamoto, Chihiro Maeda, Kazuto Takaishi, and Tadashi Ema
   Conference: 72nd SPSJ Annual Meeting, Gunma (May, 2023)
   Type: Poster

3. New synthetic methods for CO_2-based polymers using epoxides, CO_2, and iso(thio)cyanates, and their degradation methods.
   Koichi Nakaoka, Satoshi Muranaka, Io Yamamoto, Chihiro Maeda, Kazuto Takaishi, and Tadashi Ema
   Conference: 12th JACI/GSC Symposium, Tokyo (June, 2023)
   Type: Poster

Acknowledgement

The studies presented in this thesis entitled "One-Pot Synthesis of Chemicals Using CO_2 as Chemical Feedstock" have been carried out under the supervision of Professor Dr. Tadashi Ema at the Division of Applied Chemistry, Graduate School of Natural Science and Technology, Okayama University during 2021–2024.

I would like to express my sincerest gratitude to Professor Dr. Tadashi Ema for his overall guidance, warm encouragement, and valuable discussions throughout this work. I would also like to express my acknowledgement to Dr. Kazuto Takaishi and Dr. Chihiro Maeda for their overall support during the course of this work. I would also like to thank Dr. Yukinari Sunatsuki (Okayama University) for X-ray analysis of metal complexes and Ms. Tomoko Amimoto (Hiroshima University) for the measurement of mass spectra of polymers.

I express my special gratitude to Mr. Chao Guo, Mr. Fan Yang, Mr. Yuta Saiki, Mr. Satoshi Muranaka, and Mr. Io Yamamoto for their active assistance and all other Lab members for their friendship and kind help. I would like to offer my special thanks to all faculty members at Okayama University.

Finally, I would like to express my heartiest gratitude to my wife Ms. Shoko Nakaoka, my daughter Ms. Yuzuki Nakaoka, and my son Mr. Itsuki Nakaoka for their constant assistance and encouragement.

March, 2024

Koichi Nakaoka
Division of Applied Chemistry
Graduate School of Natural Science and Technology
Okayama University